Hydrographic Observations at the Woods Hole Oceanographic Institution Hawaii Ocean Time-series Site: 2012 – 2013 Data Report #9

Fernando Santiago-Mandujano, Daniel McCoy, Cameron Fumar, Craig Nosse, Albert Plueddemann, Robert Weller, Roger Lukas, Jefrey Snyder, Sean Whelan, Nan Galbraith and Ethan Roth

January, 2015

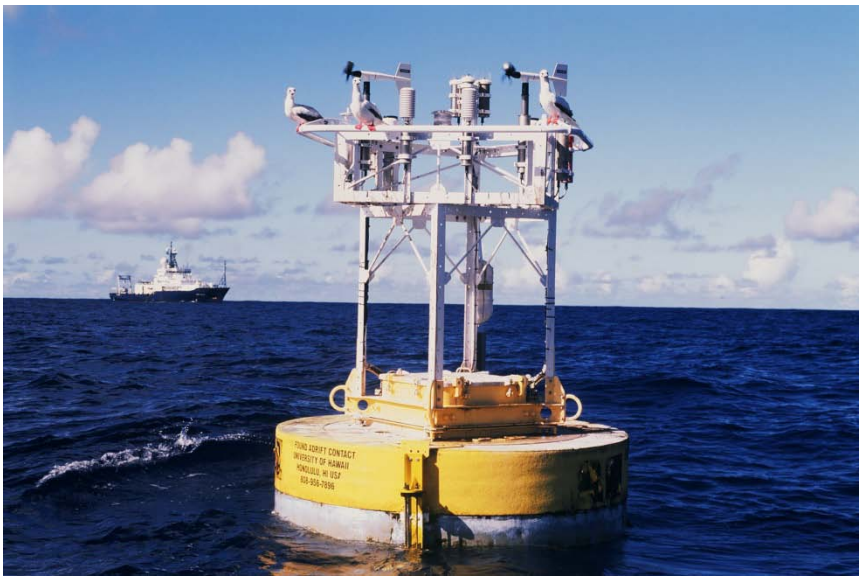

SCHOOL OF OCEAN AND EARTH SCIENCE AND TECHNOLOGY
UNIVERSITY OF HAWAI'I AT MĀNOA
SOEST Publication no. 9258

Acknowledgments

Many people participated in the WHOTS mooring deployment/recovery cruises. They are listed in Tables 2.1 and 2.4. We gratefully acknowledge their contributions and support. Thanks are due to all the personnel of the Upper Ocean Processes Group (UOP) at WHOI who prepared the WHOTS buoy's instrumentation and mooring; to Alison Andrews, Jennifer George, Ethan Roth, David Hashisaka, Branden Nakahara, and Nicholas Seymour for their technical assistance with the moored and shipboard instrumentation; to Kellie Terada for her excellent project support, and to Joseph Gum for his shore-based support. We gratefully acknowledge the support from the colleagues at Sea-Bird for helping us maintain the quality of the CTD data. We would also like to thank the captains and crew of the Ship *Hi'ialakai* and especially the University of Hawaii (UH) Marine Center staff for their efforts. The WHOTS Ocean Reference Station mooring is funded by the National Oceanic and Atmospheric Administration (NOAA) through the Cooperative Institute for Climate and Ocean Research (CICOR) under Grant No. NA09OAR4320129 to the Woods Hole Oceanographic Institution. Support for preparation and processing of subsurface instrumentation at WHOI is via a subcontract from the UH NSF project (OCE-0926766).

Table of Contents

1. Introduction 1
2. Description of the WHOTS-9 Mooring Cruises 3
   A. WHOTS-9 Cruise: WHOTS-9 Mooring Deployment 3
   B. WHOTS-10 Cruise: WHOTS-9 Mooring Recovery 5
3. Description of WHOTS-9 Mooring 7
4. WHOTS-9 and -10 cruise shipboard observations 11
   A. Conductivity, Temperature and Depth (CTD) profiling 11
      1. Data acquisition and processing 12
      2. CTD sensor calibration and corrections 12
         Pressure 12
         Temperature 13
         Conductivity 16
         Dissolved Oxygen 18
   B. Water sampling and analysis 19
   C. Thermosalinograph data acquisition and processing 20
      1. WHOTS-9 Cruise 20
      2. WHOTS-10 Cruise 20
         Temperature Calibration 20
         Nominal Conductivity Calibration 21
         Data Processing 21
         Bottle Salinity and CTD Salinity Comparisons 21
         CTD Temperature Comparisons 22
   D. Shipboard ADCP 22
      1. WHOTS-9 Deployment Cruise 22
      2. WHOTS-10 Deployment Cruise 23
5. Moored Instrument Observations 24
   A. MicroCAT/SeaCAT data processing procedures 24
      1. Internal Clock Check and Missing Samples 25
      2. Pressure Drift Correction and Pressure Variability 25
      3. Temperature Sensor Stability 27
         Comparisons with VMCM and ADCP temperature sensors 29
      4. Conductivity Calibration 34
   B. Acoustic Doppler Current Profiler 46
      1. Compass Calibrations 46
      2. ADCP Configurations 49
      3. ADCP data processing procedures 50
   C. Vector Measuring Current Meter (VMCM) 61
   D. Global Positioning System Receiver and ARGOS Positions 67
   E. MAVS Acoustic Velocity Sensor 70
6. Results 73
   A. CTD Profiling Data 74
   B. Thermosalinograph data 85
   C. MicroCAT/SeaCAT data 87
   D. Moored ADCP data 102
   E. Moored and Shipboard ADCP comparisons 111

F. Next Generation Vector Measuring Current Meter data (VMCM) 133
G. GPS data..... 134
H. Mooring Motion..... 135
7. References..... 137
8. Appendices..... 139
A. Appendix 1: WHOTS-9 300 kHz ADCP Configuration 139
B. Appendix 2: WHOTS-9 600 kHz ADCP Configuration 140
C. Appendix 3: WHOTS-9 VMCM report..... 141

1. Introduction

In 2003, Robert Weller (Woods Hole Oceanographic Institution [WHOI]), Albert Plueddemann (WHOI) and Roger Lukas (University of Hawaii [UH]) proposed to establish a long-term surface mooring at the Hawaii Ocean Time-series (HOT) Station ALOHA (22°45'N, 158°W) to provide sustained, high-quality air-sea fluxes and the associated upper ocean response as a coordinated part of the HOT program, and as an element of the global array of ocean reference stations supported by the National Oceanic and Atmospheric Administration's (NOAA) Office of Climate Observation.

With support from NOAA and the National Science Foundation (NSF), the WHOI HOT Site (WHOTS) surface mooring has been maintained at Station ALOHA since August 2004. The objective of this project is to provide long-term, high-quality air-sea fluxes as a coordinated part of the HOT program and contribute to the goals of observing heat, fresh water and chemical fluxes at a site representative of the oligotrophic North Pacific Ocean. The approach is to maintain a surface mooring outfitted for meteorological and oceanographic measurements at a site near Station ALOHA by successive mooring turnarounds. These observations are being used to investigate air-sea interaction processes related to climate variability and change.

The original mooring system is described in the mooring deployment/recovery cruise reports (Plueddemann et al., 2006; Whelan et al., 2007). Briefly, a Surlyn foam surface buoy is equipped with meteorological instrumentation including two complete Air-Sea Interaction Meteorological (ASIMET) systems (Hosom et al. (1995), Colbo and Weller (2009)), measuring air and sea surface temperatures, relative humidity, barometric pressure, wind speed and direction, incoming shortwave and longwave radiation, and precipitation. Complete surface meteorological measurements are recorded every minute, as required to compute air-sea fluxes of heat, freshwater and momentum. Each ASIMET system also transmits hourly averages of the surface meteorological variables via the Argos satellite system and via iridium. The mooring line is instrumented in order to collect time series of upper ocean temperatures, salinities and velocities with the surface forcing record. This includes vector measuring current meters, conductivity, salinity and temperature recorders, and two Acoustic Doppler current profilers (ADCPs). See the WHOTS-9 mooring diagram in Figure 1-1.

The subsurface instrumentation is located vertically to resolve the temporal variations of shear and stratification in the upper pycnocline to support study of mixed layer entrainment. Experience with moored profiler measurements near Hawaii suggests that Richardson number estimates over 10 m scales are adequate. Salinity is clearly important to the stratification, as salt-stratified barrier layers are observed at HOT and in the region (Kara et al., 2000), so we use Sea-Bird MicroCATs with vertical separation ranging from 5-20 m to measure temperature and salinity. We use an RDI ADCP to obtain current profiles across the entrainment zone and another in the mixed layer. Both ADCPs are in an upward-looking configuration, one is at 126 m, using 4 m bins, and the other is a 47.5 m using 2 m bins. To provide near-surface velocity (where the ADCP estimates are less reliable) we deploy two Vector Measuring Current Meters (VMCMs).

The nominal mooring design is a balance between resolving extremes versus typical annual cycling of the mixed layer (see WHOTS Data Report 1-2, Santiago-Mandujano et al., 2007).

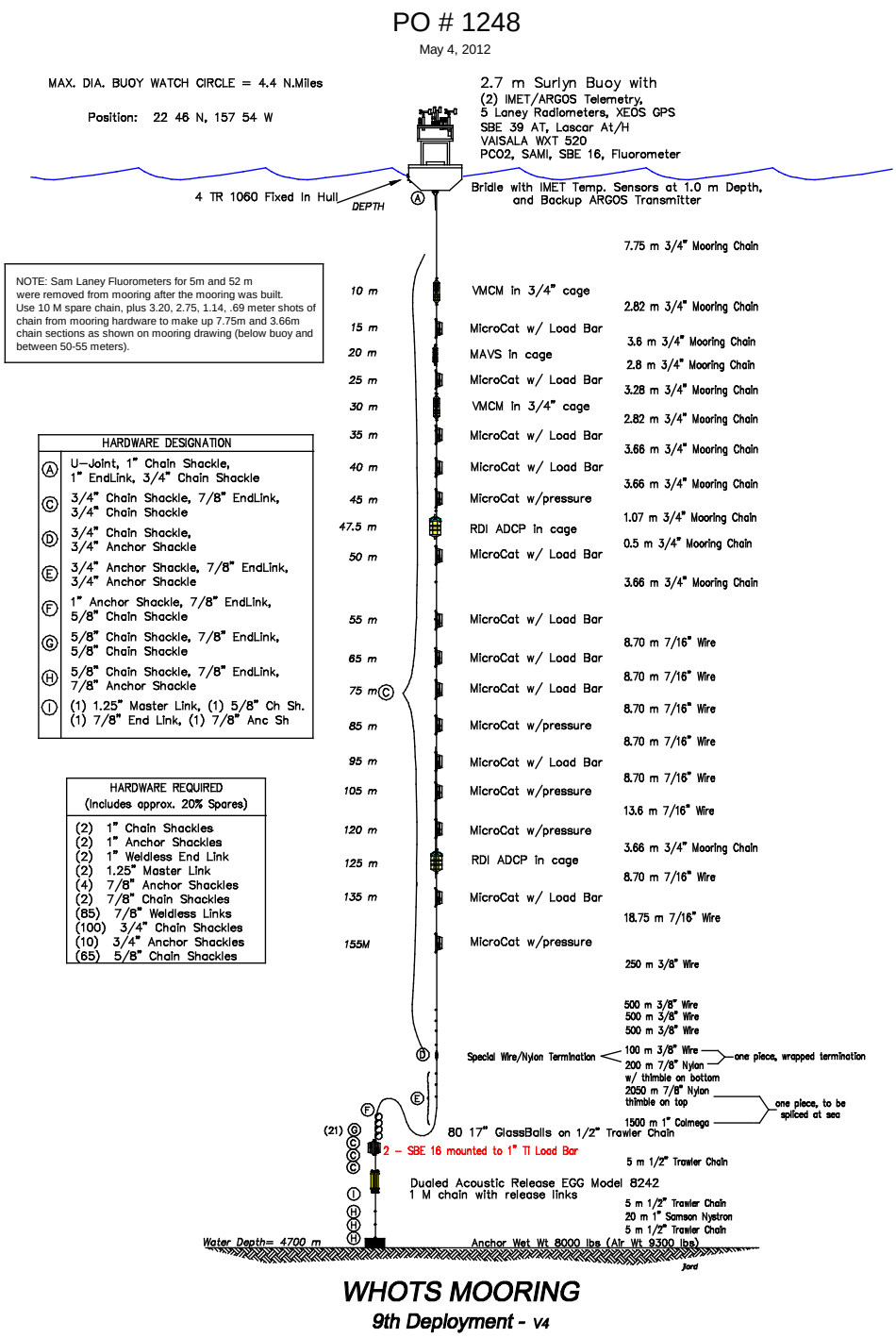

Figure 1-1. WHOTS-9 mooring design.

The ninth WHOTS mooring (WHOTS-9 mooring) was deployed in June 2012 during a 7-day cruise (WHOTS-9 cruise), and it was recovered in July 2013 during an 8-day cruise (WHOTS-10 cruise); both cruises aboard the NOAA Ship *Hi'ialakai*. A tenth mooring (WHOTS-10 mooring) was deployed during the WHOTS-10 cruise; to be recovered in July 2014.

This report documents and describes the oceanographic observations made on the ninth WHOTS mooring during a period of nearly one year, and from shipboard during the two cruises when the mooring was deployed and recovered. Sections 2 and 3, respectively, include a detailed description of the cruises and the mooring. Sampling and processing procedures of the hydrographic casts, thermosalinograph, and shipboard ADCP data collected during cruises are in Section 4. Section 5 includes the processing procedures for the data collected by the moored instruments: SeaCATs, MicroCATs, VMCMs, and moored ADCP. Plots of the resulting data and a preliminary analysis are included in Section 6.

2. Description of the WHOTS-9 Mooring Cruises

A. WHOTS-9 Cruise: WHOTS-9 Mooring Deployment

The Woods Hole Oceanographic Institution Upper Ocean Processes Group (WHOI/UOP), with the assistance of the UH group conducted the ninth deployment of the WHOTS mooring on board the NOAA Ship *Hi'ialakai* during the WHOTS-9 cruise between 12 and 19 June 2012. The WHOTS-9 mooring was deployed at HOT Station 50 on 14 June 2012 at 02:22 UTC at 22° 46.071'N, 157° 53.956'W. The scientific personnel that participated during the cruise are listed in Table 2-1.

Table 2-1. Scientific personnel on Ship Hi'ialakai during the WHOTS-9 deployment cruise.

Cruise	**Name**	**Title or function**	**Affiliation**
WHOTS-9	Plueddemann, Albert	Chief Scientist	WHOI
	Ryder, James	Scientist	WHOI
	Pietro, Ben	Engineering Assistant	WHOI
	Smith, Jason	Senior Engineering Assistant	WHOI
	Duncombe Rae, Chris	Scientist	WHOI
	Lukas, Roger	Professor/Co-PI	UH
	Nosse, Craig	Marine Research Associate	UH
	Snyder, Jefrey	Marine Electronics Technician	UH
	Fumar, Cameron	Research Associate	UH
	Andrews, Alison	Marine Technician	UH
	Hashisaka, David	Marine Research Associate	UH
	Roth, Ethan	Marine Research Engineer	UH
	Seymour, Nicholas	Marine Technician	UH
	Barteau, Ludovic	Scientist	CIRES

Cruise	Name	Title or function	Affiliation
	Park, Sang-Jong	Scientist	KOPRI

The shipboard oceanographic observations during the cruise were conducted by the UH group.

A Sea-Bird CTD (conductivity, temperature and depth) system was used to measure T, S, and O_2 profiles during ten CTD casts. The time, location, and maximum CTD pressure for each of the profiles are listed in Table 2-2. One cast was conducted to 1020 dbar at a test site near Oahu. Four CTD casts were conducted at HOT Station 52 near the WHOTS-8 mooring for comparison with subsurface instruments before its recovery; each cast was to 500 dbar. Five CTD casts were made at Station 50 near the WHOTS-9 mooring for comparison with subsurface instruments after the WHOTS-9 mooring deployment; each cast was to 500 dbar. These casts were sited approximately 200 to 500 m from the buoys and consisted of 4 yo-yo cycles between 10 dbar and 200 dbar and then to 500 dbar (5th yo-yo cycle of each cast). Four salinity samples were taken from each 500 dbar cast to calibrate the conductivity sensors used for the CTD profiling.

Table 2-2. CTD stations occupied during the WHOTS-9 deployment cruise

Station	Date	Time (GMT)	Location	Maximum pressure (dbar)
Test	6/13/12	06:03	21° 28.06' N, 158° 21.13' W	1024
50/1	6/14/12	15:49	22° 47.78' N, 157° 54.04' W	502
50/2	6/14/12	19:47	22° 47.66' N, 157° 53.81' W	502
50/3	6/14/12	23:52	22° 47.66' N, 157° 53.72' W	500
50/4	6/15/12	03:50	22° 47.66' N, 157° 53.66' W	502
50/5	6/15/12	07:50	22° 47.66' N, 157° 53.50' W	516
52/1	6/16/12	03:51	22° 41.96' N, 157° 56.38' W	502
52/2	6/16/12	07:51	22° 41.66' N, 157° 56.65' W	502
52/3	6/16/12	11:50	22° 41.75' N, 157° 56.79' W	502
52/4	6/16/12	15:51	22° 41.92' N, 157° 56.74' W	502

In addition, continuous acoustic Doppler current profiler (ADCP) and near surface thermosalinograph data were obtained while underway.

The Ship *Hi'ialakai* was equipped with an RD Instruments Ocean Surveyor 75 kHz ADCP, set to function in broadband and narrowband configurations. Broadband data was unavailable for this cruise. The configuration information is shown in Table 2-3. The ADCP used input from a S.G. Brown gyrometer and a Furuno GP 90 GPS receiver to establish the heading and attitude of the ship while an Applanix POSMV4 system archived attitude data for use in post-processing.

A complete description of these operations is available in the WHOTS-9 cruise report (Plueddemann *et al.*, 2013).

Table 2-3. Configuration of the Ocean Surveyor 75kHz ADCP on board the Ship Hi'ialakai during the WHOTS-9 deployment cruise. Only narrow band data were available during the cruise (see text).

	OS75NB
Sample interval (s)	900
Number of bins	60
Bin Length (m)	16
Pulse Length (m)	16
Transducer depth (m)	5
Blanking length (m)	24

Near-surface temperature and salinity data for WHOTS-9 cruise were acquired through a thermosalinograph (TSG) system aboard Ship *Hi'ialakai.* The system was comprised of a Sea-Bird model SBE-21 measuring temperature and conductivity from the ship's flow through system. These instruments were set to record data every 60 seconds. Ship *Hi'ialakai* has a thermosalinograph intake depth of 2 m at the bow of the ship, next to the bow thruster. The data were acquired continuously during the WHOTS-9 deployment cruise, with salt calibration samples taken roughly three times per day from an outlet in the flow through system located less than 0.5 m from the TSG.

B. WHOTS-10 Cruise: WHOTS-9 Mooring Recovery

The WHOI/UOP Group conducted the mooring turnaround operations during the WHOTS-10 cruise between 9 and 16 July 2013. The WHOTS-10 mooring was deployed at Station 52 on 11 July 2013 at 04:26 UTC at 22° 40.12'N, 157° 57.01'W.

The scientific personnel that participated during the cruise are listed in Table 2-4.

Table 2-4. Scientific personnel on Ship Hi'ialakai during the WHOTS-10 cruise (WHOTS-9 mooring recovery).

Cruise	**Name**	**Title or function**	**Affiliation**
WHOTS-10	Plueddeman, Albert	Chief Scientist	WHOI
	Lukas, Roger	Professor/PI	UH
	Whelan, Sean	Senior Engineering Assistant	WHOI
	Pietro, Ben	Engineering Assistant	WHOI
	Snyder, Jefrey	Marine Electronic's Technician	UH
	Fumar, Cameron	Research Associate	UH
	McCoy, Daniel	Research Associate	UH

Cruise	Name	Title or function	Affiliation
	Roth, Ethan	Marine Research Engineer	UH
	George, Jennifer	Marine Research Technician	UH
	Nakahara, Branden	Marine Research Technician	UH
	Wolfe, Dan	Scientist	NOAA/CIRES

The shipboard oceanographic observations during the cruise were conducted by the UH group. A complete description of these operations is available in the WHOTS-10 cruise report (Plueddemann *et al*., 2014).

A Sea-Bird CTD system was used to measure T, S, and O_2 profiles during ten CTD casts. The time, location, and maximum CTD pressure for each of the profiles are listed in Table 2-5. One cast was conducted at a test site near Oahu to 1020 dbar. Five CTD casts were conducted at station 50 near the WHOTS-9 mooring for comparison with subsurface instruments before its recovery; each cast was to 500 dbar. Five CTD casts were made at station 52 near the WHOTS-10 mooring for comparison with subsurface instruments after the WHOTS-10 mooring deployment; each cast was to 500 dbar. Four salinity samples were taken from each 500 dbar cast to calibrate the conductivity sensors used for the CTD profiling.

Table 2-5. CTD stations occupied during the WHOTS-10 cruise (WHOTS-9 mooring recovery).

Station	Date	Time (GMT)	Location	Maximum pressure (dbar)
TEST	7/10/13	01:03	21° 28.49´ N, 158° 20.97´ W	1026
52 / 1	7/11/13	16:11	22° 40.88´ N, 157° 58.70´ W	518
52 / 2	7/11/13	19:56	22° 41.04´ N, 157° 58.67´ W	502
52 / 3	7/11/13	23:55	22° 41.12´ N, 157° 58.75´ W	506
52 / 4	7/12/13	04:05	22° 41.24´ N, 157° 58.55´ W	506
52 / 5	7/12/13	07:59	22° 41.03´ N, 157° 58.35´ W	506
50 / 1	7/13/13	15:58	22° 47.43´ N, 157° 54.09´ W	502
50 / 2	7/13/13	20:02	22° 47.63´ N, 157° 54.38´ W	504
50 / 3	7/13/13	23:58	22° 47.79´ N, 157° 53.69´ W	504
50 / 4	7/14/13	04:02	22° 47.79´ N, 157° 53.50´ W	504
50 / 5	7/14/13	07:51	22° 47.84´ N, 157° 53.60´ W	504

In addition, continuous acoustic Doppler current profiler (ADCP) and near surface thermosalinograph data were obtained while underway.

The Ship *Hi'ialakai* was equipped with an RD Instruments Ocean Surveyor 75 kHz ADCP, set to function in broadband and narrowband configurations. Configurations for each system are shown in Table 2-6. The ADCP used input from a S.G. Brown gyrometer and a Furuno GP 90 GPS receiver to establish the heading and attitude of the ship while an Applanix POSMV4 system archived attitude data for use in post-processing.

Table 2-6. Configuration of the Ocean Surveyor 75kHz ADCP on board the Ship Hi'ialakai during the WHOTS-10 cruise.

	OS75BB	OS75NB
Sample interval (s)	900	900
Number of bins	80	60
Bin Length (m)	8	16
Pulse Length (m)	8	16
Transducer depth (m)	5	5
Blanking length (m)	16	24

Near-surface temperature and salinity data during the WHOTS-10 cruise were acquired through the use of a thermosalinograph (TSG) system aboard Ship *Hi'ialakai.* The system was comprised of a Sea-Bird model SBE-21 thermosalinograph with internal temperature and conductivity sensors sampling water from the ship's flow through system, and an SBE-38 external temperature sensor located near the intake. These instruments were set to record data every 60 seconds. Ship *Hi'ialakai* has a thermosalinograph intake depth of 2 m. The data were acquired continuously during the WHOTS-10 deployment cruise, with salt calibration samples taken roughly three times per day from an outlet in the flow through system located less than 0.5 m from the TSG.

3. Description of WHOTS-9 Mooring

The WHOTS-9 mooring, deployed on 14 June 2012 from NOAA's Ship *Hi'ialakai*, was outfitted with two complete sets (L09 and L10) of ASIMET sensors on the buoy and underneath, and subsurface instruments from 10 to 155 m depth (Figure 1-1). The WHOTS-9 recovery on 14 July 2013 resulted in 395 days on station.

The buoy tower also contains a radar reflector, two marine lanterns, and two independent Argos satellite transmission systems that provide continuous monitoring of buoy position. A Xeos Melo Global Positioning System (GPS) receiver, a SBE-39 temperature sensor adapted to measure air temperature and a Vaisala WXT-520 multi-variable (temperature, humidity, pressure, wind and precipitation) were also mounted on the tower. A fourth positioning system (SiS Argos transmitter) was mounted beneath the hull. Several other instruments were mounted on the buoy. A pCO_2 system, a pumped SBE-16 CTD and a SAMI-2 pH sensor were mounted to the underside of the buoy. The SHB-16 hosted turbidity and dissolved oxygen sensors. Five radiometers and a chlorophyll fluorometer were also mounted in one of the buoy access tubes.

Four internally-logging RBR TR-1060 temperature sensors and two SBE-37 MicroCATs were bolted to the underside of the buoy hull measuring sea surface temperature (SST) and salinity. The RBRs measured SST once every 60 sec between 80-95 cm below the surface, and the MicroCATs were at 1.55 m.

Instrumentation provided by UH for the WHOTS-9 mooring included 15 SBE-37 Microcats, an RDI 300 kHz Workhorse ADCP, an RDI 600 kHz Workhorse ADCP, and a Nobska MAVS acoustic velocity sensor. The Microcats all measured temperature and conductivity, with 6 also measuring pressure. WHOI provided two Vector Measuring Current Meters (VMCMs), and two Seacats (SBE-16) installed near the bottom of the mooring.

Table 3-1 provides a listing of the WHOTS-9 subsurface instrumentation at their nominal depths on the mooring, along with serial numbers, sampling rates and other pertinent information. Also included in the table are the four RBR TR-1060 and two MicroCATs from WHOI bolted to the underside of the buoy hull. A cold water spike was induced to the UH Microcats before deployment and after recovery by placing an ice pack in contact with their temperature sensor to check for any drift in their internal clock.

The RDI 300 kHz Workhorse Sentinel ADCP, SN 7637, with an additional external battery pack, was deployed at 125 m with transducers facing upwards. The instrument was set to ping at 4-second intervals for 160 seconds every 10 minutes. This burst sampling was designed to minimize aliasing by occasional large ocean swell orbital motions. Bin size was set for 4 m. The total number of ensemble records was 58,165. The first ensemble was at 6/07/2012 00:00:00Z, and the last was at 7/15/2013 21:50:00Z. This instrument also measured temperature.

The RDI 600 kHz Workhorse Sentinel ADCP, SN 13917, with an additional external battery pack, was deployed at 47.5 m with transducers facing upwards. The instrument was set to ping at 2-second intervals for 160 seconds every 10 minutes. This burst sampling was designed to minimize aliasing by occasional large ocean swell orbital motions. Bin size was set for 2 m. The total number of ensemble records was 58,154. The first ensemble was at 6/07/2012 00:00:00, and the last was at 7/15/2013 19:59:59. This instrument also measured temperature.

The two VMCMs, SN 011 and 061 were deployed at 10 m and 30 m depth respectively. The instruments were prepared for deployment by the WHOI/UOP group and set to sample at 1-minute intervals. These instruments also measured temperature.

A Nobska MAVS SN 10261 acoustic velocity sensor was deployed a 20 m in a downward orientation. The instrument was set to ping at 2-second intervals for 160 seconds every 30 minutes. This burst sampling was designed to minimize aliasing by occasional large ocean swell orbital motions. The deployment of the MAVS was largely unsuccessful, as 3 of the instrument's 4 transducers failed less than 4 months into the deployment.

Table 3-1. WHOTS-9 mooring subsurface instrument deployment information. All times are in UTC. The RBR instruments indicate their location on the buoy in degrees clockwise from the vane.

SN:	Instrument	Depth	Pressure SN	Sample Interval (sec)	Start Logging Data(UTC)		Cold Spike In (UTC)		Cold Spike Out (UTC)		Time in Water (UTC)	
14977	RBR, 120 deg	0.8	N/A	60	6/4/2012	1:00:00	N/A		N/A		6/13/2012	19:30
14878	RBR, 180 deg	0.8	N/A	60	6/4/2012	1:00:00	N/A		N/A		6/13/2012	19:30
14978	RBR, 180 deg	0.95	N/A	60	6/4/2012	1:00:00	N/A		N/A		6/13/2012	19:30
14882	RBR, 240 deg	0.8	N/A	60	6/4/2012	1:00:00	N/A		N/A		6/13/2012	19:30
1306	Microcat	1.55	N/A	60	6/9/2012	0:18:00	N/A		N/A		6/13/2012	19:30
1419	Microcat	1.55	N/A	300	6/7/2012	0:39:00	N/A		N/A		6/13/2012	19:30
11	VMCM	10	N/A	60	6/14/2012	4:00:00	N/A		N/A		6/13/2012	18:32
3382	Microcat	15	N/A	180	06/07/12	0:00:00	06/08/12	1:06:00	06/08/12	1:30:00	06/13/12	18:31
10261	MAVS	20	N/A	1800	06/07/12	0:00:00	N/A		N/A		06/13/12	18:26
4663	Microcat	25	N/A	180	06/07/12	0:00:00	06/08/12	1:06:00	06/08/12	1:30:00	06/13/12	18:23
61	VMCM	30	N/A	60	6/14/2012	4:00:00	N/A		N/A		6/13/2012	18:18
3633	Microcat	35	N/A	180	06/07/12	0:00:00	06/08/12	1:06:00	06/08/12	1:30:00	06/13/12	18:14
3381	Microcat	40	N/A	180	06/07/12	0:00:00	06/08/12	1:06:00	06/08/12	1:30:00	06/13/12	18:08
3668	Microcat	45	5579	240	06/07/12	0:00:00	06/08/12	1:06:00	06/08/12	1:30:00	06/13/12	18:03
13917	600 kHz ADCP	47.5	N/A	600	06/07/12	0:00:00	N/A		N/A		06/13/12	19:49
3619	Microcat	50	N/A	180	06/07/12	0:00:00	06/08/12	1:06:00	06/08/12	1:30:00	06/13/12	19:49
3620	Microcat	55	N/A	180	06/07/12	0:00:00	06/08/12	1:06:00	06/08/12	1:30:00	06/13/12	19:52
3621	Microcat	65	N/A	180	06/07/12	0:00:00	06/08/12	1:06:00	06/08/12	1:30:00	06/13/12	19:57
3632	Microcat	75	N/A	180	06/07/12	0:00:00	06/08/12	1:06:00	06/08/12	1:30:00	06/13/12	20:00
4699	Microcat	85	10209	240	06/07/12	0:00:00	06/08/12	1:06:00	06/08/12	1:30:00	06/13/12	20:03
3791	Microcat	95	N/A	180	06/07/12	0:00:00	06/08/12	1:06:00	06/08/12	1:30:00	06/13/12	20:06
2769	Microcat	105	2949	240	06/07/12	0:00:00	06/08/12	1:06:00	06/08/12	1:30:00	06/13/12	20:13
4700	Microcat	120	9944	240	06/07/12	0:00:00	06/08/12	1:06:00	06/08/12	1:30:00	06/13/12	20:15
7637	300 kHz ADCP	125	N/A	600	06/07/12	0:00:00	N/A		N/A		06/13/12	20:19
3669	Microcat	135	5700	240	06/07/12	0:00:00	06/08/12	1:06:00	06/08/12	1:30:00	06/13/12	20:23
4701	Microcat	155	10211	240	06/07/12	0:00:00	06/08/12	1:06:00	06/08/12	1:30:00	06/13/12	20:34
1880	Seacat	4631	N/A	1800	6/4/2012	1:00:00	N/A		N/A		6/14/2012	2:00
1881	Seacat	4631	N/A	1800	6/4/2012	1:00:00	N/A		N/A		6/14/2012	2:00

All WHOTS-9 instruments were successfully recovered; recovery information for the C-T instruments is shown in Table 3-2. The MicroCATs at 25 m (SN 4663), 45 m (SN 3668), and 50 m (SN 3619) did not have their conductivity cell guard upon recovery. There was no apparent damage to any of the conductivity cells of these instruments. We question whether the guards came off due to mooring vibrations which could have loosened screws that were not tight enough. All instruments except for the RBRs and the MicroCAT SN 1306 at 1.55 m returned full data records. SN 1306 stopped recording on June 6, 2013, and its data had to be retrieved from the ASIMET L09 data logger. Table 3-2 has an initial evaluation of the data quality; more details are in Section 5A.

Table 3-2. WHOTS-9 RBR, MicroCAT Recovery Information. All times stated are in UTC.

Depth (m)	Sea-Bird Serial #	Time out of water	Time of Spike	Time Logging Stopped	Samples Logged	Data Quality
0.8	RBR 14977	07/15/2013 03:13	N/A	06/21/2012 12:41	110,142	Good
0.8	RBR 14878	07/15/2013 03:13	N/A	09/26/2012 8:58	249,599	Good
0.95	RBR 14978	07/15/2013 03:13	N/A	12/7/2012 9:20	353,301	Good
0.8	RBR 14882	07/15/2013 03:13	N/A	09/27/2012 23:1	251,882	Good
1.55	SBE 1306	07/15/2013 03:13	N/A	06/6/2013 02:13	104,856	Good
1.55	SBE 1419	07/15/2013 03:13	N/A	07/15/2013 20:49	116,307	Good
15	SBE-37SM31486 - 3382	07/15/2013 03:30	07/15/2013 5:30:15	07/15/2013 16:36:00	193,772	Good
25	SBE-37SM42760 - 4663	07/15/2013 03:37	07/15/2013 5:30:15	07/15/2013 07:08:00	193,582	Good Recovered without cell guard
35	SBE-37SM36805 - 3633	07/15/2013 03:43	07/15/2013 5:30:15	07/15/2013 16:28:30	193,769	Good
40	SBE-37SM31486 - 3381	07/15/2013 03:46	07/15/2013 5:30:15	07/15/2013 16:46:00	193,775	Good
45	SBE-37SM36805 - 3668	07/15/2013 03:47	07/15/2013 5:30:15	07/15/2013 07:44:00	145,196	Good Recovered without cell guard
50	SBE-37SM36805 - 3619	07/15/2013 02:02	07/15/2013 5:30:15	07/15/2013 16:31:00	193,770	Questionable conductivity after 3/2013. Recovered without cell guard
55	SBE-37SM36805 - 3620	07/15/2013 01:59	07/15/2013 5:30:15	07/15/2013 07:03:30	193,581	Good
65	SBE-37SM36805 - 3621	07/15/2013 01:56	07/15/2013 5:30:15	07/15/2013 07:41:00	193,594	Good
75	SBE-37SM36805 - 3632	07/15/2013 01:52	07/15/2013 5:30:15	07/15/2013 16:33:00	193,771	Good
85	SBE-37SM42760 - 4699	07/15/2013 01:47	07/15/2013 5:30:15	07/15/2013 07:47:00	145,197	Good
95	SBE-37SM36805 - 3791	07/15/2013 01:43	07/15/2013 5:30:15	07/15/2013 16:59:30	193,779	Good
105	SBE-37SM31486 - 2769	07/15/2013 01:37	07/15/2013 5:30:15	07/15/2013 16:51:00	145,333	Good
120	SBE-37SM47260 - 4700	07/15/2013 01:28	07/15/2013 5:30:15	07/15/2013 07:17:00	145,189	1 dbar drift in pressure
135	SBE-37SM36805 - 3669	07/15/2013 01:20	07/15/2013 5:30:15	07/15/2013 07:13:00	145,188	Questionable pressure after 7/2013
155	SBE-37SM42760 - 4701	07/15/2013 01:13	07/15/2013 5:30:15	07/15/2013 07:35:00	145,194	Good
4631	SBE-16 - 1880	07/14/2013 18:41	NA	07/15/2013 19:00	19,525	Conductivity drift and an offset near the end of the record
4631	SBE-16 - 1881	07/14/2013 18:41	NA	07/15/2013 19:00	19,525	Good

The data from the upward-looking 300 kHz ADCP at 125 m was good; the instrument was pinging upon recovery. There appears to be no obviously questionable data from this ADCP apart from near-surface artifacts.

The data from the upward-looking 600 kHz ADCP at 47.5 m was good; the instrument was pinging upon recovery. There appears to be no initial questionable data from this ADCP apart from near-surface artifacts.

4. WHOTS-9 and -10 cruise shipboard observations

The hydrographic profile observations made during the WHOTS cruises were obtained with a Sea-Bird CTD package with dual temperature, salinity and oxygen sensors. This CTD was installed on a rosette-sampler with 5 L Niskin bottles for calibration water samples. In addition, the Ship *Hi'ialakai* came equipped with a thermosalinograph system which provided a continuous depiction of temperature and salinity of the near-surface layer. Horizontal currents over the depth range of 30-1000 m were measured from the shipboard 75 kHz Ocean Surveyor (OS75) ADCP (narrowband) with a vertical resolution of 16m for the WHOTS-9 cruise. Broadband mode for the OS75 was available in addition for WHOTS-10 cruise, providing additional current data over the range of 20-650 m with a vertical resolution of 8m.

A. Conductivity, Temperature and Depth (CTD) profiling

Continuous measurements of temperature, conductivity, dissolved oxygen and pressure were made with the UH Sea-Bird SBE-9/11Plus CTD underwater unit #09P43777-0850 (referred to as #0850) during the WHOTS-9 and WHOTS-10 cruises. The CTD was equipped with an internal Digiquartz pressure sensor and pairs of external temperature, conductivity, and oxygen sensors.

Each of the temperature-conductivity sensor pairs used a Sea-Bird TC duct which circulated seawater through independent pump and plumbing installations. The CTD configuration also included two oxygen sensors, installed in the plumbing for each sensor set. In both cruises, the CTD was mounted in a vertical position in the lower part of a rosette sampler, with the sensors' water intakes located at the bottom of the 12-place rosette.

The package was deployed on a conducting cable, which allowed for real-time data acquisition and display. The deployment procedure consisted in lowering the package to 10-15 dbar and waiting until the CTD pumps started operating. The CTD was then raised until the sensors were close to the surface to begin the CTD cast. The time and position of each cast was obtained via a GPS connection to the CTD deck box. Six Niskin bottles were used on the rosette. Four salinity samples were taken on each cast for calibration of the conductivity sensors.

1. Data acquisition and processing.

CTD data were acquired at the instrument's highest sampling rate of 24 samples per second. Digital data were stored on a laptop computer and, for redundancy, the analog signal was recorded on VHS video tapes. Backups of CTD data were made onto USB storage cards.

The raw CTD data were quality controlled and screened for spikes as described in the WHOTS Data Report 1 (Santiago-Mandujano et al., 2007). Data alignment, averaging, correction and reporting were done as described in Tupas *et al*. (1993). Spikes in the data occur when the CTD samples the disturbed water of its wake. Therefore, samples from the downcast were rejected when the CTD was moving upward or when its acceleration exceeded 0.5 m s^{-2} in magnitude. The data were subsequently averaged into 2-dbar pressure bins after calibrating the CTD conductivity with the bottle salinities.

The data were additionally screened by comparing the T-C sensor pairs. These differences permitted identification of problems with the sensors. The data from only one T-C pair, whichever was deemed most reliable, is reported here. Only data from the downcast are reported, as upcast data are contaminated by rosette wake effects.

Temperature is reported in the ITS-90 scale. Salinity and all derived units were calculated using the UNESCO (1981) routines; salinity is reported in the practical salinity scale (PSS-78). Oxygen is reported in μmol kg^{-1}.

2. CTD sensor calibration and corrections

Pressure

The pressure calibration strategy for CTD pressure transducer SN 101430 used during WHOTS-9 and WHOTS-10 cruises employed a high-quality quartz pressure transducer as a transfer standard. Periodic recalibrations of this lab standard were performed with a primary pressure standard. The only corrections applied to the CTD pressures were a constant offset determined at the time that the CTD first enters the water on each cast. In addition, a span correction determined from bench tests on the sensor against the transfer standard was applied.

Transfer Standard Calibration

The transfer standard is a Paroscientific Model 760 pressure gauge equipped with a 10,000-PSI transducer. This instrument was purchased in March 1988, and was originally calibrated against a primary standard. Subsequent recalibrations have been performed every 2.5 years on average either at the Northwest Regional Calibration Center, at the Scripps Institute of Oceanography or at Fluke Electronics (DH Instruments Division). The latest calibrations were conducted at the Scripps Institute of Oceanography in April 1999, May 2001, May 2003, and July 2005; and at Fluke in July 2009 and November 2012.

CTD Pressure Transducer SN 51412 Bench Tests

CTD pressure transducer bench tests were done using an Ametek T-100 pump and a manifold to apply pressure simultaneously to the CTD pressure transducer and to the transfer standard. All these tests generated calibration data at six pressure levels between 0 and 4500 dbar, for both increasing and decreasing pressures. Pressure sensor SN 101430 was used during the WHOTS-9 and WHOTS-10 cruises. The results of the bench tests on this sensor are shown in Table 4-1. The 0-dbar offset is near zero and decreased slightly between 2012 and 2013, however, a more accurate offset was later determined for the time that the CTD first enters the water on each cast. The hysteresis from the bench tests has been small and showing a slight increase. A linear pressure dependent offset is applied during data collection to correct for the 0-4500 dbar span offset of about 1.24 dbar (Table 4-1), which had a small increase between 2012 and 2013.

Table 4-1. CTD pressure sensor #101430 calibrations against the transfer standard

Calibration Date	Offset @ 0 dbar	0-4500 dbar offset	Hysteresis
1 August 2013	-0.14	1.39	0.14
10 January 2013	-0.17	1.31	0.13
7 August 2012	-0.10	1.15	0.09
8 February 2012	0.00	1.19	0.06
12 August 2011	0.04	1.32	0.05
20 January 2011	0.15	1.20	0.10
12 August 2010	0.20	1.20	0.15
8 January 2010	0.20	1.30	0.16
9 September 2009	0.21	1.30	0.13
7 January 2009	0.28	1.10	0.10
26 August 2008	0.31	1.20	0.09
4 January 2008	0.27	1.10	0.12
24 July 2007	0.19	1.10	0.10
28 February 2007	0.05	1.00	0.08

Temperature

Three Sea-Bird SBE-3-Plus temperature transducers (#1416, #2454, and #5519) were used during WHOTS-9 and -10 cruises, and were calibrated at Sea-Bird before and after each cruise to an accuracy better than 0.5 x 10^{-3}°C. Sensor #5519 is a new sensor acquired in January 2012. Calibration coefficients obtained at Sea-Bird are listed in Table 4-2. These coefficients were used in the following formula that gives the temperature (in °C) as a function of the frequency signal (*f*):

$$Temperature = 1/\{a+b[ln(fo/f)]+c[ln^2(fo/f)+d[ln^3(fo/f]\}-273.15$$

For each sensor, we calculated the 0-30°C average offset for each calibration relative to the oldest one, and applied a linear fit to these offsets. A single baseline calibration was chosen and a temperature-independent offset relative to the baseline calibration was applied to the data to remove the temporal trend due to the sensor drift. The maximum drift correction for WHOTS cruises was less than 1.0 x 10^{-3}°C. The baseline calibration was selected as the one for which the trend-corrected average from 0-5°C was nearest to the ensemble mean of these averages.

Table 4-2. Calibration coefficients for Sea-Bird temperature sensors. RMS residuals from calibration give an indication of calibration quality.

SN	*Date yymmdd*	*f0*	*a*	*b*	*c*	*d*	*RMS (m°C)*
1416	130418	6233.46	3.68120966e-03	6.01717330e-04	1.46100832e-05	1.78997011e-06	0.28
1416	121221	6233.51	3.68120975e-03	6.01723831e-04	1.46108158e-05	1.78360634e-06	0.28
1416	120907	6233.47	3.68120979e-03	6.01715632e-04	1.46341513e-05	1.81681657e-06	0.28
1416	120512	6233.55	3.68121004e-03	6.01736349e-04	1.46939412e-05	1.86140829e-06	0.24
1416	120211	6233.55	3.68120995e-03	6.01726937e-04	1.46850658e-05	1.86458252e-06	0.28
1416	111208	6233.66	3.68120871e-03	6.01722327e-04	1.47288631e-05	1.91968969e-06	0.27
1416	110804	6233.73	3.68121041e-03	6.01714830e-04	1.46343735e-05	1.81119240e-06	0.25
1416	110331	6233.80	3.68120909e-03	6.01701993e-04	1.46000054e-05	1.77202876e-06	0.25
2454	120216	2885.37	3.68121225e-03	6.02188034e-04	1.67634669e-05	2.37714945e-06	0.02
2454	111208	2885.40	3.68121094e-03	6.02190055e-04	1.67787094e-05	2.39362837e-06	0.02
2454	110803	2885.43	3.68121237e-03	6.02181187e-04	1.67431280e-05	2.36267504e-06	0.02
2454	110331	2885.53	3.68121054e-03	6.02184632e-04	1.67414323e-05	2.35175902e-06	0.04
5519	131106	3004.26	3.68121451e-03	5.90896972e-04	1.51213894e-05	1.74135275e-06	0.07
5519	130806	3004.23	3.68121296e-03	5.90816769e-04	1.48852058e-05	1.53655316e-06	0.06
5519	130418	3004.28	3.68121296e-03	5.90834864e-04	1.48967247e-05	1.53354844e-06	0.06
5519	121222	3004.27	3.68121327e-03	5.90833374e-04	1.48869620e-05	1.52359138e-06	0.07
5519	120906	3004.24	3.68121318e-03	5.90826616e-04	1.49005183e-05	1.55385022e-06	0.06
5519	120512	3004.24	3.68121292e-03	5.90838747e-04	1.49380321e-05	1.58313788e-06	0.05

A small residual pressure effect on the temperature sensors documented in Tupas et al. (1997) has been removed from measurements obtained with our sensors. Another correction to our temperature measurements was for the viscous heating of the sensor tip due to the water flow past it (Larson and Pederson, 1996). This correction is thoroughly documented in Tupas et al. (1997).

Dual sensors were used during all casts of the WHOTS-9 and -10 cruises. Sensors #1416 and #2454 were used during WHOTS-9; and sensors #1416 and #5519 were used during WHOTS-10. The temperature differences between sensor pairs were calculated for each cast to evaluate the quality of the data, and to identify possible problems with the sensors. All sensors performed correctly during the cruises, showing temperature differences within expected values. The mean temperature difference in the water column was typically less than 2 x 10^{-3} °C in the 1000 m casts, with a standard deviation of less than 0.5 x 10^{-3} °C below 500 dbar. The largest variability in temperature difference between sensor pairs was observed in the thermocline, where the standard deviation reached nearly 1 x 10^{-2} °C. These differences are not unexpected, since each sensor has independent water intakes it is possible that when the CTD passes through

this steep gradient region each sensor measures water from slightly different levels, yielding significant temperature differences.

Temperature sensor #1416

This sensor was used during the WHOTS-9 and -10 cruises. This sensor has maintained a stable drift for a long time. The calibrations from February 2009 through April 2013 (Table 4-2) yielded a sensor drift of 3.80 x 10^{-6} ºC day^{-1}, with an intercept of 5.7 x 10^{-4} ºC and a RMS residual of 3.9 x 10^{-4} ºC, which was used to obtain the drift correction for cruise WHOTS-9. When corrected for linear drift to 15 June 2012 (the mid-date of the cruise), the 12 May 2012 calibration gave the smallest deviation in the 0-5 ºC temperature range from the set of all calibrations (also corrected for linear drift to 15 June 2012). A drift correction was obtained using this calibration as a baseline. The resulting drift correction for the cruise was 0.13 m°C, and was applied to the data (Table 4-3).

The calibrations from February 2009 through November 2013 yielded a sensor drift of 3.84 x 10^{-6} ºC day^{-1}, with an intercept of -6.8 x 10^{-5} ºC and a RMS residual of 3.7 x 10^{-4} ºC, which was used to obtain the drift correction for cruise WHOTS-10. When corrected for linear drift to 12 July 2013 (the mid-date of the cruise), the 21 December 2012 calibration gave the smallest deviation in the 0-5 ºC temperature range from the set of all calibrations (also corrected for linear drift to 12 July 2013). A drift correction was obtained using this calibration as a baseline. The resulting drift correction for the cruise was 0.78 m°C, and was applied to the data (Table 4-3).

Temperature sensor #2454

This sensor was used during the WHOTS-9 cruise. The calibrations from September 2008 through April 2013 (Table 4.2) yielded a sensor drift of 4.85 x 10^{-6} ºC day^{-1} with an intercept of 2.4 x 10^{-5} ºC and a RMS residual of 5.2 x 10^{-4} ºC, and was used to obtain the drift correction for the cruise. When corrected for linear drift to 15 June 2012 (the mid-date when the sensor was used), the 21 December 2012 calibration gave the smallest deviation in the 0-5 ºC temperature range from the set of all calibrations (also corrected for linear drift to 15 June 2012). A drift correction was obtained using this calibration as a baseline. The resulting drift correction for the cruise was -0.92 m°C, and was applied to the data (Table 4-3).

Temperature sensor #5519

This sensor was also used during the WHOTS-10 cruise. The calibrations between February 2012 and November 2013 (Table 4.2) were used to calculate the sensor drift and the drift corrections. A linear fit to the 0-30°C average offset from each calibration relative to 17 February 2012 gave an intercept of 1.88 x 10^{-5} °C with a slope of -3.08 x 10^{-7} ºC day^{-1}. The RMS deviation of the offsets from this fit was 4.0 x 10^{-5} °C. The 6 September 2012 calibration showed a small deviation from the 0-5°C ensemble mean of all the calibrations (all corrected for linear drift to the cruise date, July 12, 2013) and was used as a baseline. A drift correction was obtained using this baseline calibration (Table 4-3). This correction was 0.10 x 10^{-3} °C and deemed insignificant.

Table 4-3. Temperature (T) and Conductivity (C) sensors used during the WHOTS cruises, including temperature drift correction and the thermal inertia parameter (alpha). Dual temperature and conductivity sensors were used during both cruises. The data reported here are from the sensors marked with (*).

Cruise	T-sensor #	T-correction (m°C)	C-sensor #	alpha
WHOTS-9	1416 (*)	0.13	3162 (*)	0.037
WHOTS-9	2454	-0.92	3984	0.020
WHOTS-10	1416 (*)	0.78	3162 (*)	0.037
WHOTS-10	5519	0.10	3984	0.020

Conductivity

Two Sea-Bird SBE 4C conductivity sensors (#3162, and #3984) were used during the WHOTS cruises. Sensor #3984 is a new sensor acquired in early 2012. Dual sensors were used during all the cruise casts. As mentioned earlier, only the data from the most reliable sensor (and its corresponding temperature sensor pair, as shown in Table 4-3) are reported here.

Sensor #3162 was calibrated at Sea-Bird in February 2012, and in April 2013; sensor #3984 was calibrated in January 2012, and in March 2013. The nominal conductivity calibrations were used for data acquisition. Final calibration was determined empirically from salinities of discrete water samples acquired during each cast. Prior to empirical calibration, conductivity was corrected for thermal inertia of the glass conductivity cell using the recursive filter given by Lueck (1990) and Lueck and Picklo (1990). Sensor parameters alpha and beta, which characterize the initial magnitude of the thermal effect and its relaxation time, are needed for this correction. As recommended by Lueck (personal communication, 1990), beta was set to 0.1 s^{-1}, but alpha was calculated for each sensor to close the spread between the down- and up-cast *T-S* curves (Table 4-3).

Salinity samples were collected at selected depths during each cast and measured with a salinometer (Sect. 4.B.1). The nominally calibrated CTD salinity trace was used to identify questionable samples. Salinity samples were later quality controlled and flagged by comparing them against the empirically calibrated CTD salinities.

Calibration of each conductivity sensor was performed empirically by comparing its nominally calibrated output against the calculated conductivity values obtained from the water sample salinities, using the pressure and temperature of the CTD at the time of bottle closure. An initial estimate of bias (*b0*) and slope (*b1*) corrections to the nominal calibration were determined from a linear least squares fit to the ensemble of CTD-bottle conductivity differences as a function of conductivity, from all casts during the sensor use. This calibration was then used to identify suspect water samples. These samples were deleted from the analysis, and the calibration was repeated. Conductivity calibration coefficients for the sensors used during WHOTS cruises are given in Table 4-4.

Table 4-4. CTD Conductivity calibration coefficients obtained from comparison against bottle salinities.

Cruise	Sensor #	b0	b1
WHOTS-9	3162	-0.000057	-0.000185
WHOTS-9	3984	0.000203	0.000163
WHOTS-10	3162	0.000328	-0.000124
WHOTS-10	3984	0.000882	-0.000205

The final step of the calibration was to perform a profile-dependent bias correction, to allow for a drift of the conductivity cell with time during each cruise, or for sudden offsets due to fouling. This offset was determined by taking the median value of CTD-bottle salinity differences for each profile. No offset corrections were necessary for any of the WHOTS cruises casts.

The quality of the conductivity calibration is illustrated by Figure 4-1, which shows the differences between the corrected CTD salinities and the bottle salinities as a function of pressure for the WHOTS-9 and -10 cruises. Table 4-5 gives the mean and standard deviations for the final calibrated CTD minus water sample salinities.

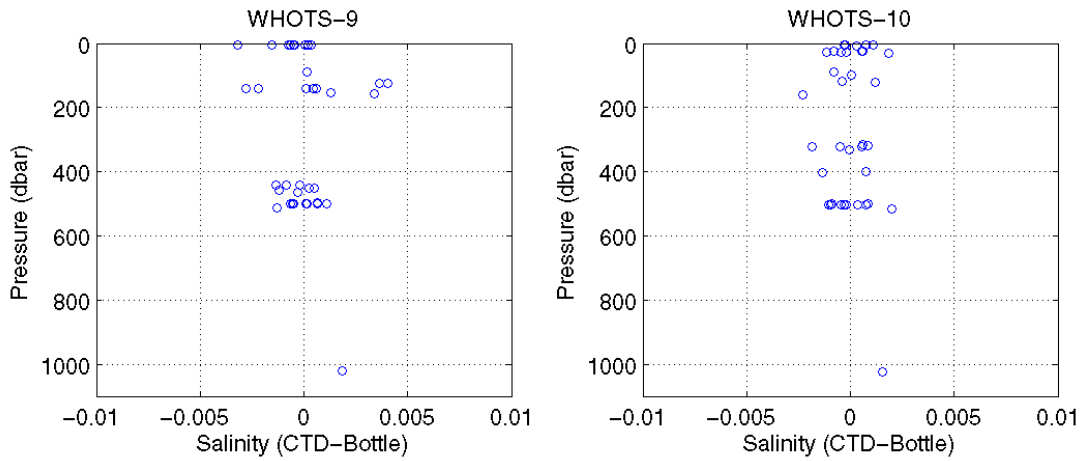

Figure 4-1. Difference between calibrated CTD salinities and bottle salinities for all the casts during WHOTS-9 and –10 deployment cruises.

Table 4-5. CTD-Bottle salinity comparison for each sensor.

		0 to 1200 dbar		500 to 1200 dbar	
Cruise	Sensor #	Mean	Standard Deviation	Mean	Standard Deviation
WHOTS-9	3162	0.0000	0.0015	0.0002	0.0012
WHOTS-9	3984	0.0000	0.0014	0.0001	0.0010
WHOTS-10	3162	0.0000	0.0010	0.0001	0.0010
WHOTS-10	3984	0.0000	0.0008	0.0001	0.0009

Salinity differences between sensor sets were calculated the same way as for the temperature in order to identify problems with any of the sensors. These differences show a behavior similar to the temperature differences in the thermocline region. Maximum absolute salinity differences of about 9 x 10^{-3} were observed at 100 dbar, decreasing to less than 2 x 10^{-3} below 200 dbar. This behavior is due to a combination of the residual temperature effect on the temperature sensors described in the previous section, and an additional residual temperature effect on the conductivity sensors (N. Larson personal communication, 1999). The temperature effect on the conductivity sensors is similar to that described for the temperature sensors, and affects the conductivity measurements when the sensor passes through intense temperature gradients.

The largest variability in the salinity difference between sensors was observed in the halocline, with standard deviations of up to 1 x 10^{-2} between 50 and 100 dbar.

Dissolved Oxygen

Three Sea-Bird SBE-43 oxygen sensors were used during the WHOTS-9 and 10 cruises: #431601, #43918, and #43262 (Table 4-6). Sensor #431601 was calibrated at Sea-Bird on 18 February 2012, and on 17 April 2013; sensor #43918 was calibrated on 11 November 2011, and sensor #43262 was calibrated on 25 May 2013. Oxygen data from the WHOTS-9 cruise were further calibrated using empirical calibrations coefficients obtained during the HOT-243 cruise conducted on 25-29 June 2012, one week after WHOTS-9, which used the same oxygen sensors. Similarly, the WHOTS-10 oxygen data were calibrated using calibration coefficients obtained during the HOT-253 cruise conducted on 24-28 June 2013, before the WHOTS-10 cruise, which used the same oxygen sensors. The CTD empirical calibration was conducted using oxygen water samples and the procedure from Owens and Millard (1985). See Tupas et al. (1997) for details on these calibrations procedures.

Table 4-6 shows the mean and standard deviation for the calibrated CTD oxygen minus water sample residuals during HOT-243 and HOT-253, whose calibrations were used for the WHOTS-9 and WHOTS-10 cruises respectively. Dual sensors were used during each cruise, and all four sensors performed well, showing small mean (less than 0.06 µmol kg^{-1} in magnitude) and standard deviation (less than 2 µmol kg^{-1}) residual values when compared with the water samples. The data reported here are from the sensors indicated in Table 4-6, and were in the same plumbing line as the temperature and conductivity sensor set whose data are also reported here (see Table 4-3).

Table 4-6. CTD-bottle dissolved oxygen comparison for each sensor during HOT-243 (calibration used for WHOTS-9 data) and HOT-253 (calibration used for WHOTS-10 data). The units are µmol kg^{-1}. The data reported here are from the sensor marked with (*).

		0 to 1200 dbar		500 to 1200 dbar	
Cruise	Sensor #	Mean	Standard Deviation	Mean	Standard Deviation
WHOTS-9/HOT-243	43918 (*)	0.01	1.30	0.02	1.13
WHOTS-9/HOT-243	431601	0.02	1.37	0.00	1.31
WHOTS-10/HOT-253	431601(*)	0.01	1.55	-0.01	1.90
WHOTS-10/HOT-253	43262	0.02	0.85	-0.05	0.83

B. Water sampling and analysis

Salinity

Salinity samples were collected by rosette sampler during CTD casts at selected depths during WHOTS-9 and -10, and sub-sampled in 250 ml glass bottles. The top of each bottle and thimble were thoroughly dried before being tightly capped to prevent water from being trapped between the cap or thimble and the bottle's mouth. It has been observed that residual water trapped in this way increases its salinity due to evaporation, and it can leak into the sample when the bottle is opened for measuring. Samples from each cruise were measured after the cruise in the laboratory at the UH using a Guildline Autosal 8400B (SN 70168). IAPSO[1] standard seawater samples were measured to standardize the Autosal, and samples from a large batch of "secondary standard" (substandard) seawater were measured after every 24-48 samples to detect drift in the Autosal. Standard deviations of the secondary standard measurements were less than ± 0.001 for WHOTS-9 and -10 cruises (Table 4-7).

The substandard water was collected by rosette sampler from 1020 m at station ALOHA during HOT cruises and drained into a 50-liter Nalgene plastic carboy. In the laboratory, the water was then thoroughly mixed in a glass carboy for 20 minutes by manually shaking, rolling and tilting the carboy vigorously, after which a 2-inch protective layer of white oil was added on top to deter evaporation. The substandard water was allowed to stand for approximately three days before it was used, and was stored in the same temperature controlled room as the Autosal, protecting it from the light with black plastic bags to inhibit biological growth. Substandard seawater batches #52 and #55 were prepared on 22 December 2011, and 19 July 2013, respectively and used for WHOTS-9 and -10 samples respectively.

Salinity samples from the WHOTS-9 cruise were measured prior to the samples from HOT-243. Samples from WHOTS-10 cruise were measured during the same session as the HOT-253 samples. The substandard statistics in Table 4-7 include the substandard samples measured for the WHOTS-9 samples and the combined WHOTS-10 and HOT-253 samples.

Table 4-7. Precision of salinity measurements of secondary lab standards.

Cruise	Mean Salinity +/- SD	# Samples	Substandard Batch #	IAPSO Batch #
WHOTS-9	34.4932 +/- 0.0003	6	52	P153
WHOTS-10 / HOT-253	34.4976 +/- 0.0001	19	55	P154

[1] International Association for Physical Sciences of the Ocean

C. Thermosalinograph data acquisition and processing

1. WHOTS-9 Cruise

Near-surface temperature and salinity data for the WHOTS-9 cruise were acquired through the Sea-Bird thermosalinograph system in the wet lab of the Ship *Hi'ialakai*. The seawater intake was situated approximately 2 m below the sea surface in the bow thruster room, and the thermosalinograph (internal) temperature and conductivity sensors were located in the ship's wet lab, about 67 m from the intake. There was no external temperature sensor during the WHOTS-9 cruise so temperature measured in the thermosalinograph were subject to heating and cooling as it passed through the ship. Data were acquired every 60 seconds for the duration of the cruise and salinity samples were taken roughly every 8 hours throughout the cruise for calibration from an outlet in the flowthrough system.

Data from the SBE-21 sensor were recorded to only one significant digit; therefore the data were not usable.

2. WHOTS-10 Cruise

Near-surface temperature and salinity data for the WHOTS-10 cruise were acquired through the use of the thermosalinograph system aboard the Ship *Hi'ialakai* described above. The system included an SBE-21 (SN 3155) thermosalinograph sensor measuring conductivity and internal temperature; and an SBE-38 (SN 0215) external temperature sensor installed near the seawater intake.

Temperature data were acquired every 60 seconds for the duration of the cruise, but the conductivity sensor stopped recording data just prior to 16 July 2013. Salinity samples were taken periodically throughout the cruise for calibration from an outlet in the flowthrough system located less than 0.5 m from the SBE-21.

Although a SBE-38 external temperature sensor was installed, no data were available from this sensor as the data were not properly recorded during the cruise.

Temperature Calibration

Since the external temperature data from the SBE-38 sensor was not available, data from the SBE-21 internal temperature sensor (last calibrated at Sea-Bird on18 November 2011) were used as a measure of the seawater temperature. However after applying an offset correction obtained by comparing to the data collected during CTD casts, these temperatures were found unreliable

as the water was subject to heating and cooling as it passed through the ship. These data were flagged as uncalibrated.

Nominal Conductivity Calibration

Data from the SBE-21 conductivity and temperature sensors were used to calculate the intake seawater salinity. These sensors were last calibrated at Sea-Bird on18 November 2011. All conductivity data from the thermosalinograph were nominally calibrated with coefficients from this calibration. However, all the final salinity data reported here were calibrated against bottle data as explained below.

Data Processing

Daily files containing navigation data recorded every 60 seconds were concatenated with the thermosalinograph data. The thermosalinograph data were then screened for gross errors, with upper and lower bounds of 18 °C and 35 °C for temperature and 3 Siemens m^{-1} and 6 Siemens m^{-1} for conductivity. There were three points outside the valid temperature range and no points outside the valid conductivity range.

A 5-point running median filter was used to detect one- or two-point temperature and conductivity glitches in the thermosalinograph data. Glitches in temperature and conductivity detected by the 5-point median filter were immediately replaced by the median. Threshold values of 0.3 °C for temperature and 0.1 Siemens m^{-1} for conductivity were used for the median filter. After running the filter, there were 140 conductivity points replaced by the median. A 3-point triangular running mean filter was used to smooth the temperature and conductivity data after passing the glitch detection.

The thermosalinograph aboard the Ship *Hi'ialakai* was set to record data every 60 seconds, but occasionally, due to an error in the acquisition software rounding routine, a record is written at a longer interval. However, there were no timing errors observed.

Data were visually scanned to flag glitches probably caused by contamination due to the introduction of bubbles to the flowthrough system during transit or during rough conditions. Of a total of 9791 data points, 1391 conductivity data points were flagged as bad. These bad points mostly occurred between 10 July 2013 and 13 July 2013. Data quality improved after. Underway conductivity stopped recording data just prior to 16 July 2013. Therefore, the final 1076 data points for conductivity are not available and set as Not a Number (NaN).

Bottle Salinity and CTD Salinity Comparisons

The thermosalinograph salinity was calibrated by comparing it to bottle salinity samples drawn from a water intake next to the thermosalinograph every 8 hours throughout the cruise. Of the 21 bottles sampled, 5 were considered outliers, while the final 4 bottles were sampled

after the system stopped collecting conductivity data. The remaining twelve salinity samples were analyzed as described in Section 0. The comparison was made in conductivity in order to eliminate the effects of temperature. The conductivity of the bottle sample was computed using the salinity of the bottle, thermosalinograph temperature and a pressure of 3.44 dbar, which includes the pressure of the flowthrough system's pump.

Salinity samples were drawn from the flowthrough system, located less than 0.5 m from the SBE-21 and consequently there should be virtually no delay between when the water passes through the thermosalinograph and it being sampled. A 90 second average centered on the sample draw time was chosen for processing purposes.

The CTD salinity data at 2 dbar from the 11 casts conducted during the cruise was used to compare with the thermosalinograph conductivity. Using the thermosalinograph temperature data and a pressure of 3.44 dbar the CTD conductivity was calculated for the 11 casts conducted while the thermosalinograph was running. One CTD cast (station 1 cast 1) was excluded from the processing as it was an obvious outlier. The SBE-21 conductivity sensor had a mean offset of 0.0071 Sm^{-1} with respect to the CTD data.

A cubic spline was fit to the time series of the differences between the bottle and thermosalinograph conductivity and a correction was obtained for the thermosalinograph conductivities. Salinity was calculated using these corrected conductivities, the thermosalinograph temperatures, and 6-dbar pressure. After correction, the mean difference between the bottle and thermosalinograph salinities was -0.0001 with a standard deviation of 0.0102. The mean CTD - thermosalinograph difference was 0.0024 with a standard deviation of 0.0095.

CTD Temperature Comparisons

There were 11 CTD casts conducted during the WHOTS-10 cruise. The 2 dbar CTD temperature data were used to compare with the thermosalinograph internal temperature. One CTD cast (station 1 cast 1) was excluded from the processing as it was an obvious outlier. No external temperature data were available post-cruise, despite a SBE-38 sensor being installed (see Sect. 4.C.2), therefore the internal temperature from the SBE-21 thermosalinograph is reported here as external temperature after adding an offset to match it to the CTD temperature data. The mean difference between the internal sensor and the CTD was -0.1995 °C, with a standard deviation of ±0.0168 °C. All the reported temperatures were flagged as uncalibrated.

D. Shipboard ADCP

1. WHOTS-9 Deployment Cruise

Currents measured by the Ship *Hi'ialaikai's* Ocean Surveyor 75 kHz narrowband ADCP were processed using the CODAS ADCP processing suite. Horizontal velocity data, latitude and longitude were processed with 15 minute ensemble averages and 10 m depth resolution. The times of the datasets from the OS75 are shown in Table 4-8.

Table 4-8. ADCP record times (UTC) for the Narrowband Ocean Surveyor 75 kHz ADCP during the WHOTS-9 cruise.

WHOTS-10	**OS75**
File beginning time	13-Jun-2012 03:30:31
File ending time	19-Jun-2012 17:00:28

2. WHOTS-10 Deployment Cruise

Currents measured by the Ship Hi'ialakai's Ocean Surveyor 75 kHz narrowband and broadband ADCP were processed using the CODAS ADCP processing suite. Horizontal velocity data, latitude and longitude were processed with 15 minute ensemble averages and 10 m depth resolution. The times of the datasets from the OS75 are shown in Table 4-9.

Table 4-9. ADCP record times (UTC) for the Narrow Band 75 kHz ADCP during the WHOTS-10 cruise.

WHOTS-10	**OS75**
File beginning time	09-Jul-2013 20:02:58
File ending time	16-Jul-2013 23:38:00

5. Moored Instrument Observations

A. MicroCAT/SeaCAT data processing procedures

Each moored MicroCAT and SeaCAT temperature, conductivity and pressure (when installed) was calibrated at Sea-Bird prior to their deployment and after their recovery on the dates shown in Table 5-1. The internally-recorded data from each instrument were downloaded on board the ship after the mooring recovery, and the nominally-calibrated data were plotted for a visual assessment of the data quality. The data processing included checking the internal clock data against external event times, pressure sensor drift correction, temperature sensor stability, and conductivity calibration against CTD data from casts conducted near the mooring during HOT and WHOTS cruises. The detailed processing procedures are described in this section.

Table 5-1. WHOTS-9 MicroCAT/SeaCAT temperature sensor calibration dates, and sensor drift during deployments. Only sensors SN 3669 at 135 m and SN 1881 at 4631 m had a drift larger than 1 mili^{o}C during the deployment (see Sect. 5.A.3).

Nominal deployment depth (m)	Sea-Bird Serial number	Pre-deployment calibration	Post-recovery calibration	Total Temperature drift during WHOTS-9 deployment (mili^{o}C)
15	SBE37SM-3382	16-Sep-2011	06-Aug-2013	-0.33
25	SBE37SM-4663	16-Sep-2011	09-Aug-2013	-1.00
35	SBE37SM-3633	16-Sep-2011	17-Aug-2013	-0.02
40	SBE37SM-3381	15-Sep-2011	29-Aug-2013	0.037
45	SBE37SM-3668	16-Sep-2011	17-Aug-2013	-0.02
50	SBE37SM-3619	16-Sep-2011	09-Aug-2013	-0.06
55	SBE37SM-3620	16-Sep-2011	03-Aug-2013	-0.02
65	SBE37SM-3621	16-Sep-2011	08-Aug-2013	-0.47
75	SBE37SM-3632	15-Sep-2011	17-Aug-2013	0.58
85	SBE37SM-4699	16-Sep-2011	29-Aug-2013	-0.11
95	SBE37SM-3791	15-Sep-2011	17-Aug-2013	0.69
105	SBE37SM-2769	15-Sep-2011	09-Aug-2013	0.64
120	SBE37SM-4700	16-Sep-2011	17-Aug-2013	-0.36
135	SBE37SM-3669	13-Oct-2011	29-Aug-2013	-3.79
155	SBE37SM-4701	15-Sep-2011	28-Aug-2013	0.84
4631	SBE16-1880	29-Mar-2011	16-Oct-2013	-0.75
4631	SBE16-1881	28-Apr-2010	16-Oct-2013	1.32

1. Internal Clock Check and Missing Samples

Before the WHOTS-9 mooring deployment and after its recovery (before the data logging was stopped), the MicroCATs temperature sensors were placed in contact with an ice pack to create a spike in the data, to check for any problems with their internal clocks, and for possible missing samples (Table 3-2). The cold spike was detected by a sudden decrease in temperature. For all the instruments, the clock time of this event matched correctly the time of the spike (within the sampling interval of each instrument). No missing samples were detected for any of the instruments.

2. Pressure Drift Correction and Pressure Variability

Some of the MicroCATs used in the moorings were outfitted with pressure sensors (Table 3-1). Biases were detected in the pressure sensors by comparing the on-deck pressure readings (which should be zero for standard atmospheric pressure at sea level of 1029 mbar) before deployment and after recovery. Table 5-2 shows the magnitude of the bias for each of the sensors before and after deployment. To correct for this offset, a linear fit between the initial and final on-deck pressure offset as a function of time was obtained, and subtracted from each sensor. Figure 5-1 shows the linearly corrected pressures measured by the MicroCATs during the WHOTS-9 deployment. For all the sensors, the mean difference from the nominal instrument pressure (based on the deployed depth) was less than 1 dbar. The standard deviation of the pressure for the duration of the record was also less than 1 dbar for all sensors, with the deeper sensors showing a larger standard deviation. The range of variability for all sensors was about ± 3 dbar, except for sensor SN 3669 at 135 dbar which shows large variability near the end of the record, probably due to failure. These data starting on May 11, 2013 until the end of the record were flagged as bad.

The causes of pressure variability can be several, including density variations in the water column above the instrument; horizontal dynamic pressure (not only due to the currents, but also due to the motion of the mooring); mooring position, etc. (see WHOTS Data Report 1, Santiago-Mandujano et al., 2007).

Table 5-2. Pressure bias of MicroCATs with pressure sensor. Sensor 3669 failed near the end of the record and its bias after recovery was unreliable (see text).

Deployment	Depth (m)	Sea-Bird Serial #	Bias before deployment (dbar)	Bias after recovery (dbar)
WHOTS-9	45	37SM31486-3668	0.01	-0.14
WHOTS-9	85	37SM31486-4699	0.56	0.48
WHOTS-9	105	37SM31486-2769	0.00	-0.08
WHOTS-9	120	37SM31486-4700	0.02	-0.75
WHOTS-9	135	37SM31486-3669	0.08	NA
WHOTS-9	155	37SM31486-4701	-0.04	-0.10

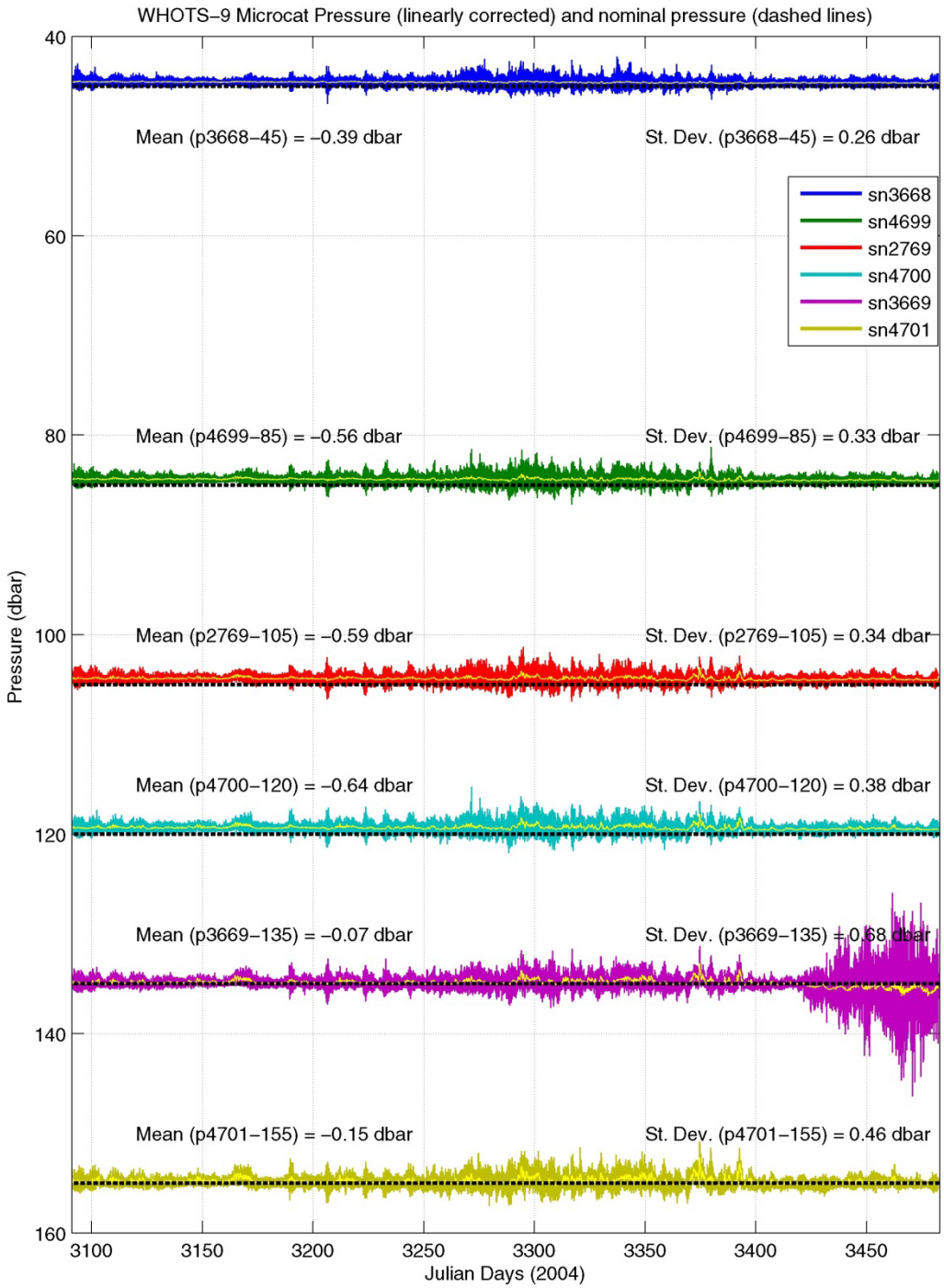

Figure 5-1. Linearly corrected pressures from MicroCATs during WHOTS-9 deployment. The yellow line is a 5-hour running mean. The horizontal dashed line is the sensor's nominal pressure, based on deployed depth.

3. Temperature Sensor Stability

The MicroCAT and SeaCAT temperature sensors were calibrated at Sea-Bird before and after each deployment (see Table 5-1). Sea-Bird's evaluation of each sensor's drift was used to calculate the temperature offset for the duration of the deployment (Table 3-1 and Table 3-2). These values turned out to be insignificant (not higher than 1 m °C) for all sensors deployed above 200 m, except for sensor SN 3669. This sensor's drift was -2.16 m°C/yr according to Sea-Bird's evaluation, and was corrected assuming that the pre-deployment calibration was correct and by subtracting this drift to the data. The drift was calculated from the pre-deployment calibration date throughout the duration of the WHOTS-9 deployment. Comparisons between the MicroCAT and CTD data from casts conducted near the mooring during HOT cruises confirmed that the temperature drift of the rest of the moored instruments was insignificant. The two SeaCATs deployed near the bottom (SN 1880 and 1881) were drift corrected as in the case of sensor SN 3669, their respective drift rates were -0.33 m°C/yr and 0.41 m°C/yr. Figure 5-8 (upper panel) shows the temperature differences between both instruments before and after the correction. After the correction the temperature differences were in the -1.0 to 2.0 m°C range.

A temperature comparison between the two MicroCATs installed underneath the buoy (SN 1306 and SN 1419) show the consistency and inferred stability of the sensors for the duration of the deployment (Figure 5-7, upper panel).

Temperature comparisons between one of the WHOTS-9 near-surface MicroCATs (SN 1306) and the 4 RBR surface temperature sensors in the buoy hull (Table 3-1) are shown in Figure 5-2. All the RBR instruments stopped recording early, instruments #4882 and #4878 lasted 109 and 107 days respectively during the deployment; #4977 has the shortest record of 10 days, and #4978 has the longest with 179 days. None of the instruments show any obvious bias when compared to the Microcat measurements.

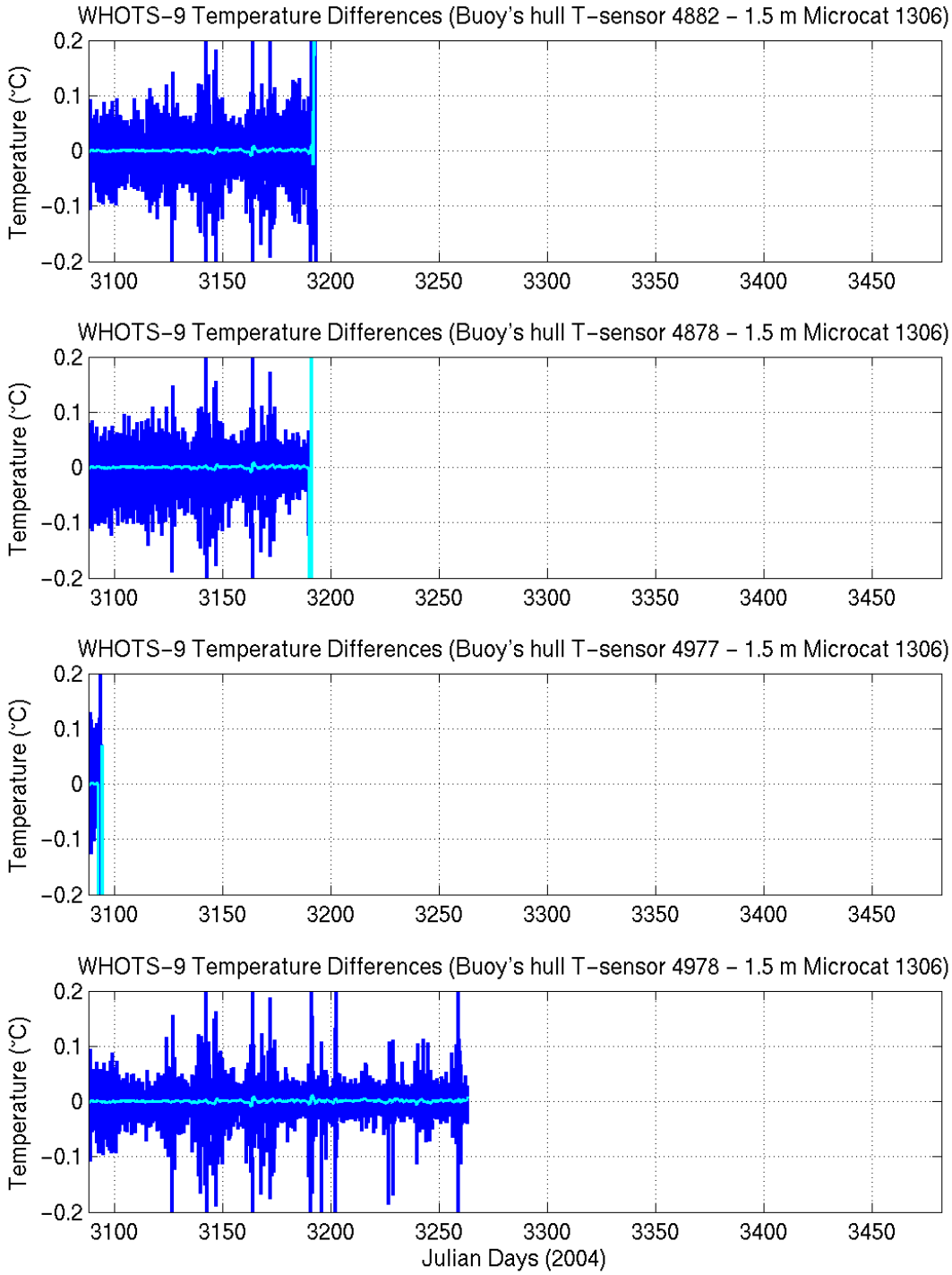

Figure 5-2. Temperature difference between MicroCAT SN 1306 at 1.5 m, and near-surface temperature sensors SN 4882(upper panel), 4878 (second panel), 4977 (third panel), and SN 4978(bottom panel), during WHOTS-9 deployment. The light blue line is a 24-hour running mean of the differences.

In addition to the temperature sensors in the Sea-Bird and the RBR instruments, there were additional temperature sensors in the VMCMs (at 10 and 30 m), and in the ADCPs (at 47.5 m and 125 m). In order to evaluate the quality of the temperatures from these sensors, comparisons with the temperatures from adjacent MicroCATs were conducted.

Comparisons with VMCM and ADCP temperature sensors

The upper panel of Figure 5-3 shows the difference between the 10-m VMCM and the 15-m MicroCAT temperatures during WHOTS-9, after adding a 0.053 °C offset correction to the VMCM. The offset was the mean difference between the uncorrected VMCM and the 15-m MicroCAT data. Also shown for comparison in the lower panel of the figure are the differences between MicroCAT temperatures at 15 and 25 m. The temperature fluctuations in the differences between the 15 and 25-m MicroCATs seem to be around zero.

Temperature differences between the 30-m VMCM and the temperatures from adjacent MicroCATs at 25 and 35-m during WHOTS-9 are shown in Figure 5-4. For comparison, the differences between the MicroCATs temperatures are also shown. These plots indicate that there was no offset in the 30-m VMCM with respect to the adjacent MicroCATs (top and middle plots).

Temperature differences between the 47.5-m ADCP and the temperatures from adjacent MicroCATs at 45 and 50-m during WHOTS-9 are shown in Figure 5-5. For comparison, the differences between the MicroCATs temperatures are also shown. These plots indicate that there was no offset in the 47.5-m ADCP with respect to the adjacent MicroCATs (top and middle plots).

Temperature differences between the 125-m ADCP and the temperatures from adjacent MicroCATs at 120 and 135-m during WHOTS-9 are shown in Figure 5-6. For comparison, the differences between the MicroCATs temperatures are also shown. It is difficult to assess the quality of the ADCP temperature from these comparisons, as these sensors were located at the top of the thermocline, where we expect to find large temperature differences between adjacent sensors. However, an indication of the quality of the ADCP temperatures is given in the upper panel plot, which shows temperatures fluctuating closely around zero during short periods (e.g. day 3350), when apparently the mixed layer deepened close to these levels (see bottom panel in Figure 5-6).

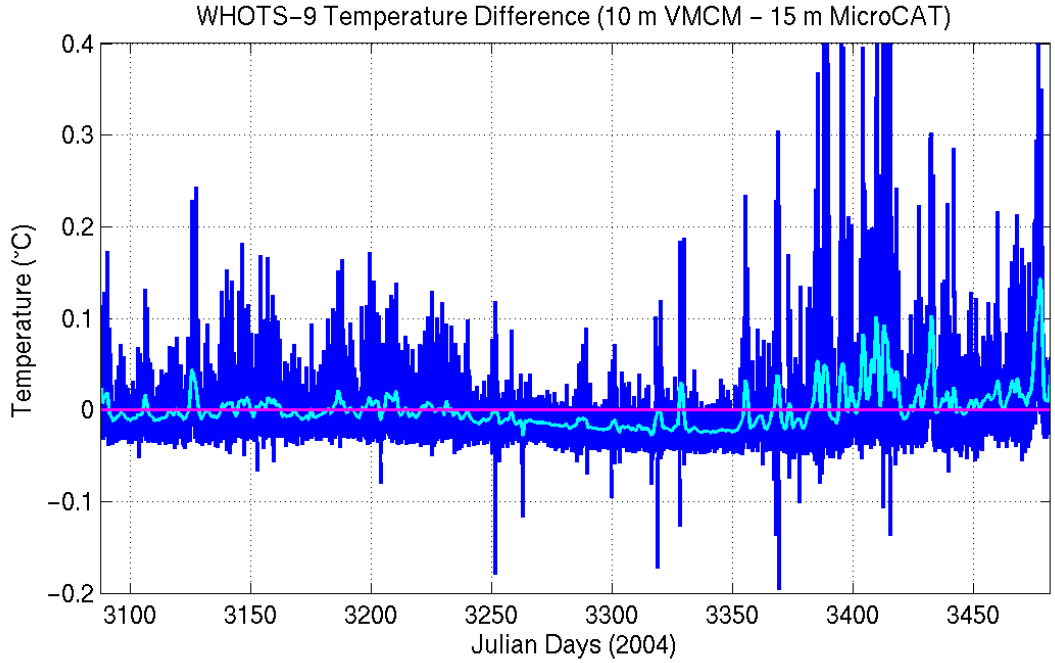

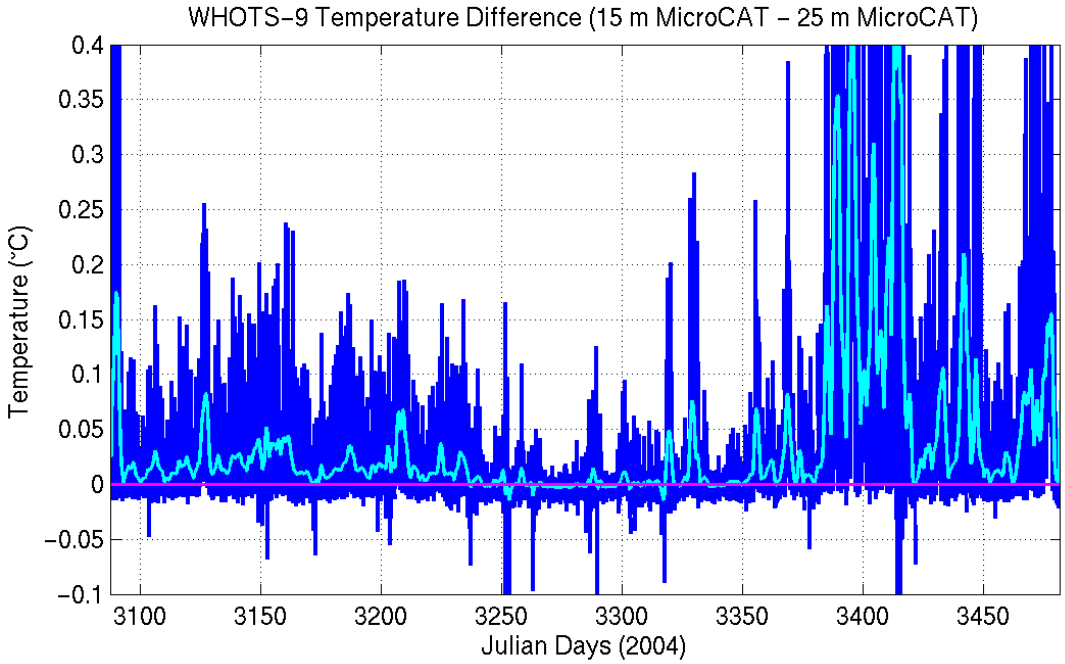

Figure 5-3. Temperature difference between the 10-m VMCM and the 15-m MicroCAT during the WHOTS-9 deployment (upper panel). Temperature difference between the 15-m MicroCAT and the 25-m MicroCAT during the WHOTS-9 deployment (lower panel). The light blue line is a 24-hour running mean of the differences.

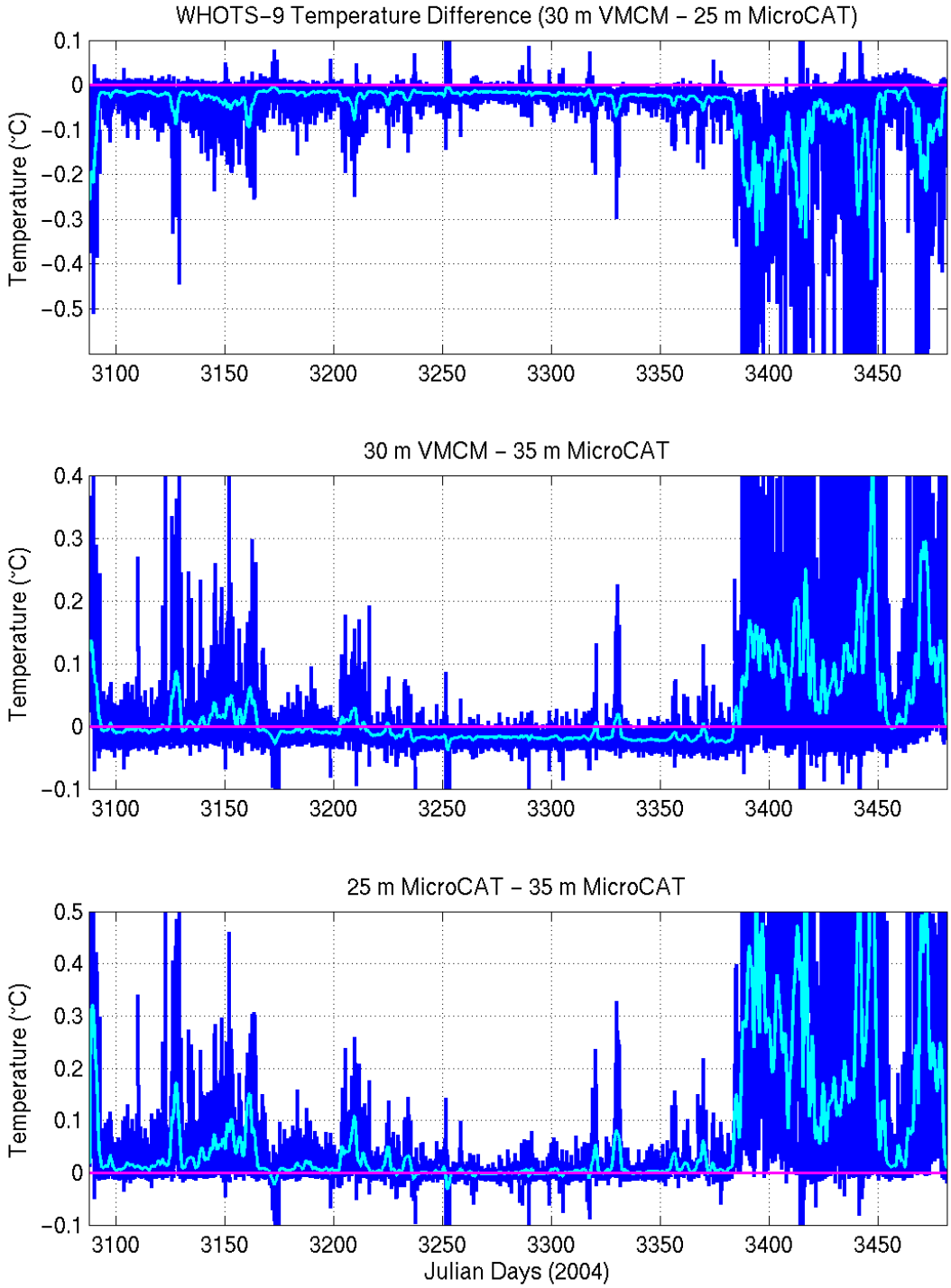

Figure 5-4. Temperature difference between the 30-m VMCM and the 25-m MicroCAT during the WHOTS-9 deployment (upper panel); between the 30-m VMCM and the 35-m MicroCAT (middle panel); and between the 25-m and the 35-m MicroCATs (lower panel). The light blue line is a 24-hour running mean of the differences.

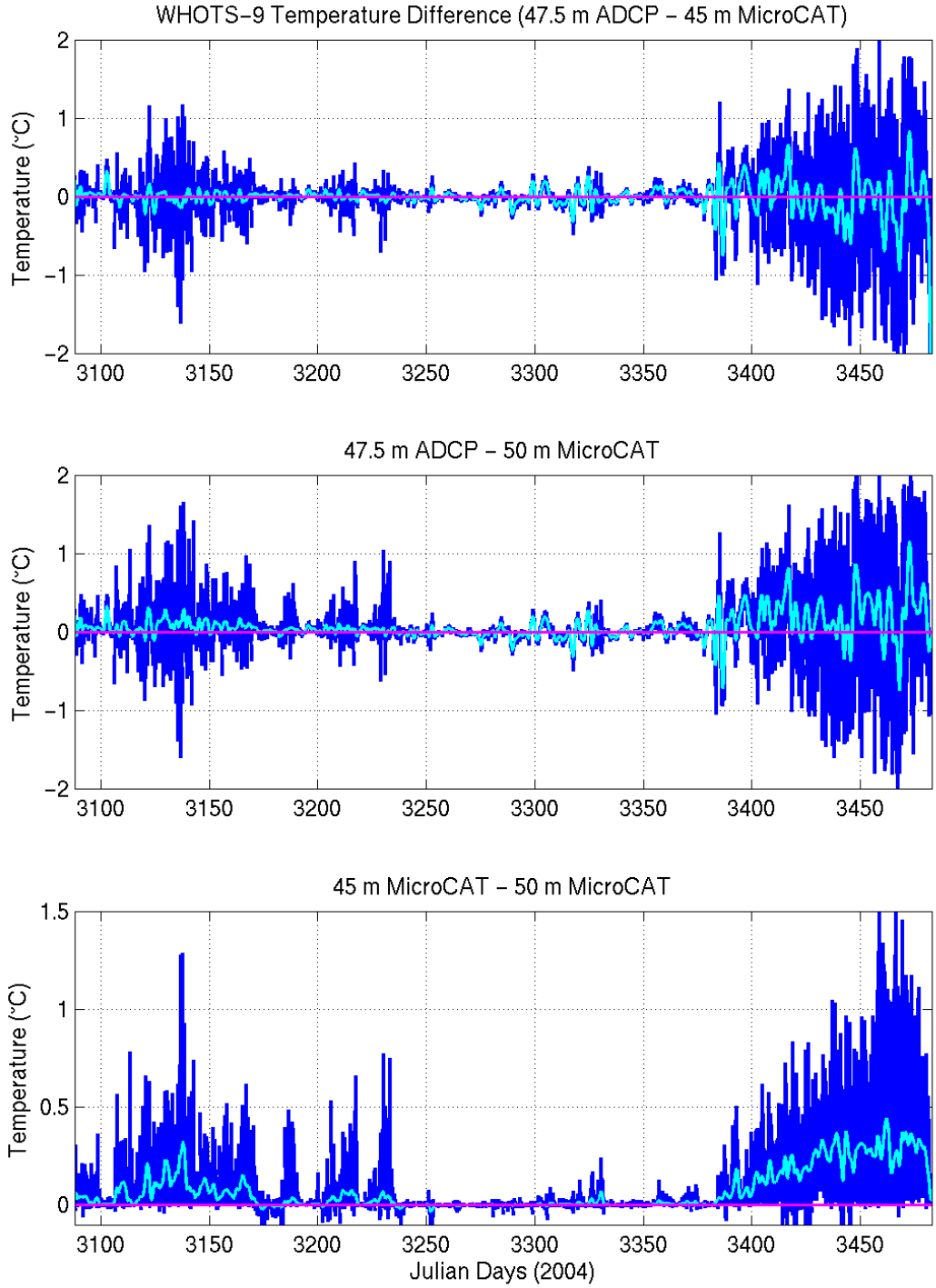

Figure 5-5. Temperature difference between the 47.5-m ADCP and the 45-m MicroCAT during the WHOTS-9 deployment (upper panel); between the 47.5-m ADCP and the 50-m MicroCAT (middle panel); and between the 45-m and the 50-m MicroCATs (lower panel). The light blue line is a 24-hour running mean of the differences.

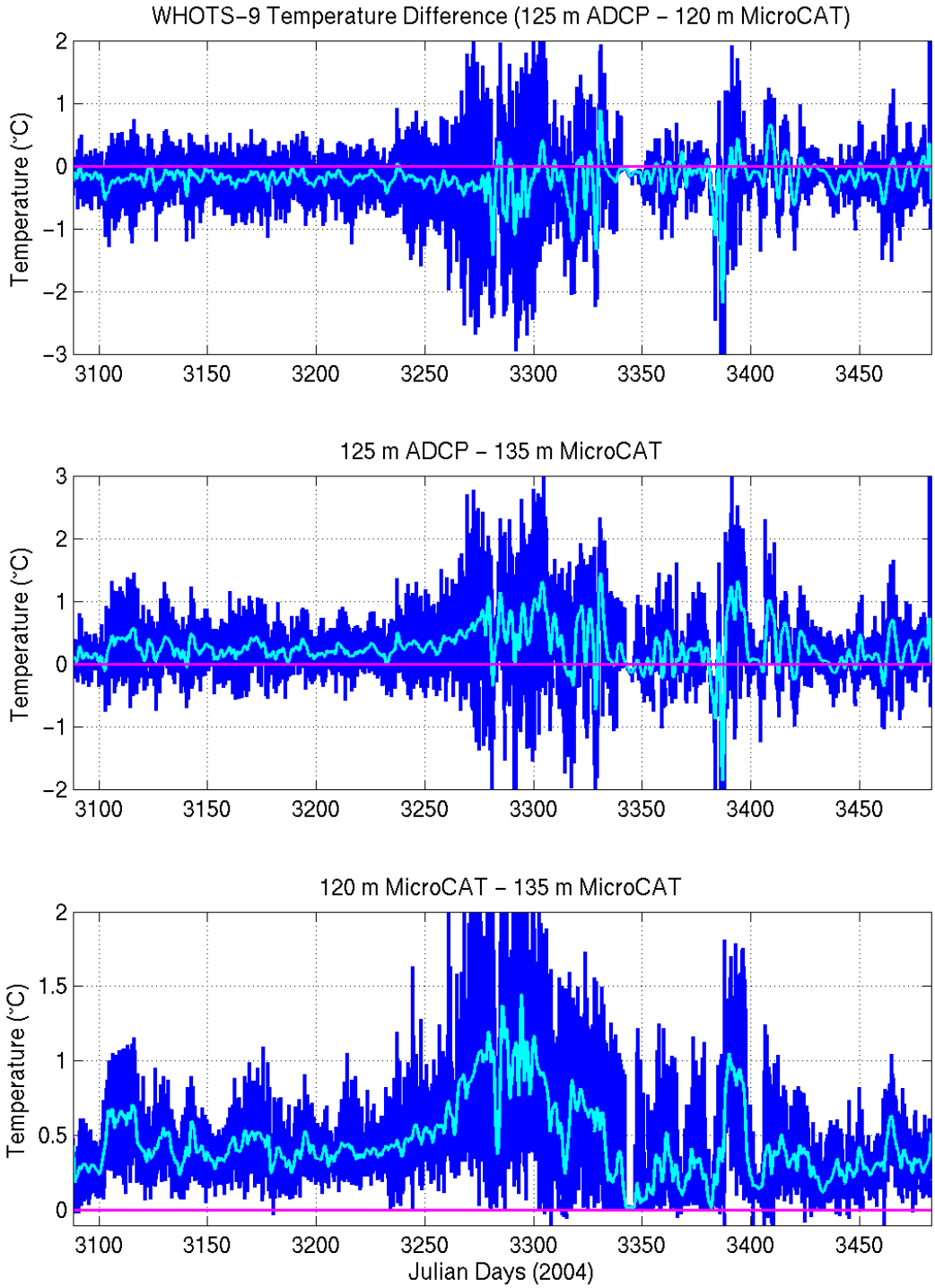

Figure 5-6. Temperature difference between the 125-m ADCP and the 120-m MicroCAT during the WHOTS-9 deployment (upper panel); between the 125-m ADCP and the 135-m MicroCAT (middle panel); and between the 120-m and the 135-m MicroCATs (lower panel). The light blue line is a 24-hour running mean of the differences.

4. Conductivity Calibration

The results of the Sea-Bird post-recovery conductivity calibrations indicated that some of the MicroCAT and SeaCAT conductivity sensors experienced relatively large offsets from their pre-deployment calibration. These were qualitatively confirmed by comparing the mooring data against CTD data from casts conducted between 200 m and 5 km from the mooring during HOT cruises. The causes of the conductivity offsets are not clear, and there may have been multiple causes (see Freitag et. al, (1999) for a similar experience with conductivity cells during COARE). For some instruments the offset was negative, caused perhaps by biofouling of the conductivity cell while for others the offset was positive, caused possibly by scouring of the inside of the conductivity cell (possible by the continuous up and down motion of the instrument in an abundant field of diatoms). A visual inspection of the instruments after recovery did not show any obvious signs of biofouling, and there were no cell scourings reported in the post-recovery inspections at Sea-Bird. However three of the instruments (25, 45 and 50 m) were recovered without their cell guards, and without their anti-fouling device. These instruments experienced large offsets during the deployment as reported below.

Corrections of the MicroCATs conductivity data were conducted by comparing them against CTD data from profiles and yo-yo casts conducted near the mooring during HOT cruises, and during deployment/recovery cruises. Casts conducted between 200 and 1000 m from the mooring were given extra weight in the correction, as compared to those conducted between 1 and 5 km away. Casts more than 5 km away from the mooring were not used. Given that the CTD casts are conducted at least 200 m from the mooring, the alignment between CTD and MicroCAT data was done in density rather than in depth. For cases in which the alignment in density was not possible due to large conductivity offsets (causing unrealistic mooring density values), alignment in temperature space was done. A cubic least-squares fit (LSF) to the CTD-MicroCAT/SeaCAT differences against time was applied as a first approximation, and the corresponding correction was applied.

Some of the sensors had large offsets and/or obvious variability that could not be explained by a cubic LSF (see below). For these sensors, a stepwise correction was applied matching the data to the available CTD cast data, and then using the differences between consecutive sensors to determine when the sensor started to drift. For instance, during periods of weak stratification the conductivity difference between neighboring sensors A, B, and C could reach near-zero values, in particular for instruments near the surface, which are the ones most prone to suffer conductivity offsets. A sudden conductivity offset observed during this period between sensors A and B, but not between sensors A and C could indicate the beginning of an offset for sensor B.

Given that the deepest instruments on the mooring are less likely to be affected by biofouling and consequent sudden conductivity drift, the deep instruments served as a good reference to find any possible malfunction in the shallower ones. Therefore the deepest instruments' conductivity was corrected first, and the correction was continued sequentially upwards toward the shallower ones.

As a quality control to the conductivity corrections, the buoyancy frequency between neighboring instruments was calculated using finite differences. Over- or under-corrected conductivities yielded instabilities in the water column (negative buoyancy frequency) that were easy to detect and were obviously not real when lasting for several days. Based on this, the conductivity correction of the corresponding sensors was revised.

Corrections of the deep SeaCATs conductivity data were conducted following similar procedures as for the shallow instruments by comparing them against CTD data from near-bottom profiles conducted during HOT cruises. Instrument SN 1880 had a large drift and offset during the deployment, which were successfully corrected (see below).

Another characteristic of the offsets in the conductivity sensors is that their development is not always linear in time, and their behavior can be highly variable (see WHOTS Data Report 1, Santiago-Mandujano et al., 2007). This is clearly illustrated by the results from two MicroCATs logging data at the same depth during WHOTS-9. Figure 5-7 shows the temperature and conductivity differences between MicroCATs #1306 and #1419 that were located on the buoy hull (about 1.55 m below the surface). The temperature sensors did not show any significant drift for the duration of the deployment (see Section 5.A.3), however the conductivity differences show significant variability. Comparisons with CTD data showed that instrument #1306 had a small conductivity drift, which was corrected as indicated above, the middle panel in Figure 5-7 shows the difference between the corrected #1306 and the uncorrected #1419 conductivities. This figure shows that #1419 started with a large offset of -0.04 S/m, and had a slow near-constant negative drift at the beginning of the deployment until day 3250, when a large positive drift started to develop lasting about 50 days. After this day there was a slow positive drift until day 3370, followed by a negative drift until day 3440 and a large positive drift until day 3450, after which the instrument reached a near-zero offset and nearly no drift. Instrument #1419 conductivities were corrected based on this comparison and the differences between these instruments after this correction are shown in the lower panel of Figure 5-7.

A correction was also applied to the deep SeaCATs conductivities. Both instruments were deployed at the same depth (4631 m). Comparisons with near-bottom CTD data showed that instrument SN 1881 had a small conductivity drift, which was corrected following the procedures outlined above. Instrument SN 1880 suffered a larger drift and a sudden large offset on 4 June 2013 as indicated by the salinity differences between both uncorrected sensors in Figure 5-8 (lower panel). This instrument's conductivities were also corrected following the above procedures. After correction, the salinity differences between both instruments were in the +-0.002 g/kg range.

The corrections applied to each of the conductivity sensors during WHOTS-9 can be seen in Figure 5-9. Most of the instruments had a drift of less than 0.009 Siemens/m for the duration of the deployment, which was corrected with a linear or cubic least-squares fit. The instruments

deployed at 25, 45 and 50 m that were recovered without their cell guard and anti-fouling device had additional problems.

MicroCAT #4663 at 25 m experienced a conductivity offset of about -0.04 Siemens/m on 24 December 2012. After correcting as explained above, some of the data still did not pass the buoyancy frequency quality control and data from 24 December 2012 through 8 April 2013 were flagged as bad, and from this date until the end of the deployment the data were flagged suspect.

MicroCAT #3668 at 45 m had a conductivity offset of about -0.04 Siemens/m starting on 9 March 2013. After applying a correction, some of the data did not pass the buoyancy frequency quality control and data from 9 March 2013 through 8 April 2013 were flagged as bad.

MicroCAT #3619 at 50 m had a large conductivity offset of -0.3 Siemens/m starting on 29 November 2012. After applying a correction, the data did not pass the buoyancy frequency quality control and all data from this date until the end of the deployment were flagged as bad.

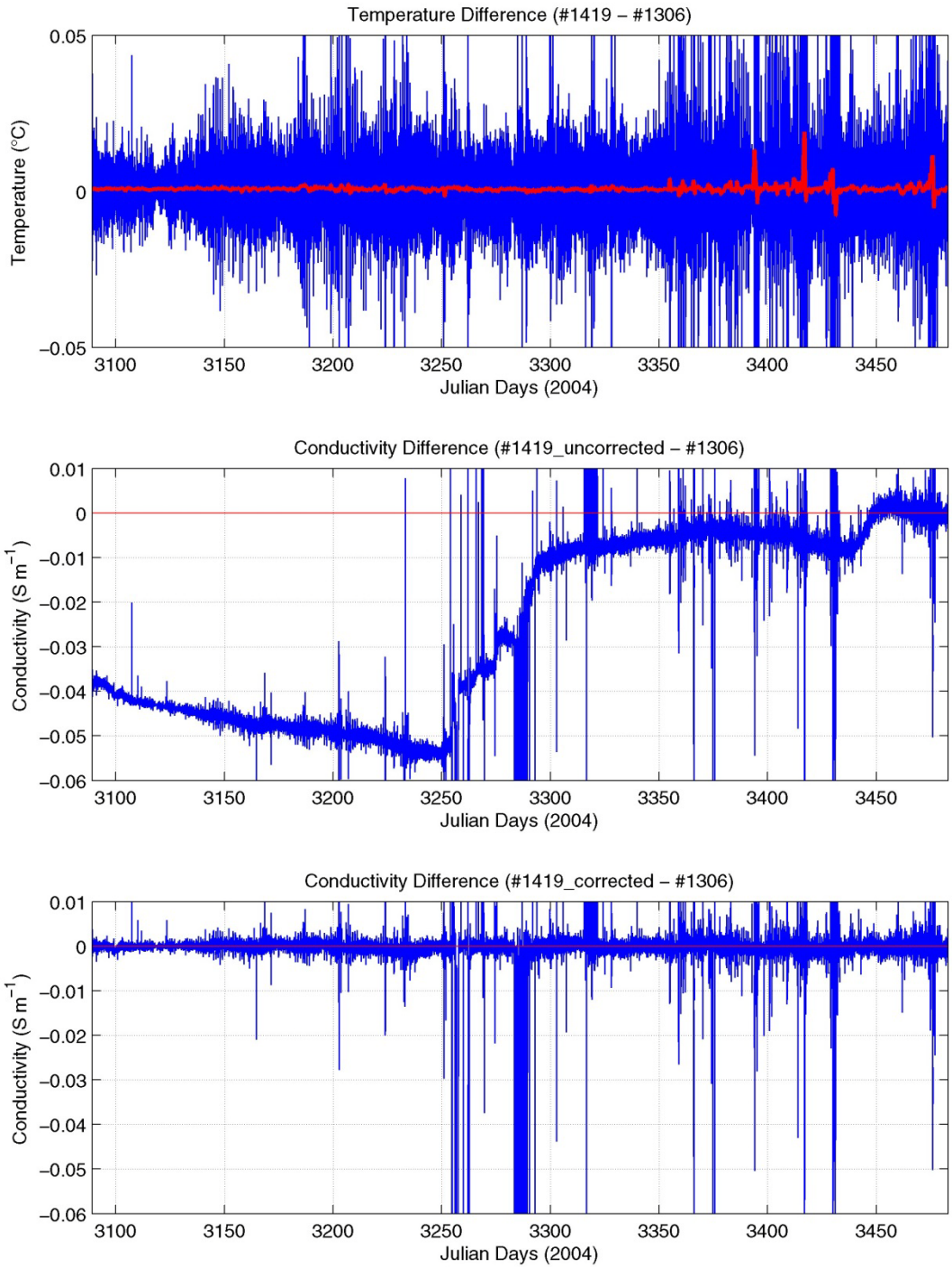

Figure 5-7. Temperature difference (top panel), and conductivity difference between MicroCATs #1419 and #1306 during WHOTS-9, with an uncorrected #1419 sensor (middle panel), and a corrected #1419 sensor (bottom panel). The red line in the top panel is a 12-hr running mean.

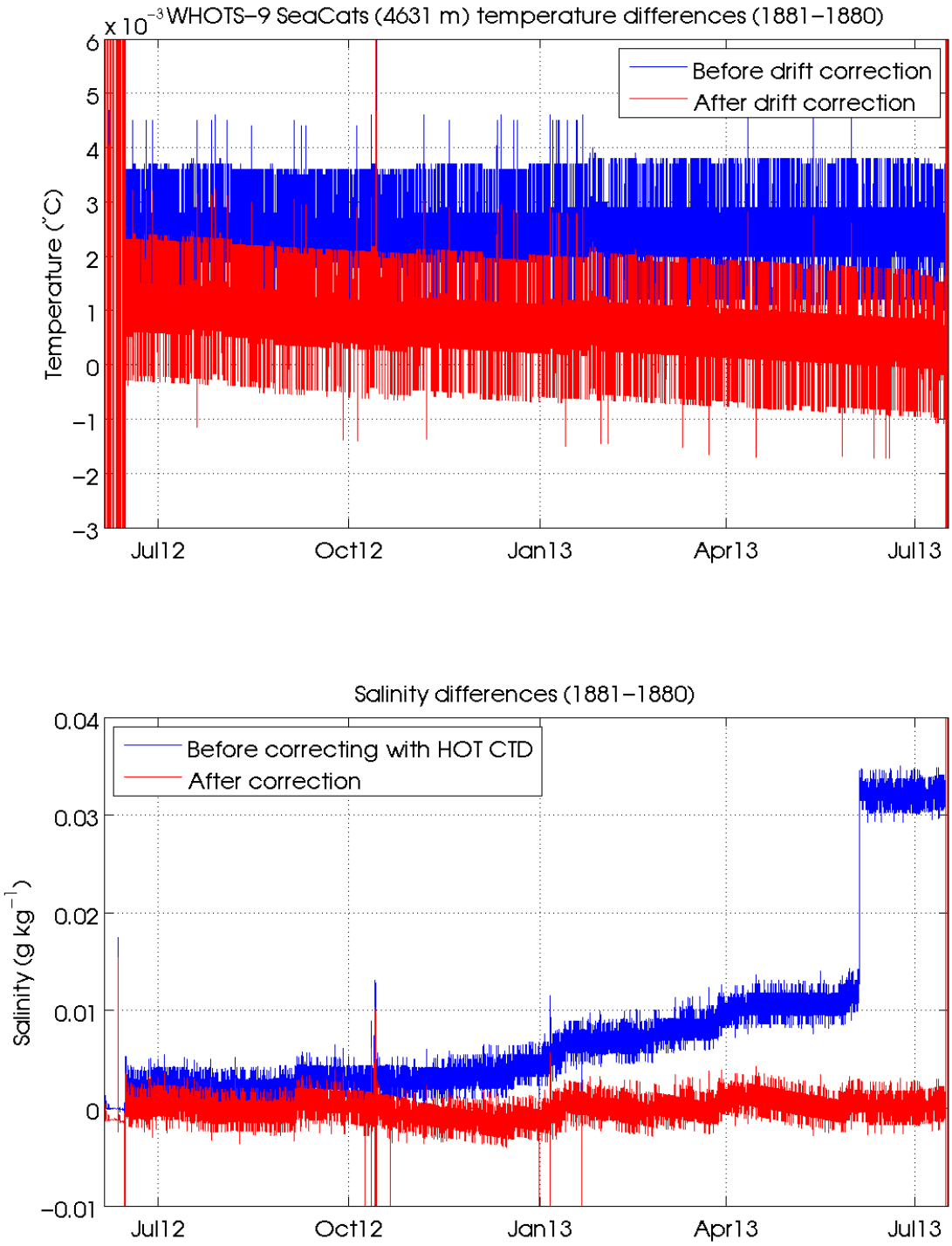

Figure 5-8. Temperature differences (top panel), and salinity differences (bottom panel) between SeaCATs #1880 and #1881 during WHOTS-9. The blue (red) lines are the differences before (after) correcting the data following procedures indicated in the text.

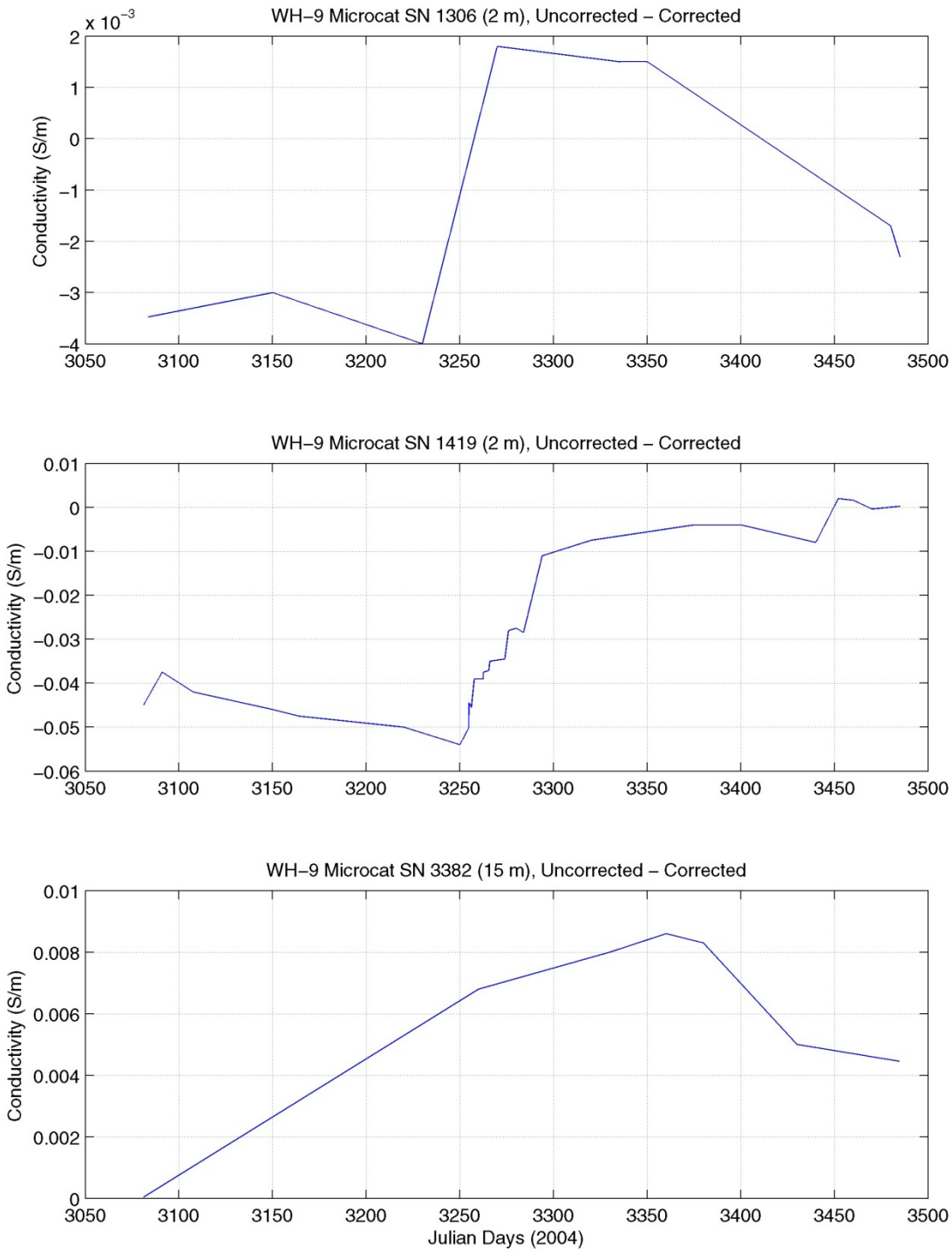

Figure 5-9. Conductivity sensor corrections for MicroCATs and SeaCATs during WHOTS-9

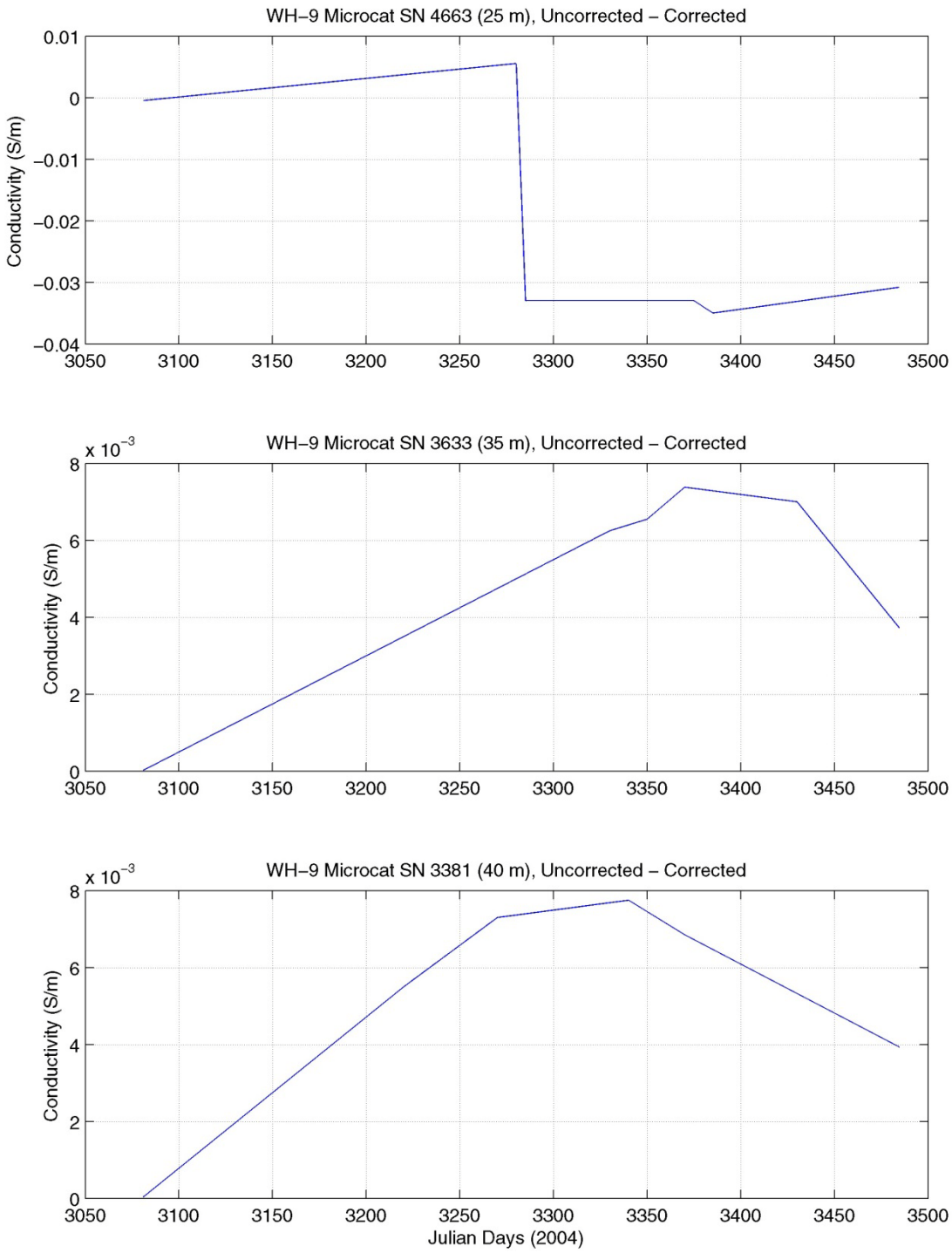

Figure 5-9. (Contd.)

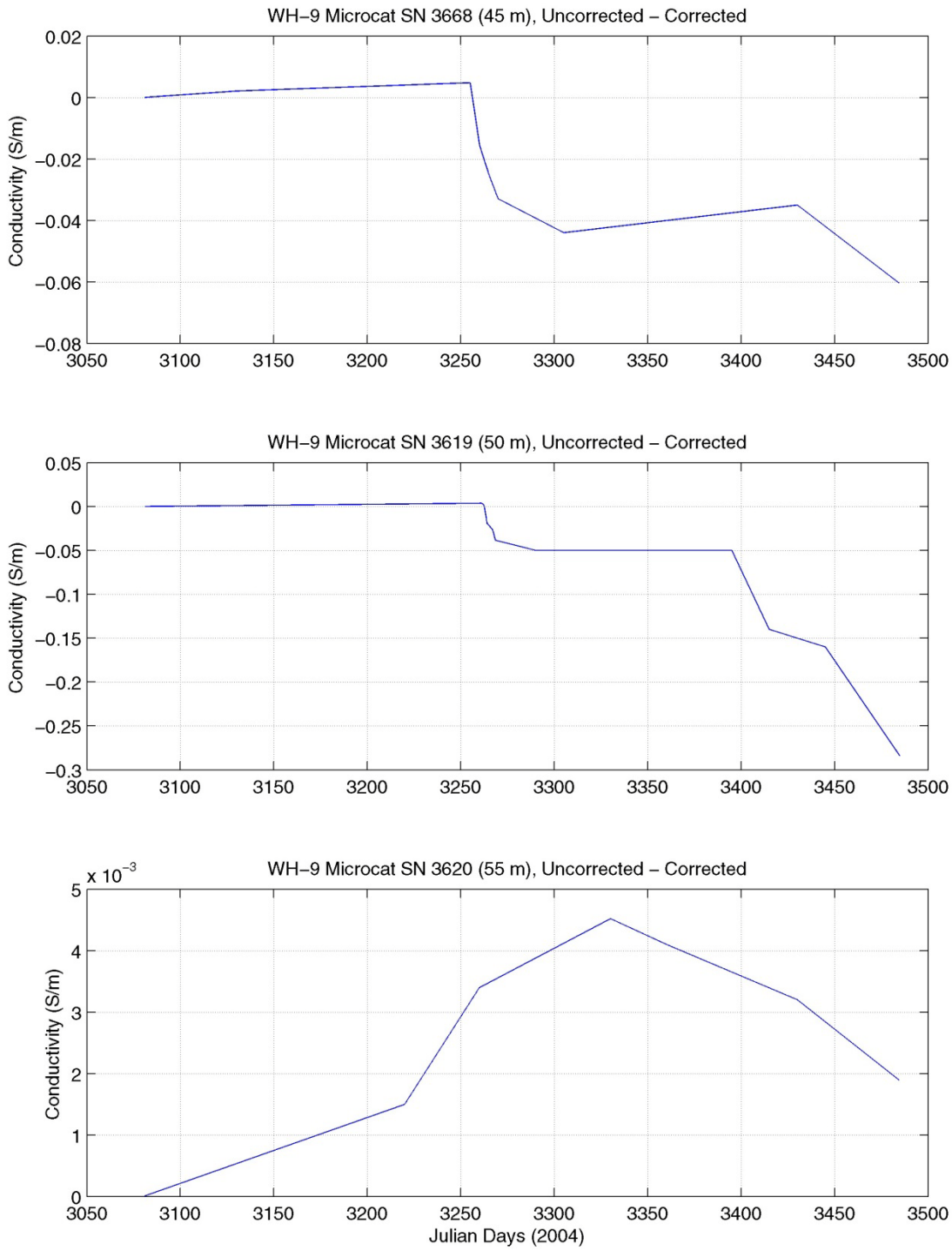

Figure 5-9. (Contd.)

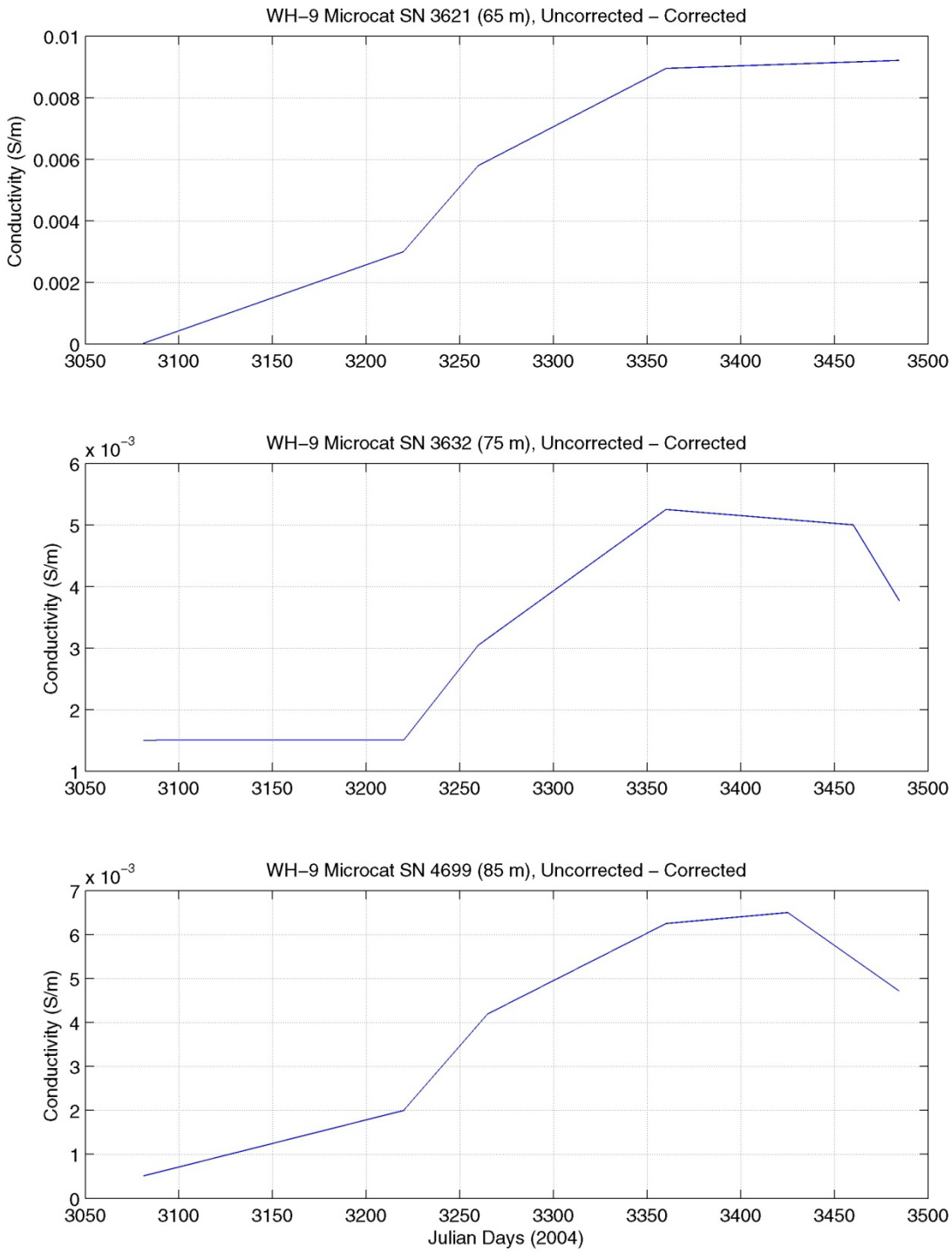

Figure 5-9. (Contd.)

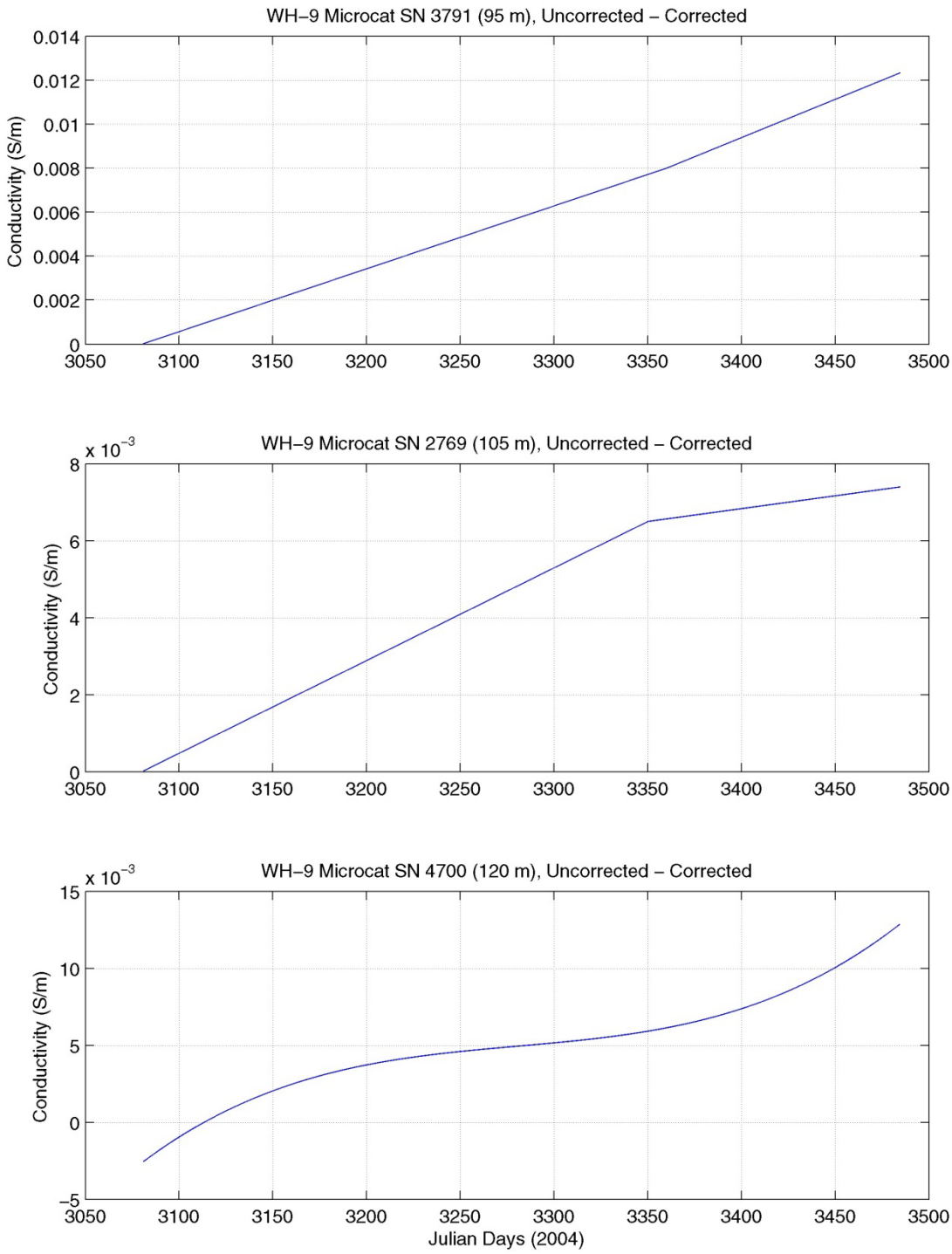

Figure 5-9. (Contd.)

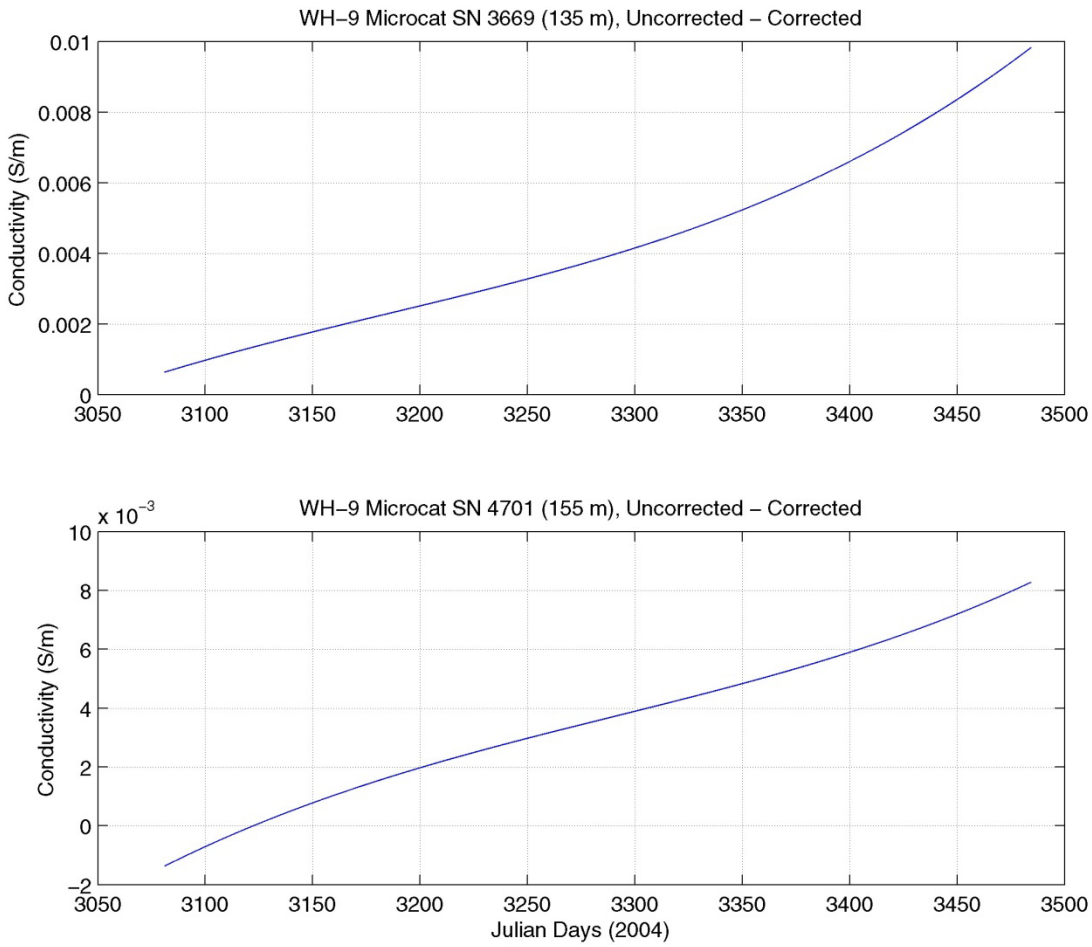

Figure 5-9. (Contd.)

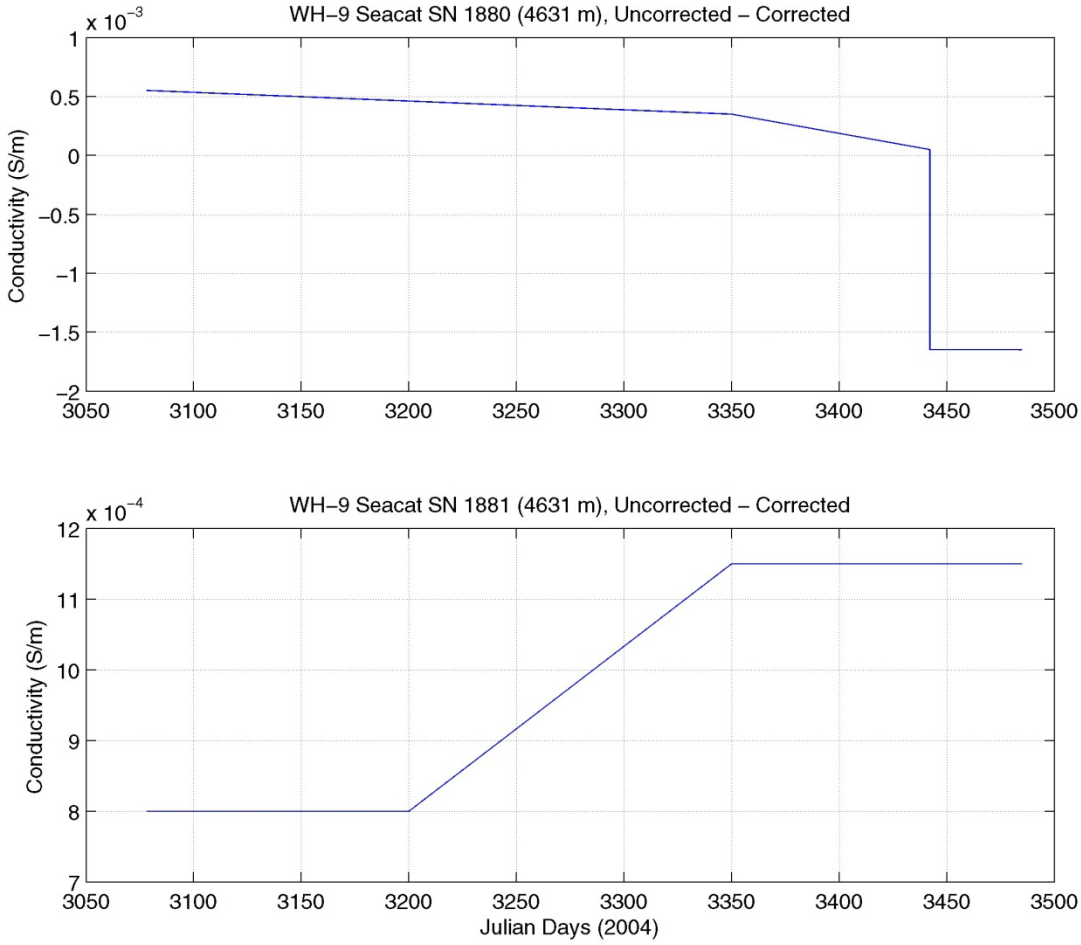

Figure 5-9. (Contd.)

B. Acoustic Doppler Current Profiler

Two Teledyne/RD Instruments broadband Workhorse Sentinel ADCP's were deployed on the WHOTS-9 mooring. A 600 kHz ADCP was deployed at 47.5 m depth in the upward-looking configuration, and a 300 kHz ADCP was deployed at 125 m, also in the upward-looking configuration. The instruments were installed in aluminum frames along with an external battery module to provide sufficient power for the intended period of deployment. The four ADCP beams were angled at 20° from the vertical line of the instrument. The ADCP was set to profile across 30 range cells of 4 m with the first bin centered 6.2 m from the transducer. The maximum range of the instrument was just short of 125 m. The specifications of the instrument are shown in Table 5-3.

Table 5-3. Specifications of the ADCP's used for the WHOTS-9 mooring.

Instrument	Description
ADCP	*RDI Workhorse Sentinel, 300KHz* Model: WHS300-I-UG129; Serial Number: 7637 *RDI Workhorse Sentinel, 600KHz* Model: WHS600-I; Serial Number: 13917
Battery module	*300 kHz* Model: WH-EXT-BATTERY; Serial Number: 3426 *600 kHz* Model: WH-EXT-BCL; Serial Number: 3818

1. Compass Calibrations

Pre-Deployment

Prior to the WHOTS-9 deployment a field calibration of the internal ADCP compass was performed at the football field of the University of Hawai'i at Manoa on 9 May 2012 for both the 300 kHz and the 600 kHz instruments. Each instrument was mounted in the deployment cage along with the external battery module and was located away from potential sources of magnetic field disturbances. The ADCP was mounted to a turntable, which was aligned with magnetic north using a surveyor's compass. Using the built-in RDI calibration procedure, the instrument was tilted in one direction between 10 and 20 degrees and then rotated through 360 degrees at less than 5 ° /sec. The ADCP was then tilted in a different direction and a second rotation made. Based on the results from the first two rotations, calibration parameters are temporarily loaded and the instrument, tilted in a third direction is rotated once more to check the calibration. Results from each pre-deployment field calibration are shown in Table 5-4 (Figure 5-10).

Table 5-4. Results from the WHOTS-9 pre-deployment ADCP compass field calibration procedure.

300 kHz (SN 7637)	Single Cycle Error (°)	Double Cycle Error (°)	Largest Double + Single Cycle Error (°)	RMS of 3rd Order and Higher + Random Error (°)	**Over all Error** (°)	Pitch Mean and Standard Deviation (°)	Roll Mean and Standard Deviation (°)
Before Calibration	10.24	0.63	0.88	0.25	**10.28**	14.90±0.85	-1.03±0.81
	8.89	1.04	9.92	0.23	**9.12**	0.51 ±0.82	11.42 ±0.99
After Calibration	0.45	0.12	0.57	0.20	**0.48**	-14.71 ±0.89	-0.23 ±0.82

600 kHz (SN 13917)	Single Cycle Error (°)	Double Cycle Error (°)	Largest Double + Single Cycle Error (°)	RMS of 3rd Order and Higher + Random Error (°)	**Over all Error** (°)	Pitch Mean and Standard Deviation (°)	Roll Mean and Standard Deviation (°)
Before Calibration	3.19	0.15	3.33	0.17	**3.18**	-13.53 ±0.77	-0.12 ±0.85
	3.20	0.54	3.74	0.15	**3.21**	-0.27 ±0.80	-10.95 ±0.92
After Calibration	0.18	0.10	0.28	0.12	**0.23**	12.29 ±0.79	-0.29 ±0.83

Post-Deployment

After the WHOTS-9 mooring was recovered, the performance of the ADCP compass was tested at the football field of the University of Hawai'i at Manoa on 12 August 2013 with an identical compass calibration procedure as during the pre-deployment calibration. Results from the WHOTS-9 post-deployment ADCP compass field calibration procedure are listed in Table 5-5 (Figure 5-11).

Table 5-5. Results from the WHOTS-9 post-deployment ADCP compass field calibration procedure

300 kHz	Single Cycle Error (°)	Double Cycle Error (°)	Largest Double + Single Cycle Error (°)	RMS of 3rd Order and Higher + Random Error (°)	**Over all Error** (°)	Pitch Mean and Standard Deviation (°)	Roll Mean and Standard Deviation (°)
After Calibration	0.95	0.51	1.46	0.19	**1.22**	0.90±0.76	-0.31±0.73

600 kHz	Single Cycle Error (°)	Double Cycle Error (°)	Largest Double + Single Cycle Error (°)	RMS of 3rd Order and Higher + Random Error (°)	**Over all Error** (°)	Pitch Mean and Standard Deviation (°)	Roll Mean and Standard Deviation (°)
After Calibration	2.85	0.12	2.97	0.18	**2.87**	-0.30±0.74	0.80±1.03

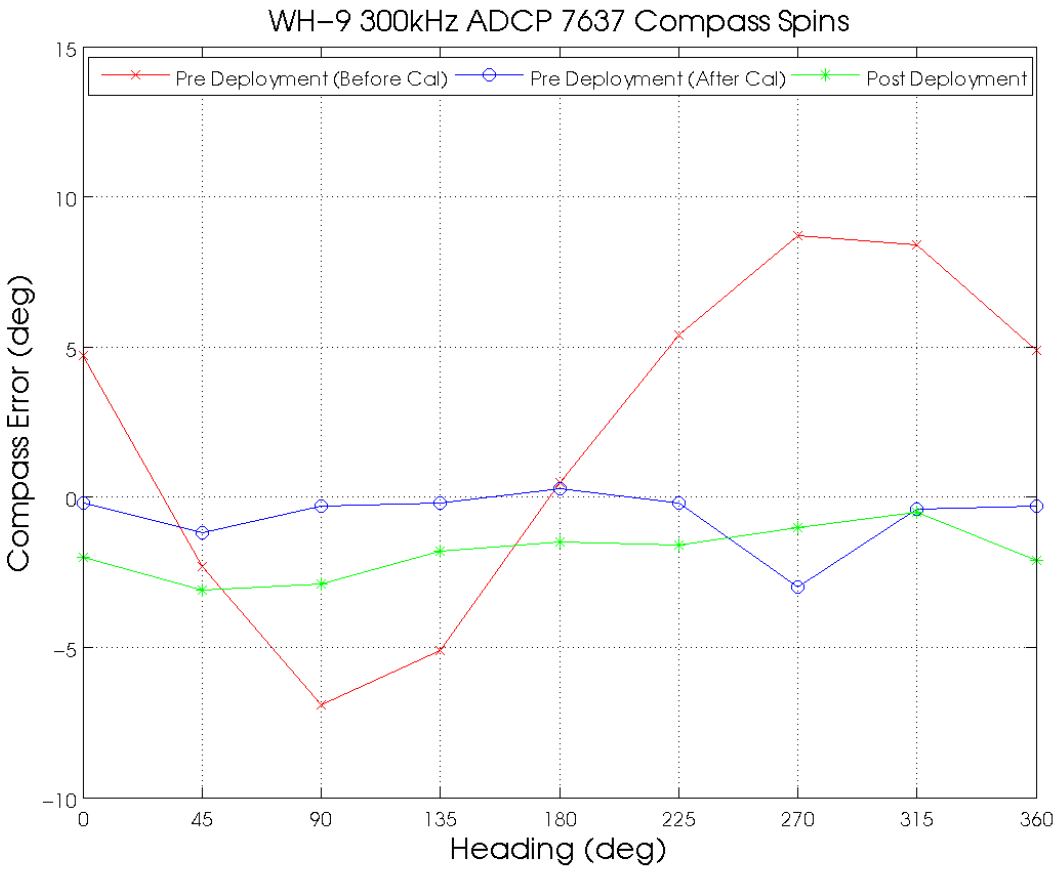

Figure 5-10. Results of the post-cruise compass calibration, conducted August 2013 on ADCP SN7637 at the University of Hawai'i at Manoa.

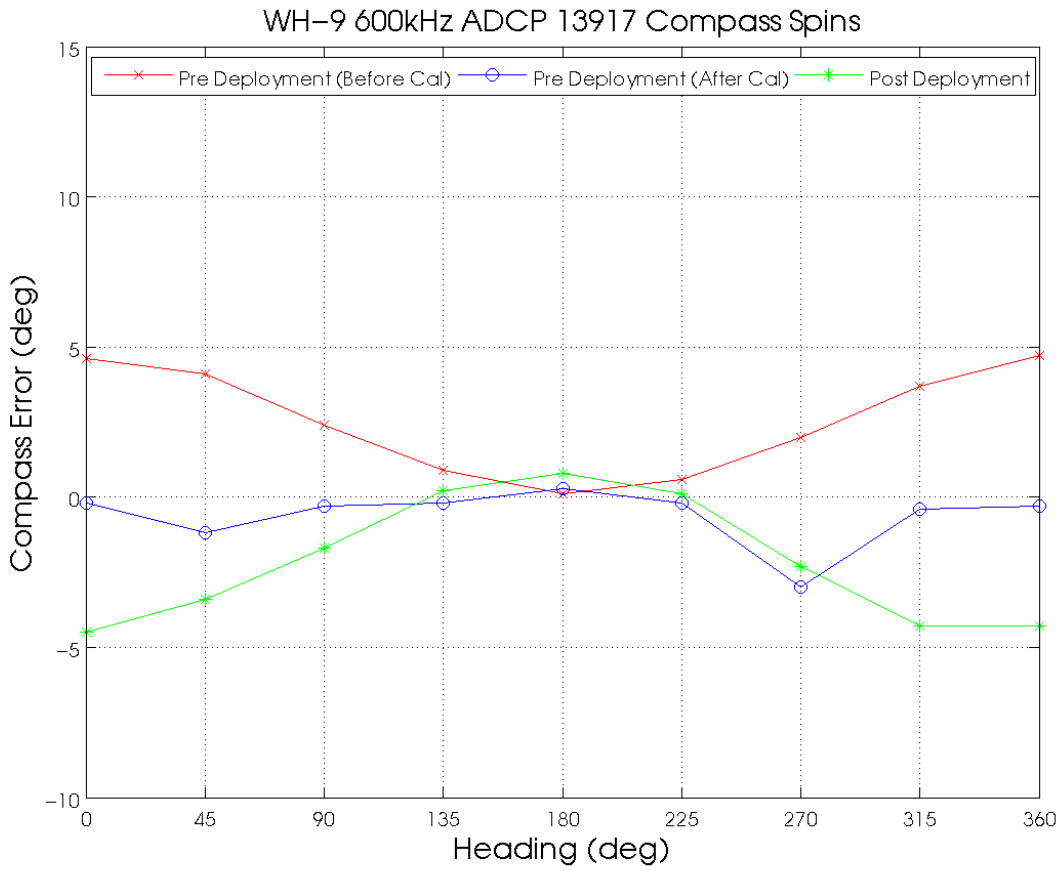

Figure 5-11. Results of the post-cruise compass calibration, conducted 12 August 2013, on ADCP SN13917 at the University of Hawai'i at Manoa.

2. ADCP Configurations

Individual configurations for the two ADCP's on the WHOTS-9 mooring are detailed in Appendices 1 and 2. The salient differences for each of the ADCP's are summarized below.

300 kHz (125m)

The ADCP, set to a beam frequency of 300 kHz, was configured in a burst sampling mode consisting of 40 pings per ensemble in order to resolve low-frequency wave orbital motions. The interval between each ping was 4 seconds so the ensemble length was 160 seconds. The interval between ensembles was 10 minutes. Data were recorded in earth coordinates with a heading bias of 9.52° E used. This heading bias was corrected in post-deployment processing to a heading bias of 10.18° E. False targets, usually fish, were screened by setting the threshold maximum to 70 counts. Velocity data were rejected if the difference in echo intensity among the four beams exceeded this threshold.

600 kHz (47.5m)

The ADCP, set to a beam frequency of 600 kHz, was configured in a burst sampling mode consisting of 80 pings per ensemble. The interval between each ping was 2 seconds so the ensemble length was also 160 seconds. The interval between ensembles was 10 minutes. Data were recorded in earth coordinates with a heading bias of 9.52° E used. This heading bias was corrected in post-deployment processing to a heading bias of 10.18° E. The threshold maximum was also set to 70 counts. Velocity data were rejected if the difference in echo intensity among the four beams exceeded this threshold.

3. ADCP data processing procedures

Binary files output from the ADCP were read and converted to MATLAB™ binary files using scripts developed by Eric Firing's ADCP lab (http://current.soest.hawaii.edu). The beginning of the raw data files were truncated to a time after the mooring anchor was released in order to allow time for the anchor to reach the seabed and for the mooring motions that follow the impact of the anchor on the sea floor to dissipate. The pitch, roll, and ADCP temperature were examined in order to pick reasonable times that ensured good data quality but without unnecessarily discarding too much data (see Figure 5-12 and Figure 5-13). Truncation at the end of the data files were chosen to be the ensemble prior to the time that the acoustic release signal was sent to avoid contamination due to the ascent of the instrument. The times of the first ensemble from the raw data, deployment and recovery time, along with the times of the truncated records of both deployments are shown in Table 5-6.

Table 5-6. ADCP record times (UTC) during WHOTS-9 deployment.

	300 kHz	600 kHz
Raw file beginning and end times	07-Jun-2012 00:00 15-Jul-2013 21:50:00	07-Jun-2012 00:00 15-Jul-2013 19:59
Deployment and recovery times	13-Jun-2012 20:19 in water 14-Jun-2012 02:24 anchor over 14-Jul-2013 16:17 release triggered 15-Jul-2013 01:25 on deck	13-Jun-2012 19:49 in water 14-Jun-2012 02:24 anchor over 14-Jul-2013 16:17 release triggered 15-Jul-2013 02:04 on deck
Processed data beginning and end times	14-Jun-2012 03:30 14-Jul-2013 15:00	14-Jun-2012 03:30 14-Jul-2013 14:59

ADCP Clock Drift

Upon recovery, the ADCP clocks were compared with the ship's time server and the difference between the two was recorded. It was found that for 300 kHz (SN 7637) ADCP the clock on the instrument was slow by 12 seconds. The clock on the 600 kHz (SN13917) was fast by 9 minutes and 7 seconds. Past deployments of the ADCP's suggest a 9 minute difference isn't unusual. Since the drift represents just one ensemble out of a total of over 58,000, no corrections

were made. However this drift may be significant if the data are used for time dependent analysis such as tidal or spectrum analysis, a drift correction needs to be applied in those cases.

Heading Bias

As mentioned in the ADCP configuration section, the data were recorded in earth coordinates. A heading bias, the angle between magnetic north and true north, can be included in the setup to obtain output data in true earth coordinates. Magnetic variation was obtained from the National Geophysical Data Center 'Geomag' calculator. (http://www.ngdc.noaa.gov/seg/geomag). For a year long deployment a constant value is acceptable because the change in declination is small, approximately -0.02° year^{-1} at the WHOTS location. A heading bias of 9.52° was entered in the setup of the WHOTS-9 ADCP's, but was corrected to 10.18° during post-deployment processing.

Speed of sound

Due to the constant of proportionality between the Doppler shift and water speed, the speed of sound needs only be measured at the transducer head (Firing, 1991). The sound speed used by the ADCP is calculated using a constant value of salinity (35) and the temperature recorded by the transducer temperature sensor of the ADCP. Using CTD profiles close to the mooring during HOT cruises, HOT-243 to HOT-253, and from the WHOTS deployment/recovery cruises, the mean salinity at 125 dbar was 35.34 while the mean salinity at 47.5 dbar was 35.24. Mean ADCP temperature at 125 dbar was 22.19 °C and 24.52 °C at 47.5 dbar (Figure 5-14). The maximum associated mean sound velocity difference is less than 0.4 m s^{-1} which represents a change of less than 0.03%, so no correction was made.

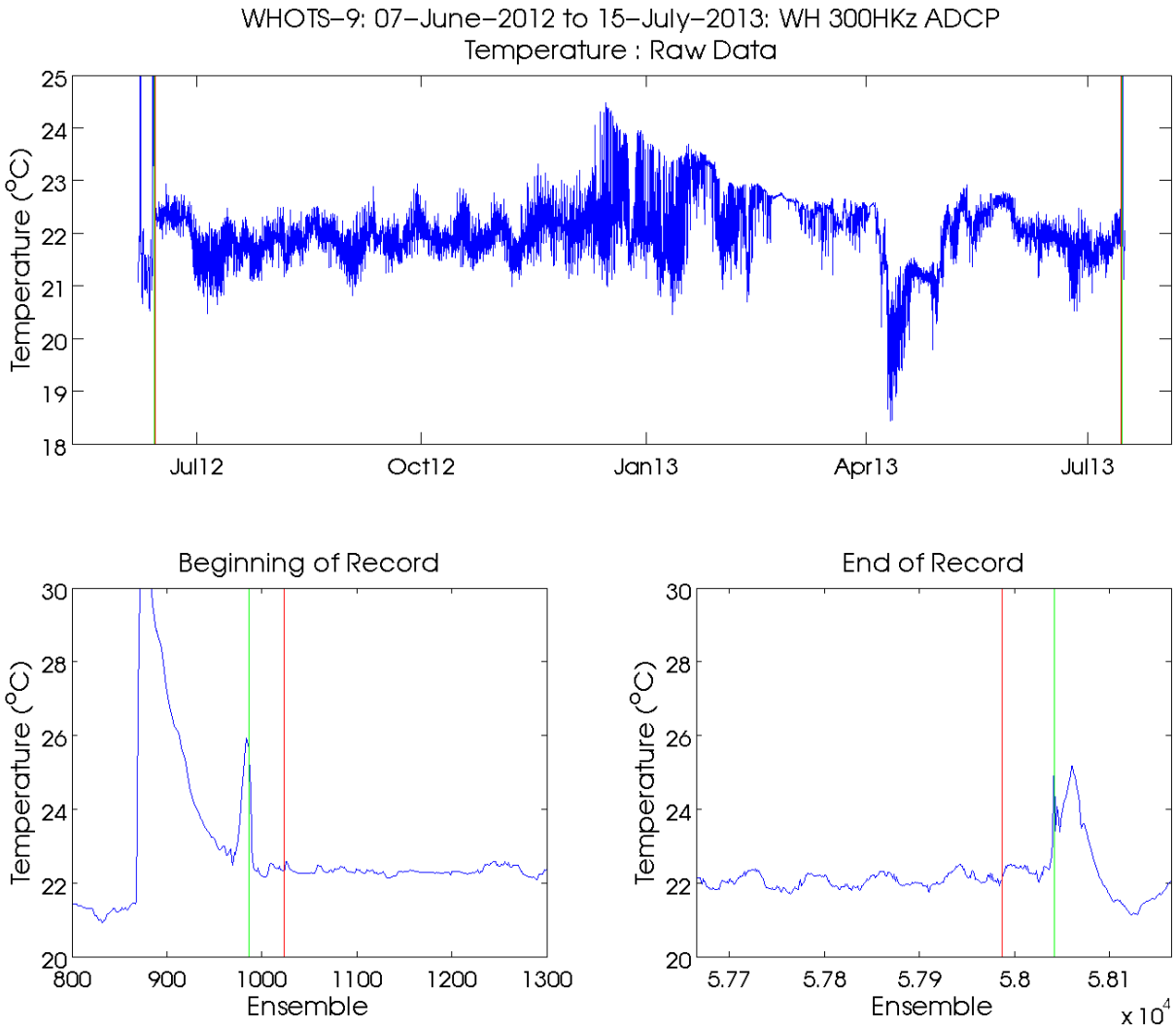

Figure 5-12. Temperature record from the 300 kHz ADCP during WHOTS-9 mooring (top panel). The bottom panel shows the beginning and end of the record with the green vertical line representing the in-water time during deployment and out-of-water time for recovery. The red line represents the anchor release and acoustic release trigger for deployment and recovery respectively.

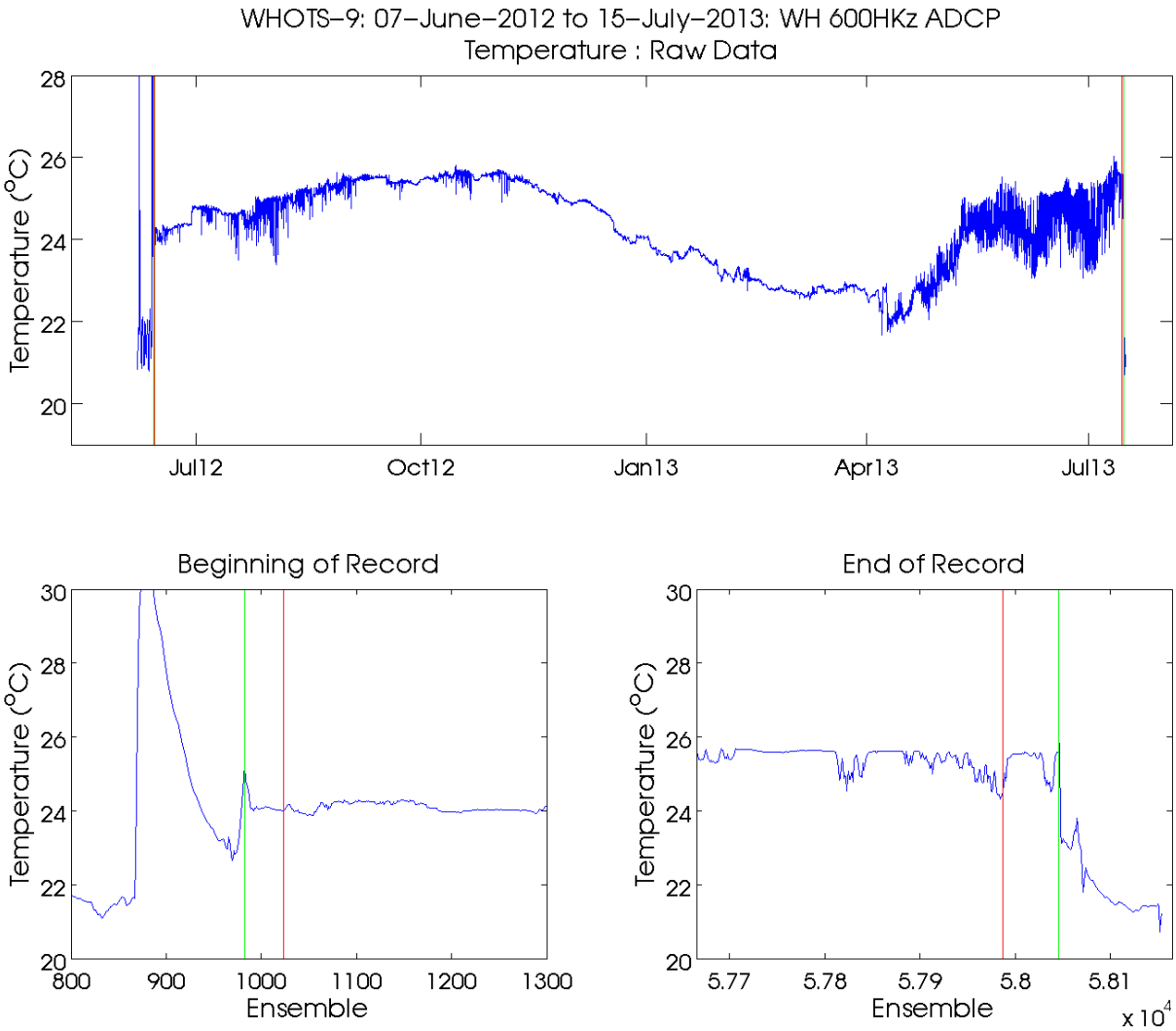

Figure 5-13. Same as Figure 5-26, but for the 600 kHz ADCP.

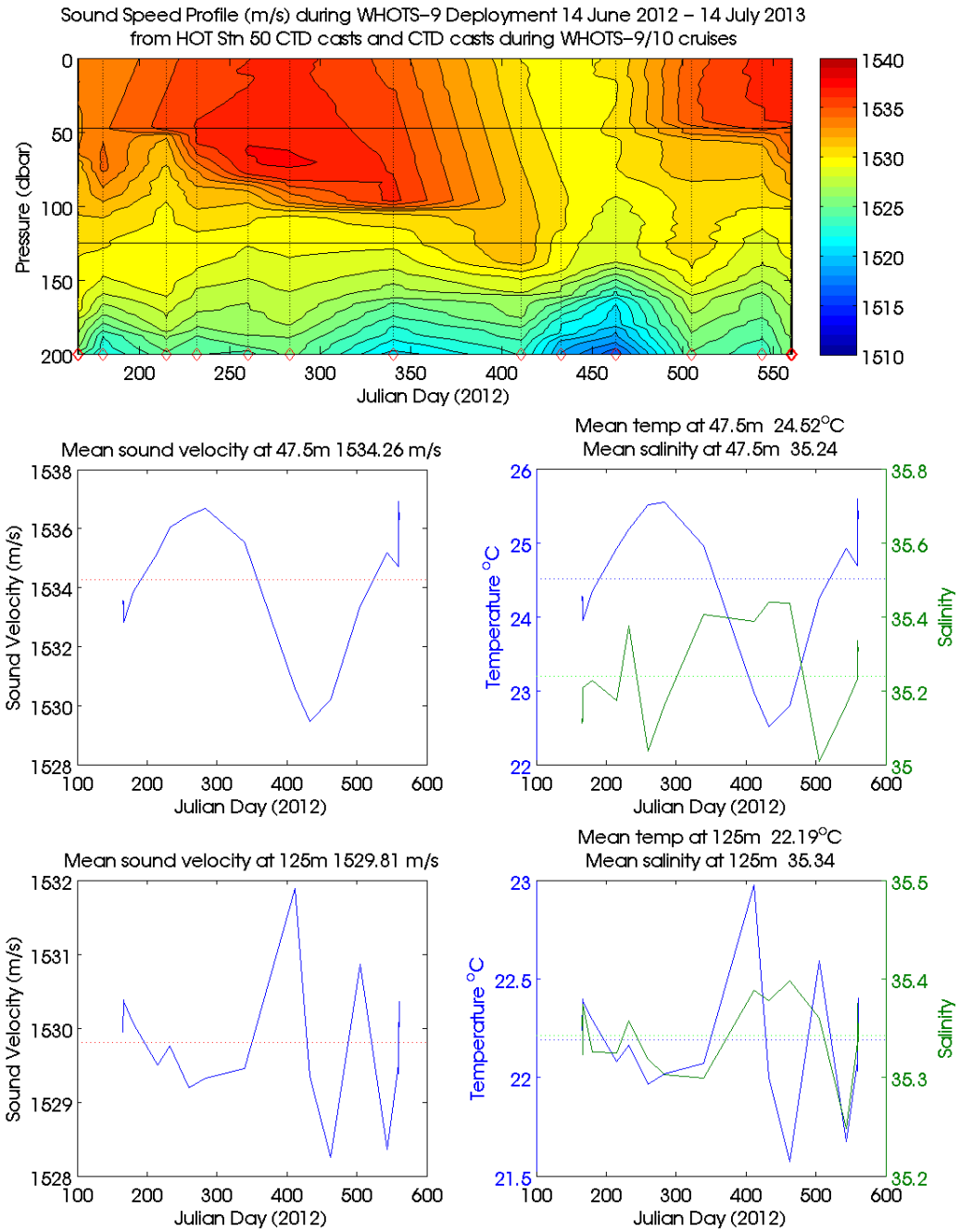

Figure 5-14. Sound speed profile (top panel) during the deployment of the WHOTS-9 mooring from 2 dbar CTD data taken during regular HOT cruises and CTD profiles taken during the WHOTS-10 recovery/deployment cruise (individual casts marked with a red diamond). The bottom left panels show the sound velocity at the depth of the ADCP's (47.5 m and 125 m), with the mean sound velocity indicated with a red line. The lower right panels show the temperature and salinity at each ADCP depth for the time series with the mean temperatures indicated with blue lines and mean salinity indicated with green lines.

Quality Control

Quality control of the ADCP data involved the thorough examination of the velocity, instrument orientation and diagnostic fields to develop the basis of the QC flagging procedures. Details of the methods used can be found in the WHOTS Data Report 1 (Santiago-Mandujano et al., 2007). The following QC procedures were applied to the WHOTS-9 deployment ADCP data.

1) The first bin (closest to the transducer) is sometimes corrupted due to what is known as ringing. A period of time is needed for the sound energy produced during a transmit pulse at the transducer to dissipate before the ADCP is able to properly receive the returned echoes. The blanking interval is used to prevent useless data from being recorded. If it is too short, signal returns can be contaminated from the lingering noise from the transducer. The default value for the blanking interval, (expressed as a distance) of 1.76 m was used for the 300 kHz ADCP, whereas an interval of 0.88 m was used for the 600 kHz ADCP. Thus bin 1 was flagged and replaced with Not a Number (NaN) in the quality controlled dataset (Figure 5-15).

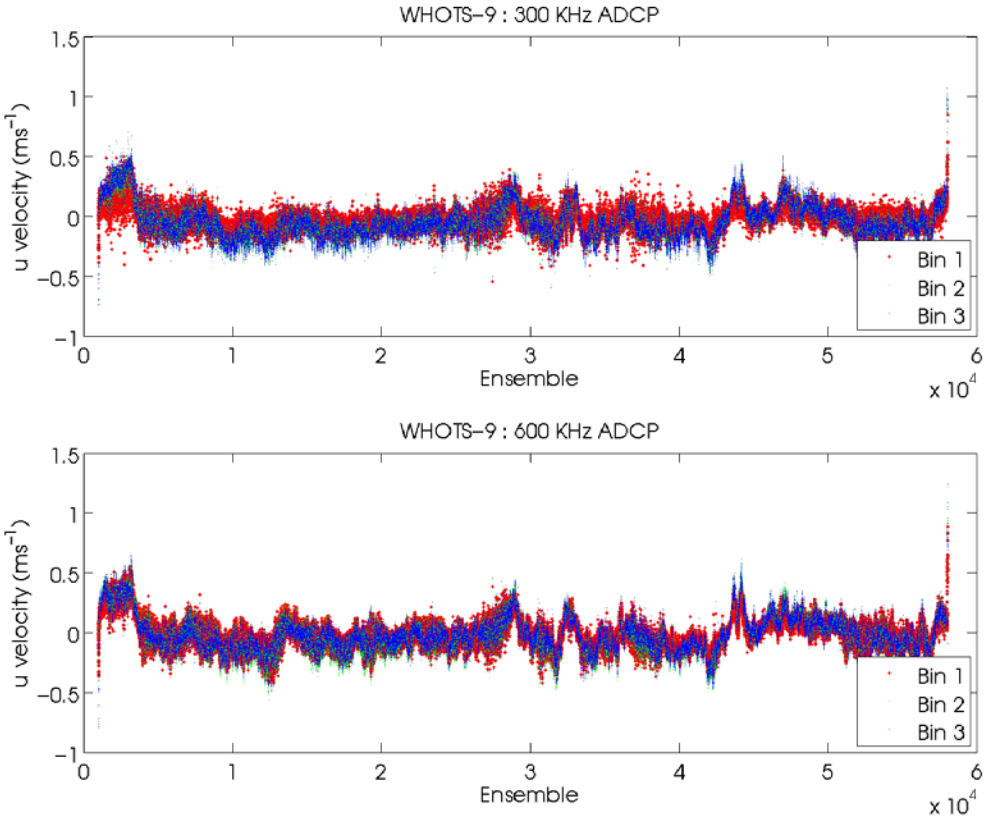

Figure 5-15. Eastward velocity component for the 300 kHz (top panel) and the 600 kHz (bottom panel) ADCPs showing the incoherence between depth 1 (red) and bins 2 (green) and 3 (blue).

2) For an upward-looking ADCP with a beam angle of 20° within range of the sea surface, the upper 6% of the depth range is contaminated with sidelobe interference (RDI, 1996). This is a result of stronger signal reflection from the sea surface (than from scatterers) overwhelming the sidelobe suppression of the transducer. Data are flagged using echo intensity (a measure of the strength of the return signal) from each beam to determine when the signal is contaminated with reflection from the sea surface. In practice, the majority of the data within the upper 4 bins (~14% of the vertical range) were flagged. These upper 4 bins range from about 15 m up to the sea surface.

3) The use of four beams (along with instrument orientation) to resolve currents into their component earth-referenced velocities provides us with a second estimate of the vertical velocity. The scaled difference between these estimates is defined as the error velocity and it is useful for assessing data quality. Error velocities with an absolute magnitude greater than 0.15 m s^{-1} (a value comparable to the standard deviation of observed horizontal velocities) were flagged and removed.

4) An indication of data quality for each ensemble is given by the "percent good" data indicator which accompanies each individual beam for each individual bin. The use of the percent good indicator is determined by the coordinate transformation mode used during the data collection. With profiles transformed into earth coordinates (as in the case of the WHOTS-9 deployment) the percent good fields show the percentage of data that was made using 4 and 3 beam solutions in each depth cell within an ensemble, and the percentage that was rejected as a result of failing one of the criteria set during the instrument setup (see Appendix 1: WHOTS-9 300 kHz ADCP Configuration). Data were flagged when data in each depth cell within an ensemble made from 3 or 4 beam solutions was 20% or less.

5) Data were rejected using correlation magnitude, which is the pulse-to-pulse correlation (in ping returns) for each depth cell. If anyone beam had a correlation magnitude of 20 counts or less, that data point was flagged.

6) Histograms of raw vertical velocity data and partially cleaned data from the ADCP [see Figure 5-16 and the WHOTS Data Report 1 (Santiago-Mandujano et al., 2007)] showed vertical velocities larger than expected, some exceeding 1 m s^{-1}. Recall that the instruments' burst sampling (4-second intervals for the 300 kHz and 2-second intervals for the 600 kHz, for 160 seconds every 10 minutes) was designed to minimize aliasing by occasional large ocean swell orbital motions (Section 3), and therefore are not the source of these large speeds in the data. These large vertical speeds are possibly fish swimming in the beams based on the histograms of the partially cleaned data; depth cells with an absolute value of vertical velocity greater than 0.3 m s^{-1} were flagged.

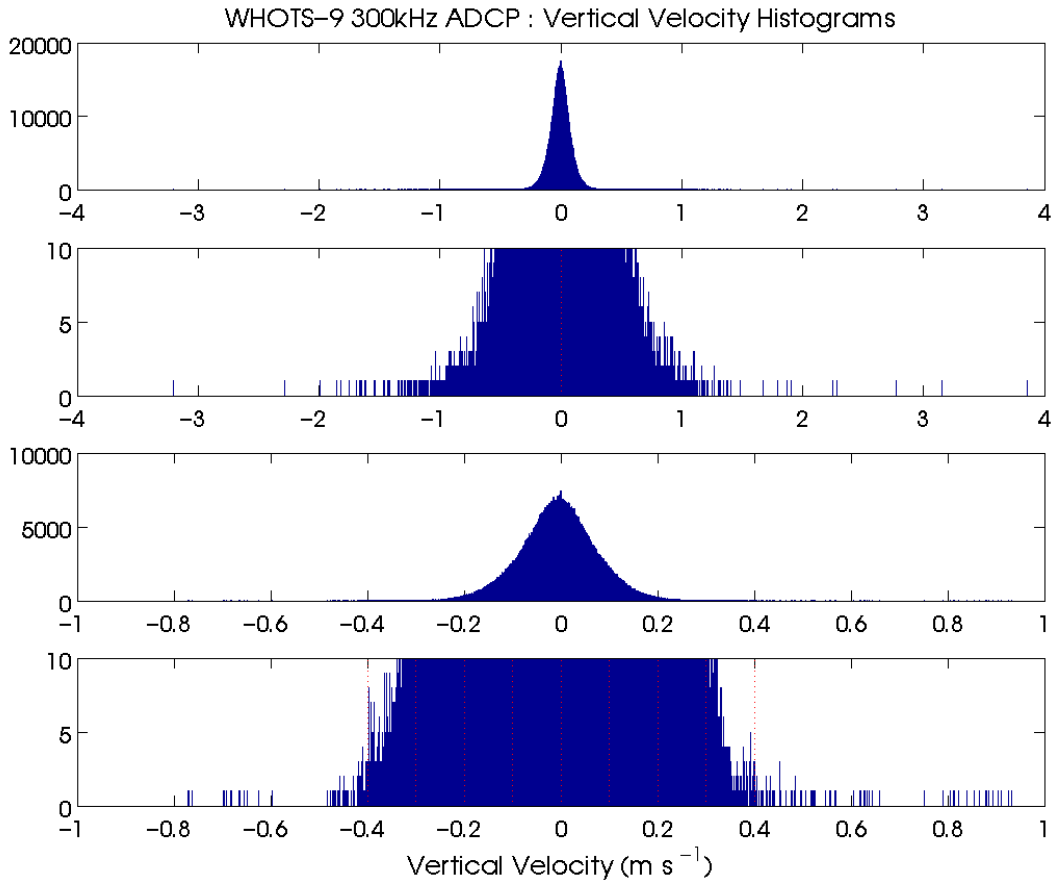

Figure 5-16. Histogram of vertical velocity of the 300 kHz ADCP for raw data (top panel) and enlarged for clarity (upper middle panel), and for partial quality controlled data (lower middle panel) and enlarged for clarity (bottom).

7) A quality control routine known as 'edgers' identifies outliers in surface bins using a five point median differencing method. The median velocity from surface bins was calculated for each ensemble, and then a five point running median of the surface bin median was calculated. This was then compared to individual velocity observations in the surface bins, and those differing by greater than 0.48 m/s were flagged.

8) A 5-pole low pass Butterworth filter with a cutoff frequency of 1/4 cycles/hour was used upon the length of the time-series to isolate low frequency flow for each bin independently. The low frequency flow is then subtracted giving a time series of high frequency velocity component fluctuations for each bin. Data points were considered outliers when their values exceeded four standard deviations from the mean (for each bin) and were removed.

9) A median residual filter used a 7-point (70 minute) median differencing method to define velocity fluctuations. A 7-point running median is calculated for each bin independently and the result is subtracted out giving time series of fluctuations relative

to the running median. Outliers greater than four standard deviations from the mean of the 7 points are flagged and removed for each bin.

10) Meticulous verification of all the quality control routines was performed through visual inspections of the quality controlled velocity data. Two methods were utilized; time-series of u and v components for multiple bins were evaluated as well as individual vertical profiles. The time-series methodology involved inspecting u and v components separately, five bins at a time, over 600 ensembles (100 hours). Any instance showing one bin behaving erratically from the other four bins was investigated further. If it seemed that there could be no reasonable rationale for the erratic points from the identified bin, the points were flagged [see Figure 5-17 and Figure 5-18 and the WHOTS Data Report 1 (Santiago-Mandujano et al., 2007)]. The intent of the vertical inspection of vertical profiles of the u and v components was to find entire profiles that were not aligned with neighboring profiles. Thirty u and v profiles were stacked at a time and were visually inspected for any anomalous data.

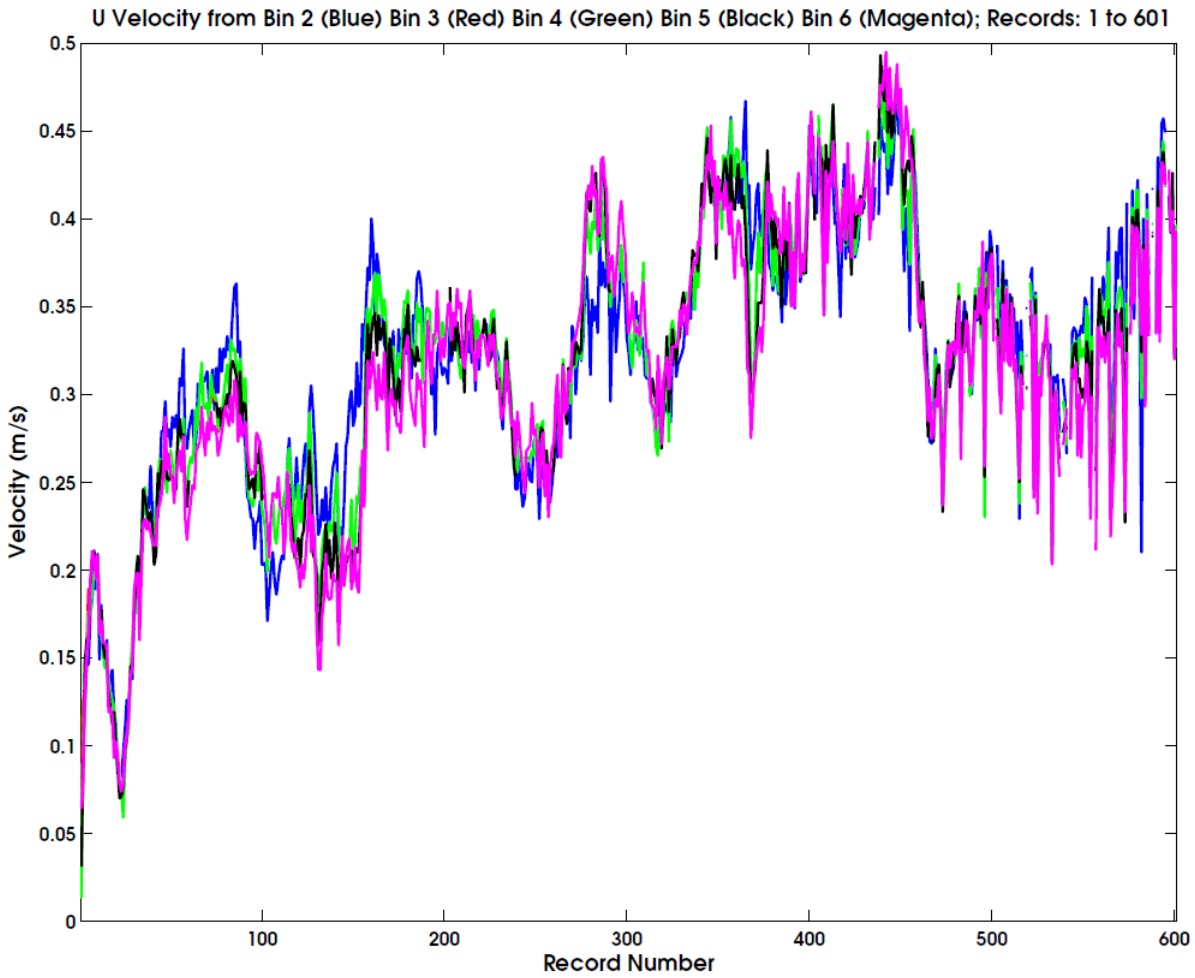

Figure 5-17. A sample of the horizontal inspection during WHOTS ADCP quality control

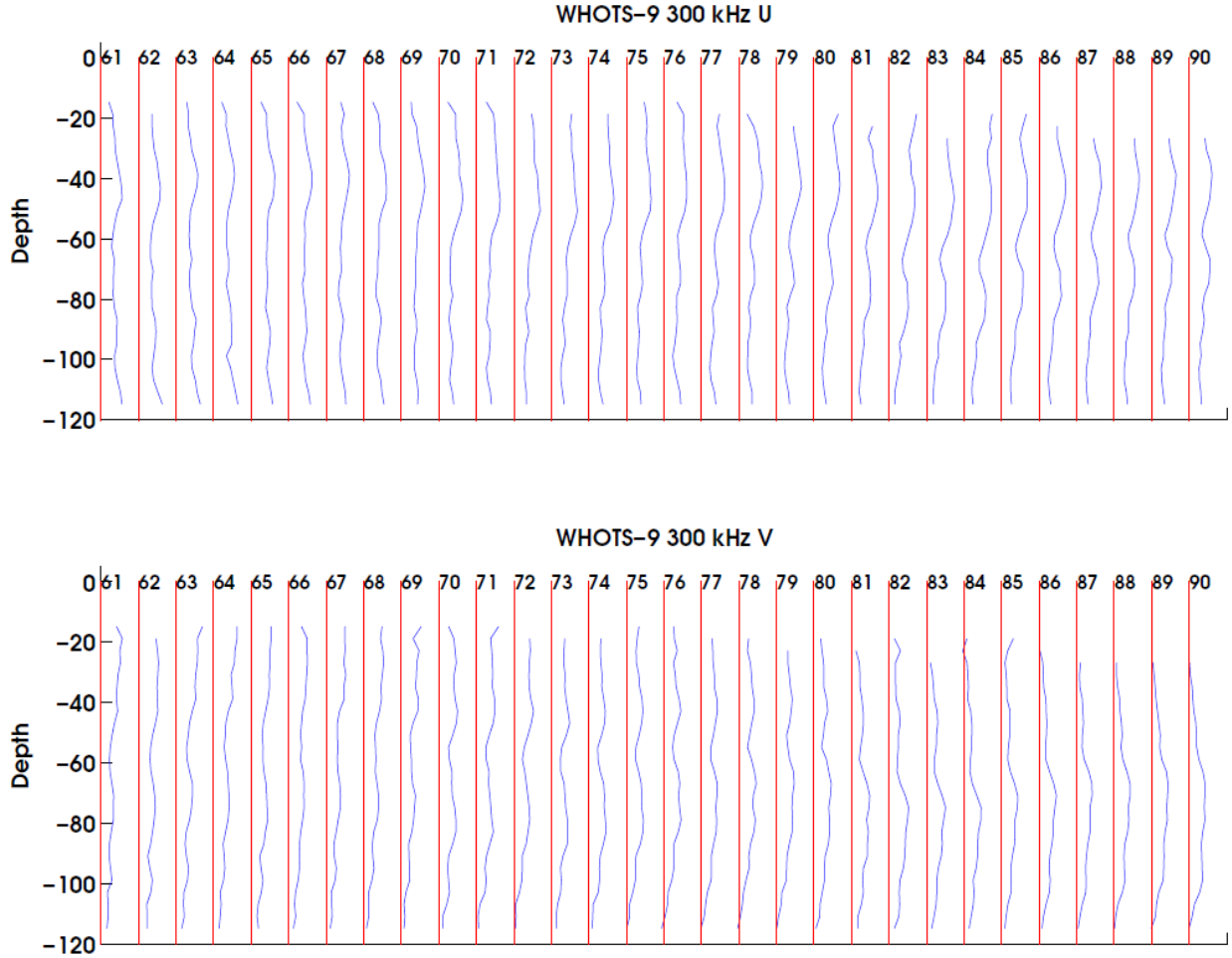

Figure 5-18. A sample of the profile consistency inspection from the WHOTS-9 ADCP quality control.

C. Vector Measuring Current Meter (VMCM)

Vector measuring current meters (VMCM) were deployed on the WHOTS-9 mooring at depths of 10 m and 30 m. VMCM data were processed by the WHOI/UOP group. A copy of the processing report is in Appendix 3 in Section 8.C. VMCM record times are shown in Table 5-7.

Table 5-7. Record times (UTC) for the VMCMs at 10 m and 30 m during the WHOTS-9 deployment

	WHOTS-9	
	VMCM011	VMCM061
Deployment and recovery times	13-Jun-2012 18:32 15-Jul-2013 03:27	13-Jun-2012 18:18 15-Jul-2013 03:40

Processed file beginning and end times	14-Jun-2012 04:00 14-Jul-2013 16:00	14-Jun-2012 04:00 14-Jul-2013 16:00

Daily (24 hour) moving averages of quality controlled 600 kHz ADCP data are compared to VMCM data interpolated to the ADCP ensemble times in the top panels of Figure 5-19 through Figure 5-22, and the difference is shown in the middle panels. The absolute value of the mean difference plus or minus one standard deviation is shown at the top of the middle panel. Velocities are not compared if greater than 80% of the ADCP data within a 24 hour average was flagged. The absolute value of mean differences for all deployments and both velocity components varied between 3 and 4 cm/s, with standard deviations between 2.5 and 5 cm/s. The VMCM data does not appear to degrade over time for any deployment. Propeller fouling would dampen measured VMCM velocity magnitudes, but a decrease in VMCM velocity magnitude compared to ADCP velocity magnitude with time is not observed.

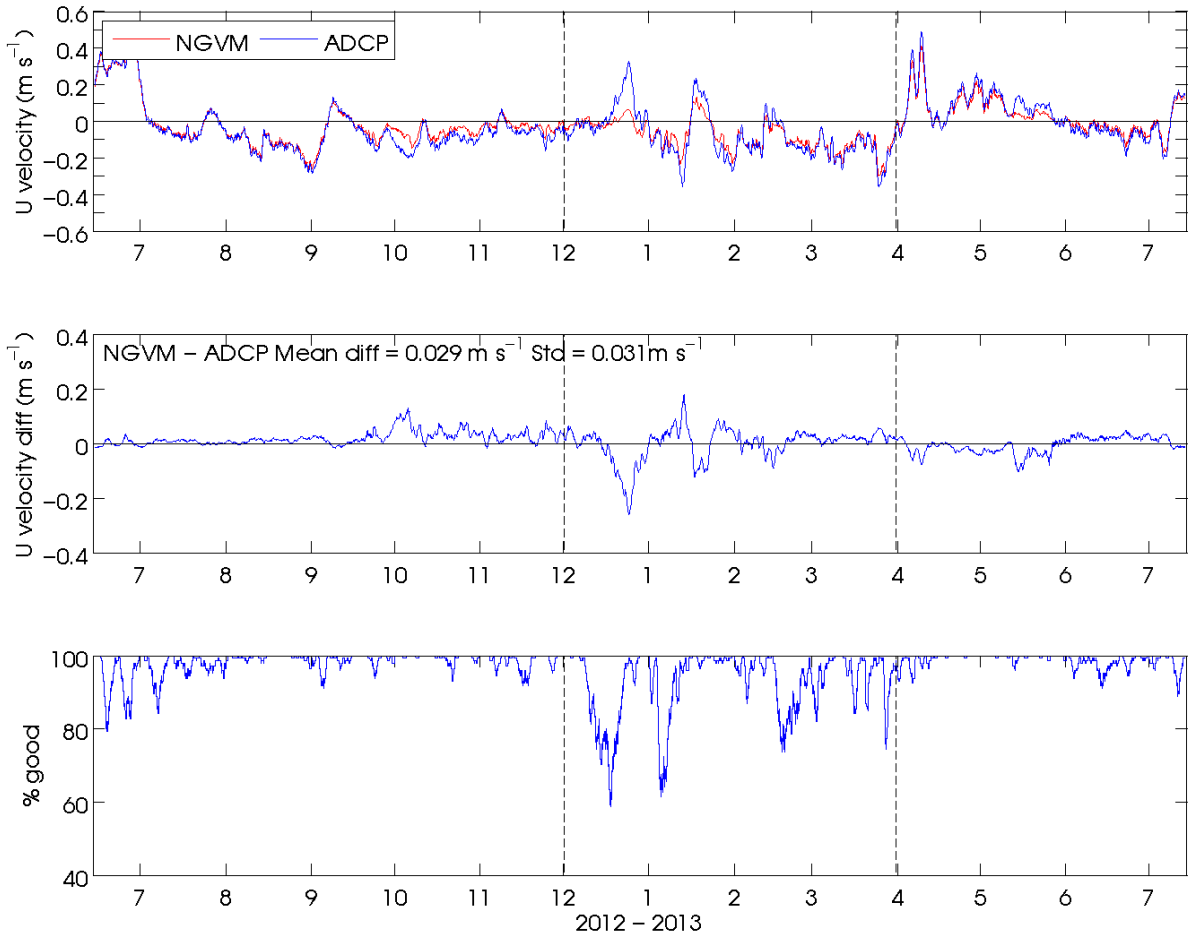

Figure 5-19. A comparison of 30 m VMCM and ADCP U velocity for WHOTS-9. The top panel shows 24 hour moving averages of VMCM zonal (U) velocity at 30 m depth (red) and ADCP U velocity from the nearest depth bin to 30 m (30.22 m). The middle panel shows the U velocity difference, and the bottom panel shows the percentage of ADCP data within the moving average not flagged by quality control methods. The dashed lines indicate a period of increased differences observed during spring months.

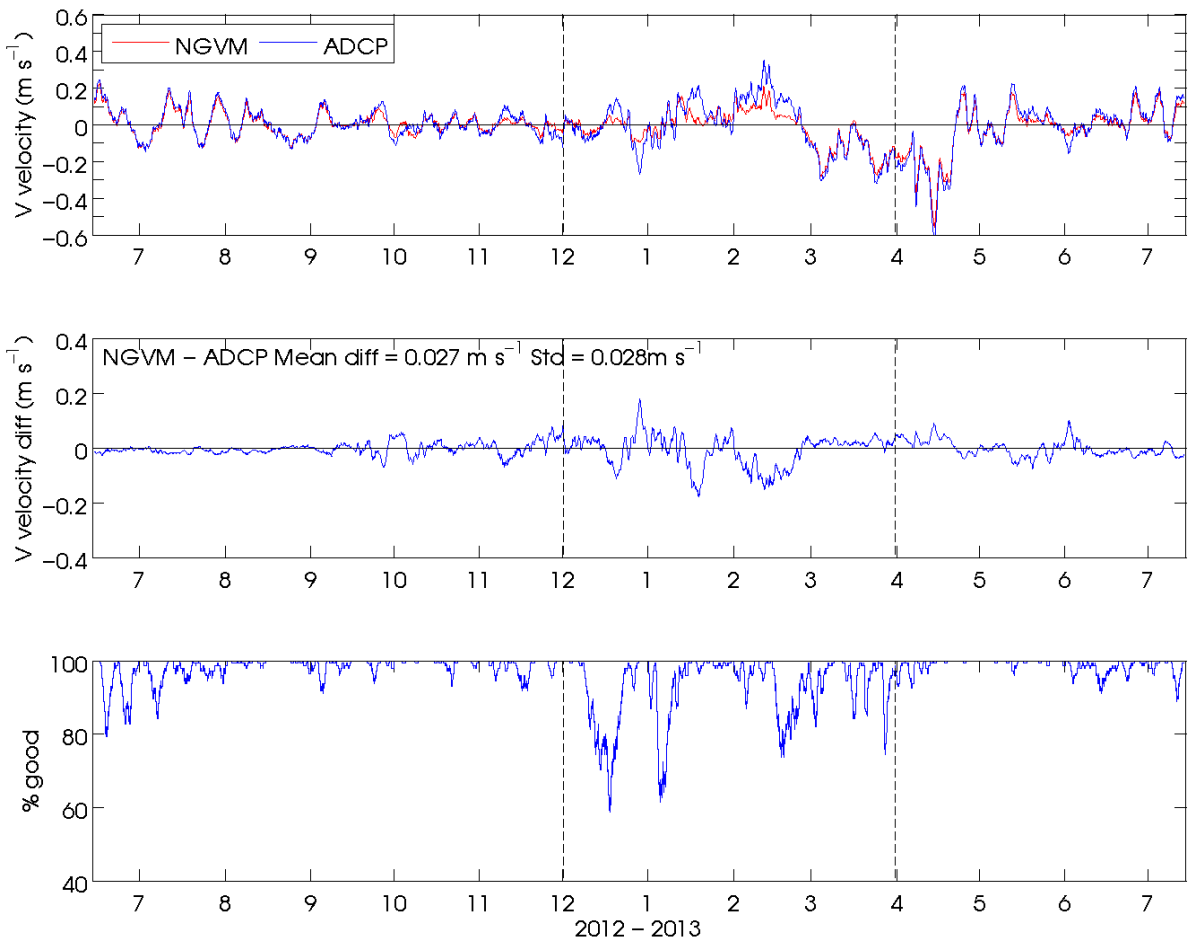

Figure 5-20. Same as in Figure 5-19 but for the meridional (V) velocity component.

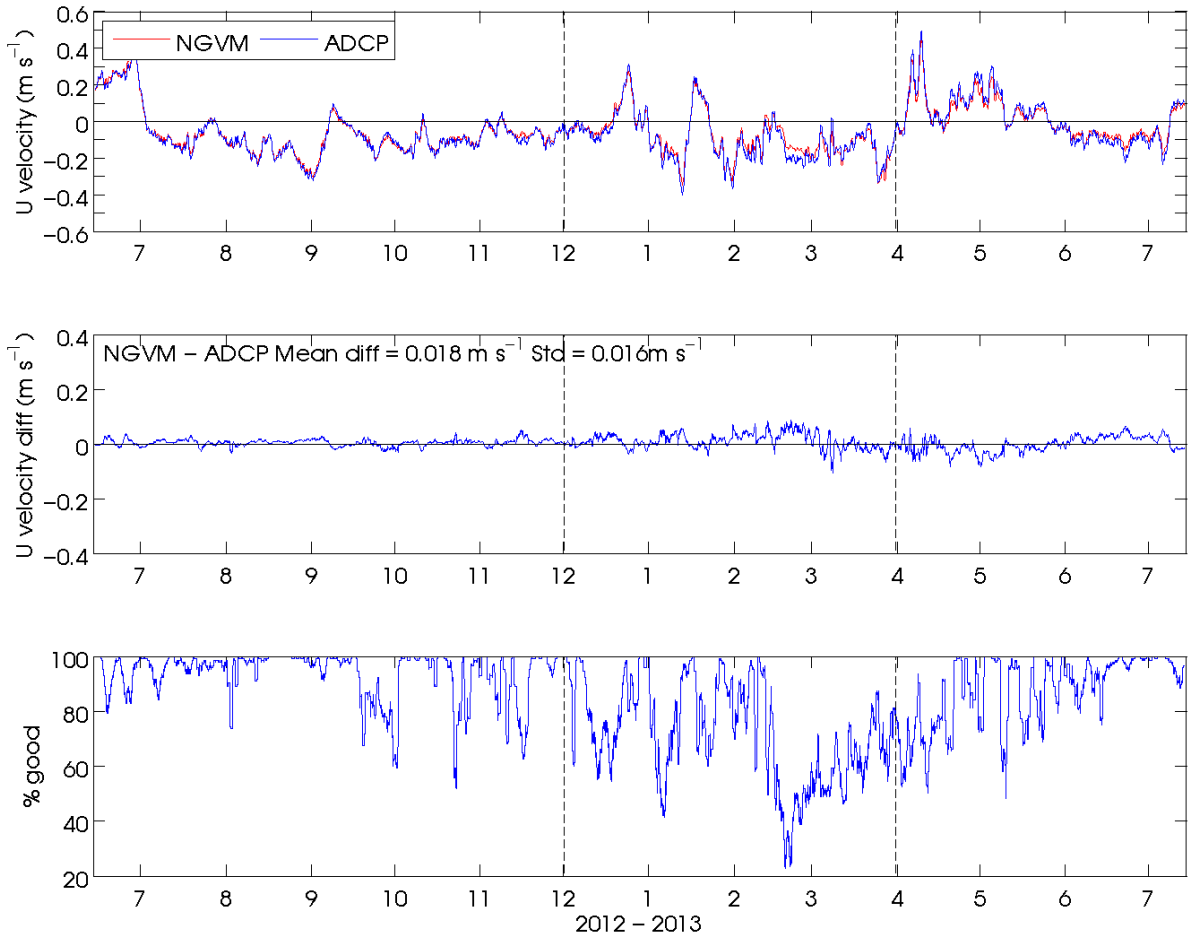

Figure 5-21. Same as in Figure 5-19 but for the 10 m VMCM.

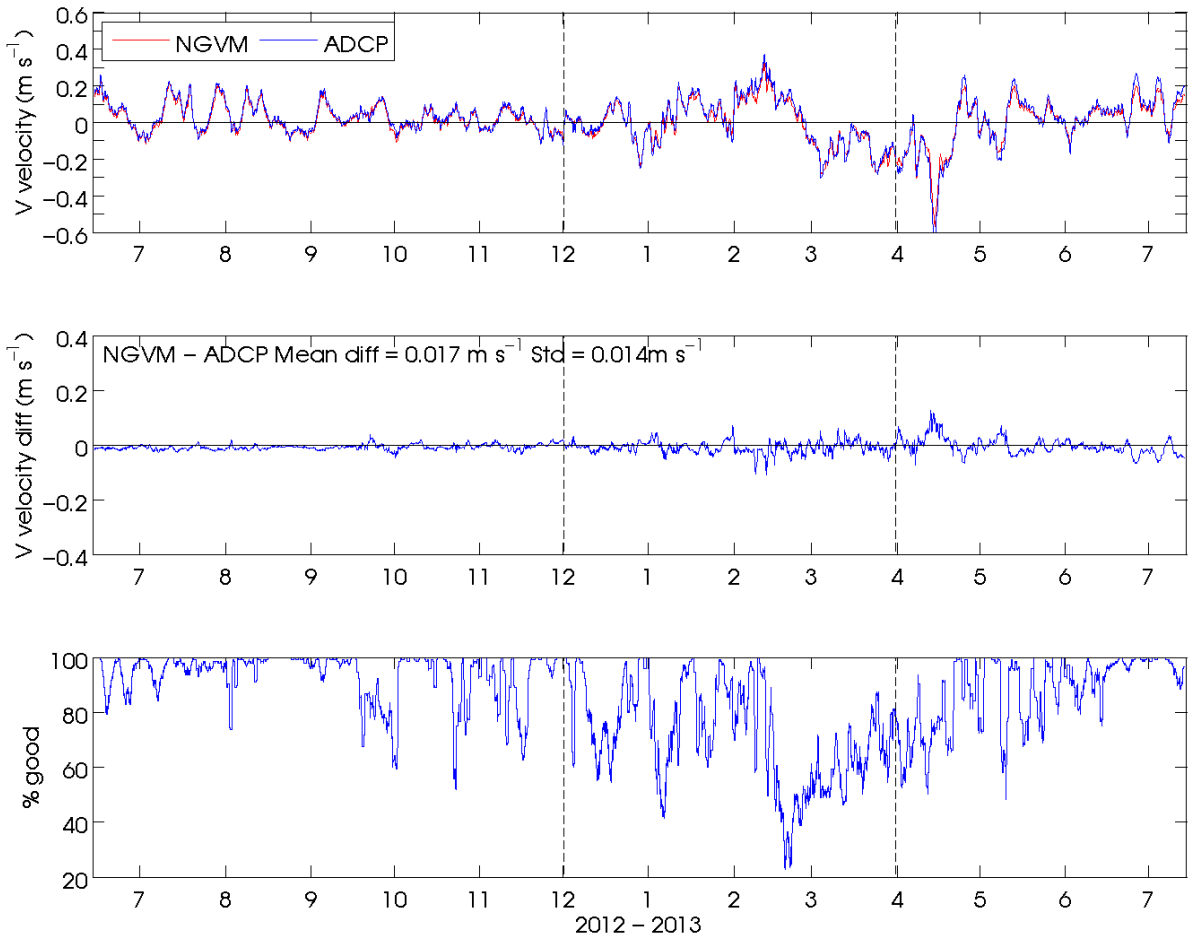

Figure 5-22. Same as in Figure 5-18 but for the V velocity component.

Velocity differences between the 10m VMCM and the 600 kHz ADCP were smaller in comparison to the 30m VMCM. A seasonal pattern in the "percent good" field is observed for both VMCM's, more notably and for a longer period in the 10m deployment. ADCP and VMCM velocities tend to agree most from summer to early winter, and larger differences often occur in late winter and spring. Specific ranges of time where VMCM velocity magnitudes are consistently larger than ADCP magnitudes in one or both components are indicated by the vertical dashed lines in Figure 5-19 through Figure 5-22.

D. Global Positioning System Receiver and ARGOS Positions

Xeos Global Positioning System receiver (IMEI 300634013701980) and ARGOS beacon SN9209 were attached to the tower top of the buoy during the WHOTS-9 deployment. Data returns from the receivers were high, but GPS data ended on 16 May 2013 (Table 5-8). The reason for the failure of the Xeos receiver is unknown.

Table 5-8. GPS and ARGOS record times (UTC) during WHOTS-9

WHOTS-9	Xeos GPS	ARGOS
Raw file beginning and end times	14-Jun-2012 03:40 16-May-2013 23:15	14-Jun-2012 04:18 16-Jul-2013 00:14

ARGOS positions were available during the WHOTS-9 deployment and they provided additional information on the buoy's motion. ARGOS data were recorded at 10 minutes intervals, although there are some small gaps at repeated times present in the records. Samples taken before mooring deployment were eliminated. Data were screened for points that were greater than 2.5 nautical miles from the surveyed anchor positions for each deployment which was considered to be the buoy watch circle radius. The velocity magnitude was calculated and positions that resulted in speeds greater than 1 m s^{-1} were removed. Data were interpolated onto a regular time grid in order to compute spectra.

For comparison, Figure 5-23 shows the ARGOS buoy's positions together with the GPS positions during the WHOTS-9 deployment. The standard deviation of the difference between these two records is about 360 m.

The ARGOS positions of the WHOTS-9 buoy for the duration of the deployment are in Figure 5-24, and shows the color-coded positions according to their data quality. The data quality is determined by its distance from the satellite track. Data of a better quality have a higher flag number: 3 is for a distance less than 150 m, 2 is for a distance between 150 and 350 m, and 1 is for a distance between 350 and 1000 m. For the duration of the deployment, the buoy had a mean position of about 3 km from the anchor, with a standard deviation of about 600 m.

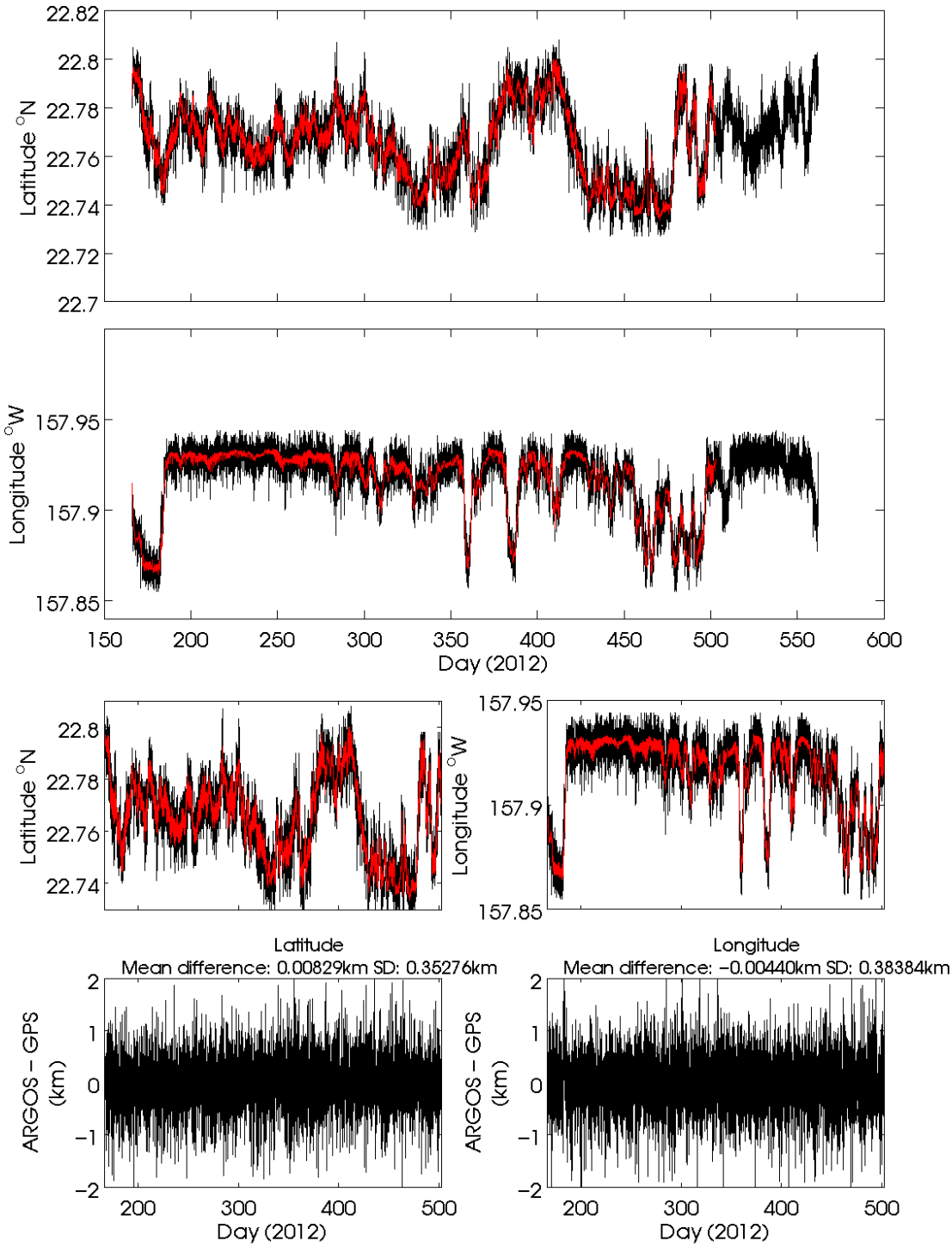

Figure 5-23. WHOTS-9 buoy position from ARGOS data (black line), and from GPS data (red line). The top and two middle panels show the latitude and longitude of the buoy. The bottom panel shows the difference between the GPS positions and the ARGOS positions interpolated to the GPS times.

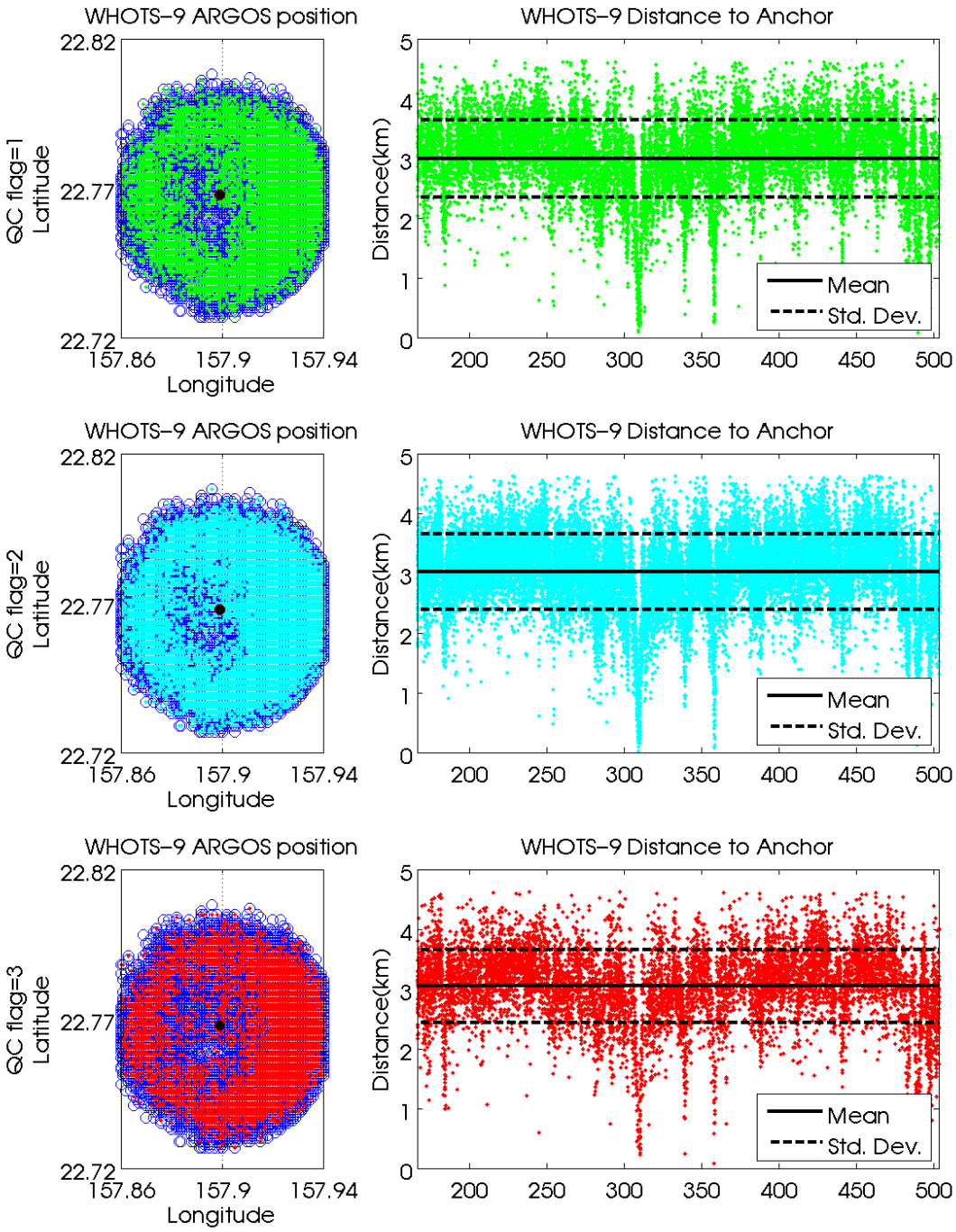

Figure 5-24. WHOTS-9 buoy ARGOS positions (circles, left panels), and distance from its anchor (dots, right panels). The data are colored according to their quality control flag, 1: green, 2: light blue, 3: red. The black circle in the center of the left side panels is the location of the mooring's anchor. The black line in the right panel plots is the mean distance between the buoy and its anchor, and the dashed line is the mean plus minus one standard deviation.

E. MAVS Acoustic Velocity Sensor

A Nobska MAVS acoustic velocity sensor (SN 10261) was deployed at 20 m on the WHOTS-9 mooring. Data return from the sensor was low, with velocity data only to September 2012 (see Figure 5-25). Data from the ‘A’ and ‘B’ transducer failed in September, with the ‘D’ transducer failing shortly thereafter in October (Figure 5-26). This issue has been observed in every deployment of the MAVS instrumentation on the WHOTS mooring. This failure has been evaluated by Nobska and it was determined that the bond between the piezoceramic transducer and the epoxy window delaminated, as electrically these transducers tested normal. This delaminated bond creates a thin air gap which separates the vibrating transducers from the water, attenuating the signal.

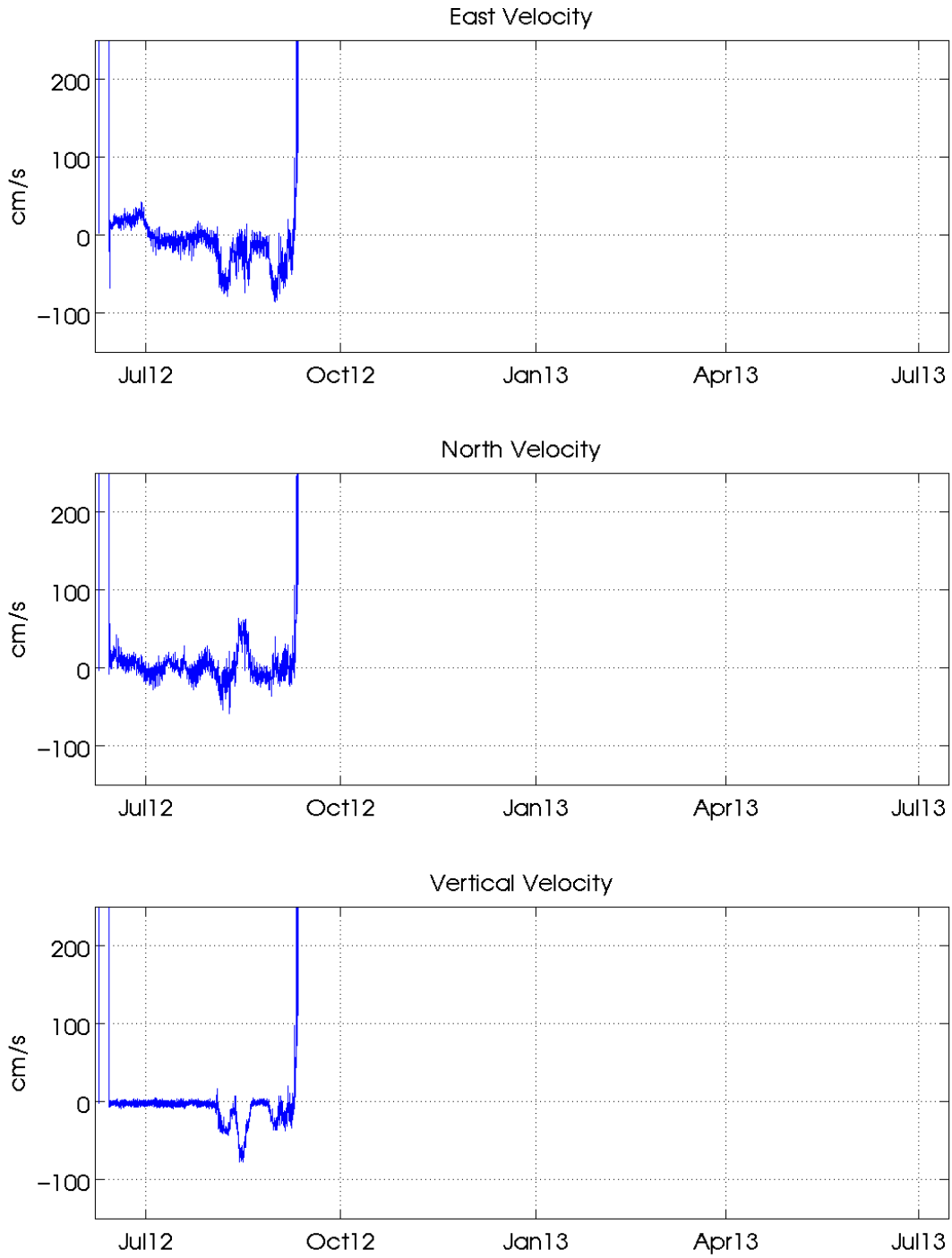

Figure 5-25. Eastward (upper panel), northward (middle panel), and upward velocity data (lower panel) as a function of time from the MAVS acoustic velocity sensor deployed at 20 m. Units are cm s^{-1}

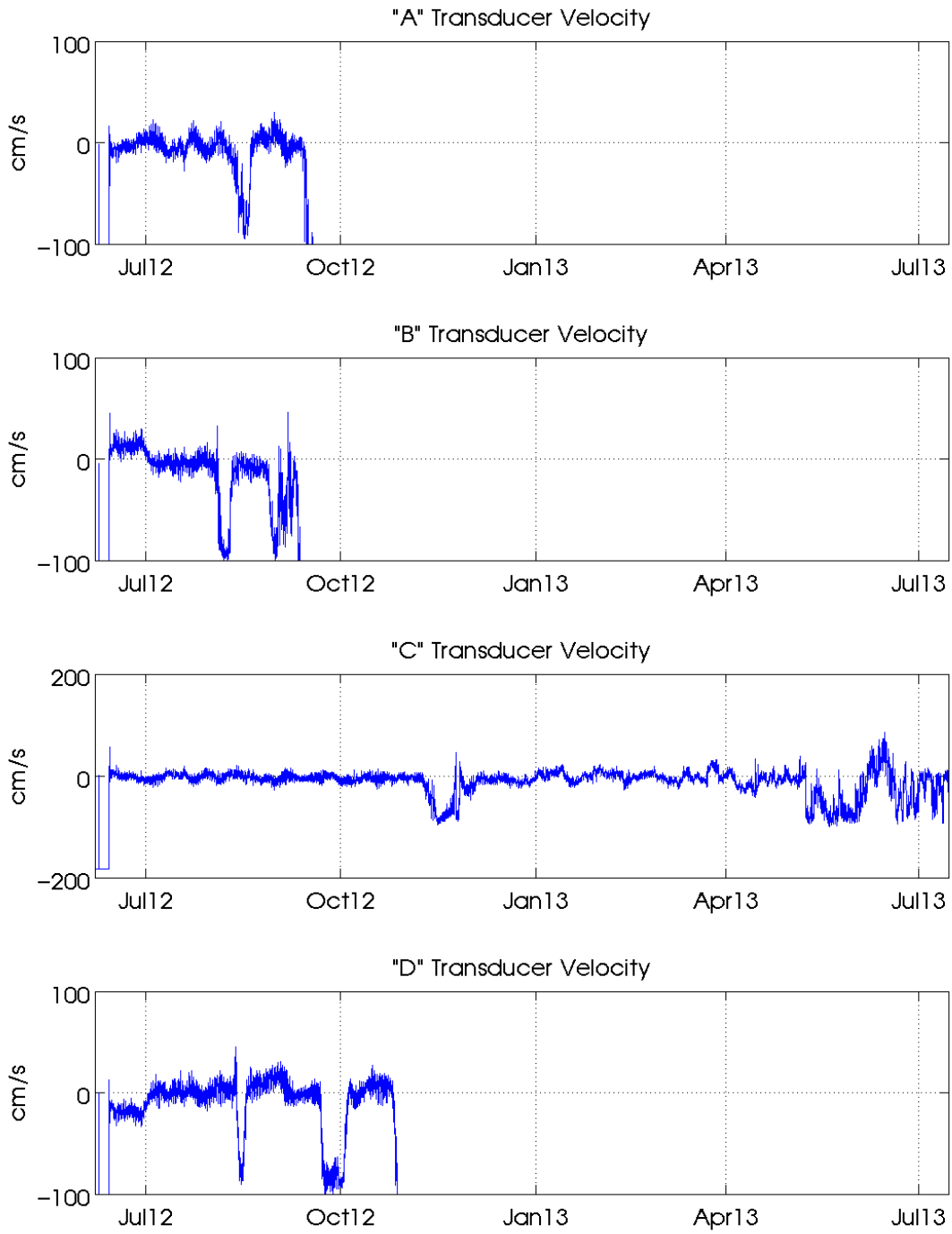

Figure 5-26. Time series of the raw acoustic velocity measured by each of the A, B, C and D transducers in cm s^{-1} from the MAVS deployed at 20 m.

6. Results

The upper ocean flow during the majority of the WHOTS-9 cruise (WHOTS-9 mooring deployment) was unusual. An anticyclonic feature developed to the east of ALOHA, and northward currents were seen early in the cruise (June 12, 2012), with southeasterly light winds (~12 kt) during the deployment of the WHOTS-9 mooring. CTD casts conducted near the mooring site (Station 50) after the deployment (Figure 6-1 through Figure 6-3), displayed a subsurface salinity maximum at 150 dbar, and stratification reaching near the surface, with a shallow mixed layer during June 14-15. The winds turned northeasterly and increased steadily to more than 20 kt starting on June 16, and the currents turned to northwestward during the recovery of the WHOTS-8 mooring. CTD casts conducted before recovering this mooring (Station 52, Figure 6-3 through Figure 6-5) showed an increasing mixed layer reaching nearly 50 m. The currents in the upper 200 m turned eastward at more than 0.5 m/s by June 18.

During the WHOTS-10 cruise (WHOTS-9 mooring recovery), Station ALOHA was under the influence of the eastern North Pacific high pressure system. East-northeasterly trade winds were up to 25 kts on July 10, 2013, and slowed to 10-15 kts by July 14. A few intense squall lines with winds up to 25 kts and heavy rain passed through on July 14-15, causing an apparent drop in the sea surface salinity as indicated by the thermosalinograph record (Figure 6-11). Near-surface currents at Station ALOHA were strongly northward early on the cruise as shown by the shipboard ADCP data (Figure 6-34 and Figure 6-35), and turned NEward prior to recovery of the WHOTS-9 mooring, apparently associated with the spinup of a cyclonic eddy feature to the north of ALOHA that was interacting with an anticyclonic feature to the southeast. The developing eddy slowly moved towards the WSW as the anticyclone moved NNW. CTD casts conducted during the cruise (Figure 6-6 through Figure 6-10) showed near-surface conditions different than those observed during the WHOTS-9 cruise. A broad salinity maximum was present with near-constant salinities between 50 and 200 dbar, and a small temperature gradient; conditions apparently associated with the anticyclonic eddy feature.

The temperature MicroCAT records during the WHOTS-9 deployment (Figure 6-13 through Figure 6-16) show obvious seasonal variability in the upper 100 m, and a sudden drop during August 2013, apparent below 40 m, but more obvious in the deeper instruments. A corresponding decrease in salinity (Figure 6-20) is also seen during August 2013 in the instruments below 100 m. The salinity records (Figure 6-17 through Figure 6-20) do not show an obvious seasonal cycle, but two instances of salinity decrease were recorded during September 2012 and May 2013 by the instruments located above 100 m.

Figure 6-25 and Figure 6-26 show contours of the WHOTS-9 MicroCAT data in context with data from the previous 8 deployments. The seasonal cycle is obvious in the temperature record, with record temperatures (higher than 26 °C) in the summer of 2004, and to a minor extent in the summer of 2005. Salinities in the subsurface salinity maximum were relatively low during the first 6 years of the record, only to increase drastically after 2008, with some episodes of lower salinity in mid-2011 and early 2012. The salinity maximum extended to near the surface during some instances in early 2010, 2011, late 2012-early 2013 and during February-March

2013. When plotted in σ_θ coordinates (Figure 6-26), the salinity maximum seems to be centered roughly between 24 and 24.5 σ_θ.

Records from the WHOTS-9 SeaCATs (Figure 6-27) deployed near the bottom of the mooring (4631 m) detected temperature and salinity changes related to episodic 'cold events' apparently caused by bottom water moving between abyssal basins (Lukas et al., 2001). These events are being monitored by instruments at the ALOHA Cabled Observatory (ACO, Howe et al., 2011), a deep water observatory located at the bottom of Station ALOHA (about 6 nautical miles west from the WHOTS-9 anchor), since June 2011. Figure 6-27 shows temperature and salinity records from the WHOTS-9 SeaCATs superimposed on the ACO data. The SeaCAT data agreed with the temperature increase and the salinity variability registered by ACO instruments during the WHOTS-9 period.

Figure 6-31 through Figure 6-33 show time series of the zonal, meridional, and vertical currents recorded with the moored ADCPs during the WHOTS-9 deployment, and Figure 6-55 shows the currents at 10 and 30 m collected by the VMCMs. Figure 6-28 through Figure 6-30 show contours of the ADCP current components in context with data from the previous deployments. In spite of the gaps in the data, an obvious variability is seen in the zonal and meridional currents, apparently caused by passing eddies. On top of this variability there have been periods of intermittent positive or negative zonal currents, for instance during 2007-2008. The contours of vertical current component (Figure 6-30) show a transition in the magnitude of the contours near 47 m, indicating that the 300 kHz ADCP located at 126 m moves more vertically than the 600 kHz ADCP located at 47.5 m.

A comparison between the moored ADCP data and the shipboard ADCP data obtained during the WHOTS-10 cruise is shown in Figure 6-34 and Figure 6-35. Some of the differences seen especially in the zonal component may be due to the mooring motion, which was not removed from the data. Comparisons between the shipboard ADCP from HOT cruises and the mooring data are compiled in Table 6-1, and shown in Figure 6-36 through Figure 6-53. The correlation coefficient from these comparisons is higher than 0.6 for the majority of the cruises.

The motion of the WHOTS-9 buoy was registered by the Xeos-GPS receiver, and its positions are plotted in Figure 6-56. The buoy was located west of the anchor for the majority of the deployment, except after April 2013 when it was east of it. Power spectrum of these data (Figure 6-57) shows extra energy at the inertial period (~31 hr). Combining the buoy motion with the tilt (a combination of pitch and roll) from the ADCP data (Figure 6-58), showed that the tilt increased as the buoy distance from the anchor increased. This was expected since the inclination of the cable increases as the buoy moves away from the anchor.

A. CTD Profiling Data

Profiles of temperature, salinity and potential density (σ_θ) from the casts obtained during the WHOTS-9 deployment cruise are presented in Figure 6-1 through Figure 6-5, together with the results of bottle determination of salinity. Figure 6-6 through Figure 6-10 are the results of the CTD profiles during the WHOTS-10 cruise.

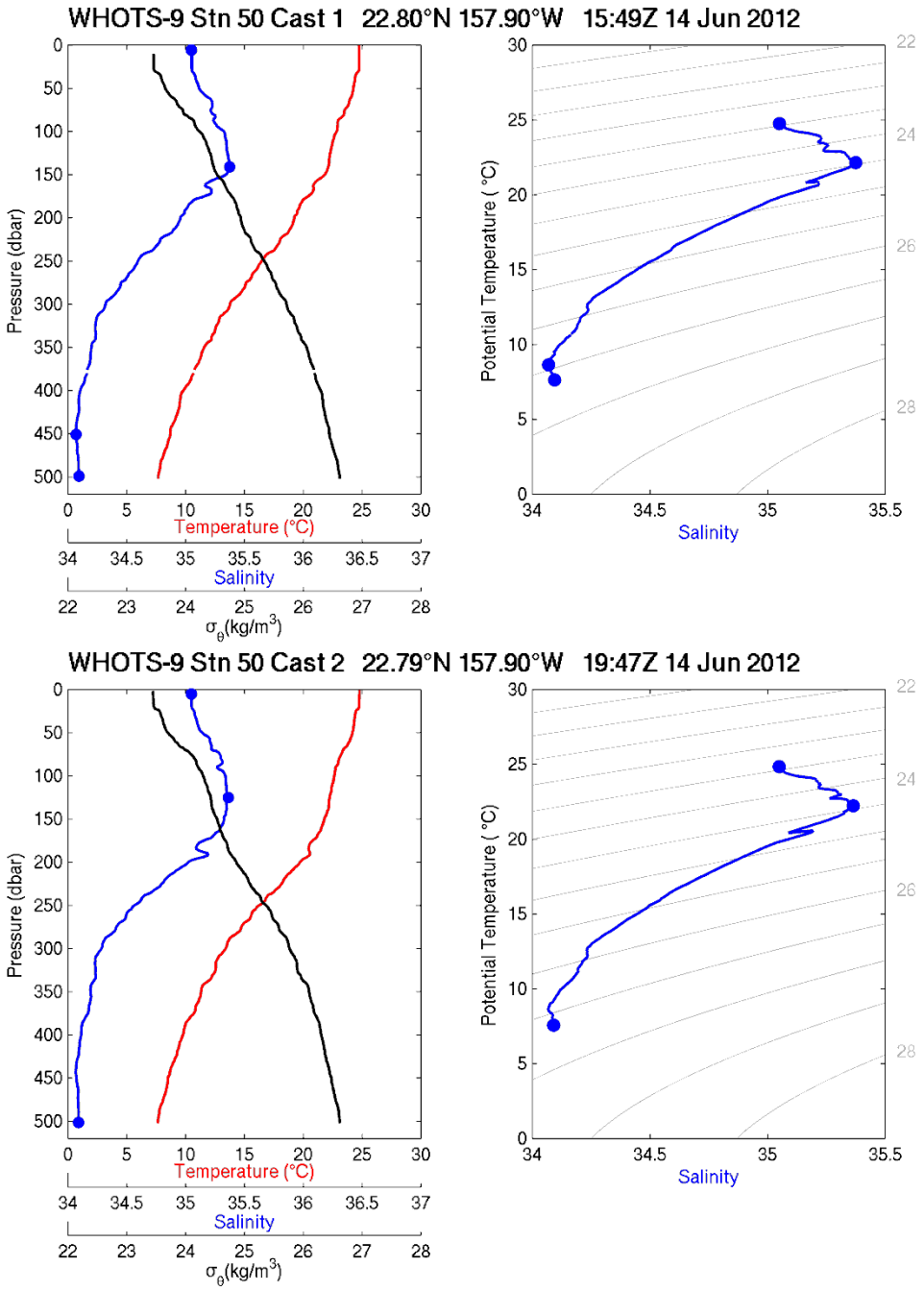

Figure 6-1. [Upper left panel] Profiles of CTD temperature, salinity, and potential density (σ_θ) as a function of pressure, including discrete bottle salinity samples (when available) for station 50 cast 1 during the WHOTS-9 cruise. [Upper right panel] Profiles of CTD salinity as a function of potential temperature, including discrete bottle salinity samples (when available) for station 50 cast 1 during the WHOTS-9 cruise. [Lower left panel] Same as in the upper left panel, but for station 50 cast 2. [Lower right panel] Same as in the upper right panel, but for station 50 cast 2.

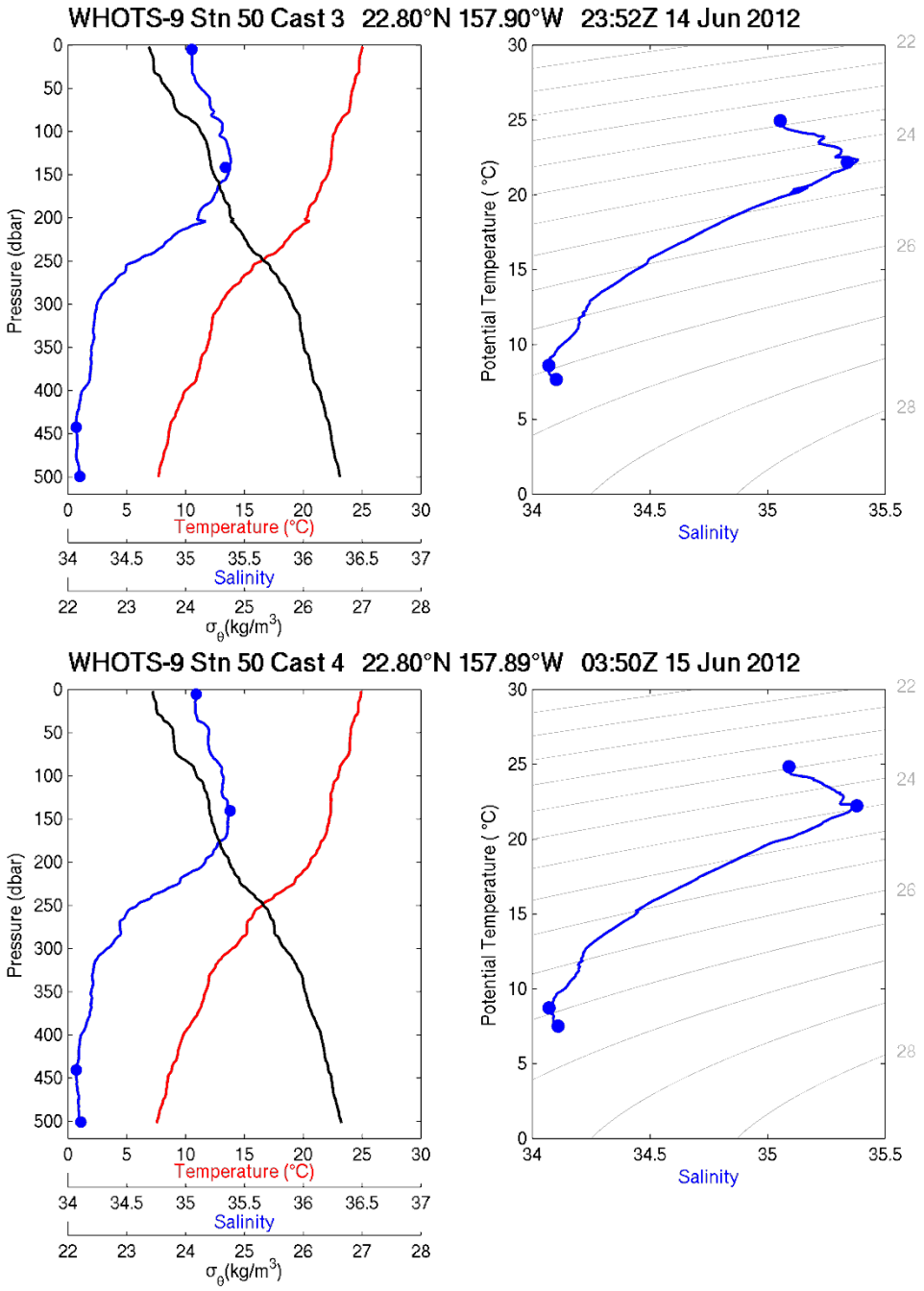

Figure 6-2. [Upper panels] Same as in Figure 6-1, but for station 50, cast 3. [Lower panels] Same as in Figure 6-1, but for station 50, cast 4.

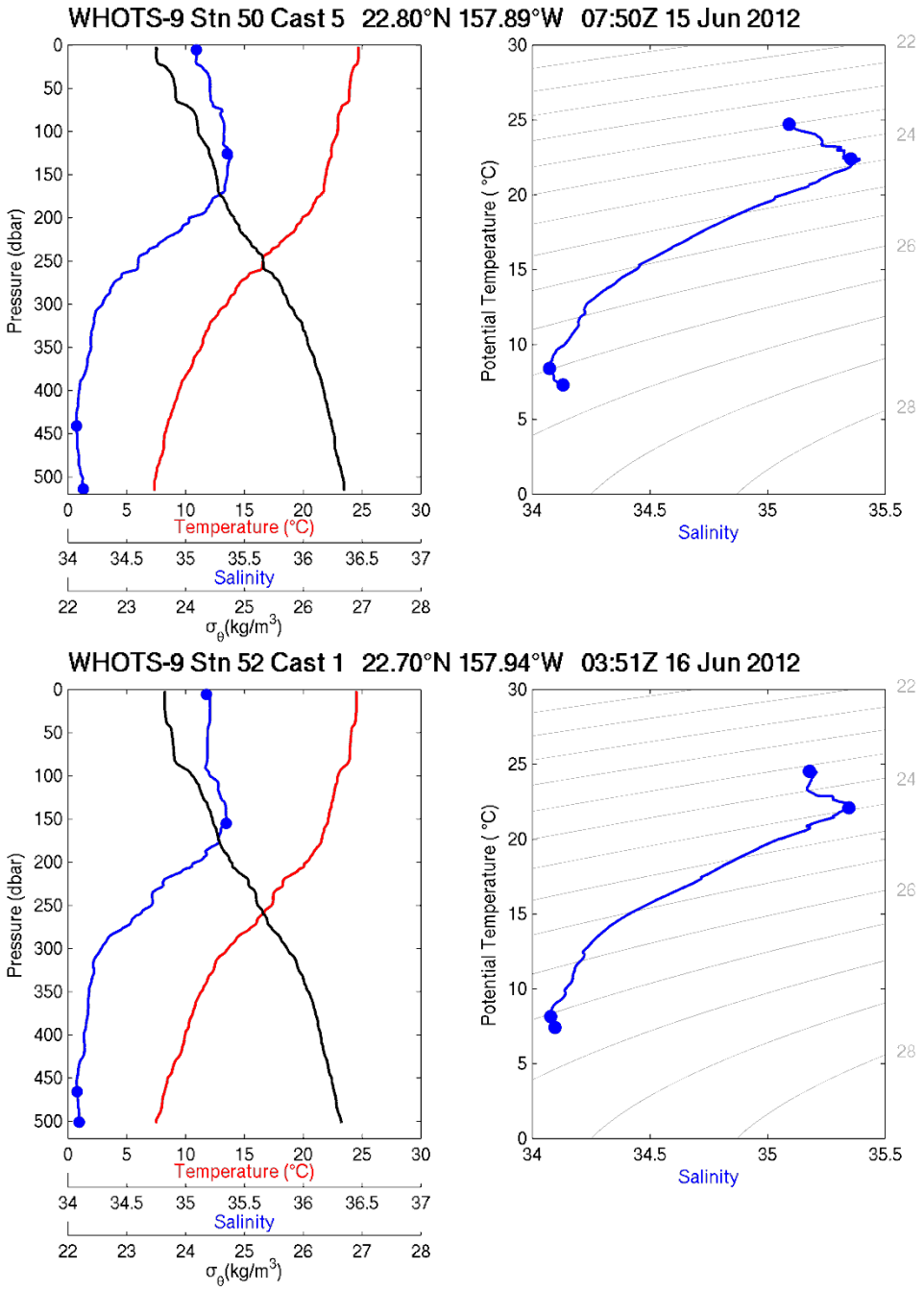

Figure 6-3. [Upper panels] Same as in Figure 6-1, but for station 50, cast 5. [Lower panels] Same as in Figure 6-1, but for station 52, cast 1.

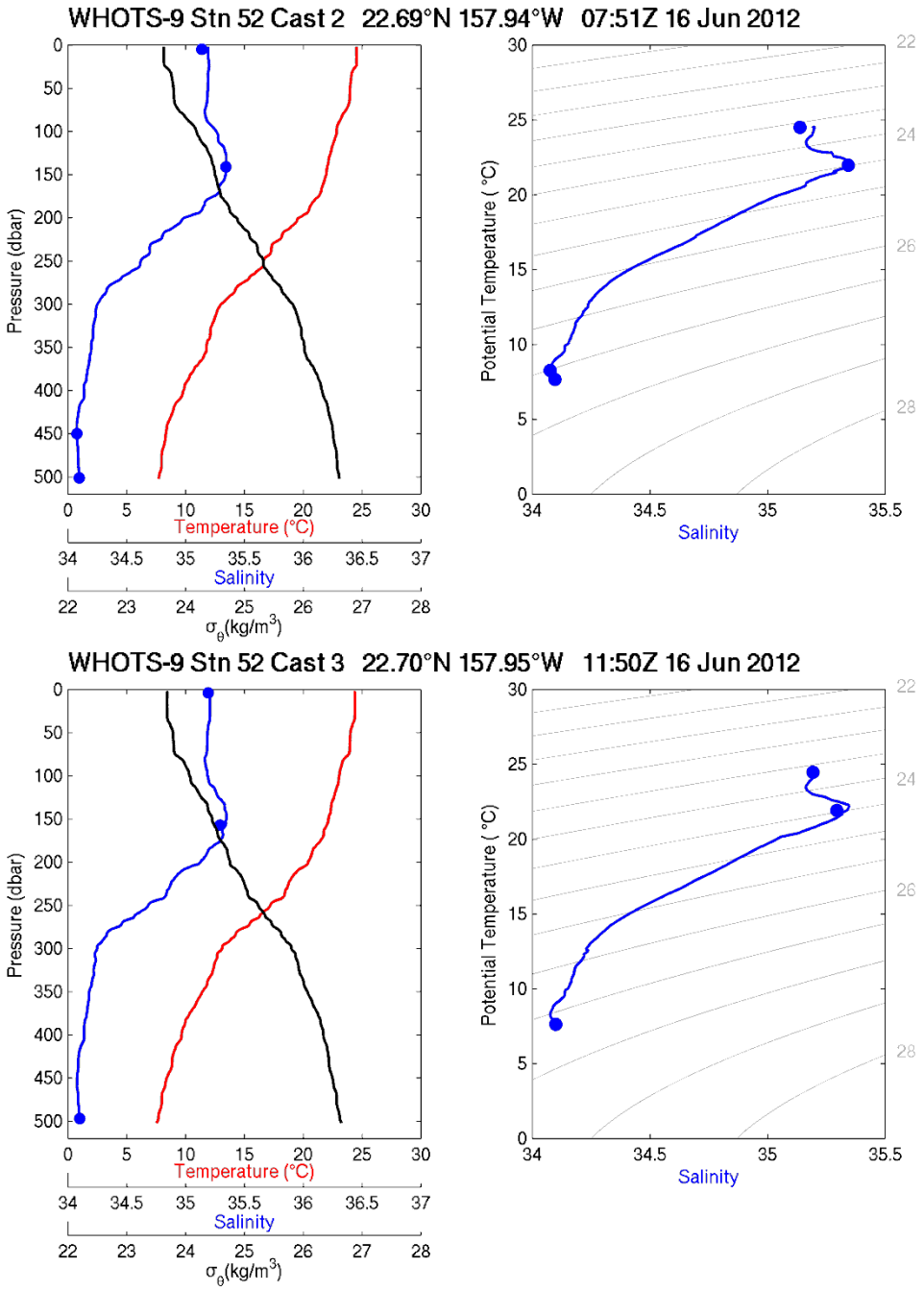

Figure 6-4. [Upper panels] Same as in Figure 6-1, but for station 52, cast 2. [Lower panels] Same as in Figure 6-1, but for station 52, cast 3.

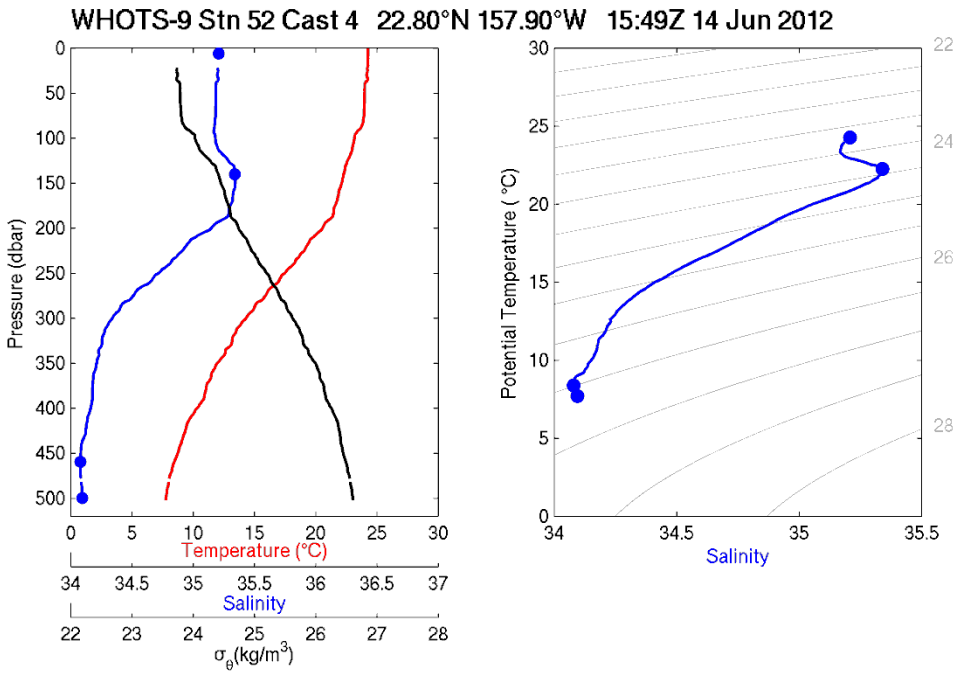

Figure 6-5. [Upper panels] Same as in Figure 6-1, but for station 52, cast 4.

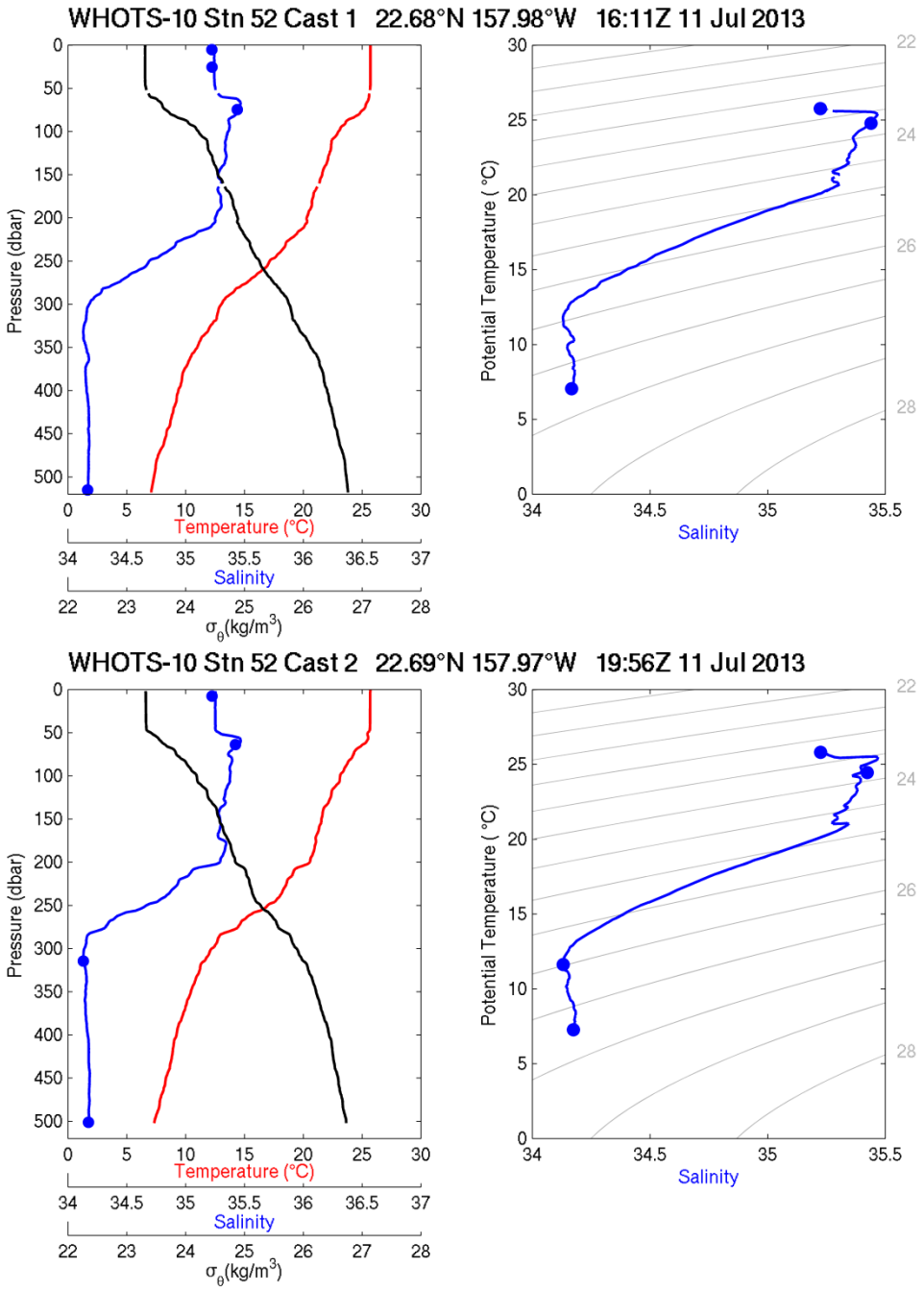

Figure 6-6. [Upper left panel] Profiles of CTD temperature, salinity, and potential density (σ_θ) as a function of pressure, including discrete bottle salinity samples (when available) for station 52 cast 1 during the WHOTS-10 cruise. [Upper right panel] Profiles of CTD salinity as a function of potential temperature, including discrete bottle salinity samples (when available) for station 52 cast 1 during the WHOTS-10 cruise. [Lower left panel] Same as in the upper left panel, but for station 52 cast 2. [Lower right panel] Same as in the upper right panel, but for station 52 cast 2.

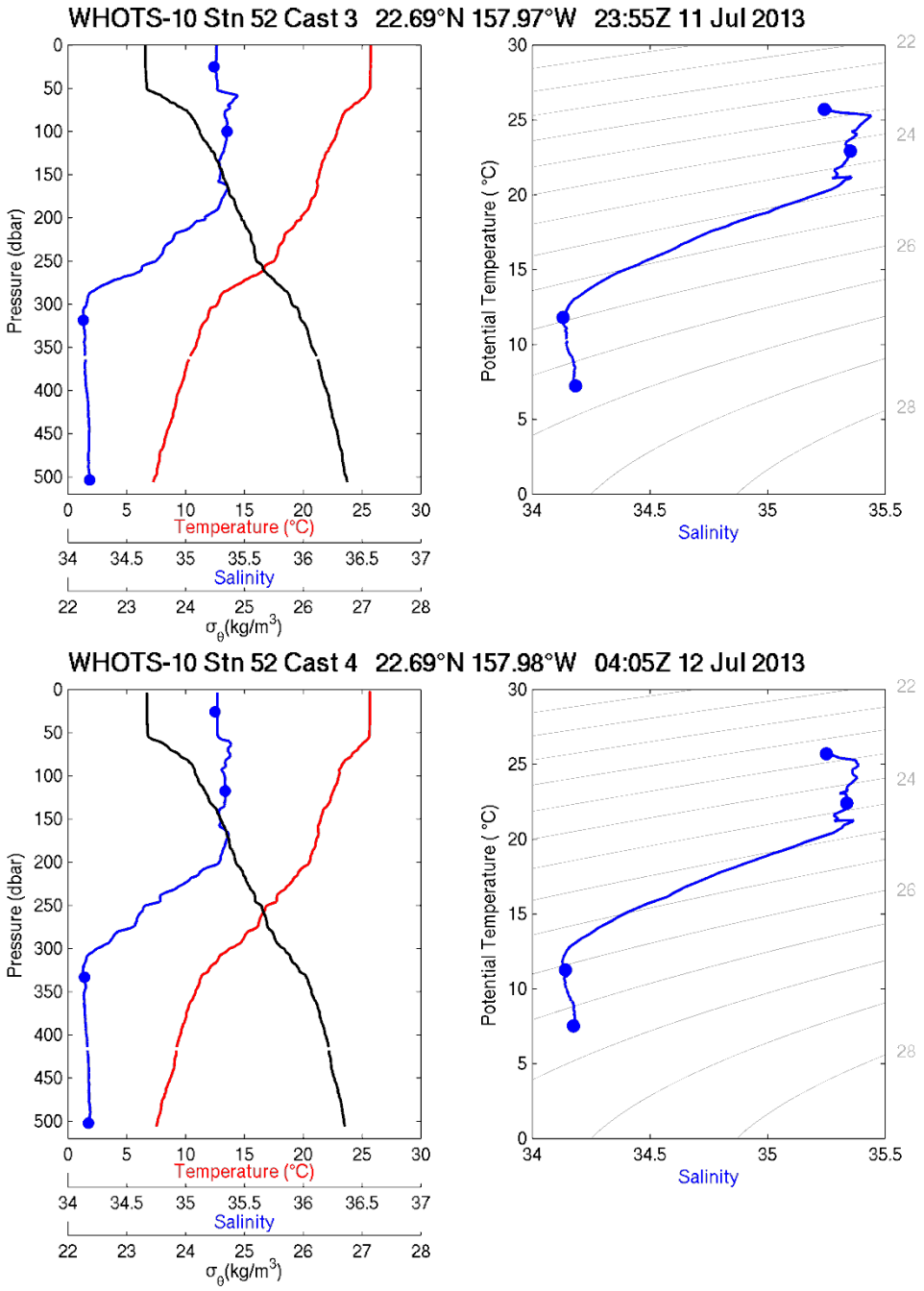

Figure 6-7. [Upper panels] Same as in Figure 6-5, but for station 52, cast 3. [Lower panels] Same as in Figure 6-5, but for station 52, cast 4.

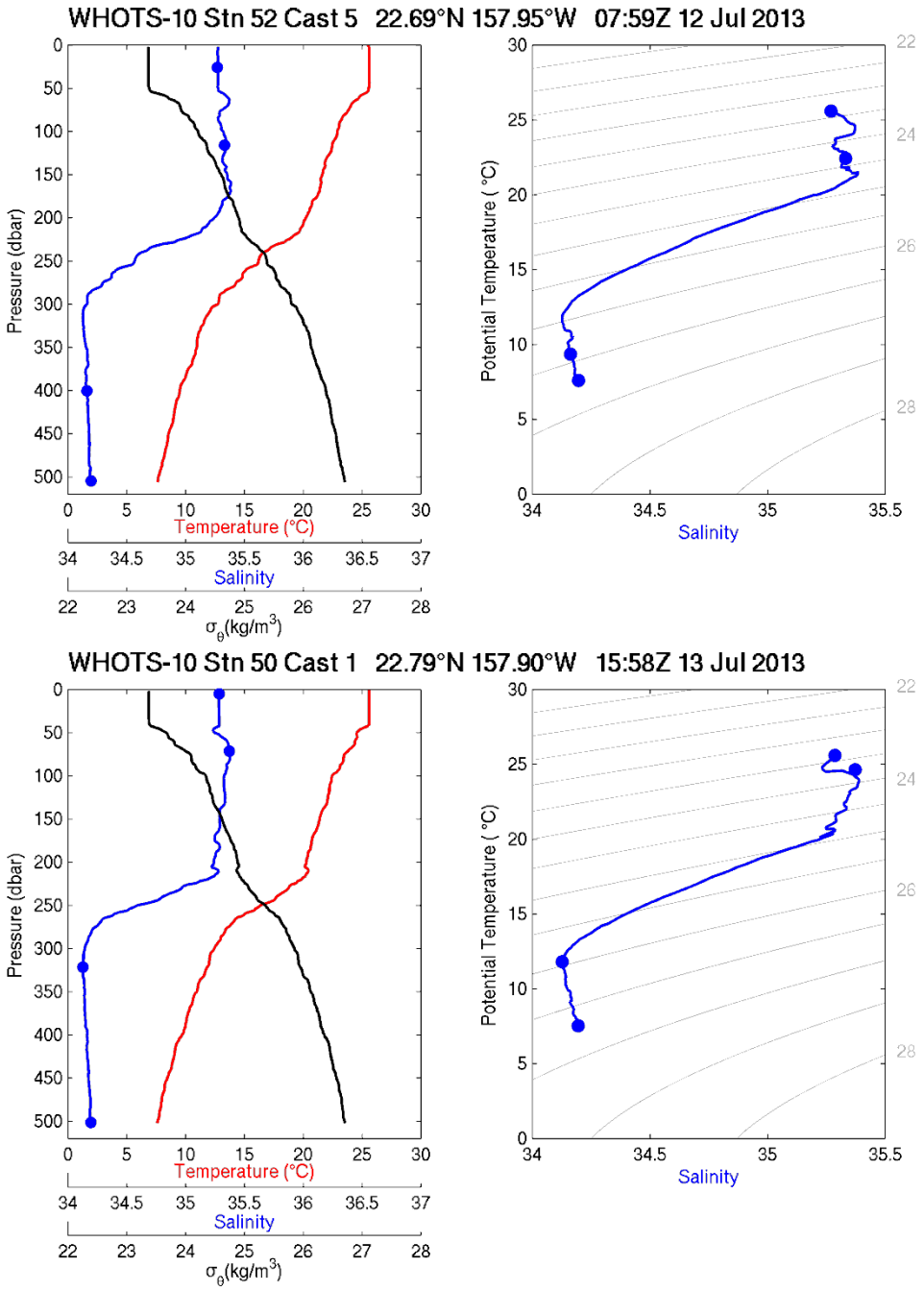

Figure 6-8. [Upper panels] Same as in Figure 6-6, but for station 52, cast 5. [Lower panels] Same as in Figure 6-6, but for station 50 cast 1.

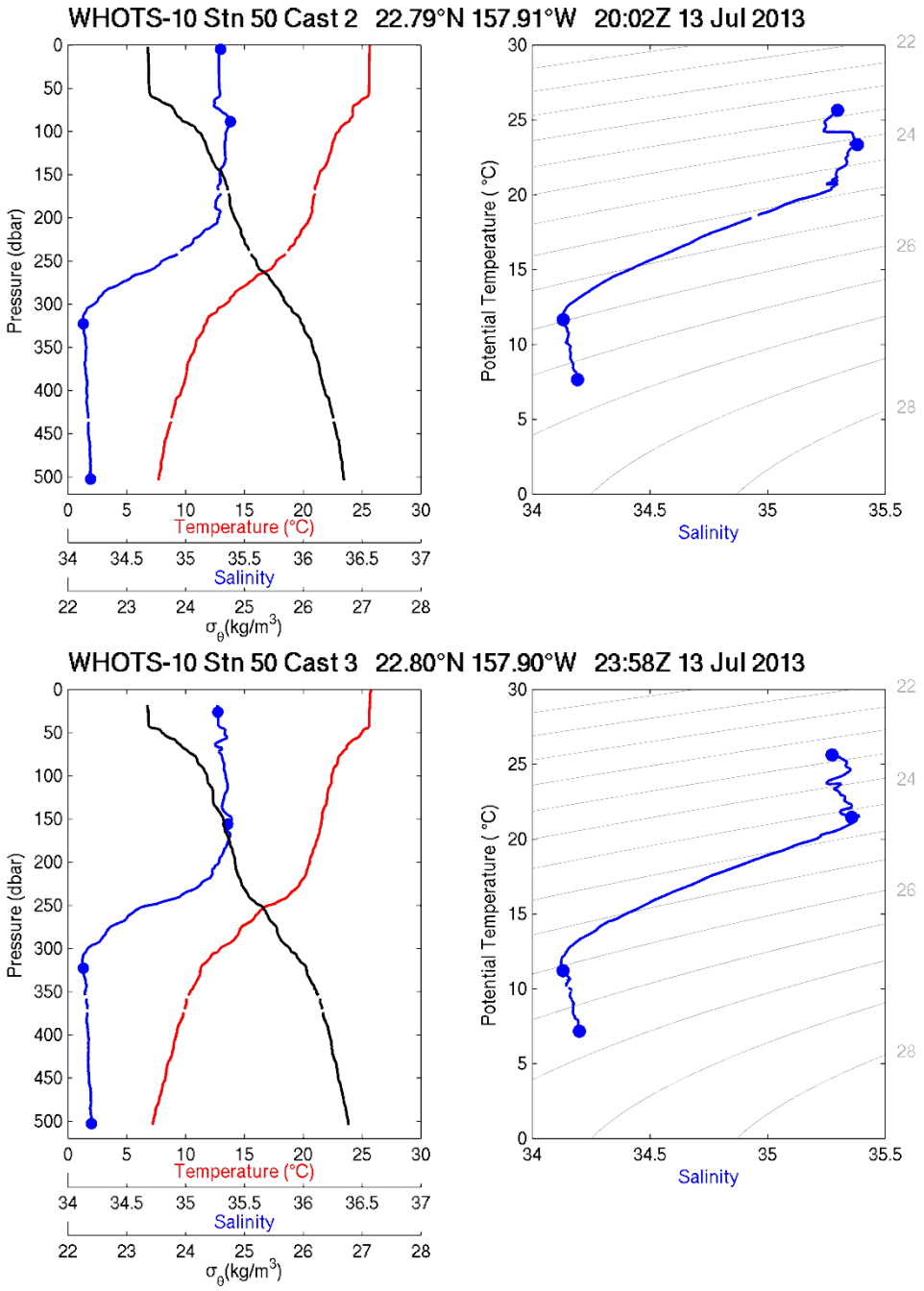

Figure 6-9. [Upper panels] Same as in Figure 6-6, but for station 50, cast 2. [Lower panels] Same as in Figure 6-6, but for station 50 cast 3.

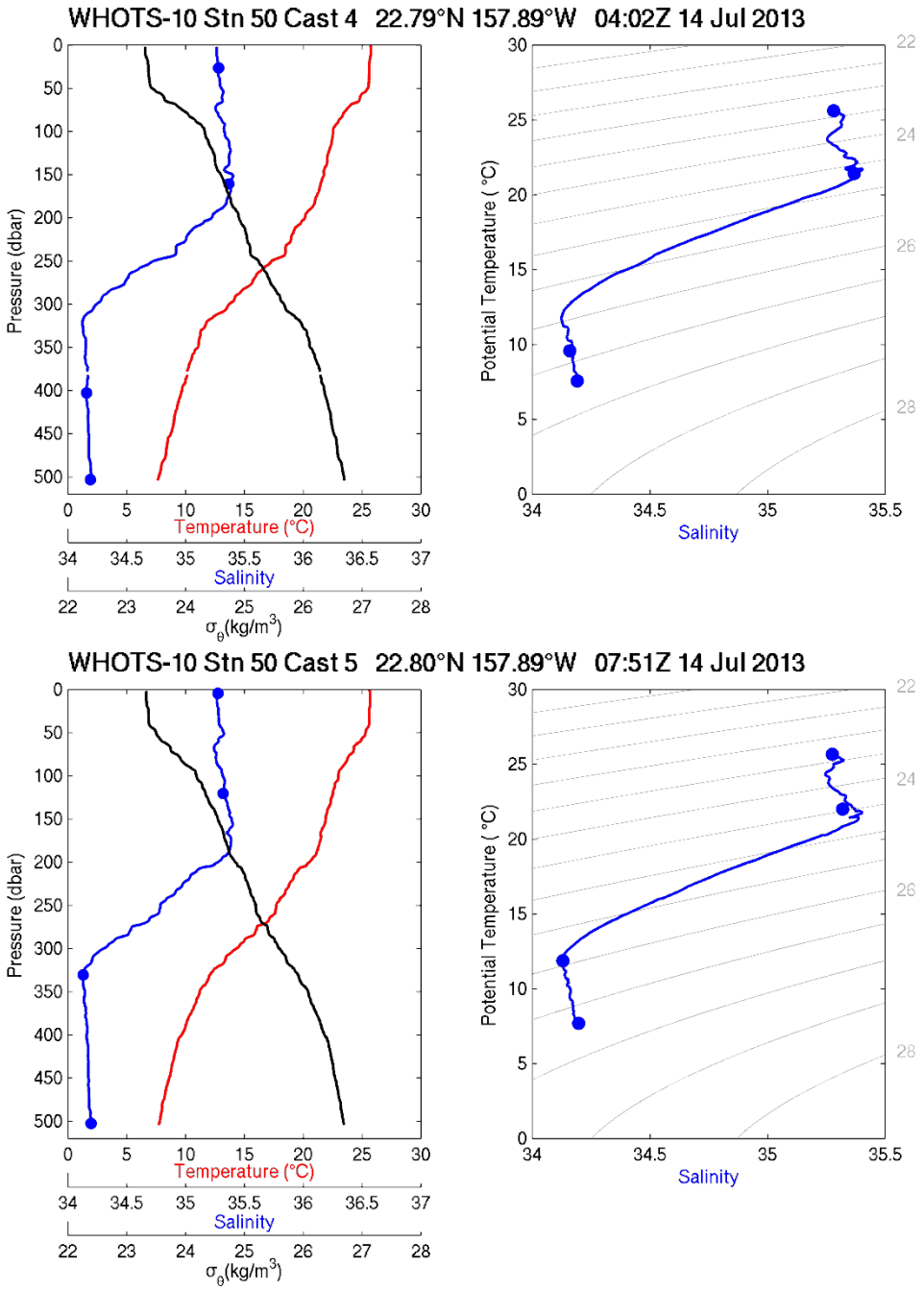

Figure 6-10. [Upper panels] Same as in Figure 6-6, but for station 50, cast 4. [Lower panels] Same as in Figure 6-6, but for station 50 cast 5.

B. Thermosalinograph data

Underway measurements of near surface temperature and near surface salinity from thermosalinograph as well as navigation for the WHOTS-10 cruise are presented in

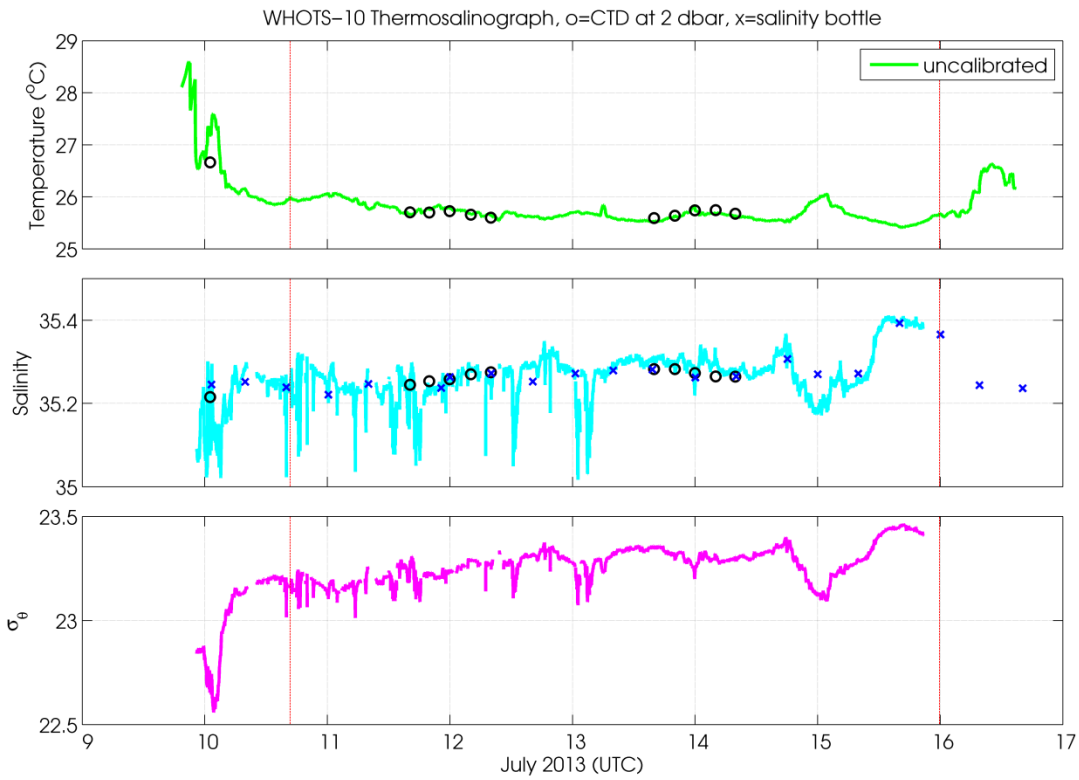

Figure 6-11 and Figure 6-12. Since external temperature data were not available, temperatures from the internal sensor are reported after correcting by an offset obtained by comparisons with the CTD cast data; however the internal sensor temperatures were affected by cooling and heating as the water traveled through the ship from the intake to the thermosalinograph (see Sect. 4.C.2), and therefore these data were flagged as uncalibrated. There were no plots generated for the WHOTS-9 cruise due to unusable data (see Sect. 4.C.1).

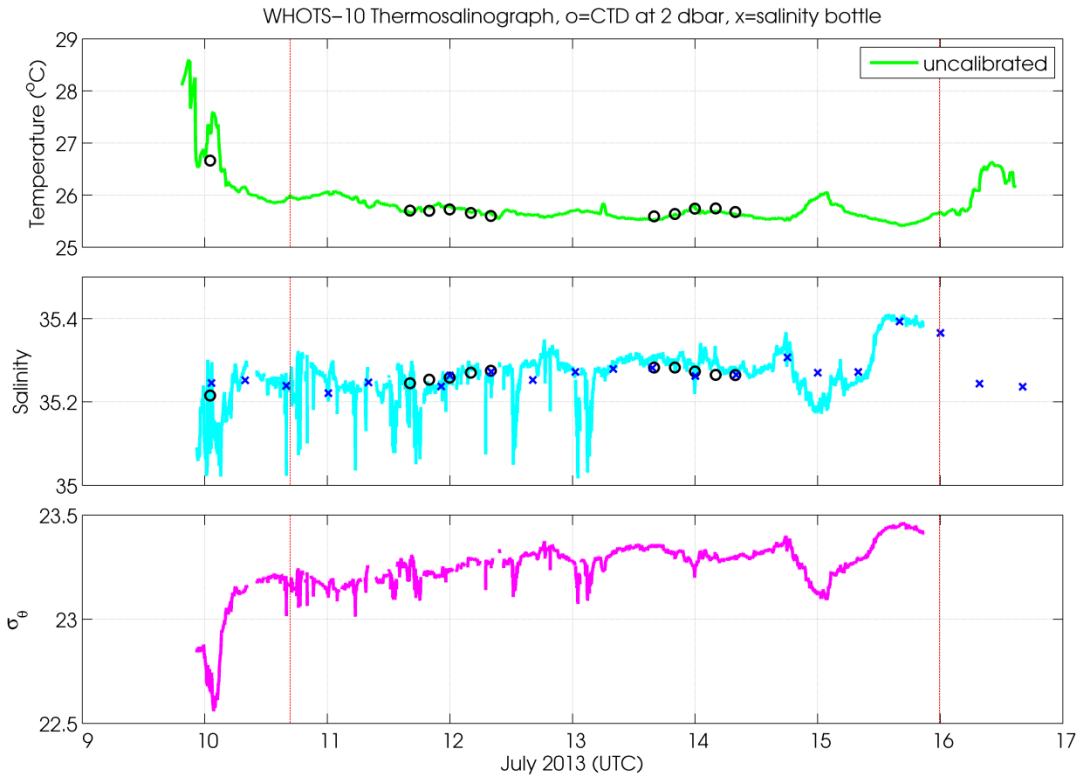

Figure 6-11. Final processed temperature (upper panel), salinity (middle panel) and potential density (σ_θ) (lower panel) data from the continuous underway system on board the RV Hi'ialakai during the WHOTS-10 cruise. Temperature and salinity taken from 6-dbar CTD data (circles) and salinity bottle sample data (crosses) are superimposed. The dashed vertical red line indicates the period of occupation of Station ALOHA and the WHOTS site.

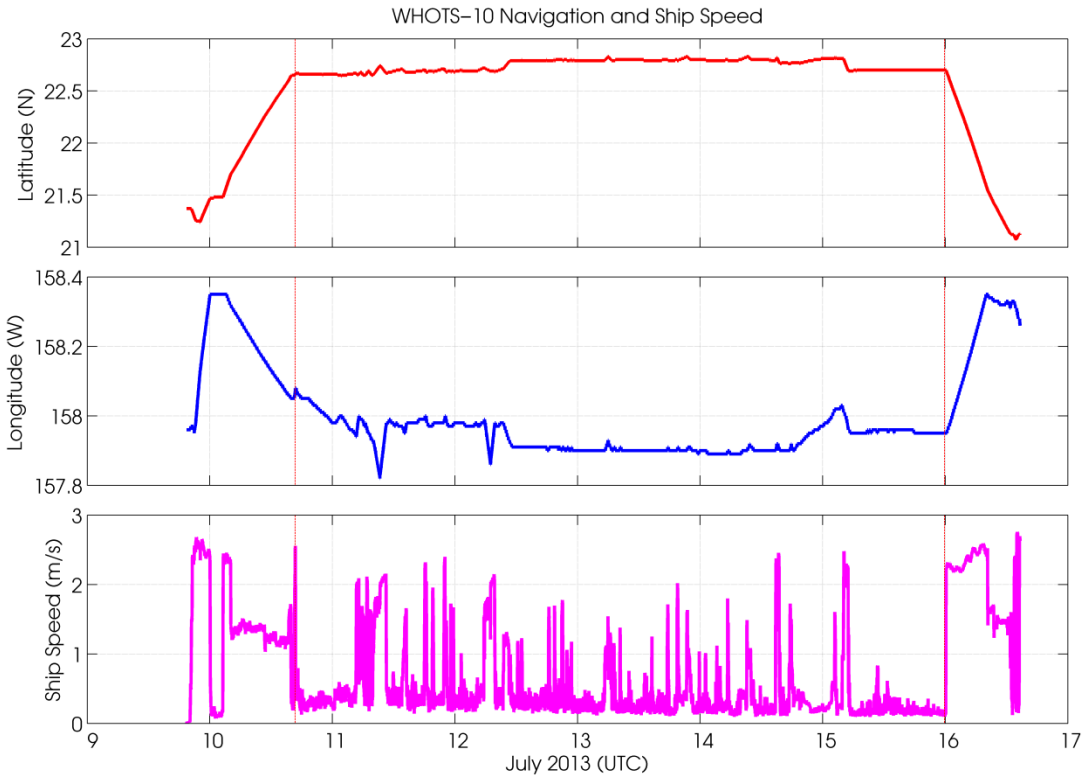

Figure 6-12. Timeseries of latitude (upper panel), longitude (middle panel), and ship's speed (lower panel) during the WHOTS-10 cruise.

C. MicroCAT/SeaCAT data

The temperature and salinity measured by MicroCATs during the mooring deployment are presented in Figure 6-13 to Figure 6-20 for each of the depths where the instruments were located. The potential density (σ_θ) is also plotted in Figure 6-21 to Figure 6-24.

Contoured plots of temperature and salinity as a function of depth are presented in Figure 6-25; and contoured plots of potential density (σ_θ) as a function of depth, and of salinity as a function of σ_θ are in Figure 6-26. The instruments at 25, 45 and 50 m had conductivity sensor problems, and sections of their data were flagged bad or suspect; these data are not included in the salinity and σ_θ plots (see Sect. 5.A.4).

The potential temperature and salinity measured by the deep SeaCATs (4631 m) during the mooring deployment are shown in Figure 6-27. Also shown in the plot are the potential temperature and salinity data obtained with a MicroCAT (SBE-37) installed in the ALOHA Cabled Observatory, about 6 nautical miles west from the WHOTS-9 anchor, the instrument is located 2 m above the bottom.

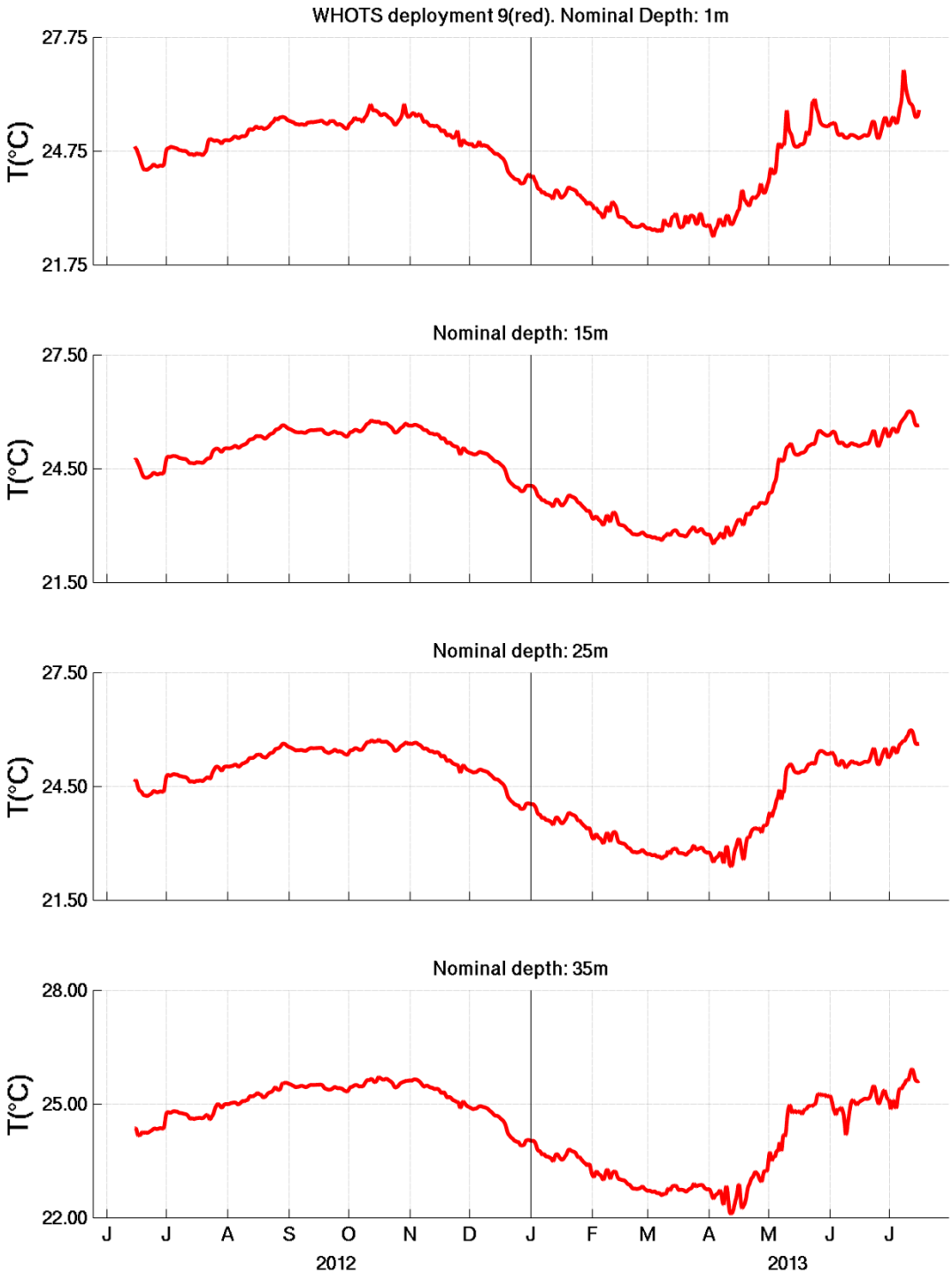

Figure 6-13. Temperatures from MicroCATs during WHOTS-9 deployment at 1, 15, 25, and 35 m.

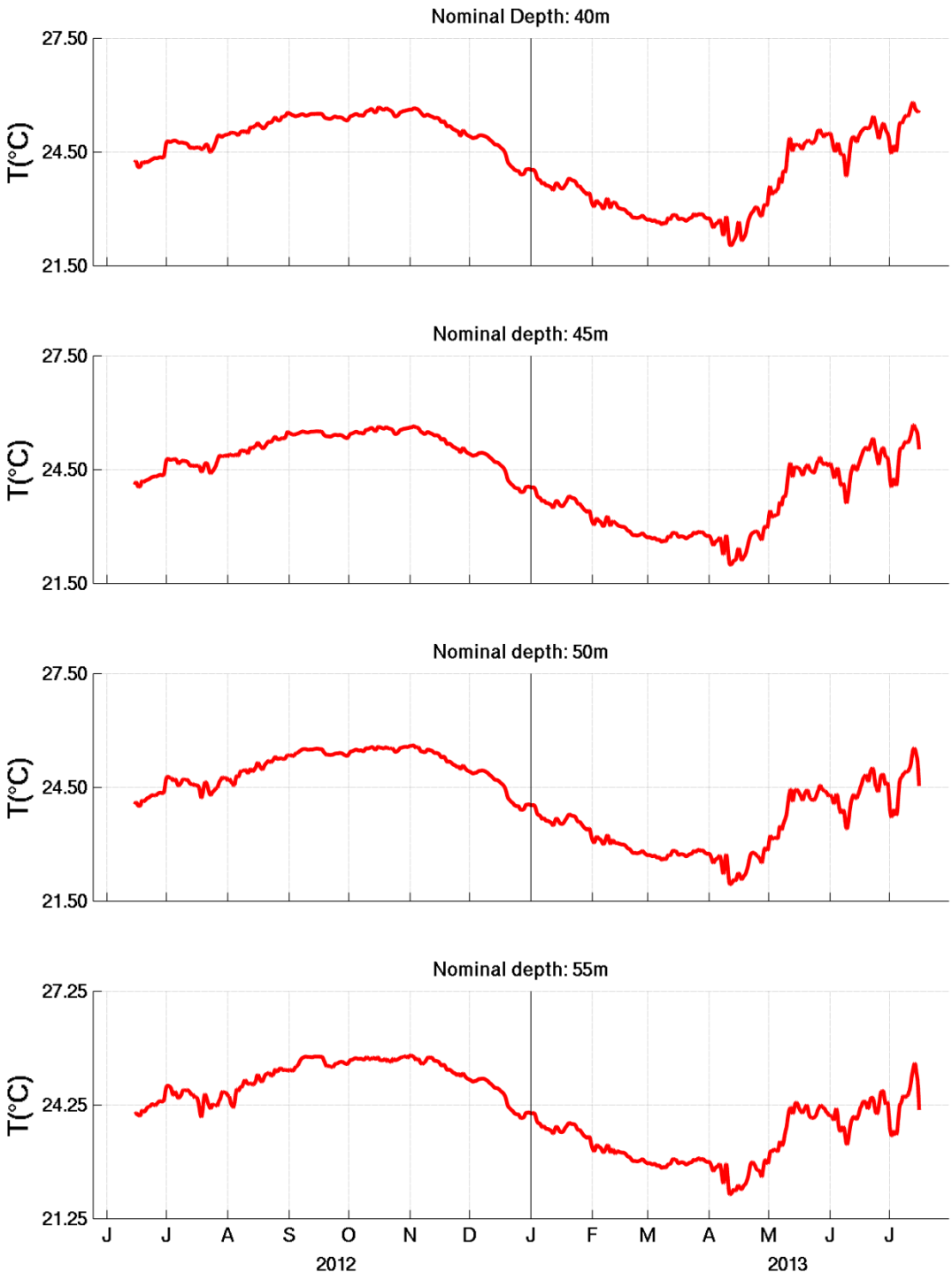

Figure 6-14. Same as in Figure 6-13, but at 40, 45, 50, and 55 m.

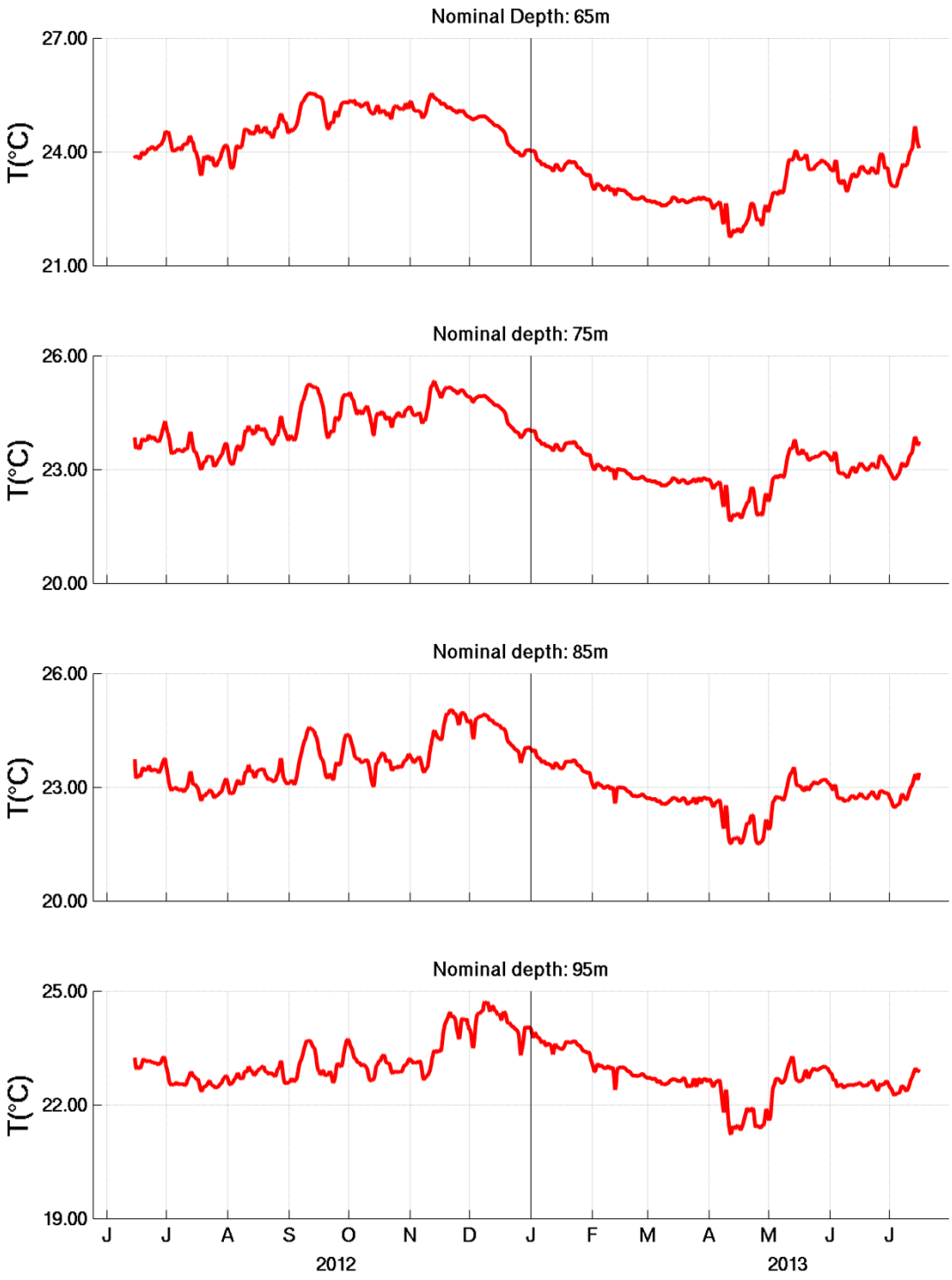

Figure 6-15. Same as in Figure 6-13, but at 65, 75, 85, and 95 m.

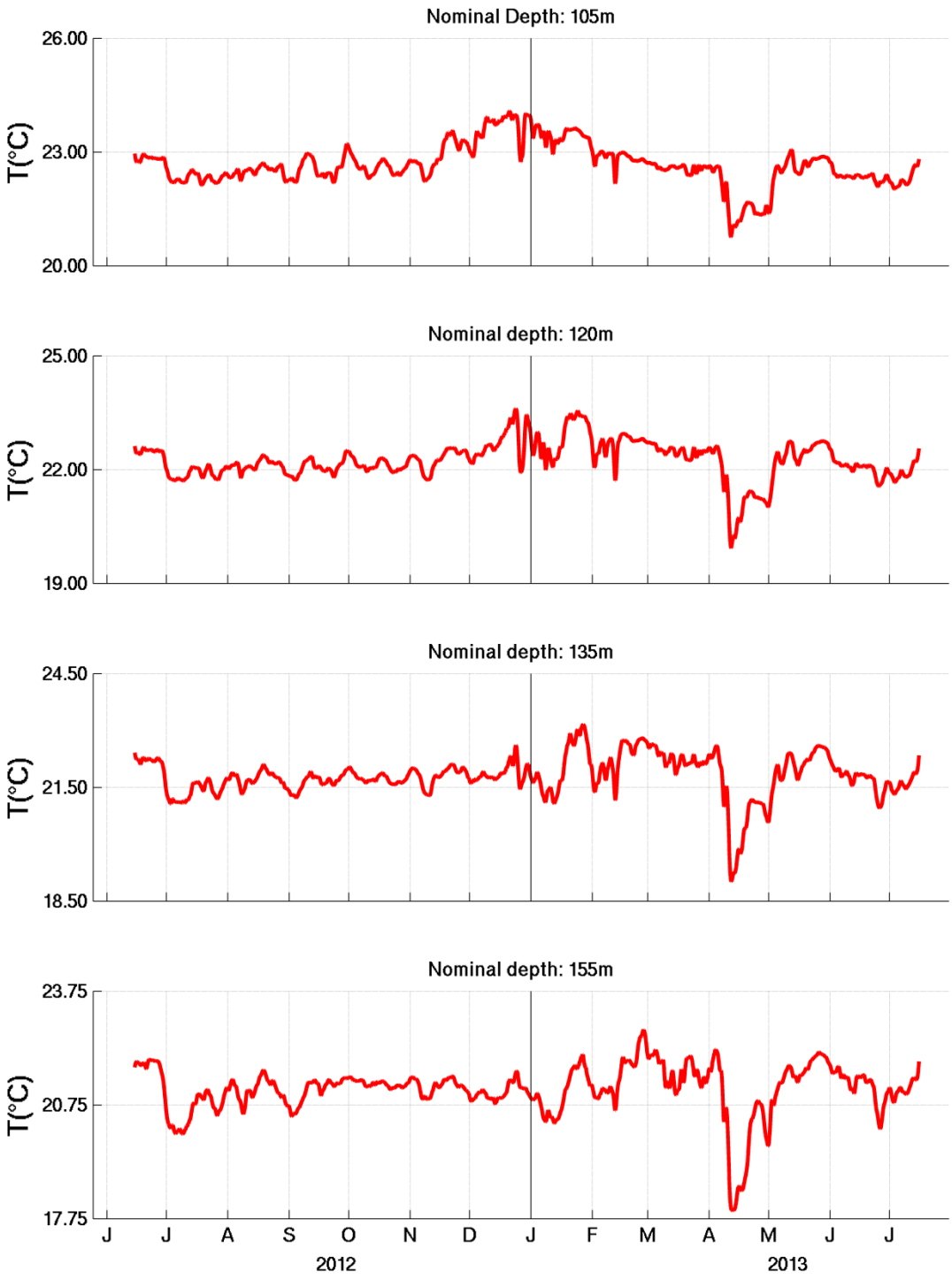

Figure 6-16. Same as in Figure 6-13, but at 105, 120, 135, and 155 m.

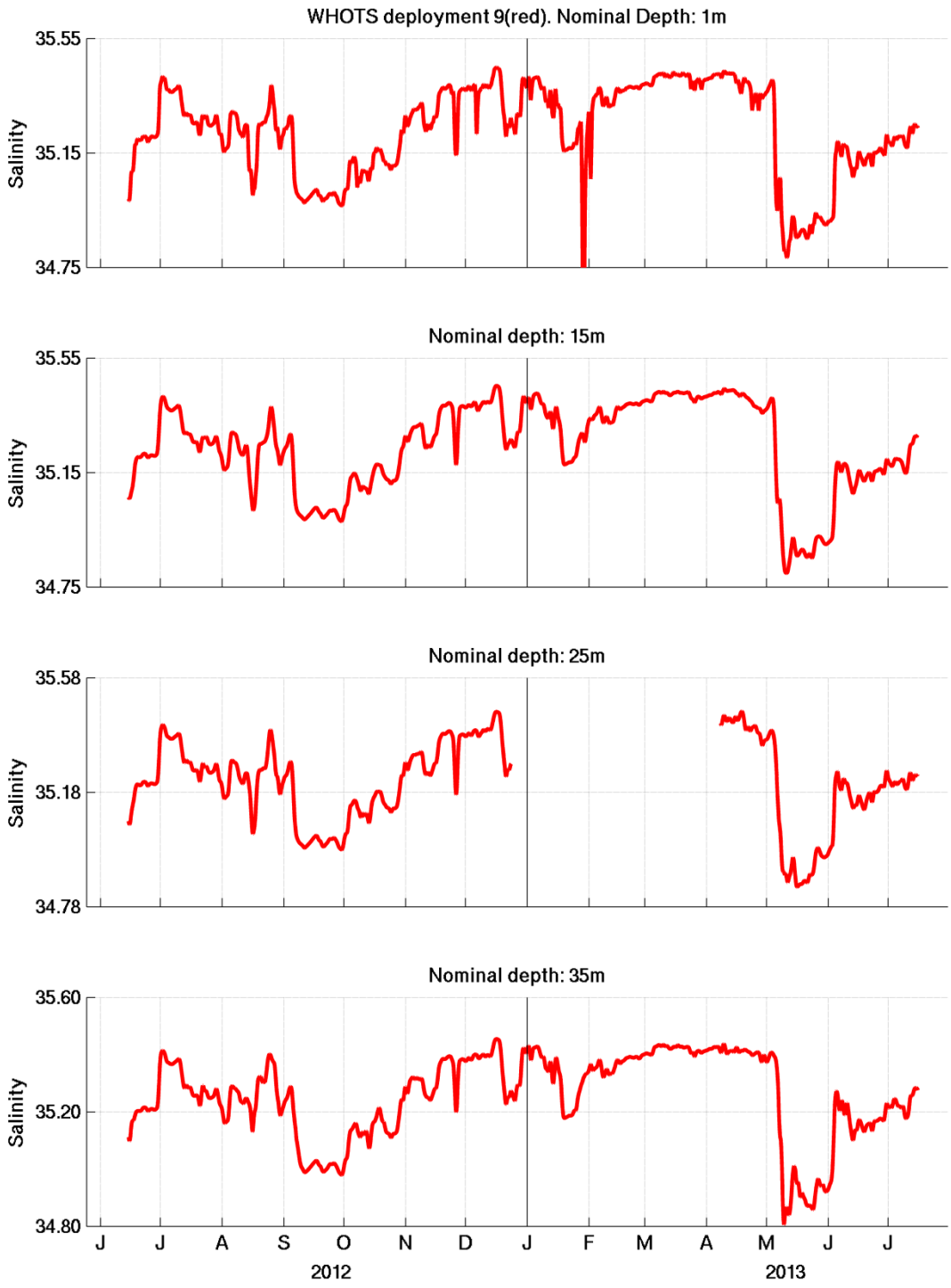

Figure 6-17. Salinities from MicroCATs during WHOTS-9 deployment at 1, 15, 25, and 35 m.

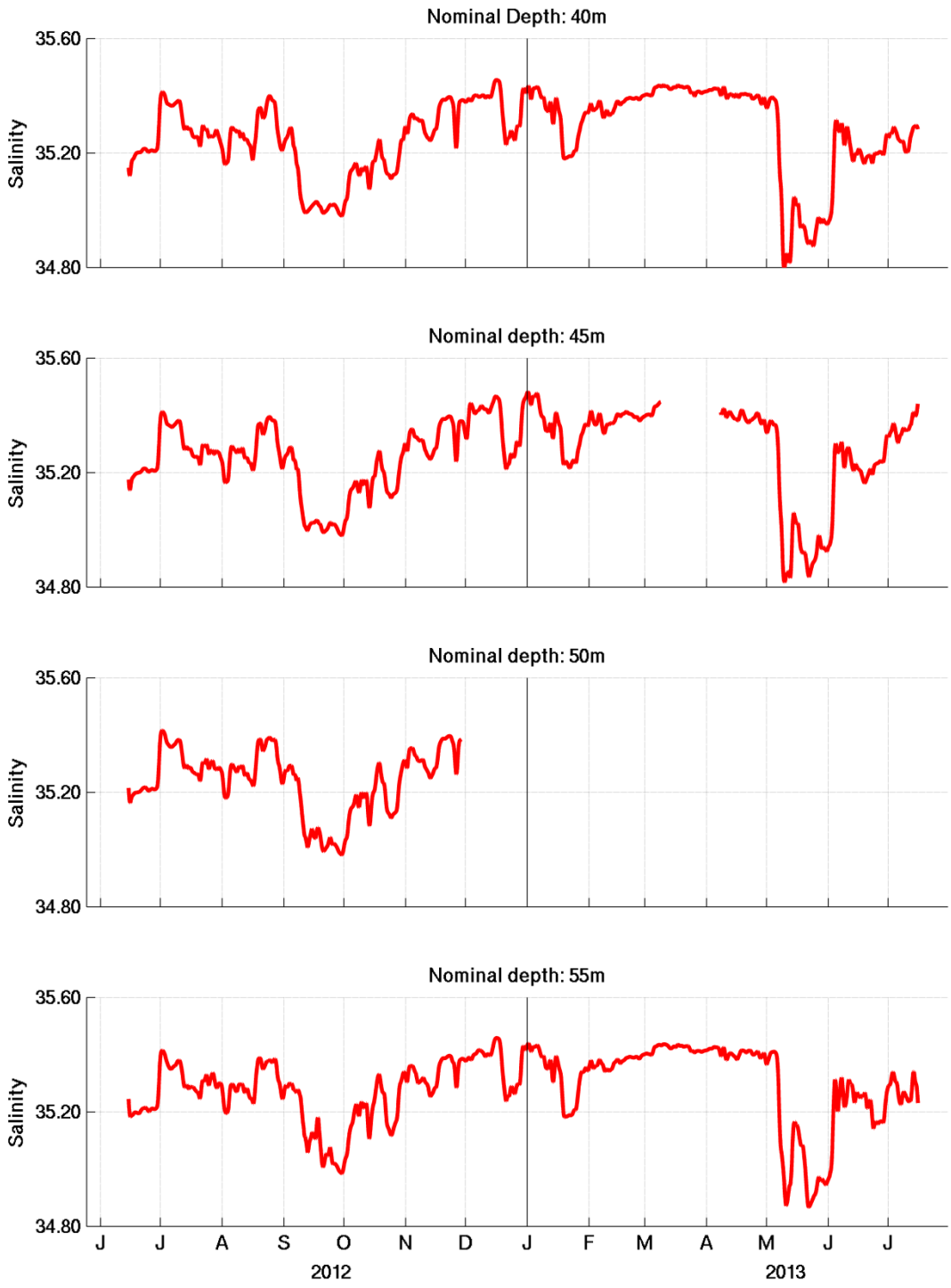

Figure 6-18. Same as in Figure 6-17, but at 40, 45, 50, and 55m.

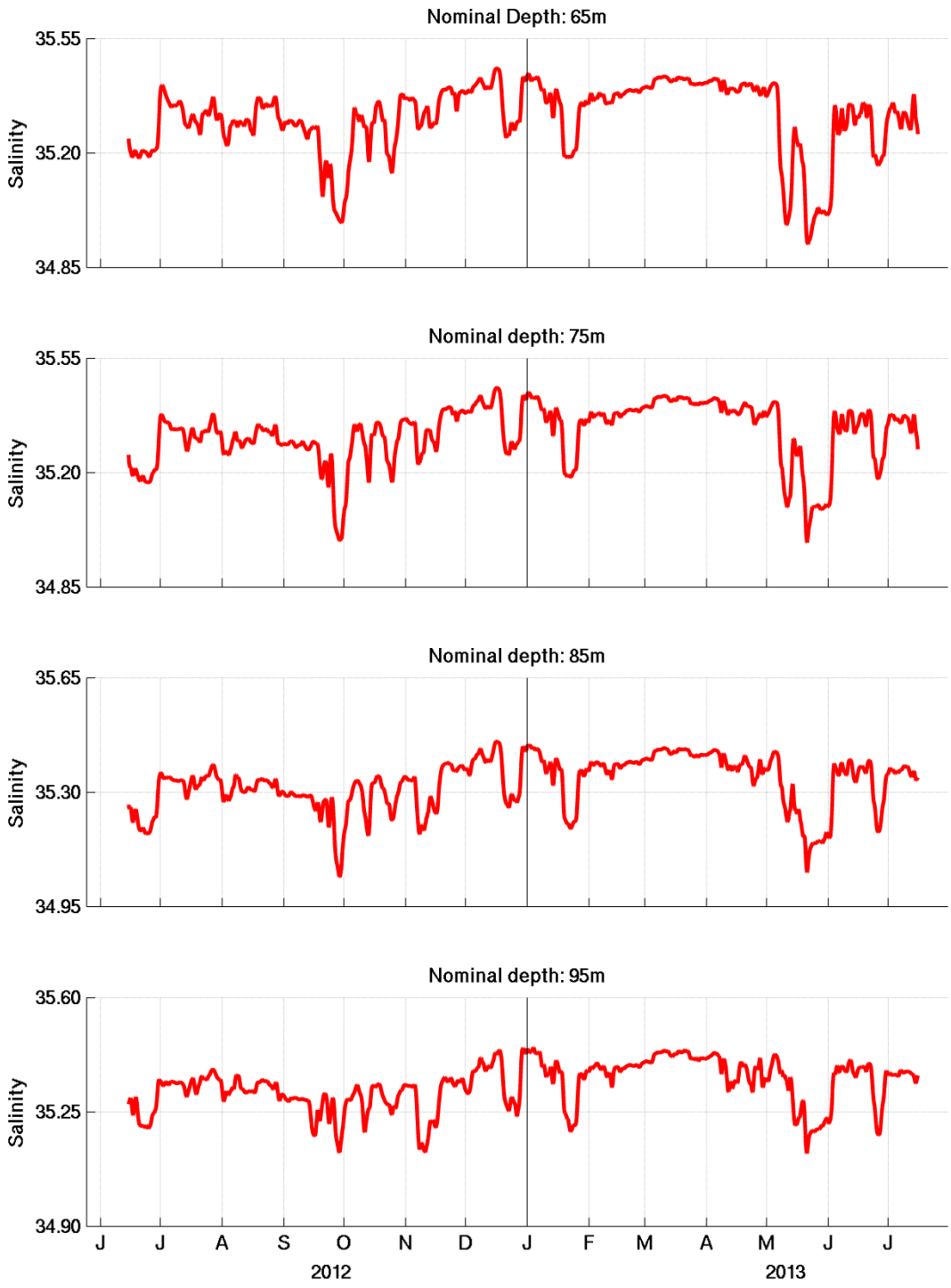

Figure 6-19. Same as in Figure 6-17, but at 65, 75, 85, and 95m.

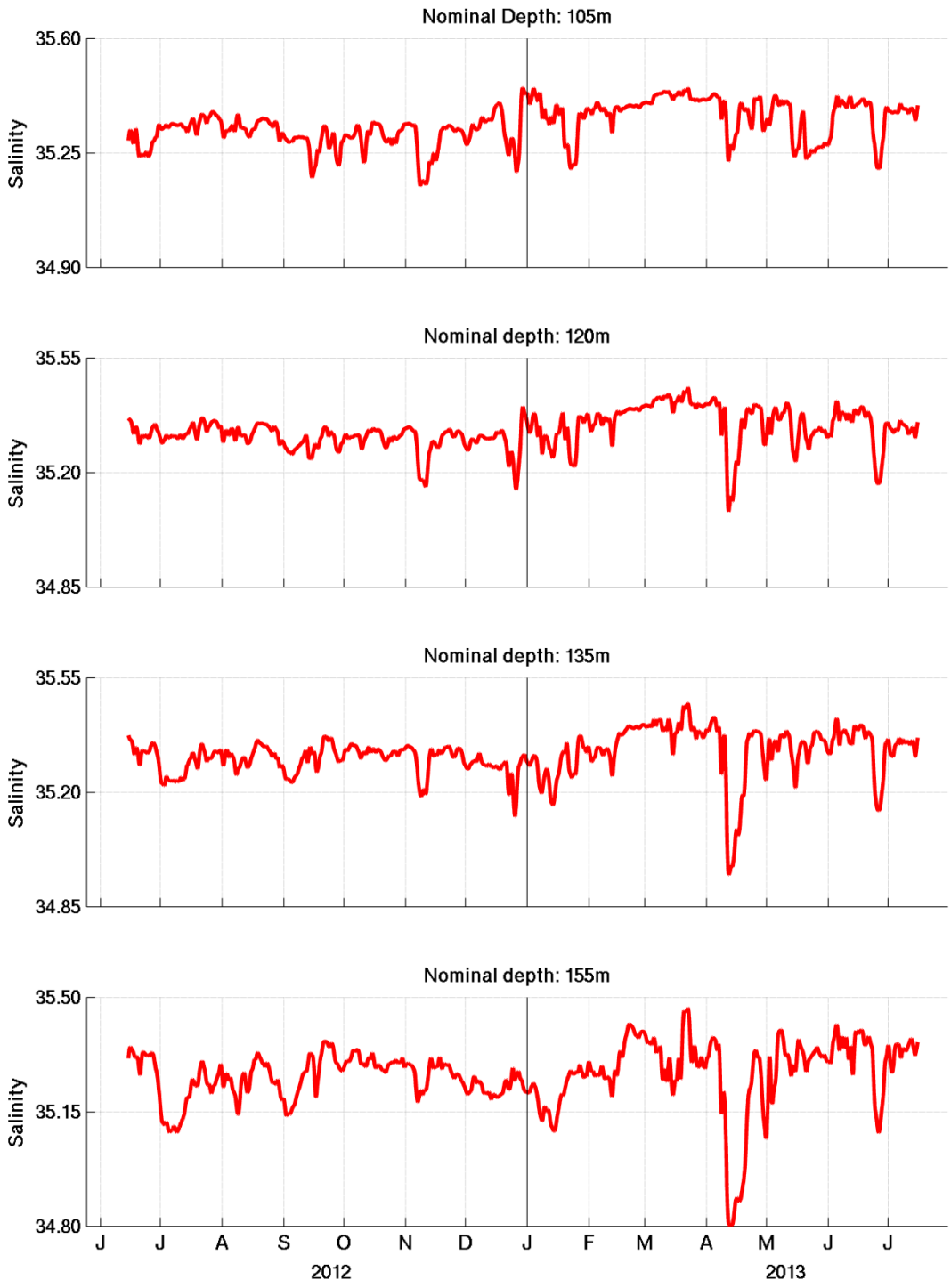

Figure 6-20. Same as in Figure 6-17, but at 105, 120, 135, and 155 m.

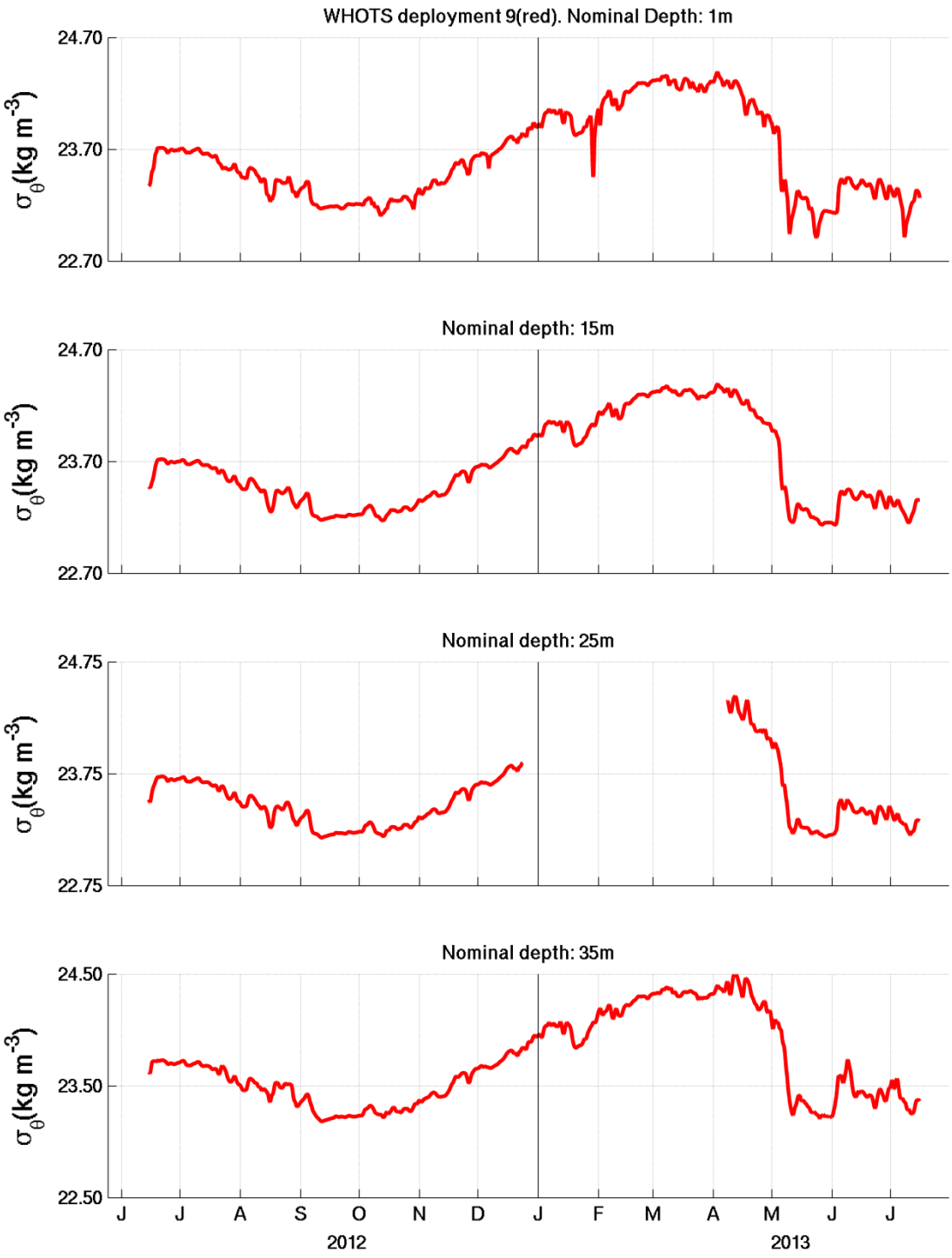

Figure 6-21. Potential density (σ_θ) from MicroCATs during WHOTS-9 deployment at 1, 15, 25, and 35 m.

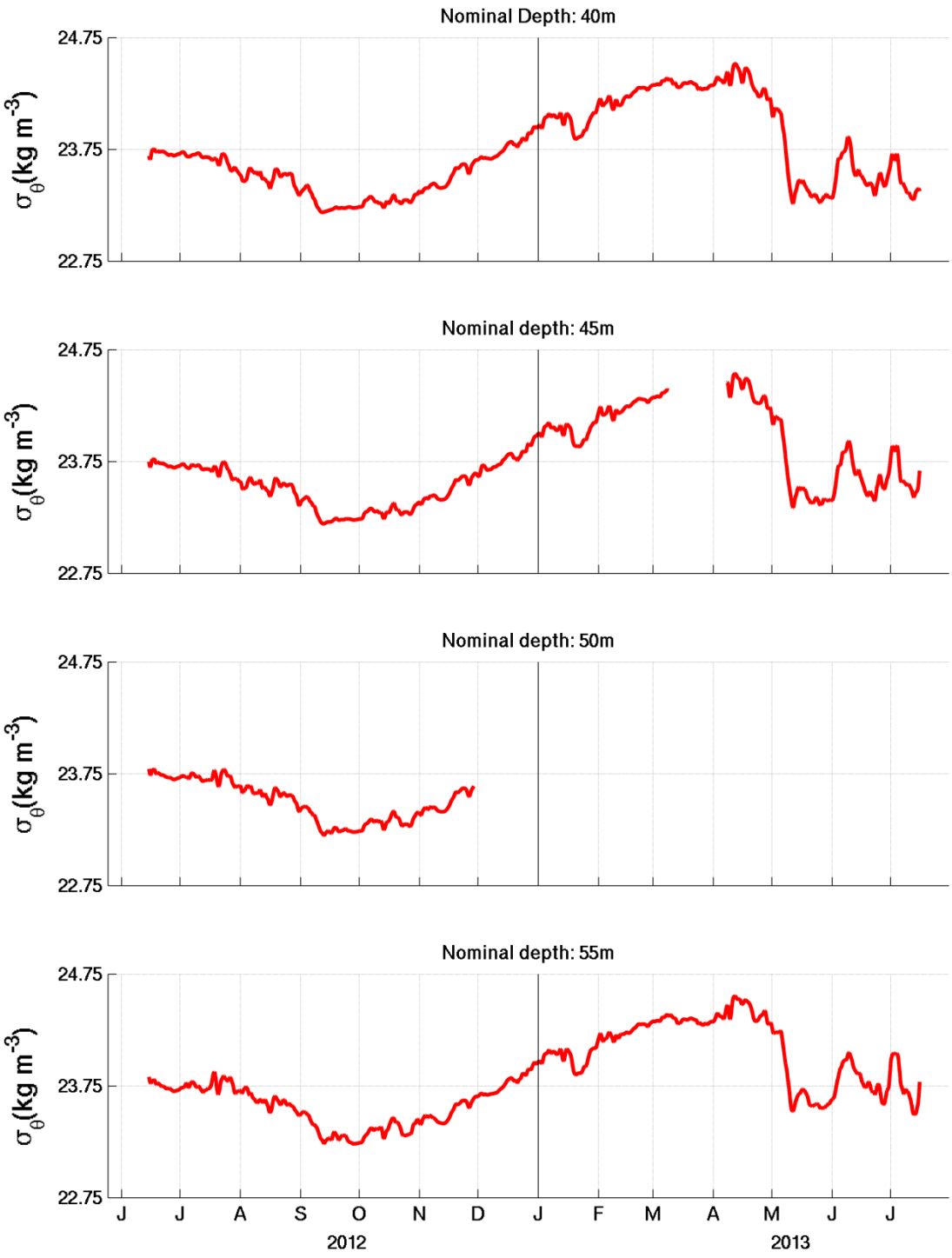

Figure 6-22. Same as in Figure 6-21but at 40, 45, 50, and 55 m.

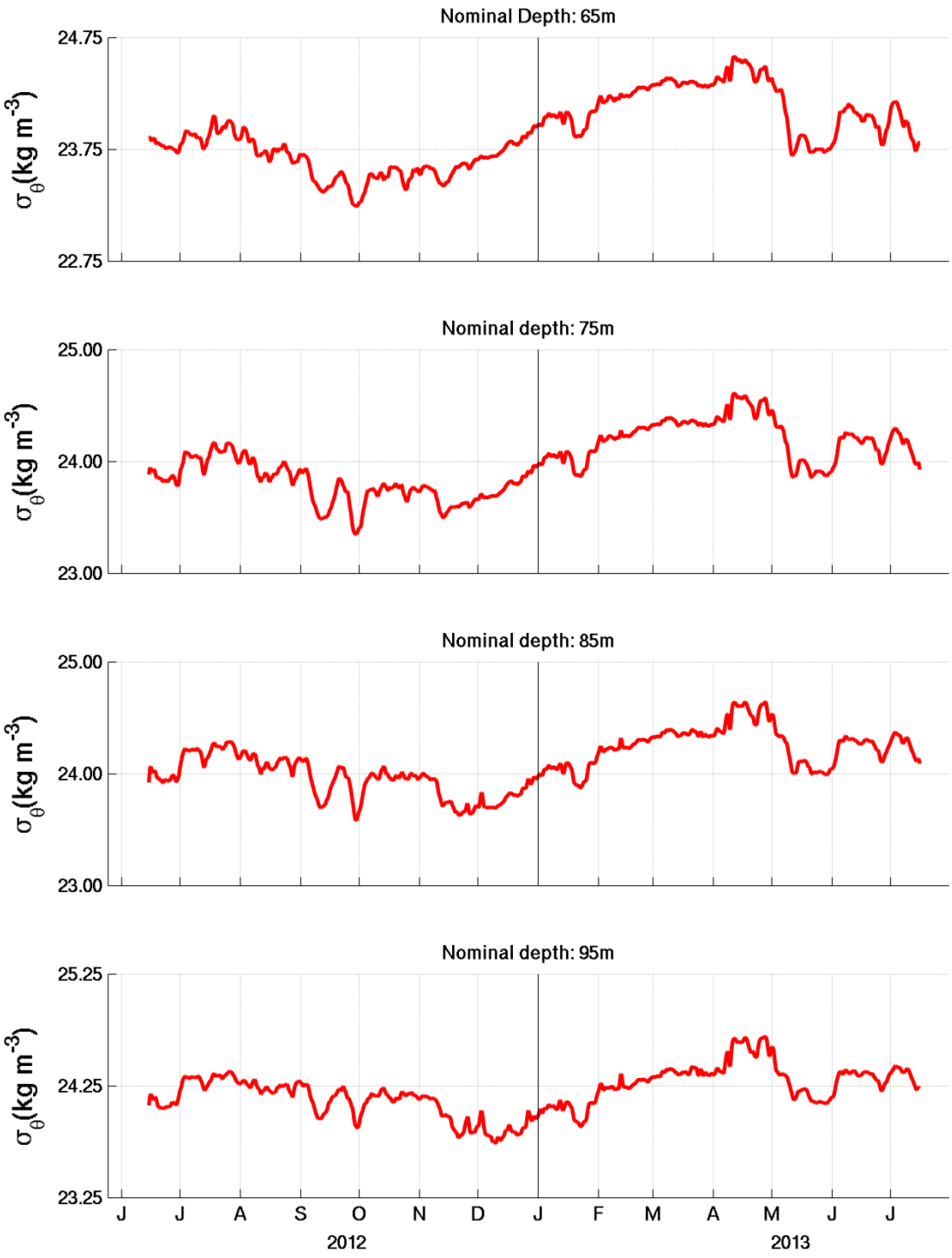

Figure 6-23. Same as in Figure 6-21but at 65, 75, 85, and 95 m.

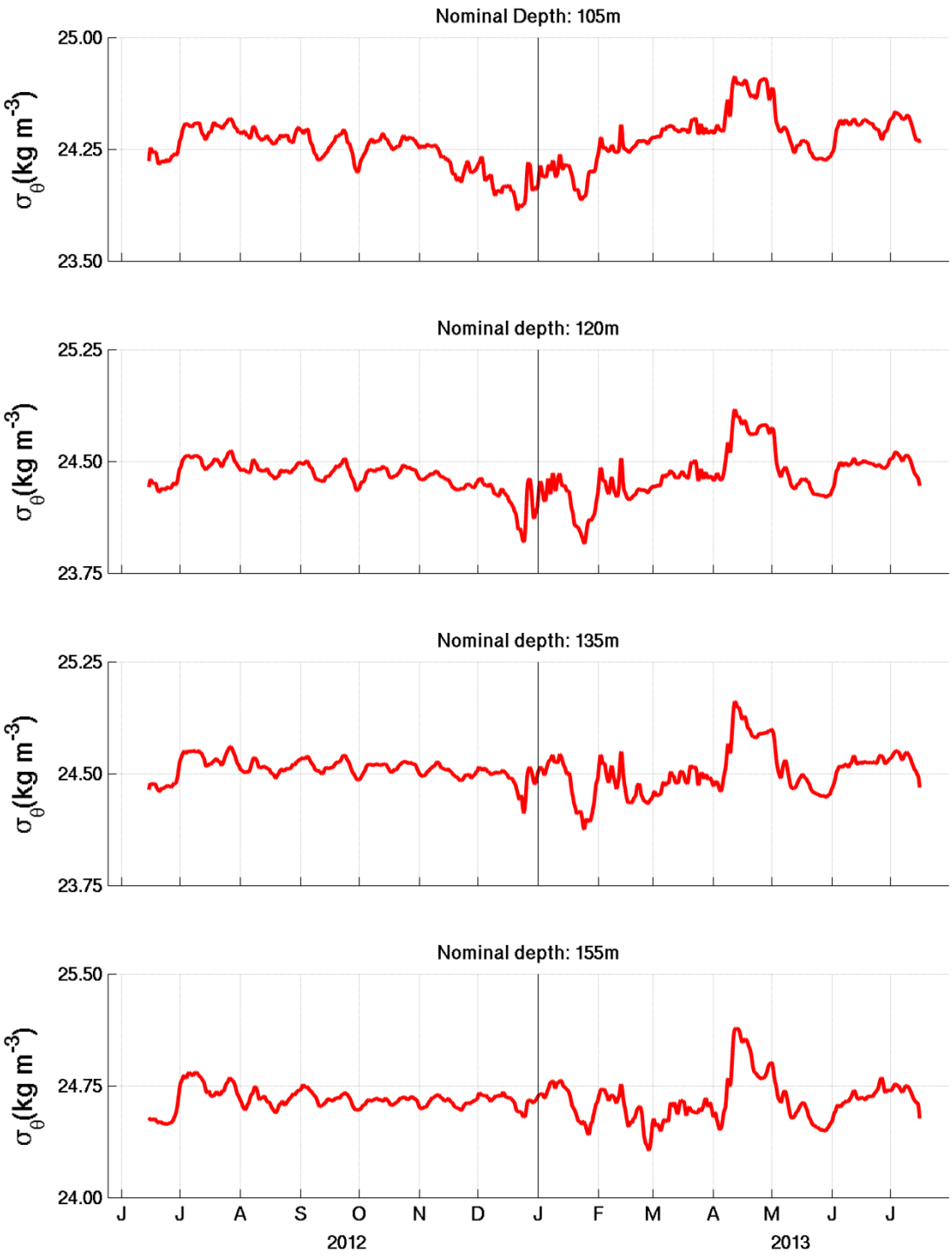

Figure 6-24. Same as in Figure 6-21but at 105, 120, 135, and 155m.

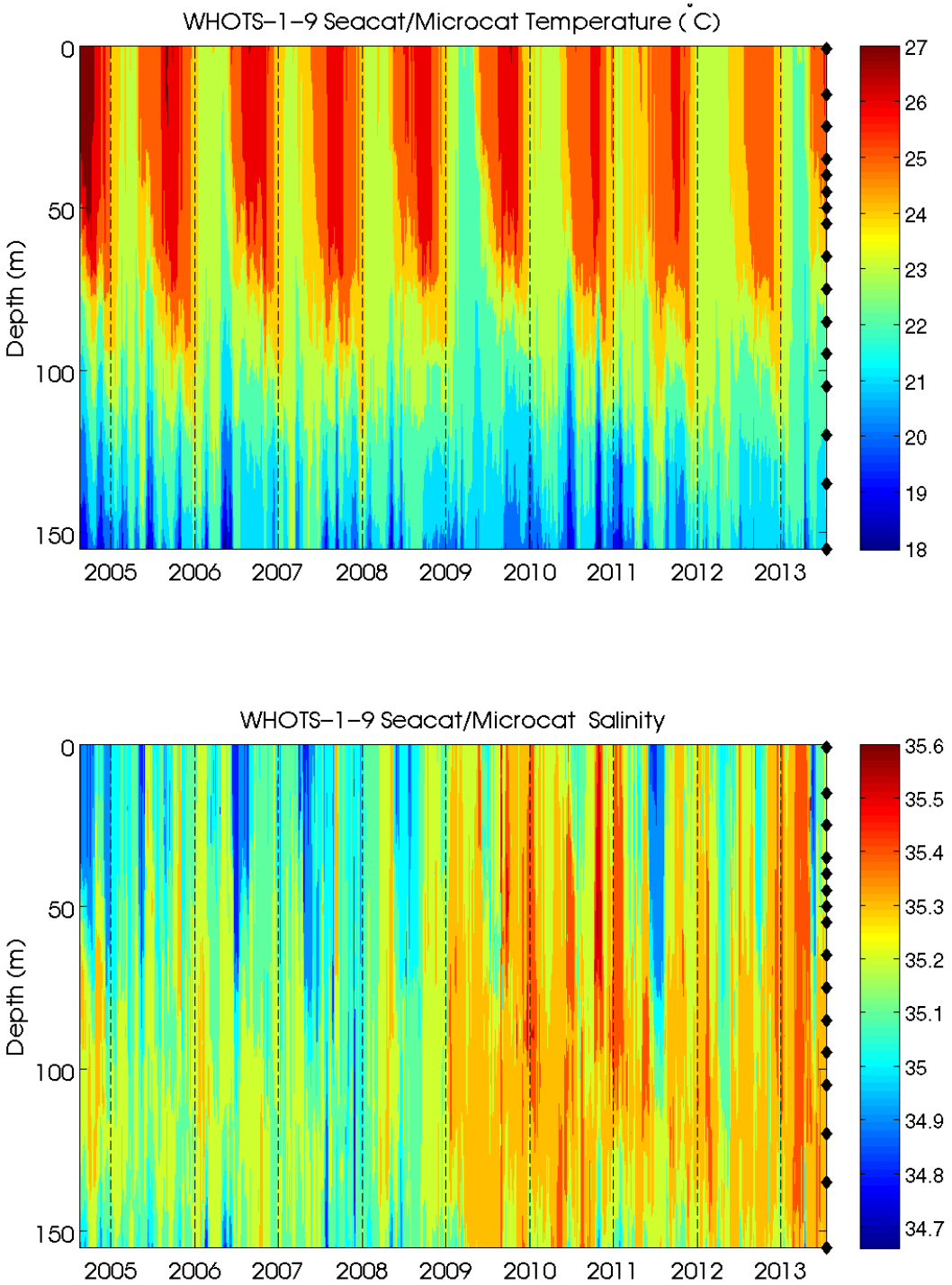

Figure 6-25. Contour plots of temperature (upper panel), and salinity (lower panel) versus depth from SeaCATs/ MicroCATs during WHOTS-1 through WHOTS-9 deployments. The diamonds along the right axis indicate the instruments depths.

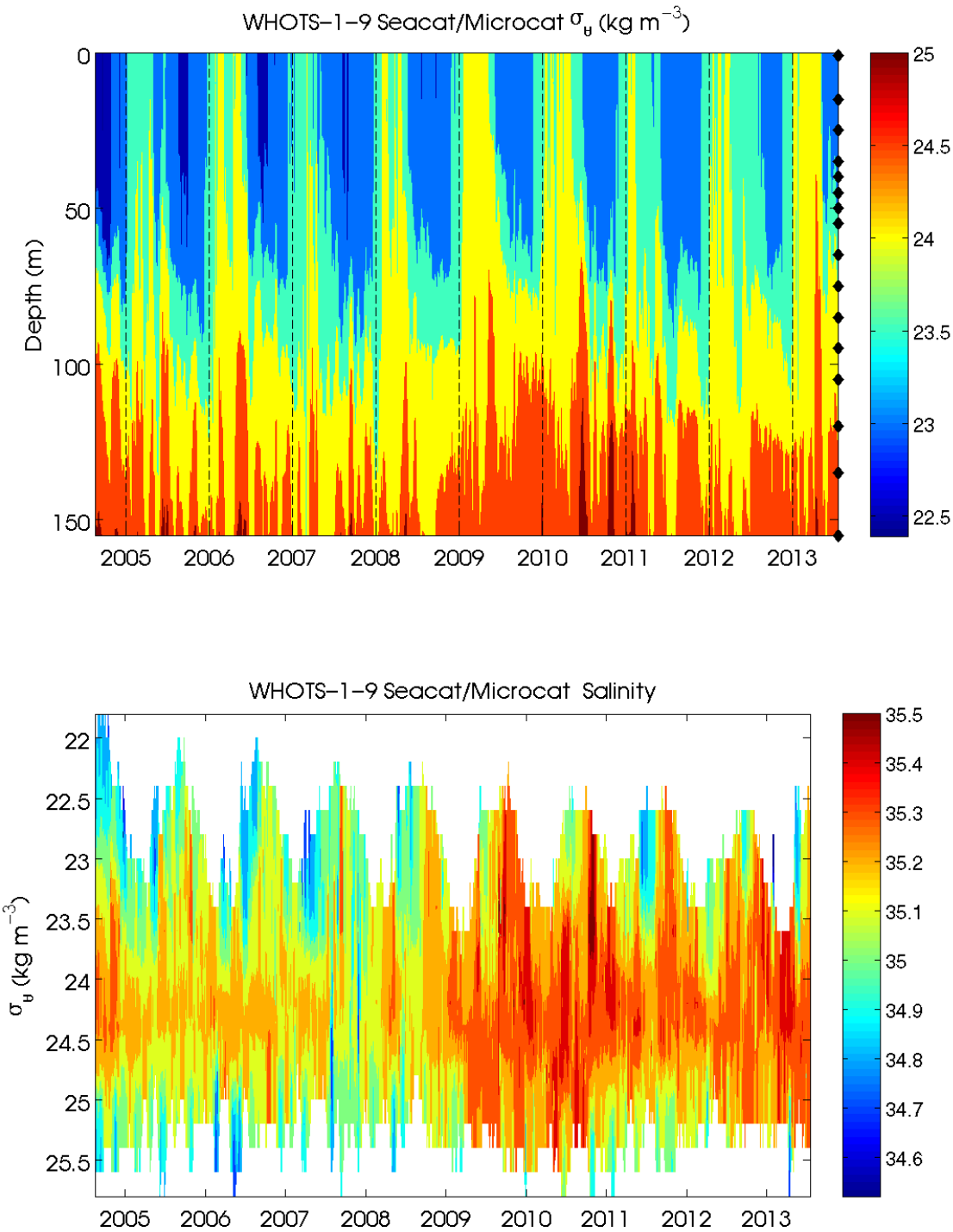

Figure 6-26. Contour plots of potential density (σ_θ , upper panel), versus depth, and of salinity versus σ_θ (lower panel) from SeaCATs/MicroCATs during WHOTS-1 through WHOTS-9 deployments. The diamonds along the right axis in the upper figure indicate the instruments depths.

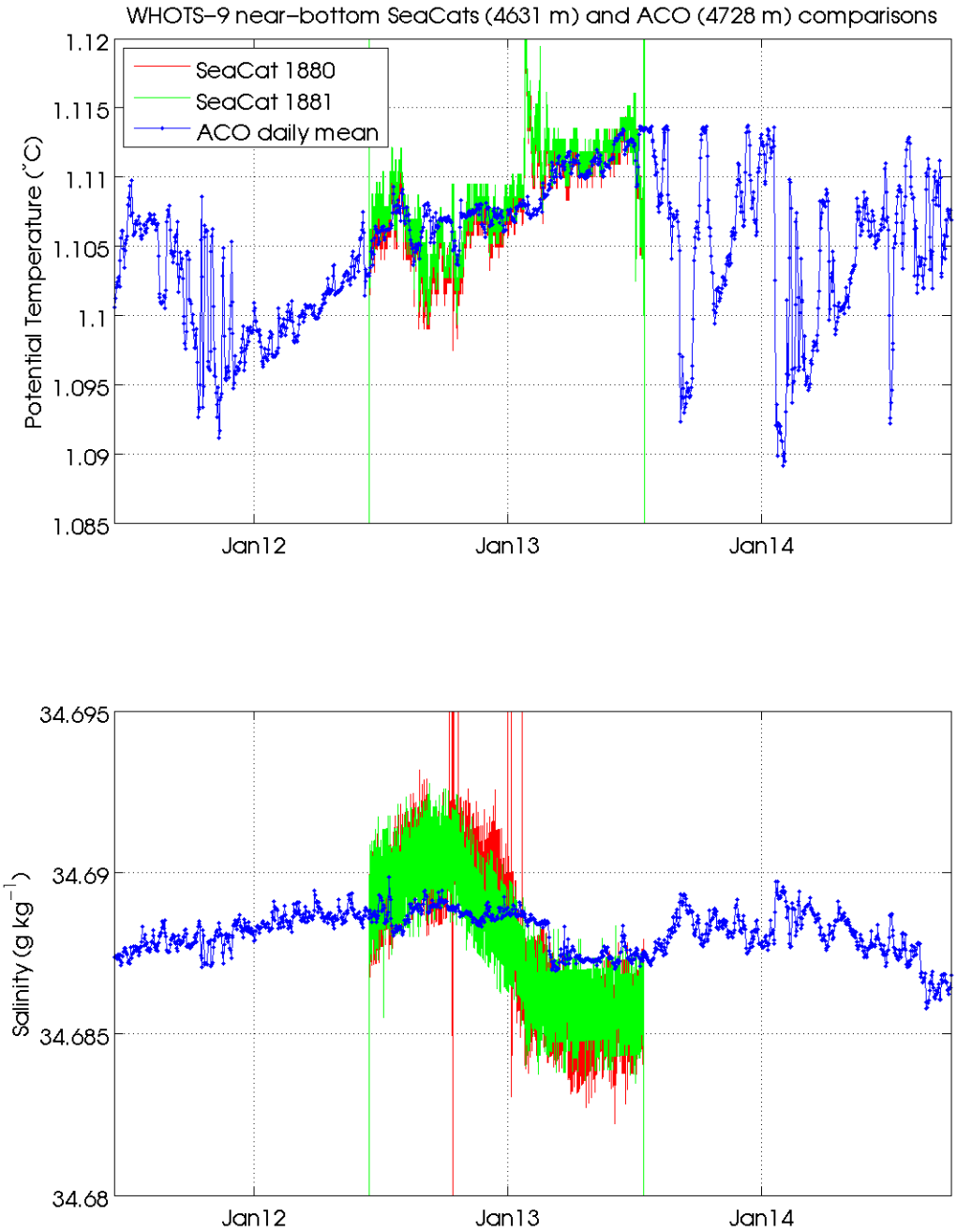

Figure 6-27 Potential temperature (upper panel) and salinity (lower panel) time-series from the ALOHA Cabled Observatory (ACO) sensors and from the WHOTS-9 SeaCATs 1880 and 1881.

D. Moored ADCP data

Contoured plots of smoothed horizontal and vertical velocity as a function of depth during the mooring deployments 1 through 9 are presented in Figure 6-28 to Figure 6-30. A staggered

time-series of smoothed horizontal and vertical velocities are shown in Figure 6-31 to Figure 6-33. Smoothing was performed by applying a daily running mean to the data and then interpolating the data on to an hourly grid.

Contours of east and north velocity components from the Ship Hi'ialakai's Ocean Surveyor broadband 75 kHz shipboard ADCP, and the moored 300 kHz ADCP from the WHOTS-9 deployment as a function of time and depth, during the WHOTS-10 cruise are shown in Figure 6-34 and Figure 6-35.

Figure 6-28. Contour plot of east velocity component (m s^{-1}) versus depth and time from the moored ADCPs from the WHOTS-1 through 9 deployments.

Figure 6-29. Contour plot of north velocity component (m s^{-1}) versus depth and time from the moored ADCPs from the WHOTS-1 through 9 deployments.

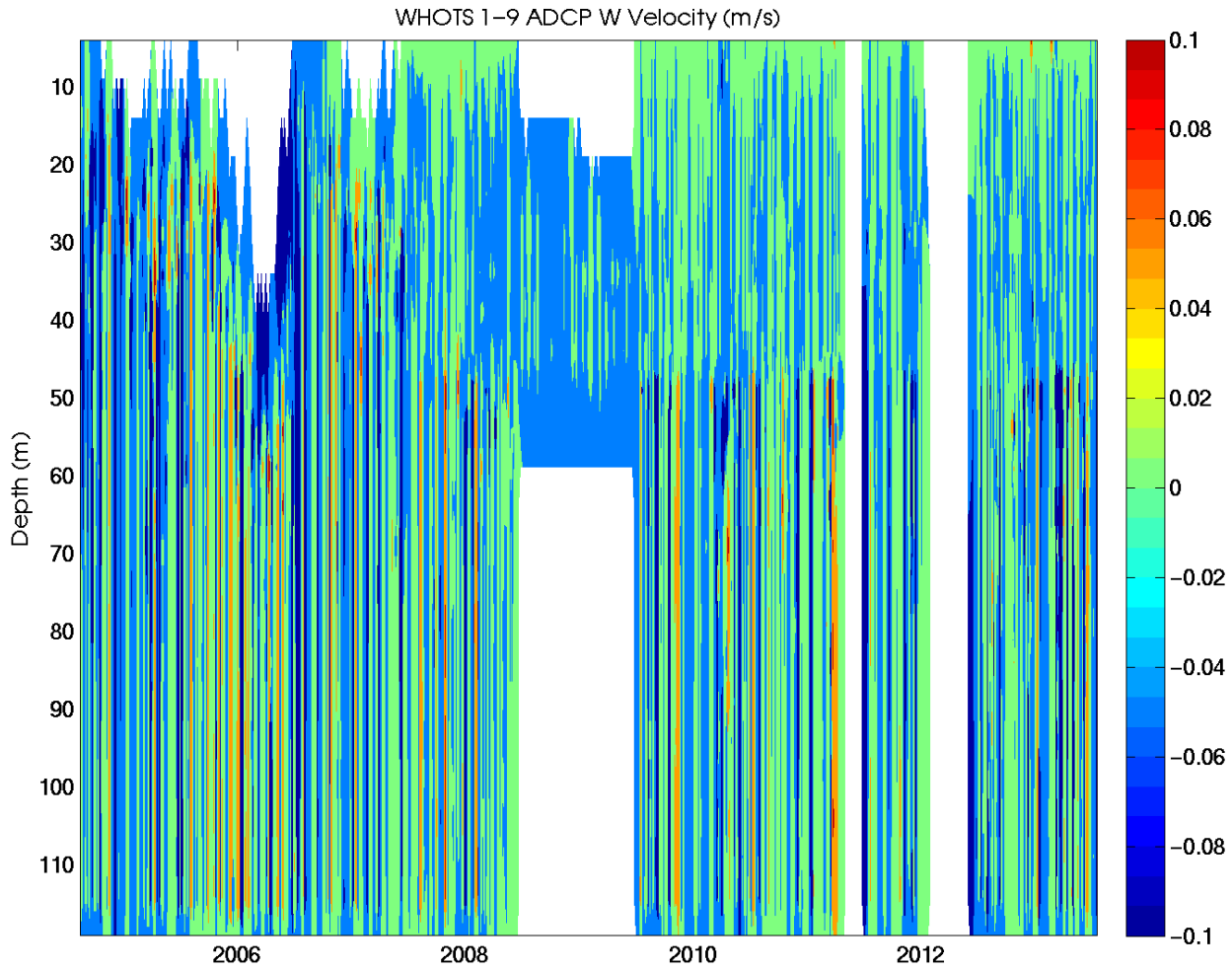

Figure 6-30.Contour plot of vertical velocity component (m s-1) versus depth and time from the moored ADCPs from the WHOTS-1through 9 deployments.

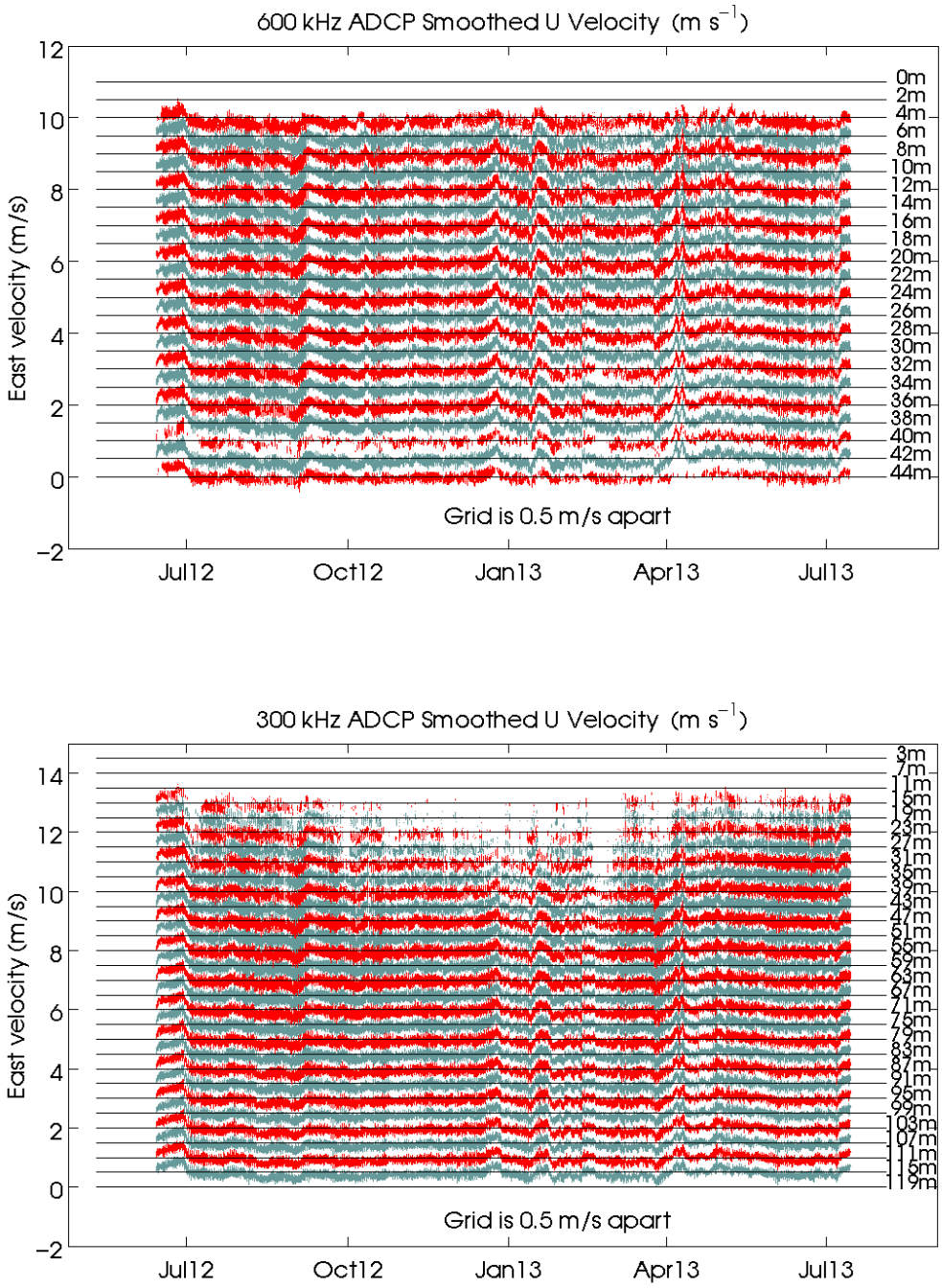

Figure 6-31. Staggered time-series of east velocity component (m s^{-1}) for each bin of the 600 kHz (upper panel), and 300 kHz (lower panel) moored ADCPs during WHOTS-9. The time-series are offset upwards by 0.5 m s^{-1}, the depth of each bin is on the right.

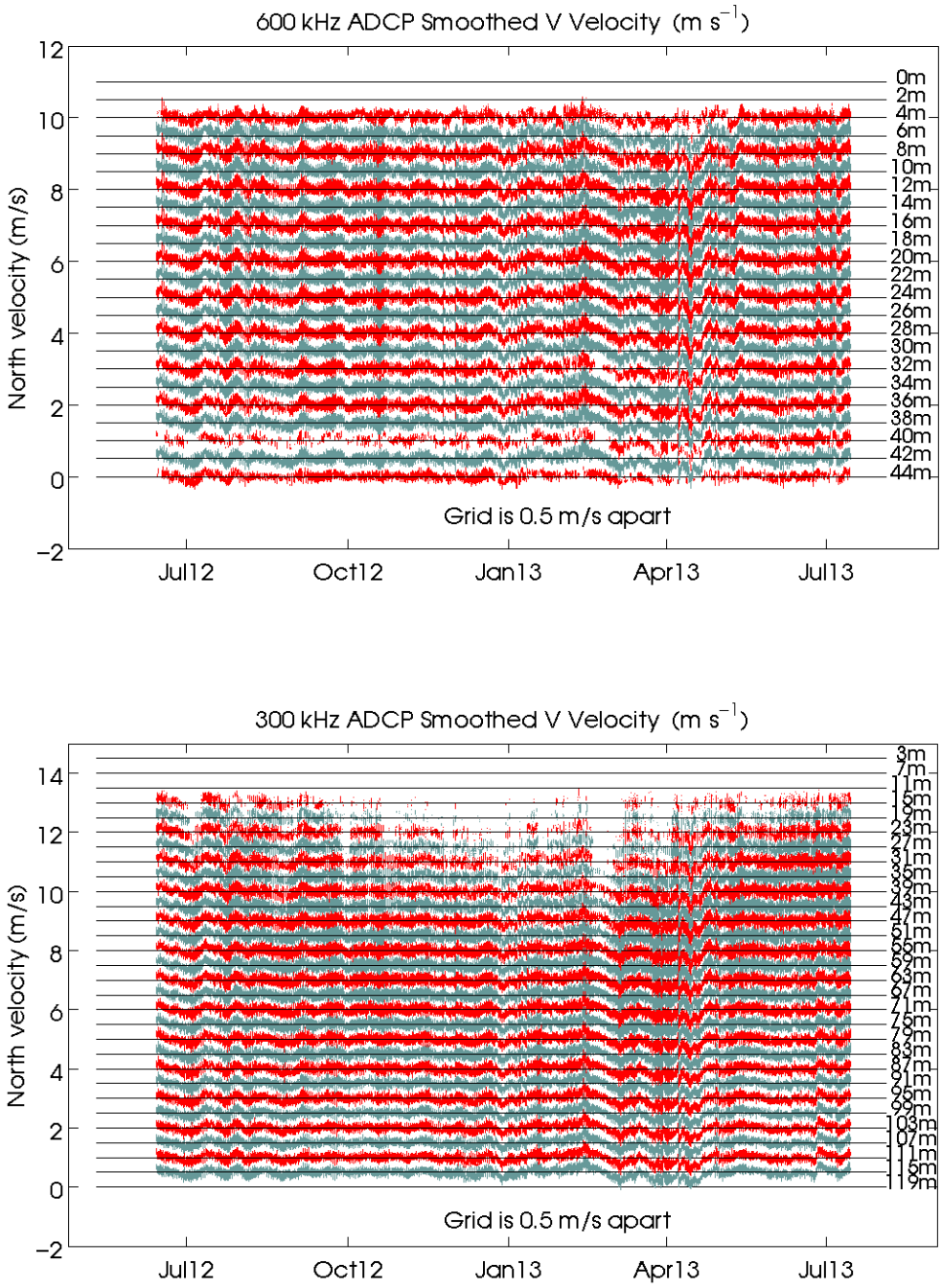

Figure 6-32. Staggered time-series of north velocity component (m s^{-1}) for each bin of the 600 kHz (upper panel), and 300 kHz (lower panel) moored ADCPs during WHOTS-9. The time-series are offset upwards by 0.5 m s^{-1}, the depth of each bin is on the right.

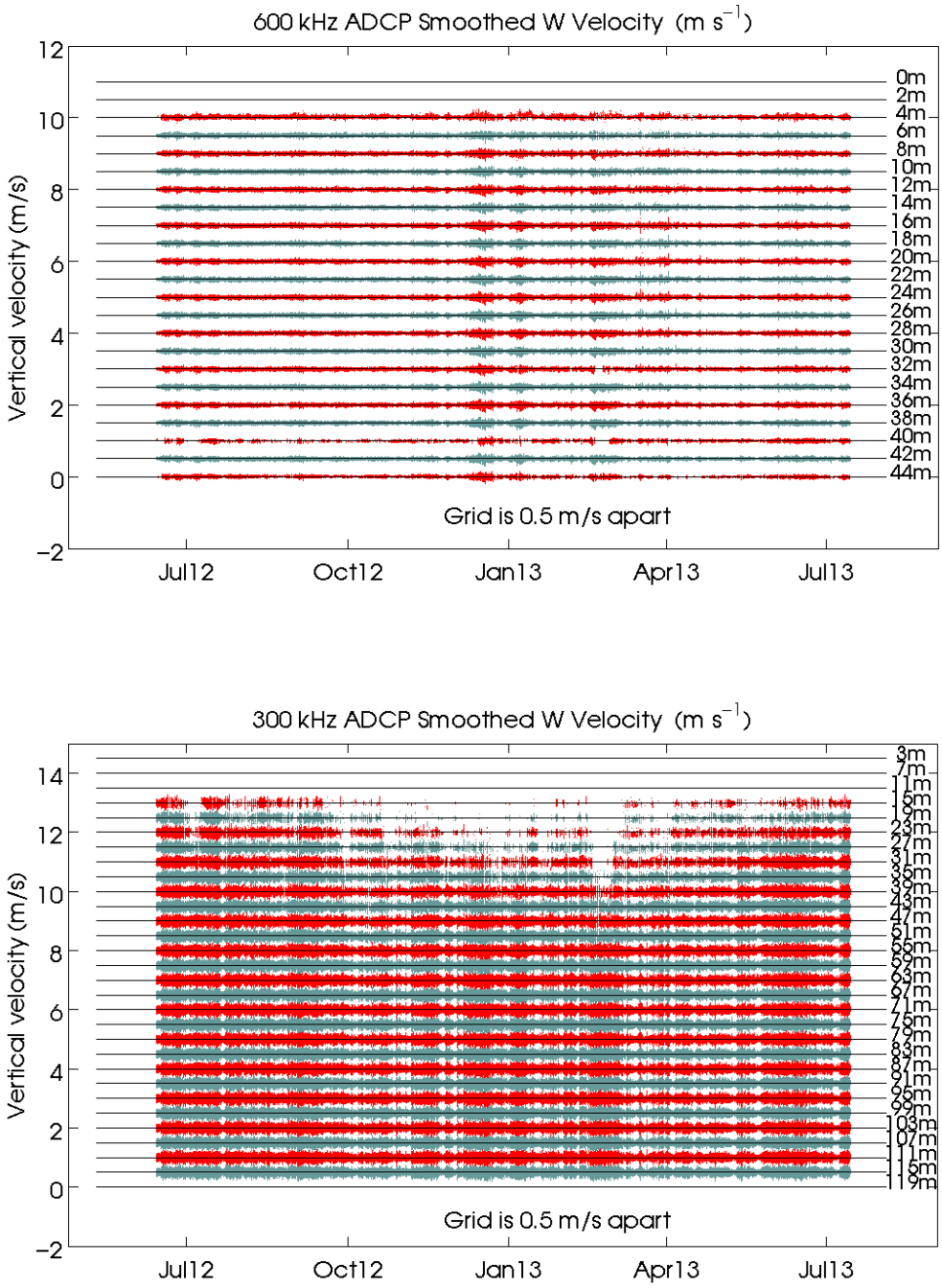

Figure 6-33. Staggered time-series of vertical velocity component (m s^{-1}) for each bin of the 600 kHz (upper panel), and 300 kHz (lower panel) moored ADCPs during WHOTS-9. The time-series are offset upwards by 0.5 m s^{-1}, the depth of each bin is on the right.

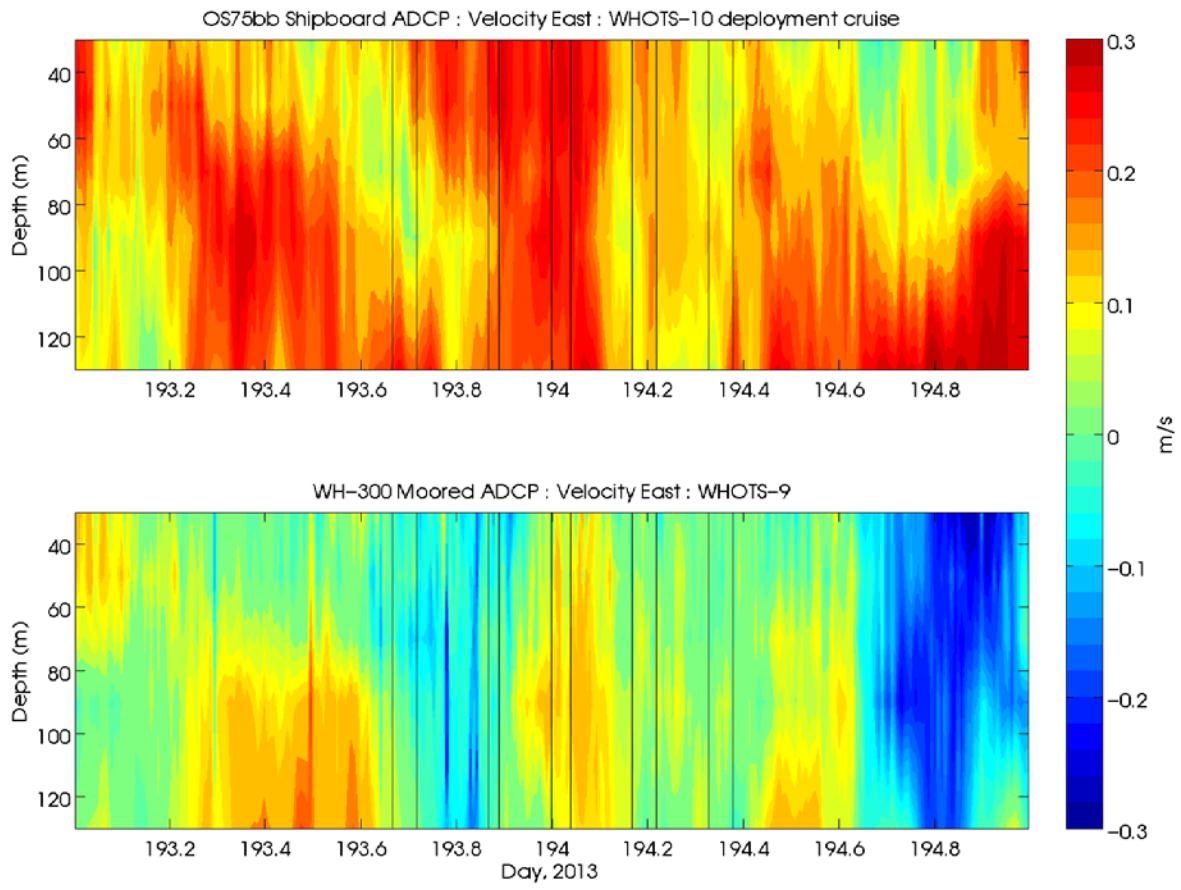

Figure 6-34. Contour of east velocity component (m s^{-1}) from the Ship Hi'ialakai's Ocean Surveyor broadband 75 kHz shipboard ADCP (upper panel), and the moored 300 kHz ADCP from the WHOTS-9 deployment as a function of time and depth, during the WHOTS-10 cruise (lower panel). Times when the CTD rosette were in the water are identified between the two sets of black lines.

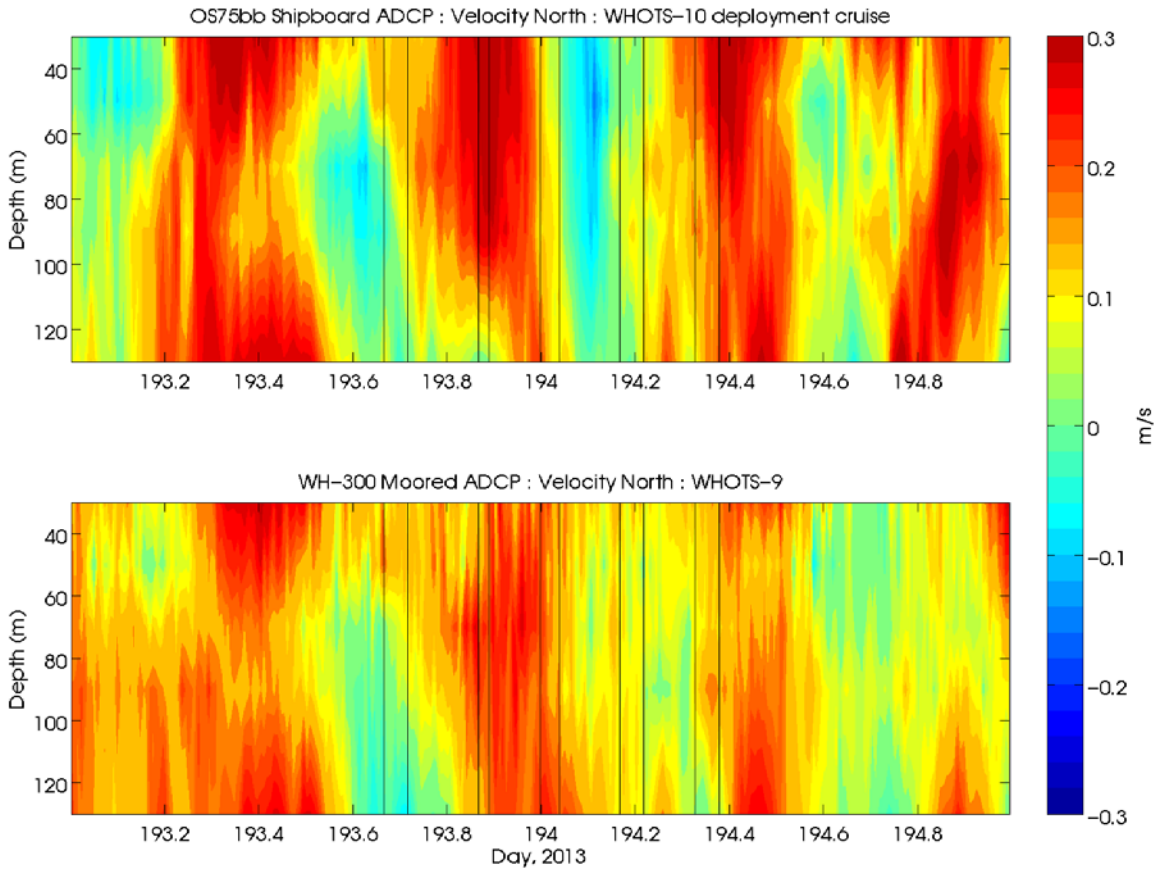

Figure 6-35. Contours of north velocity component (m s^{-1}) from the Ship Hi'ialakai's Ocean Surveyor broadband 75 kHz shipboard ADCP (upper panel), and the moored 300 kHz ADCP from the WHOTS-9 deployment as a function of time and depth, during the WHOTS-10 cruise (lower panel). Times when the CTD/rosette was in the water are identified between the two sets of black lines.

E. Moored and Shipboard ADCP comparisons

Comparisons between quality-controlled moored ADCPs during the WHOTS-9 deployment and available shipboard ADCP obtained during regular HOT cruises 243 to 253 are shown in Figure 6-36 to Figure 6-46 for the 300 kHz ADCP, and Figure 6-47 to Figure 6-54 for the 600 kHz ADCP. Median and mean velocity profiles were computed during the time when HOT CTD casts were being conducted near the WHOTS mooring specifically intended to calibrate moored

instrumentation (see 5.A.4). The shipboard profiles were taken when the ship was stationary, within 1 km of the mooring, and within 4 hours before the start and 4 hours after the end of the CTD cast conducted near the WHOTS mooring. HOT cruises conducted on the R/V *Kilo Moana* (HOT-243 to 250 and 252 to 253) had data from an RD Instruments Workhorse 300 kHz ADCP (wh300) with 4 m bin size, reaching 100 m, and averaging ensembles every 2 minutes; and from an RD Instruments Ocean Surveyor 38 kHz operating in broad band mode (os38bb) with 12 m bin size, reaching 1200 m, with 5 minute ensemble averages, and in narrow band mode (os38nb) with 24 m bin size, reaching 1500 m and also with 5 minute ensemble averages. Data from the wh300 were used for the comparisons with the moored ADCP data, or from the os75bb if the wh300 data were not available. Cruise HOT-251 on the R/V *T. Thompson* had data from an RD Instruments Ocean Surveyor 75 kHz operating in broad band mode (os75bb) with 20 m bin size, reaching 330 m, with 5 minute ensemble averages.

The moored ADCP data were collected from the upward facing 300 kHz ADCP located at 125 m and the upward facing 600 kHz ADCP located at 47.5 m over the same time period. Each of the zonal (U), and meridional (V) current components from the shipboard and moored vertical profiles were interpolated to the profile resolution of the shipboard ADCP, and ensemble mean and median profiles were obtained for each data set to compute differences and correlation coefficients between them (Table 6). Bins with less than 50% data were excluded.

Comparisons between the 300 kHz and the shipboard ADCP from HOT-245 were excluded due to a lack of comparable data. Comparisons between the moored 600 kHz and the shipboard ADCP were only evaluated for cruises featuring the Workhorse 300 kHz ADCP (wh300) due to the larger vertical resolution with the other ADCP models (os38bb, os75bb). The correlations and the vertical mean of the differences between the ensemble median and mean for each of the U and V components are shown in Table 6-1.

Table 6-1. Correlations and differences of zonal (U), and meridional (V) ensemble median and mean currents (10 to 125 m) between WHOTS-9 moored ADCP (300 and 600 kHz) and shipboard ADCP during HOT cruises. Only HOT cruises with a wh300 shipboard ADCP were compared with the 600 kHz ADCP due to lack of shallow current data in the shipboard os38bb and os75bb models (see text).

HOT Shipboard ADCP vs WHOTS Moored 300 kHz ADCP									
Cruise	**Ship ADCP Type**	**Ensemble Median U correlation**	**Vertical Mean of U median differences**	**Ensemble Median V correlation**	**Vertical Mean of V median differences**	**Ensemble Mean U correlation**	**Vertical Mean differences U**	**Ensemble Mean V correlation**	**Vertical Mean differences V**
HOT - 243	wh300	0.6403	-0.0177	0.8078	-0.0467	0.6253	-0.0131	0.8787	-0.0370
HOT - 244	wh300	0.9432	-0.0103	0.8106	-0.0174	0.9693	-0.0079	0.7882	-0.0174
HOT - 246	wh300	0.6797	0.0368	0.8431	0.0571	0.5683	0.0287	0.8352	0.0604
HOT - 247	wh300	0.6991	-0.0262	0.8701	-0.0338	0.6911	-0.0276	0.7540	-0.0371
HOT - 248	os38bb	0.6797	-0.0157	0.6433	-0.0107	0.8803	-0.0125	0.5266	0.0014
HOT - 249	os38bb	0.9722	-0.0402	0.9077	0.0341	0.9936	-0.0393	0.8280	0.0310
HOT - 250	wh300	0.7992	-0.0051	0.3688	0.0096	0.0266	0.0094	0.3543	0.0152
HOT - 251	os75bb	0.7838	0.0644	0.9484	0.0316	0.8169	0.0698	0.9615	0.0331
HOT - 252	wh300	0.9064	-0.0076	0.8485	-0.0073	0.8705	0.0089	0.7717	-0.0152
HOT - 253	wh300	0.7378	-0.0416	0.4337	-0.0597	0.7790	-0.0390	-0.1821	-0.0687
HOT Shipboard ADCP vs WHOTS Moored 600 kHz ADCP									
HOT - 243	wh300	0.8397	-0.0276	0.3300	-0.0457	0.8235	-0.0282	0.5471	-0.0501
HOT - 244	wh300	0.9214	0.0103	0.4358	-0.0358	0.9223	0.0131	0.5405	-0.0316
HOT - 245	wh300	0.9131	-0.0077	0.9752	-0.0152	0.9285	-0.0084	0.9814	-0.0220
HOT - 246	wh300	0.7095	0.0393	0.7312	0.0426	0.9279	0.0426	0.8398	0.0477
HOT - 247	wh300	0.9460	-0.0384	0.9498	-0.0199	0.9355	-0.0359	0.9698	-0.0208
HOT - 250	wh300	0.9194	-0.0087	0.8842	-0.0135	0.9666	0.0014	0.7206	-0.0115
HOT - 252	wh300	0.9671	-0.0113	0.8234	-0.0253	0.9514	-0.0175	0.9802	-0.0028
HOT - 253	wh300	0.5838	-0.0206	0.8805	-0.0237	0.3990	-0.0243	0.9286	-0.0232

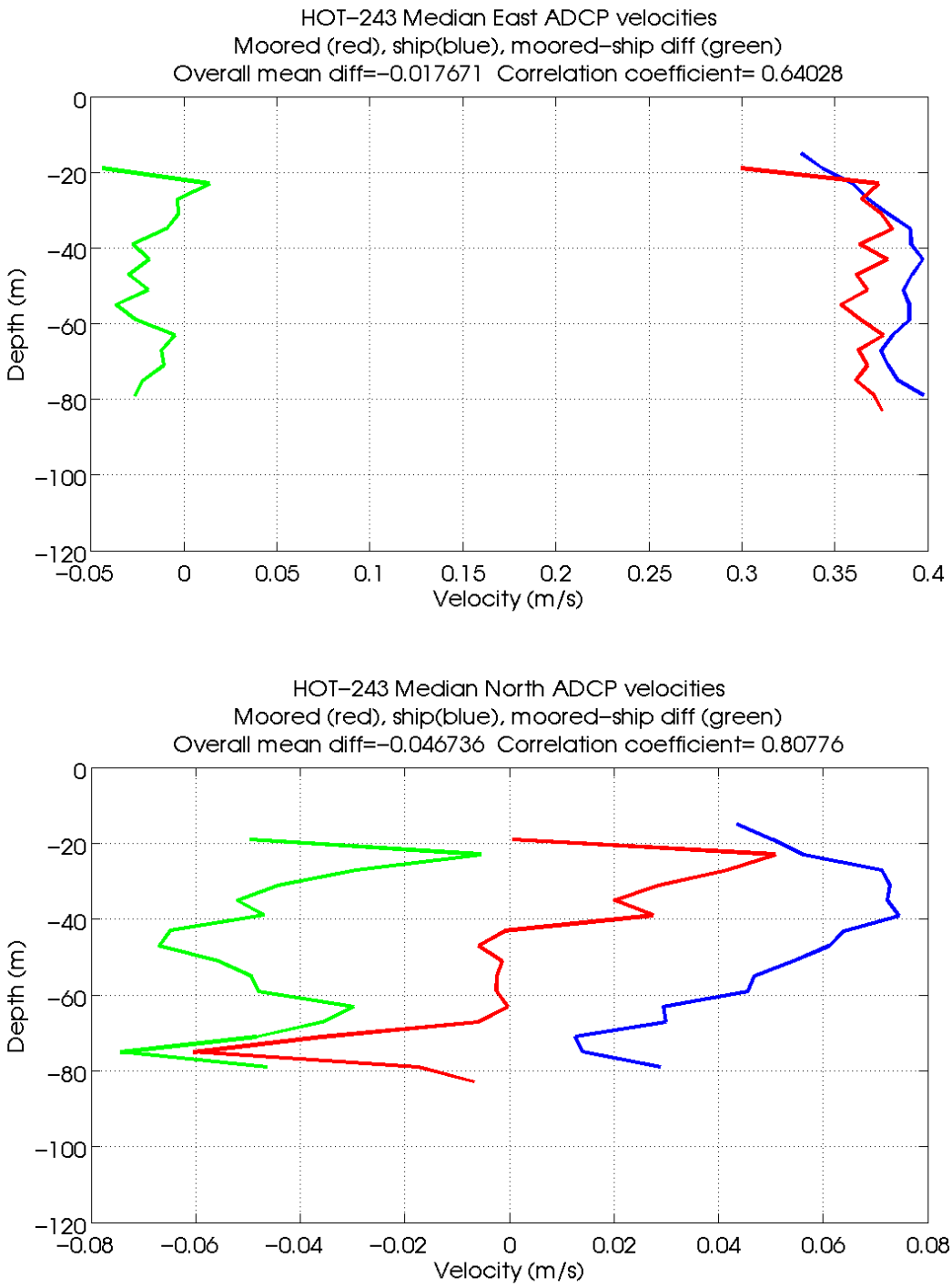

Figure 6-36. Median velocity profiles during shipboard ADCP (blue) versus moored 300 kHz ADCP (red) intercomparisons from HOT-243. Moored minus shipboard ADCP differences shown in green. Top panel shows east velocity components, bottom panel shows north velocity components.

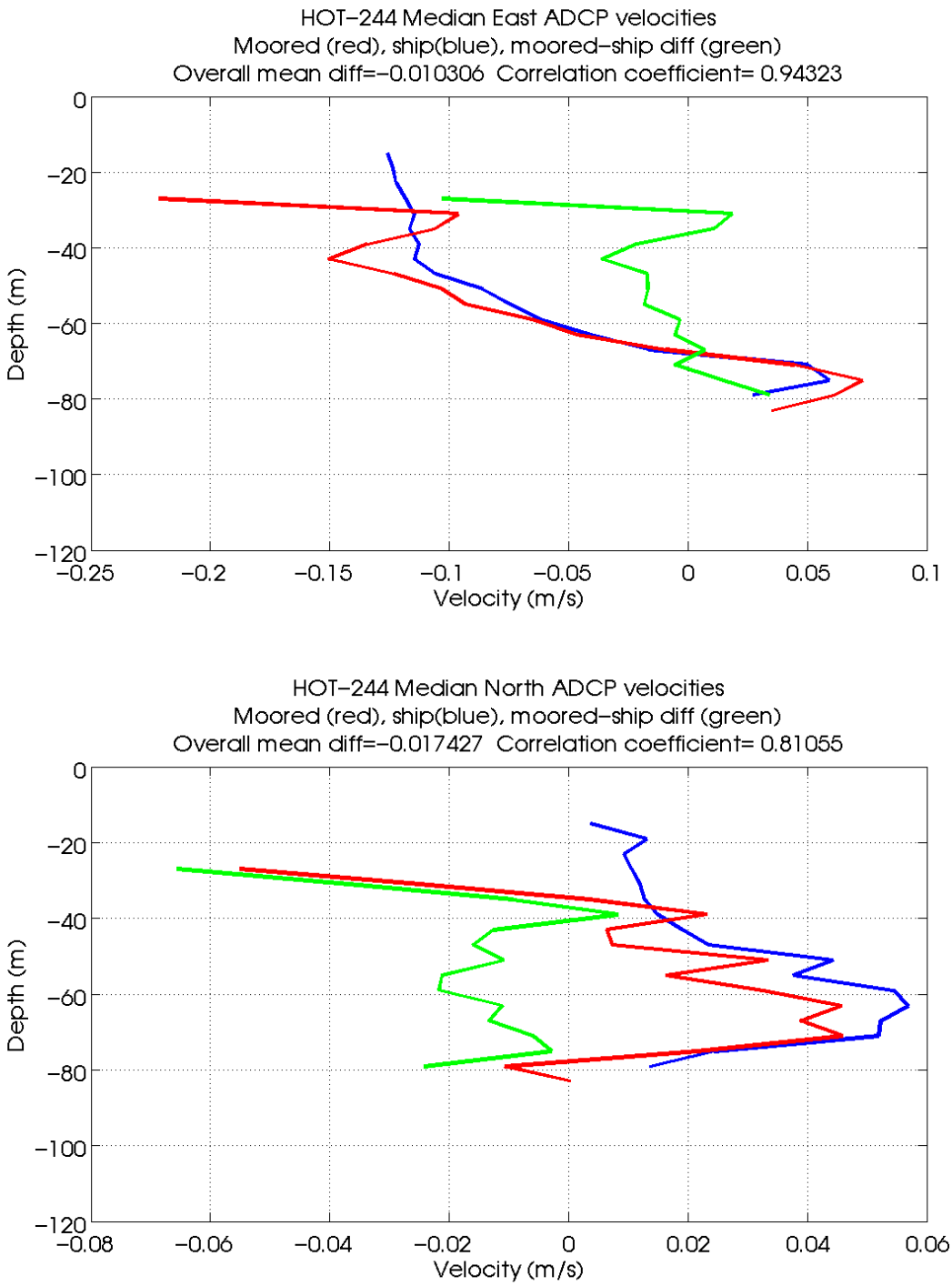

Figure 6-37. Median velocity profiles during shipboard ADCP (blue) versus moored 300 kHz ADCP (red) intercomparisons from HOT-244. Moored minus shipboard ADCP differences shown in green. Top panel shows east velocity components, bottom panel shows north velocity components.

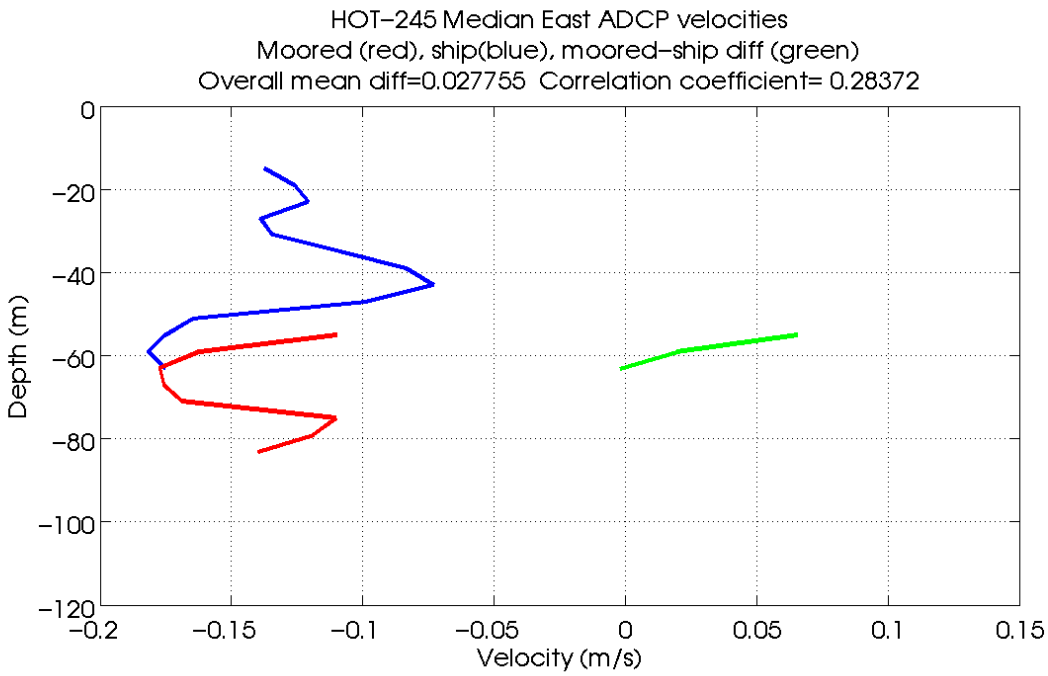

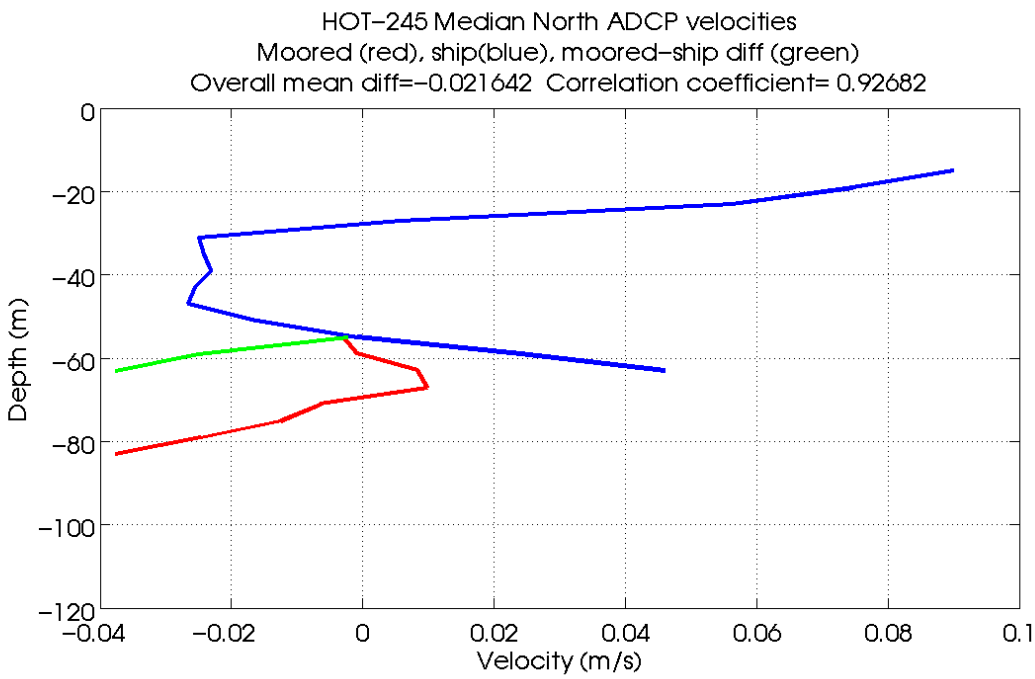

Figure 6-38. Median velocity profiles during shipboard ADCP (blue) versus moored 300 kHz ADCP (red) intercomparisons from HOT-245. Moored minus shipboard ADCP differences shown in green. Top panel shows east velocity components, bottom panel shows north velocity components.

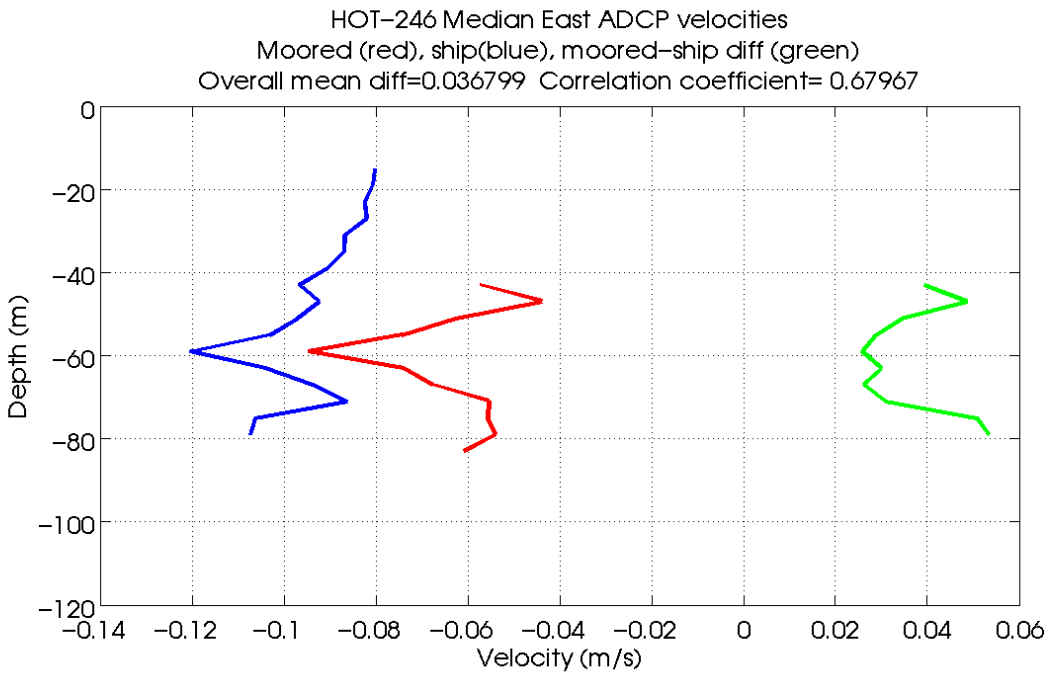

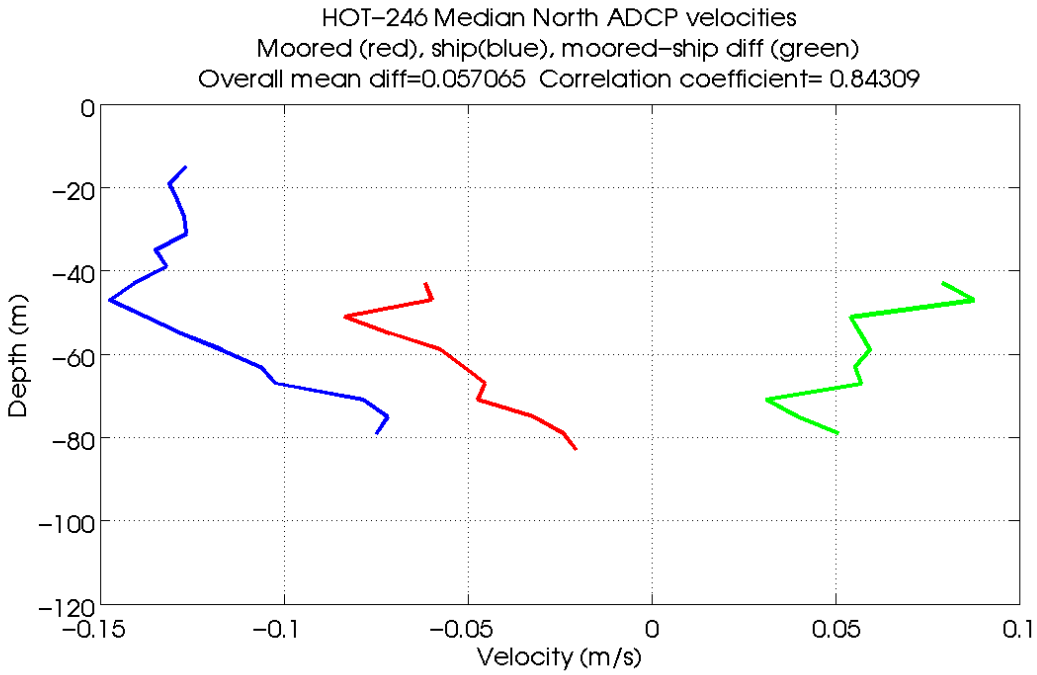

Figure 6-39. Median velocity profiles during shipboard ADCP (blue) versus moored 300 kHz ADCP (red) intercomparisons from HOT-246. Moored minus shipboard ADCP differences shown in green. Top panel shows east velocity components, bottom panel shows north velocity components.

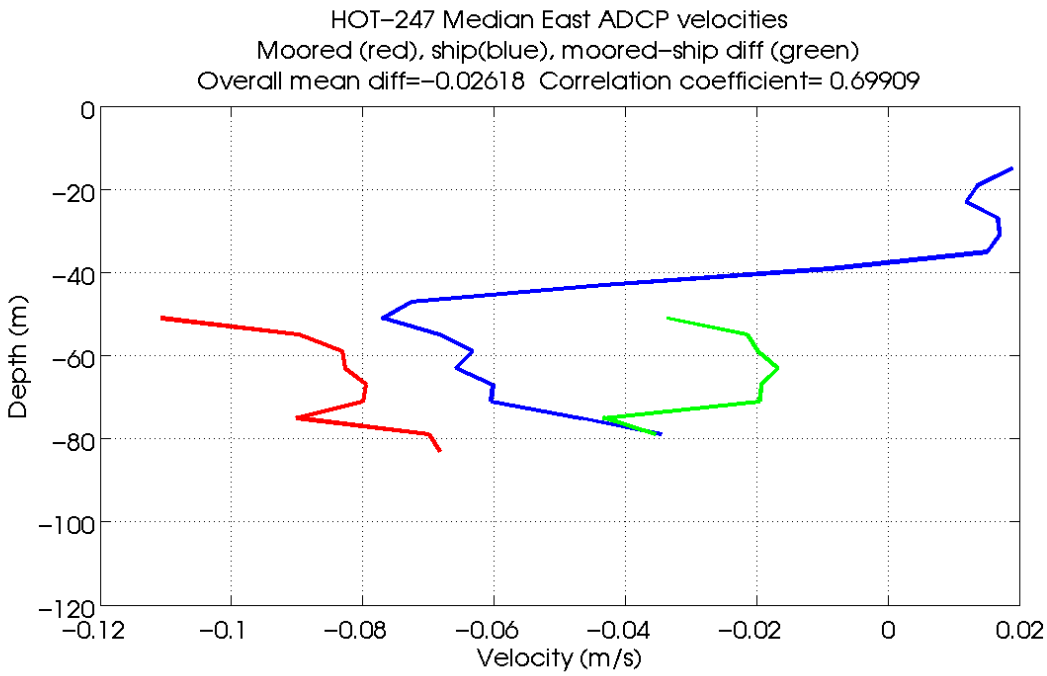

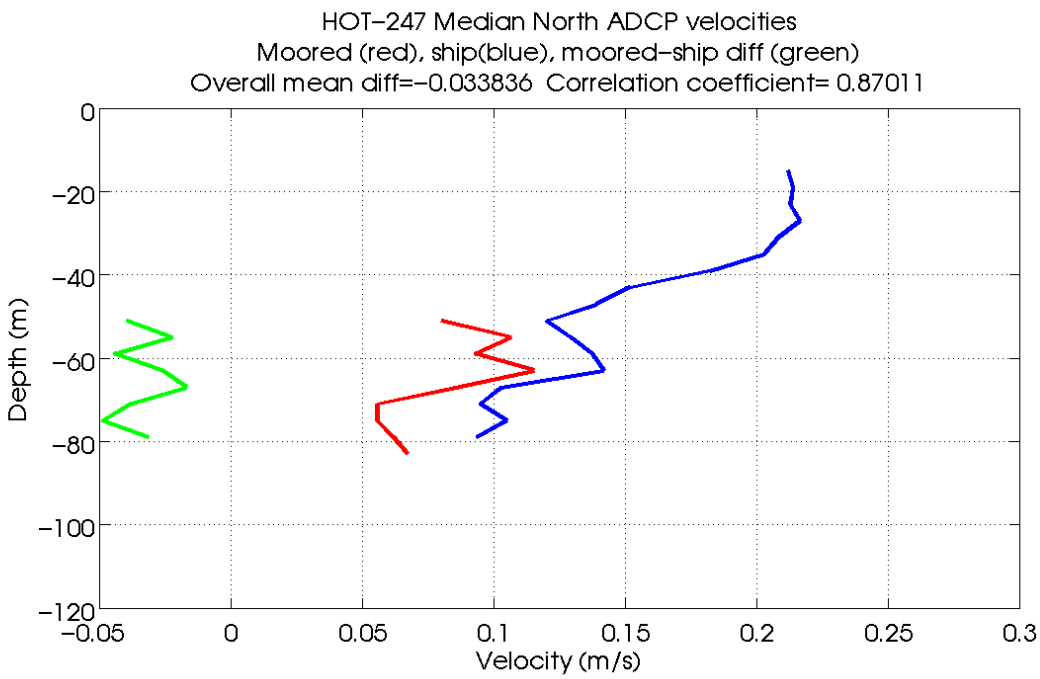

Figure 6-40. Median velocity profiles during shipboard ADCP (blue) versus moored 300 kHz ADCP (red) intercomparisons from HOT-247. Moored minus shipboard ADCP differences shown in green. Top panel shows east velocity components, bottom panel shows north velocity components.

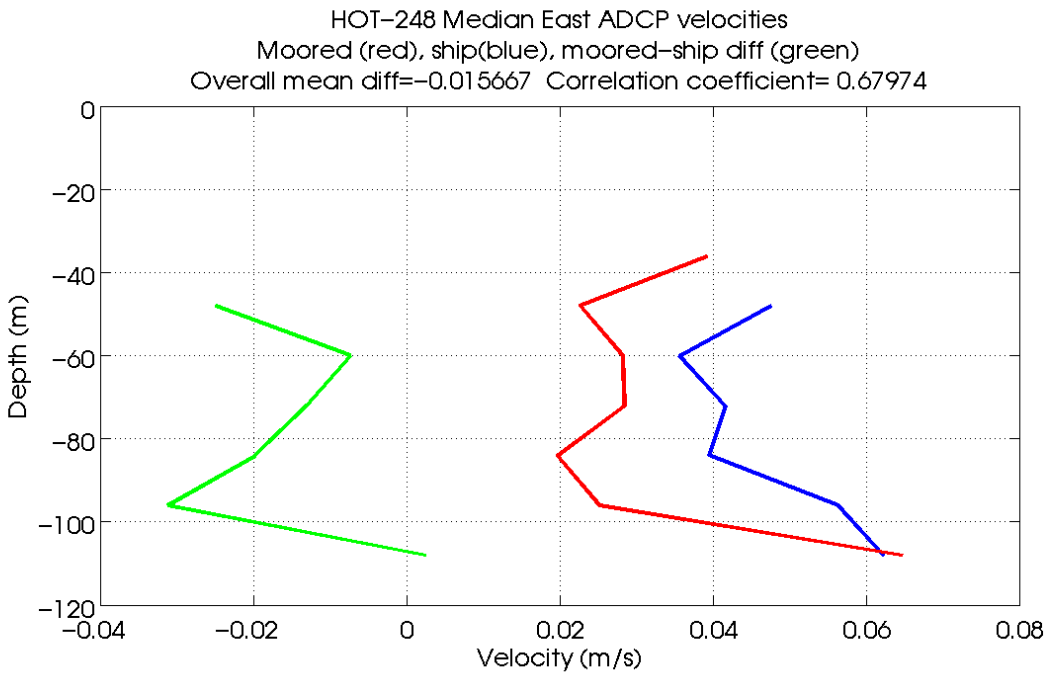

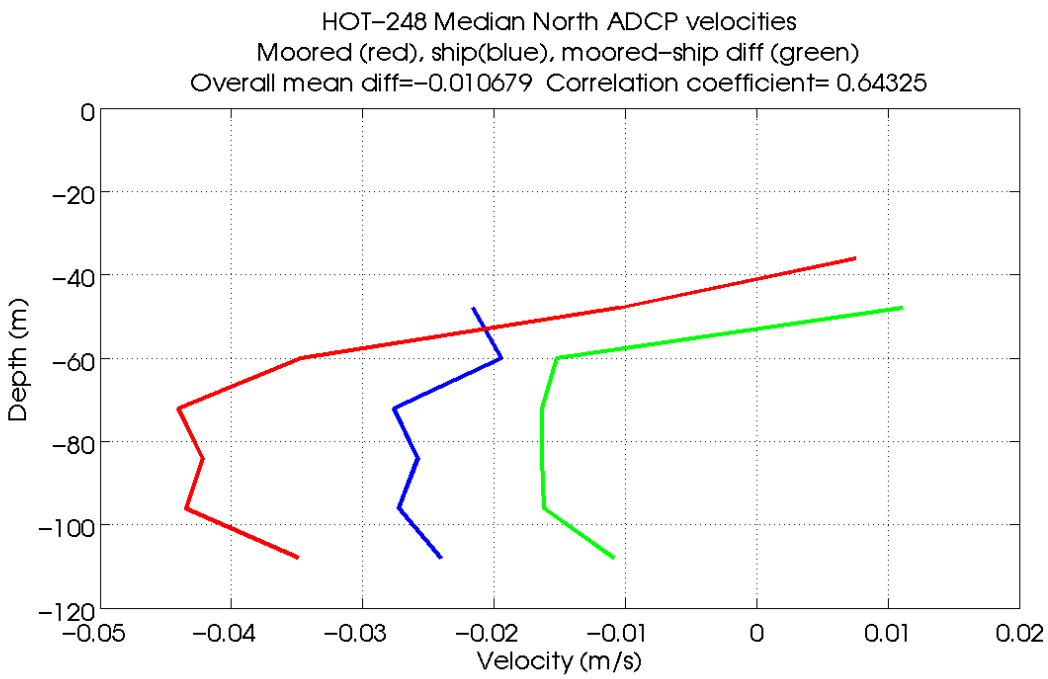

Figure 6-41. Median velocity profiles during shipboard ADCP (blue) versus moored 300 kHz ADCP (red) intercomparisons from HOT-248. Moored minus shipboard ADCP differences shown in green. Top panel shows east velocity components, bottom panel shows north velocity components.

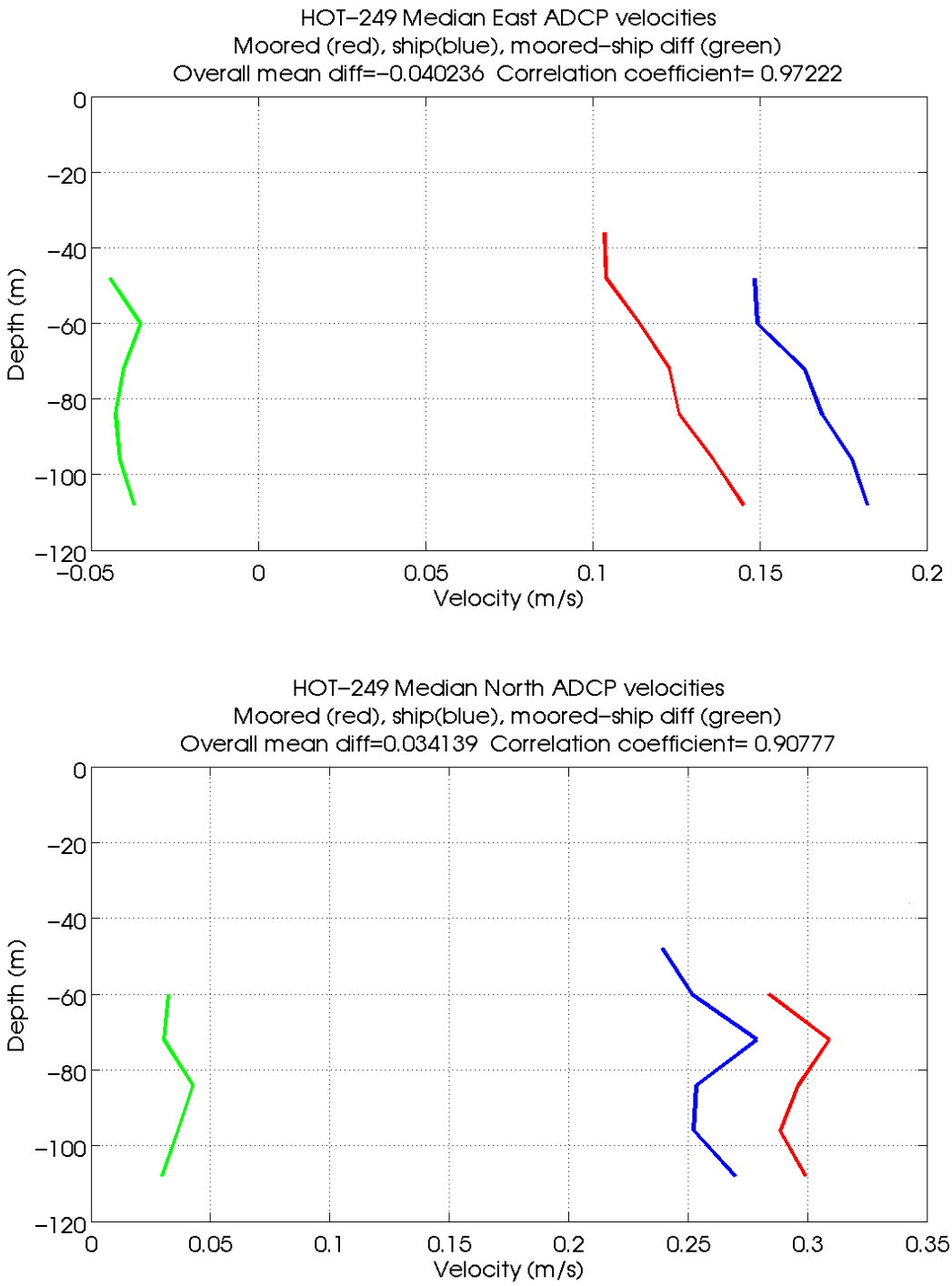

Figure 6-42. Median velocity profiles during shipboard ADCP (blue) versus moored 300 kHz ADCP (red) intercomparisons from HOT-249. Moored minus shipboard ADCP differences shown in green. Top panel shows east velocity components, bottom panel shows north velocity components.

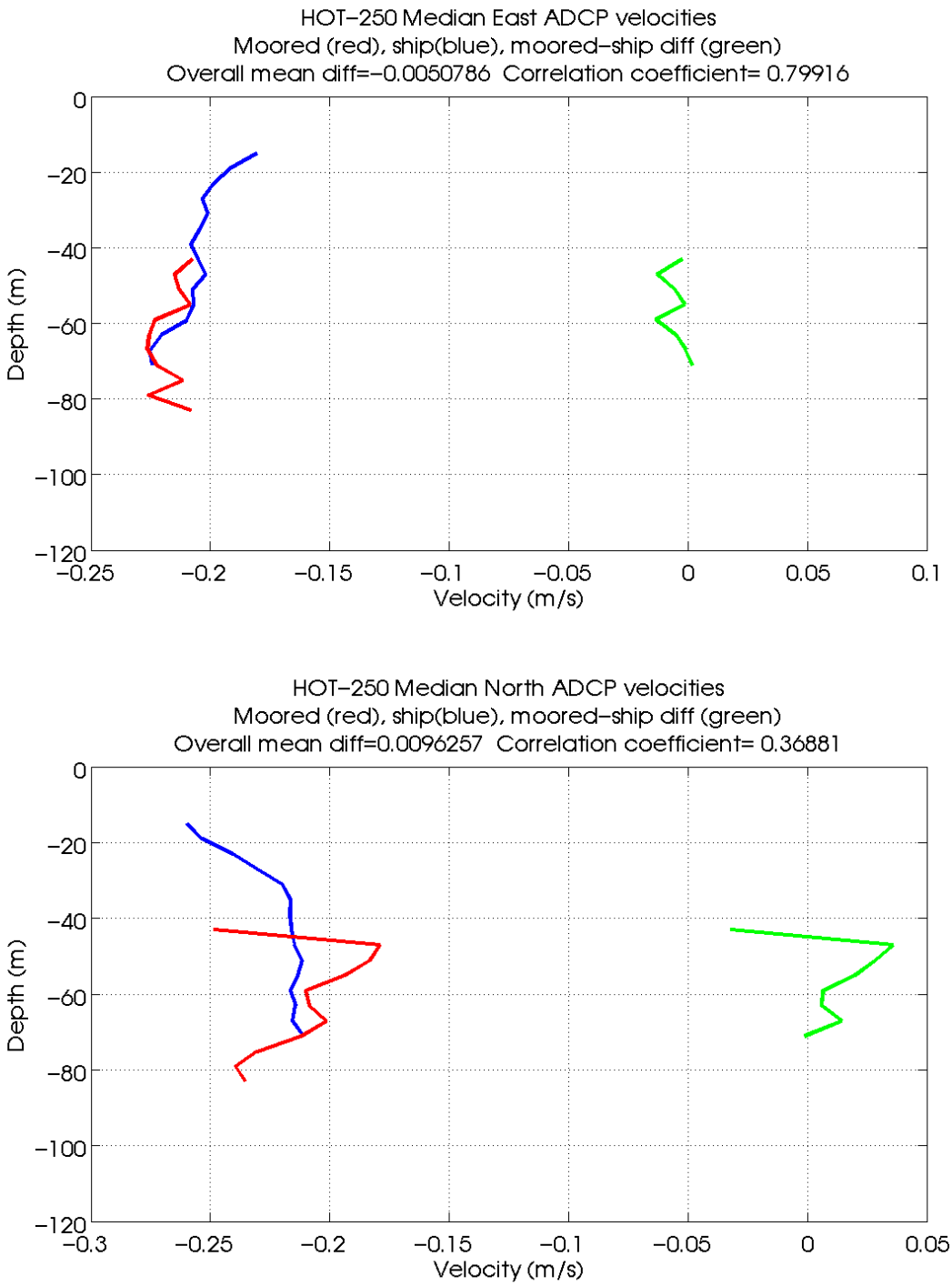

Figure 6-43. Median velocity profiles during shipboard ADCP (blue) versus moored 300 kHz ADCP (red) intercomparisons from HOT-250. Moored minus shipboard ADCP differences shown in green. Top panel shows east velocity components, bottom panel shows north velocity components.

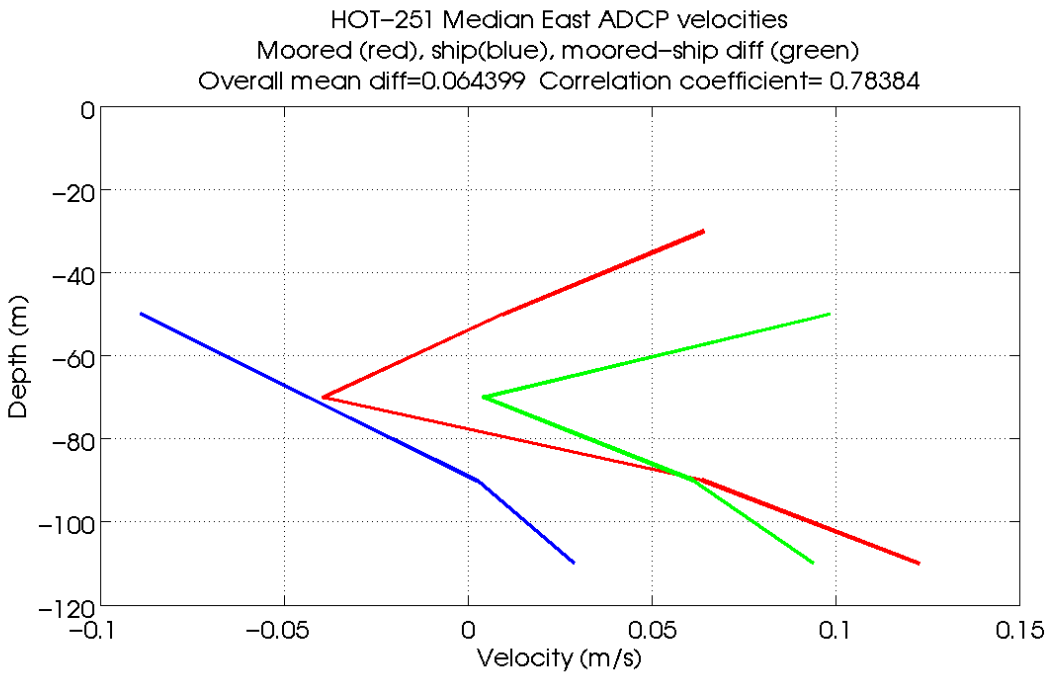

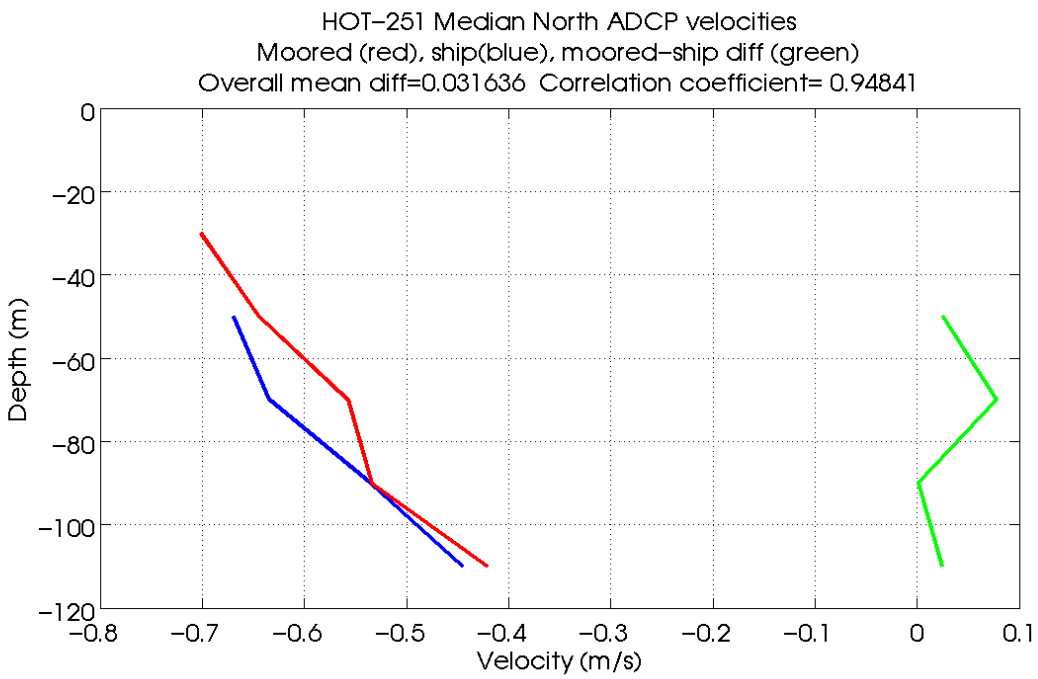

Figure 6-44. Median velocity profiles during shipboard ADCP (blue) versus moored 300 kHz ADCP (red) intercomparisons from HOT-251. Moored minus shipboard ADCP differences shown in green. Top panel shows east velocity components, bottom panel shows north velocity components.

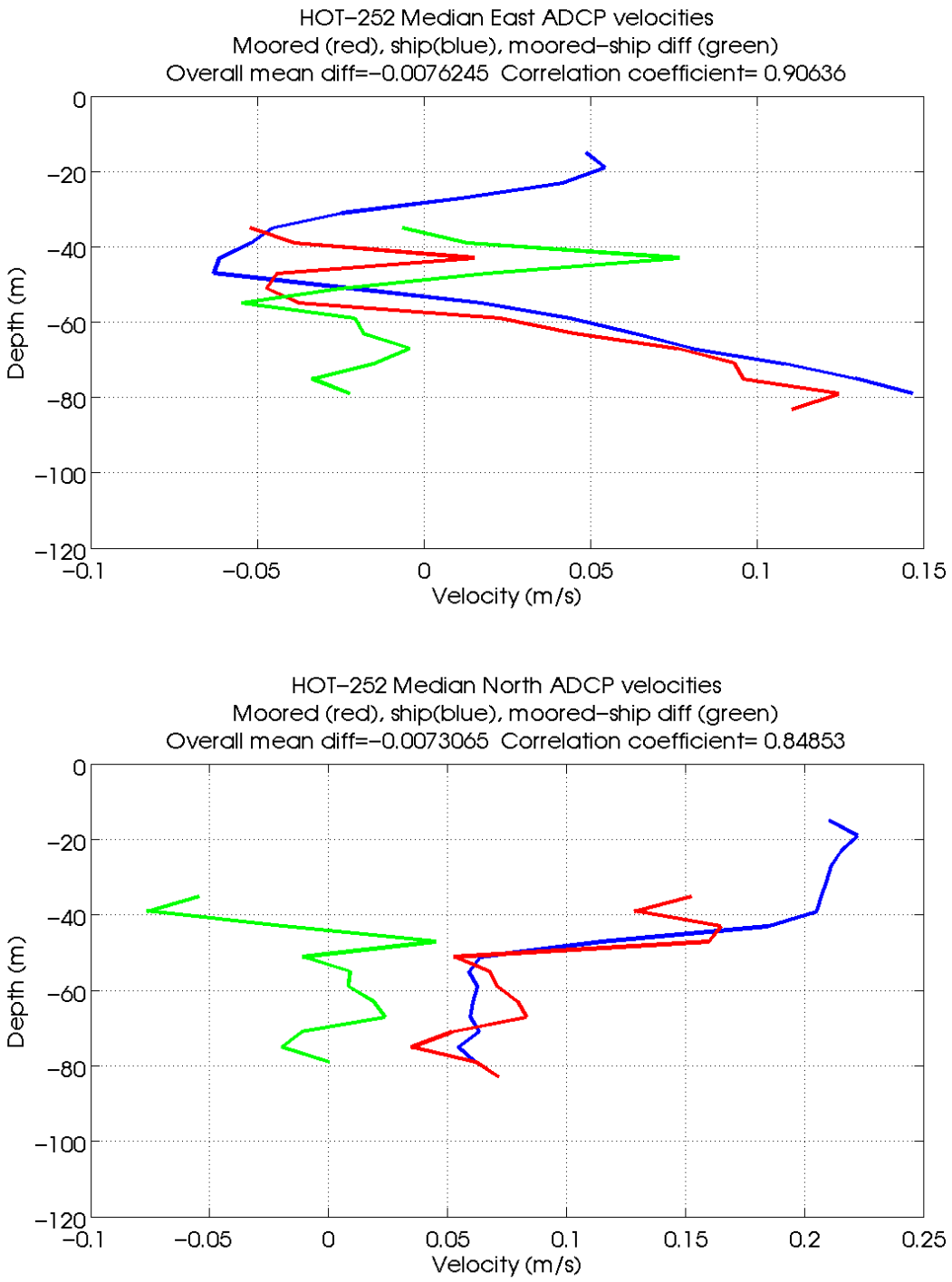

Figure 6-45. Median velocity profiles during shipboard ADCP (blue) versus moored 300 kHz ADCP (red) intercomparisons from HOT-252. Moored minus shipboard ADCP differences shown in green. Top panel shows east velocity components, bottom panel shows north velocity components.

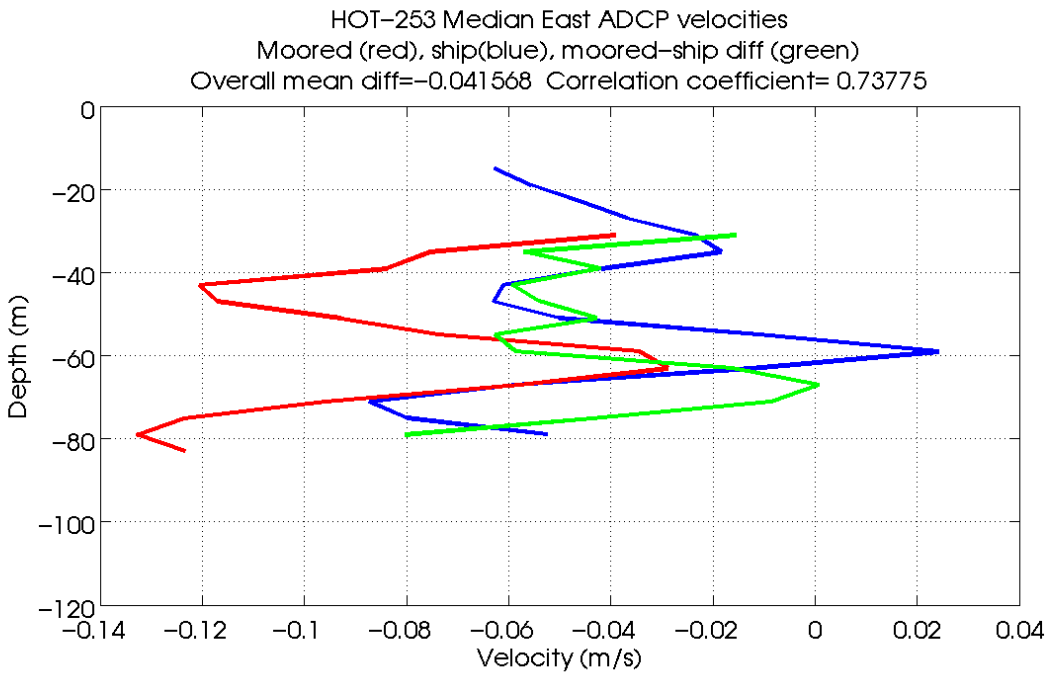

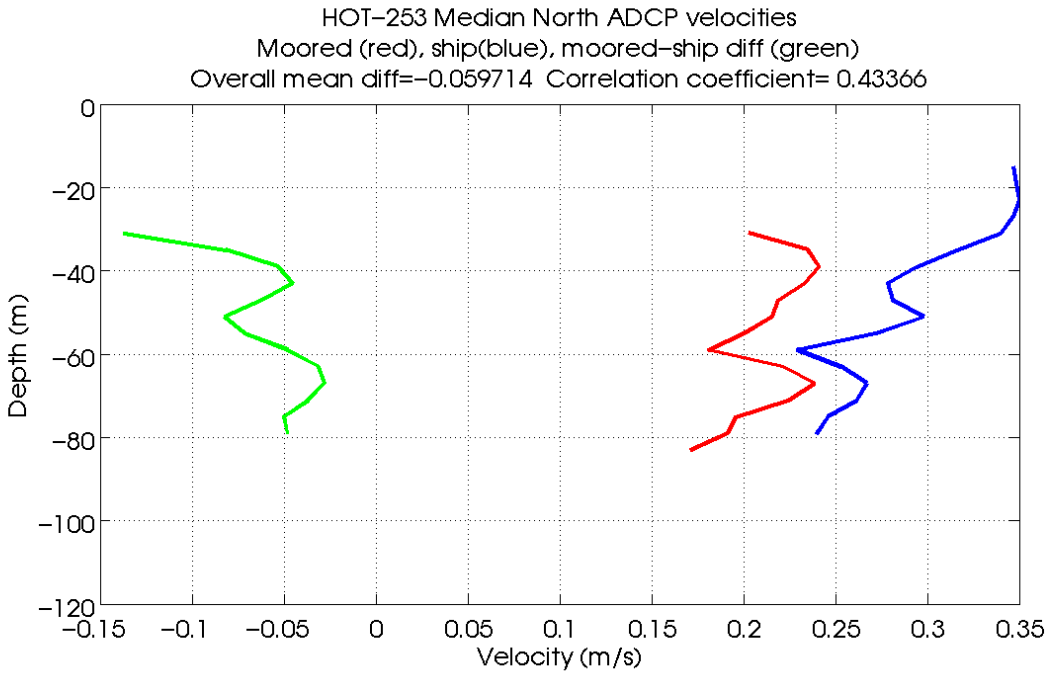

Figure 6-46. Median velocity profiles during shipboard ADCP (blue) versus moored 300 kHz ADCP (red) intercomparisons from HOT-253. Moored minus shipboard ADCP differences shown in green. Top panel shows east velocity components, bottom panel shows north velocity components.

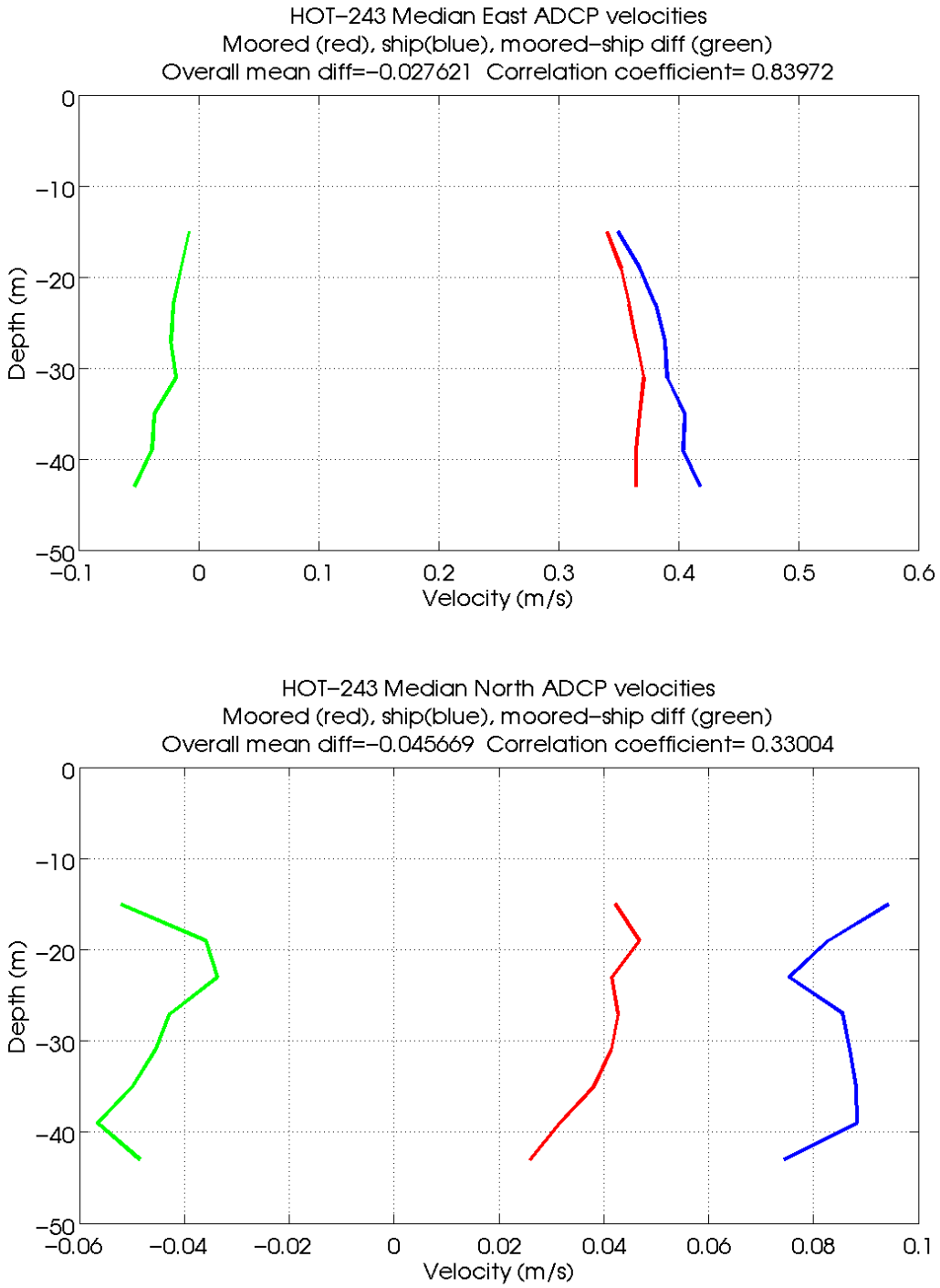

Figure 6-47. Median velocity profiles during shipboard ADCP (blue) versus moored 600 kHz ADCP (red) intercomparisons from HOT-243. Moored minus shipboard ADCP differences shown in green. Top panel shows east velocity components, bottom panel shows north velocity components.

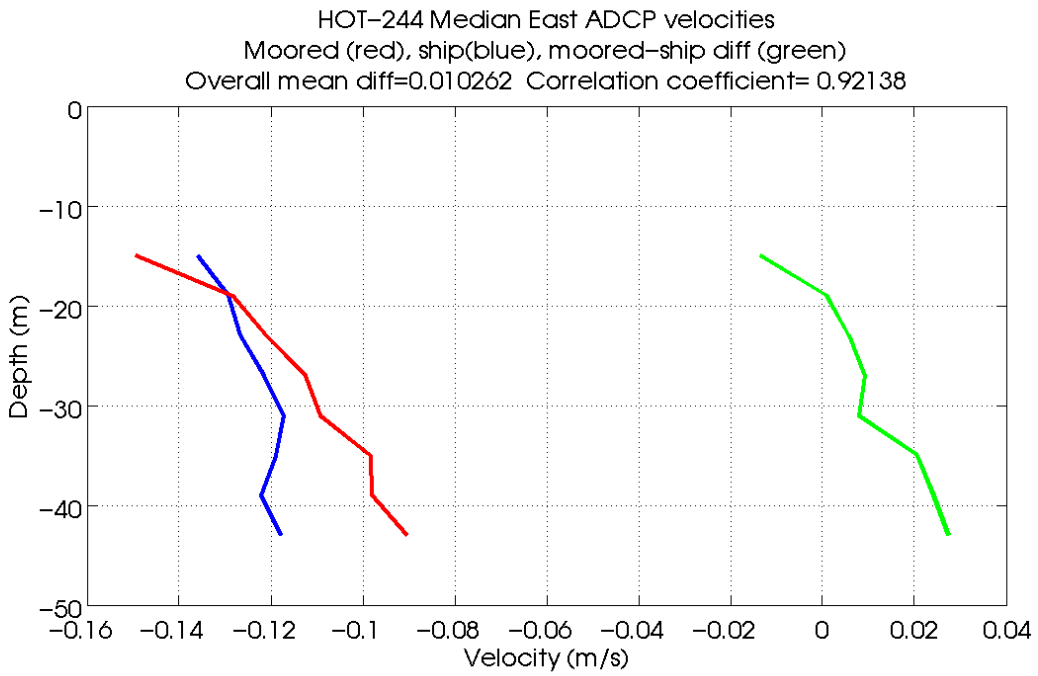

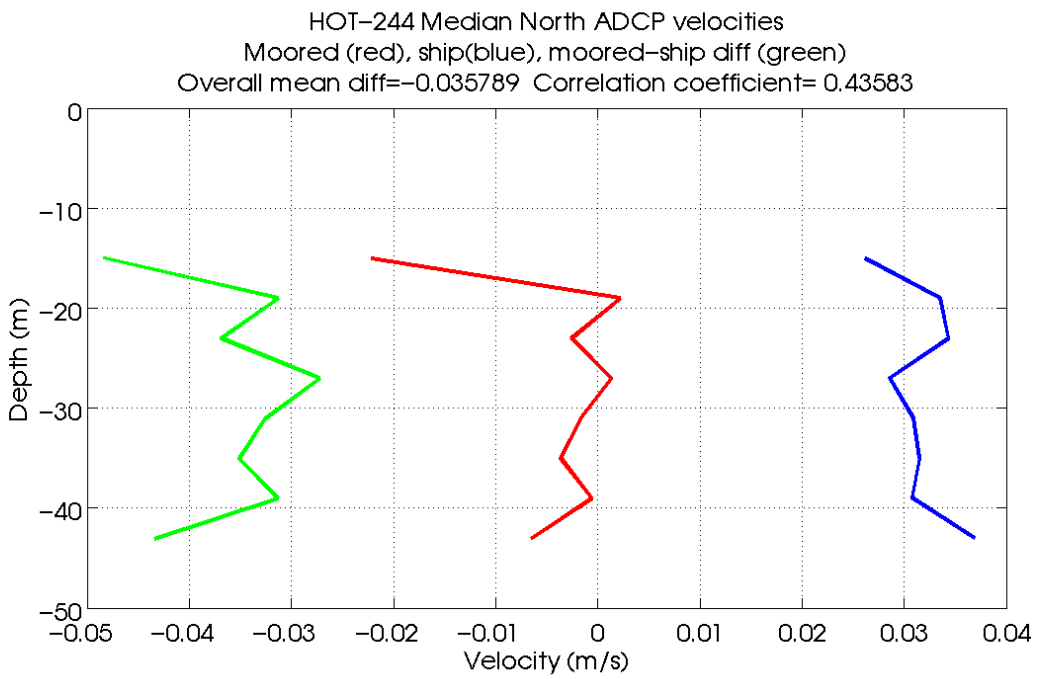

Figure 6-48. Median velocity profiles during shipboard ADCP (blue) versus moored 600 kHz ADCP (red) intercomparisons from HOT-244. Moored minus shipboard ADCP differences shown in green. Top panel shows east velocity components, bottom panel shows north velocity components.

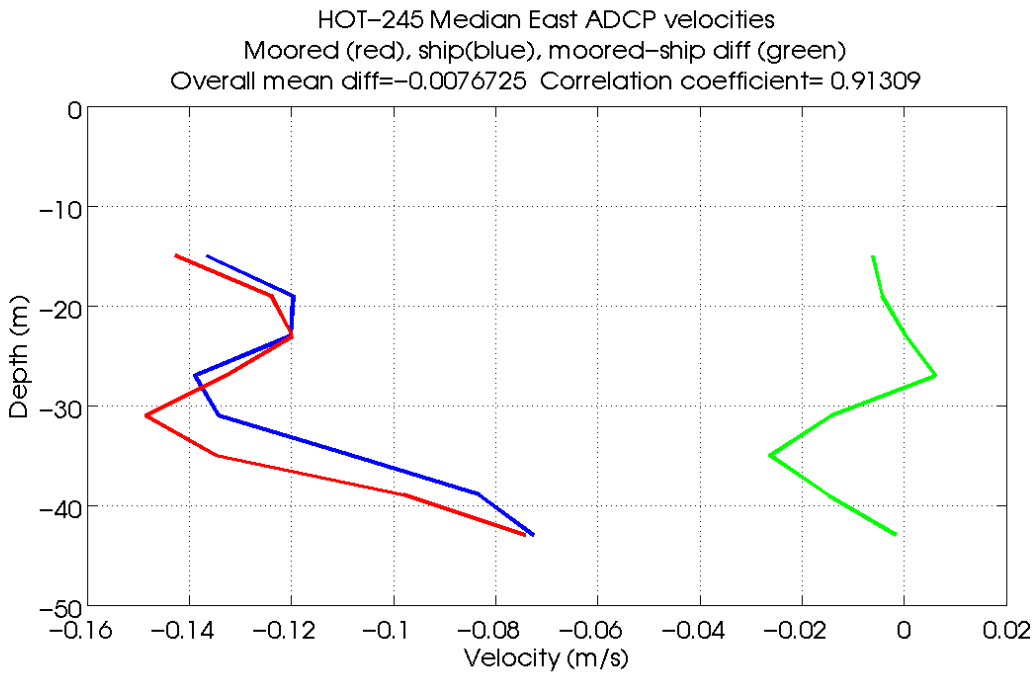

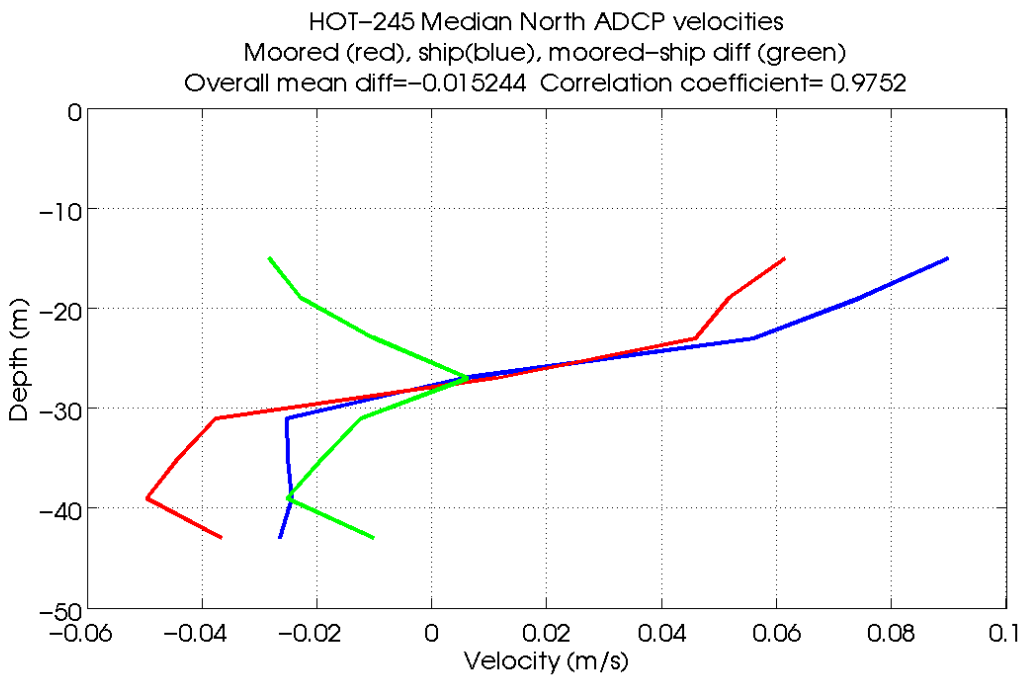

Figure 6-49. Median velocity profiles during shipboard ADCP (blue) versus moored 600 kHz ADCP (red) intercomparisons from HOT-245. Moored minus shipboard ADCP differences shown in green. Top panel shows east velocity components, bottom panel shows north velocity components.

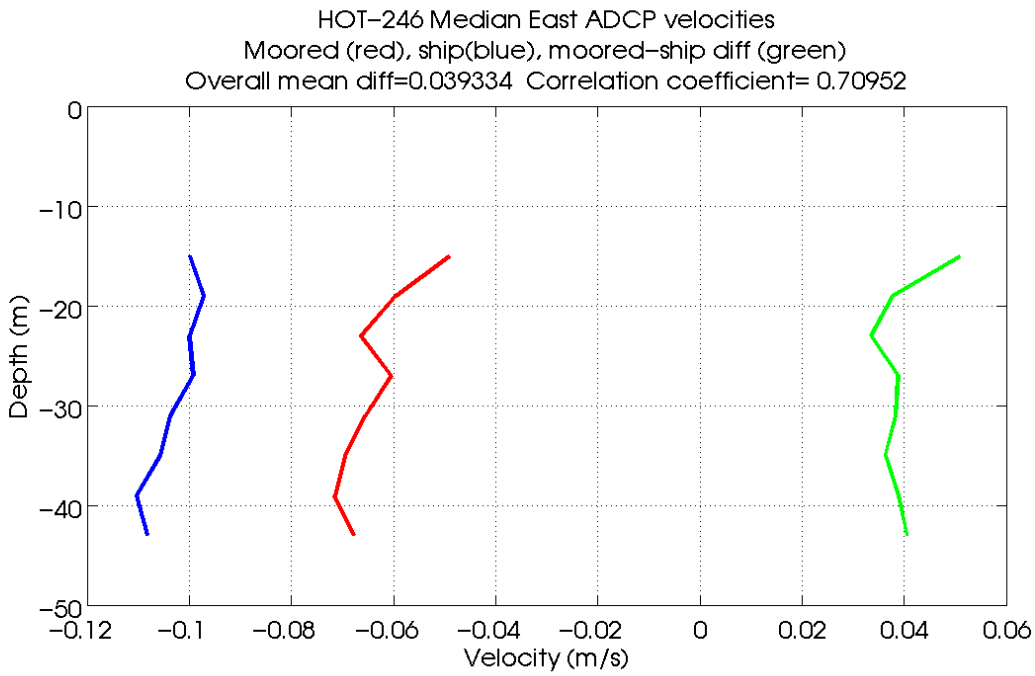

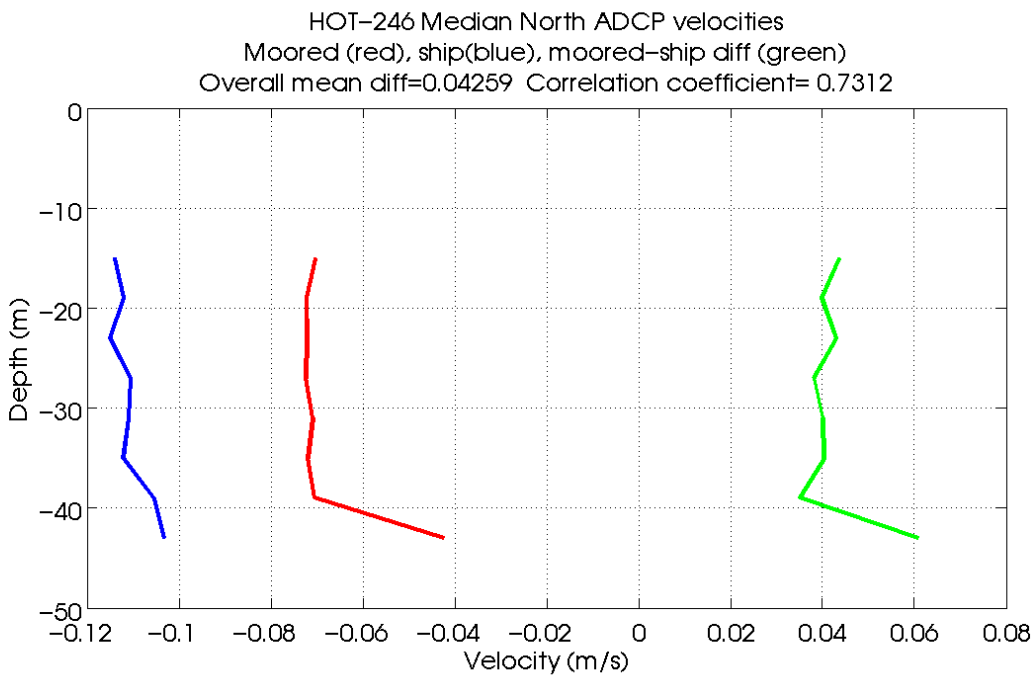

Figure 6-50. Median velocity profiles during shipboard ADCP (blue) versus moored 600 kHz ADCP (red) intercomparisons from HOT-246. Moored minus shipboard ADCP differences shown in green. Top panel shows east velocity components, bottom panel shows north velocity components.

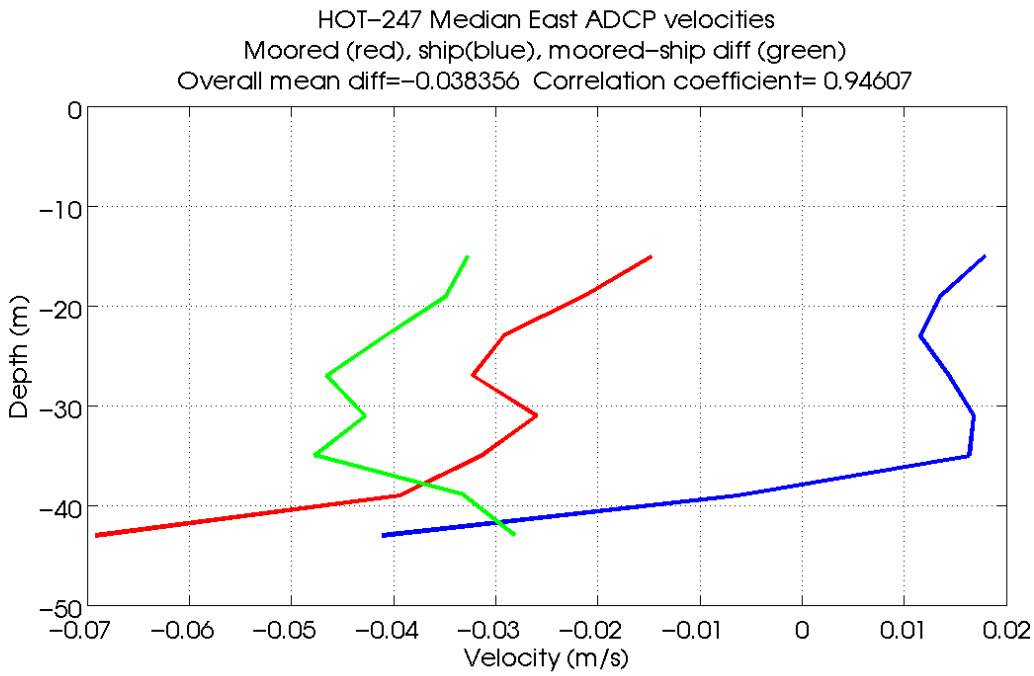

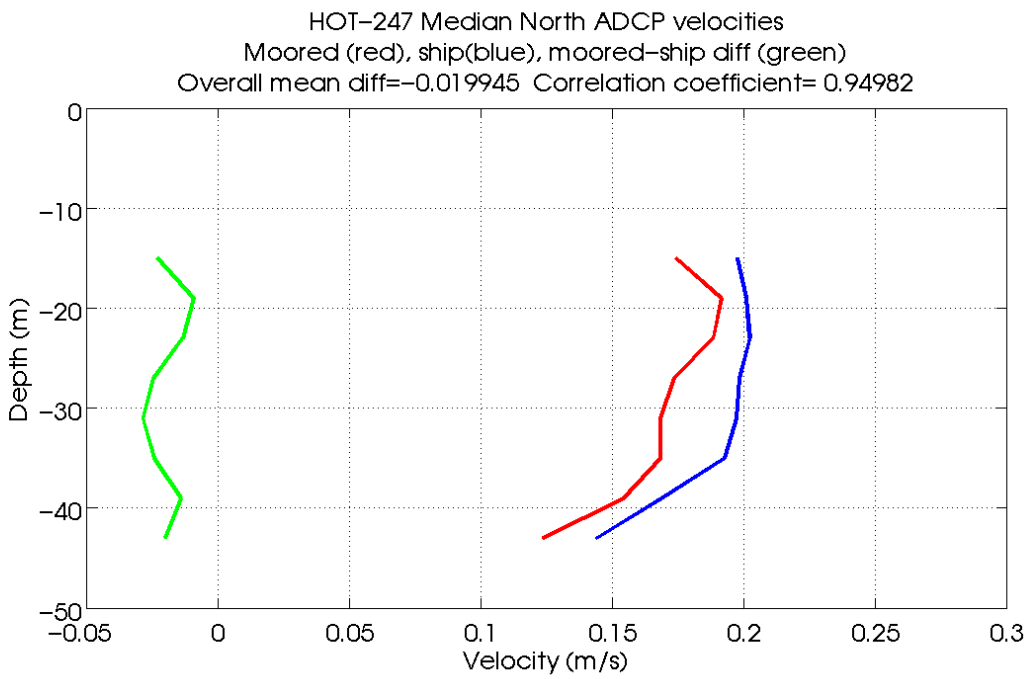

Figure 6-51. Median velocity profiles during shipboard ADCP (blue) versus moored 600 kHz ADCP (red) intercomparisons from HOT-247. Moored minus shipboard ADCP differences shown in green. Top panel shows east velocity components, bottom panel shows north velocity components.

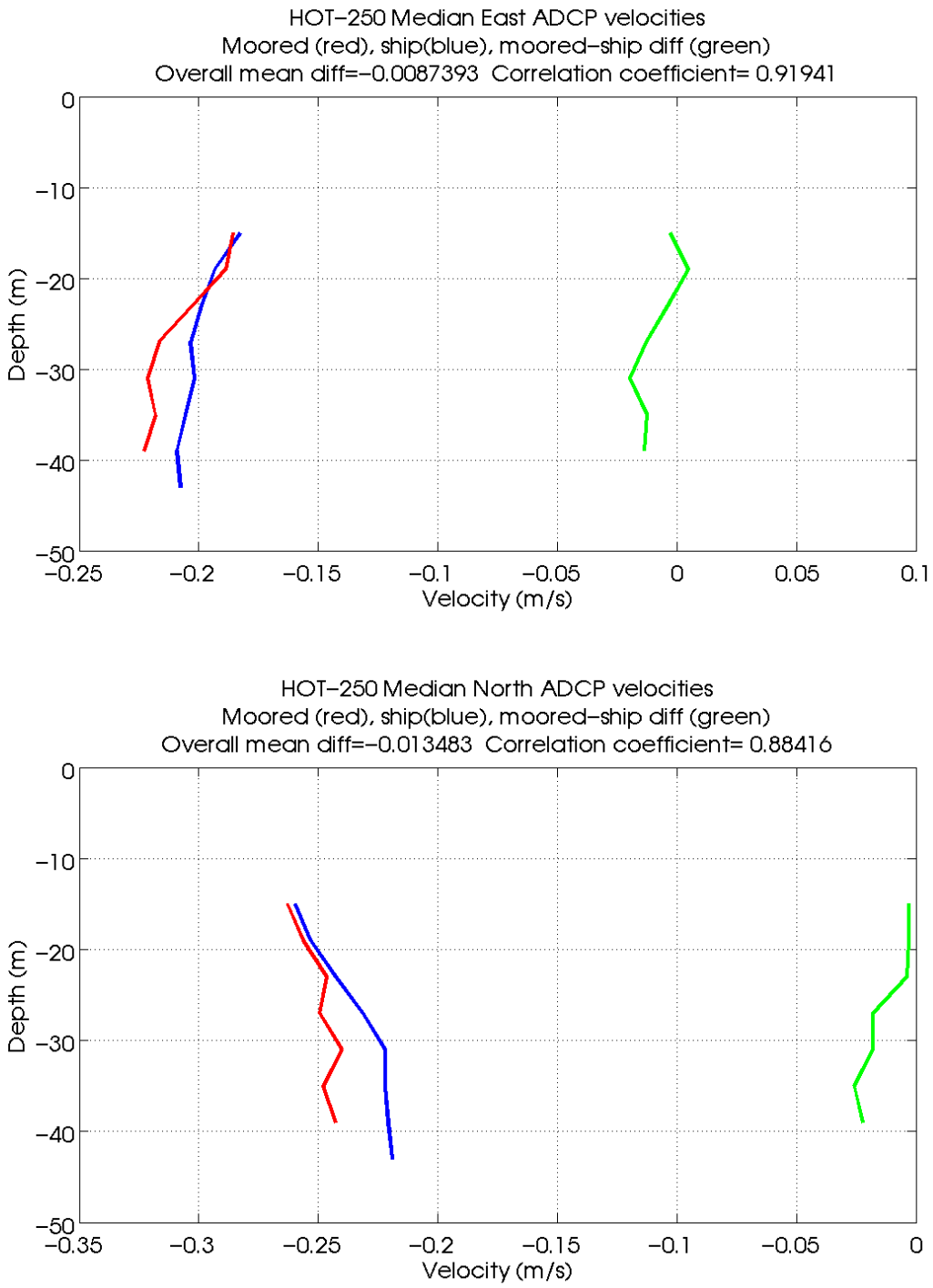

Figure 6-52. Median velocity profiles during shipboard ADCP (blue) versus moored 600 kHz ADCP (red) intercomparisons from HOT-250. Moored minus shipboard ADCP differences shown in green. Top panel shows east velocity components, bottom panel shows north velocity components.

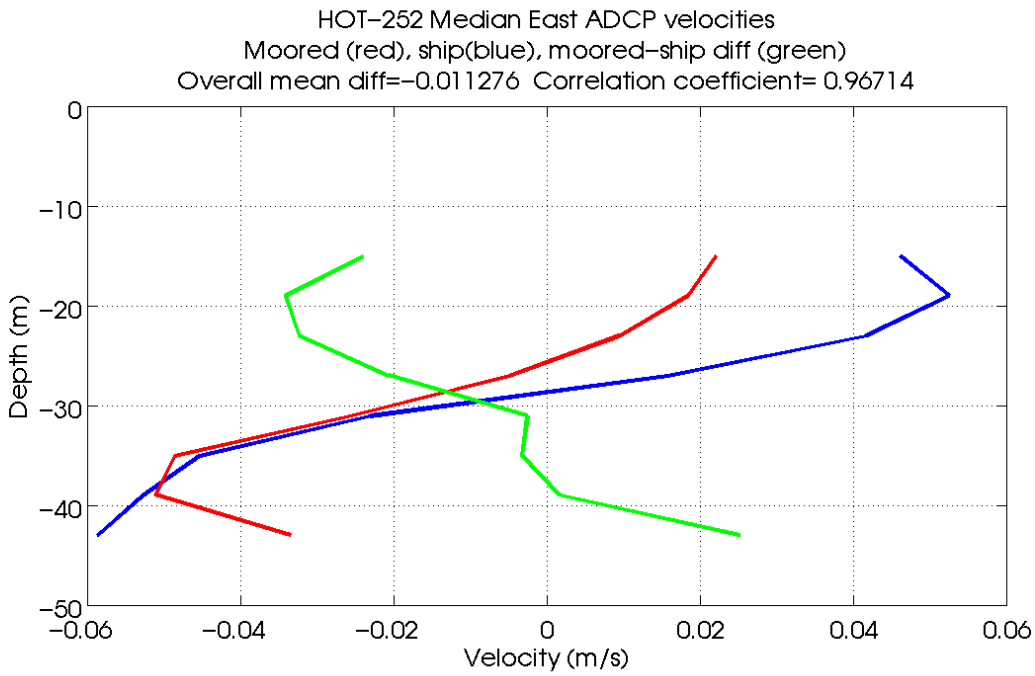

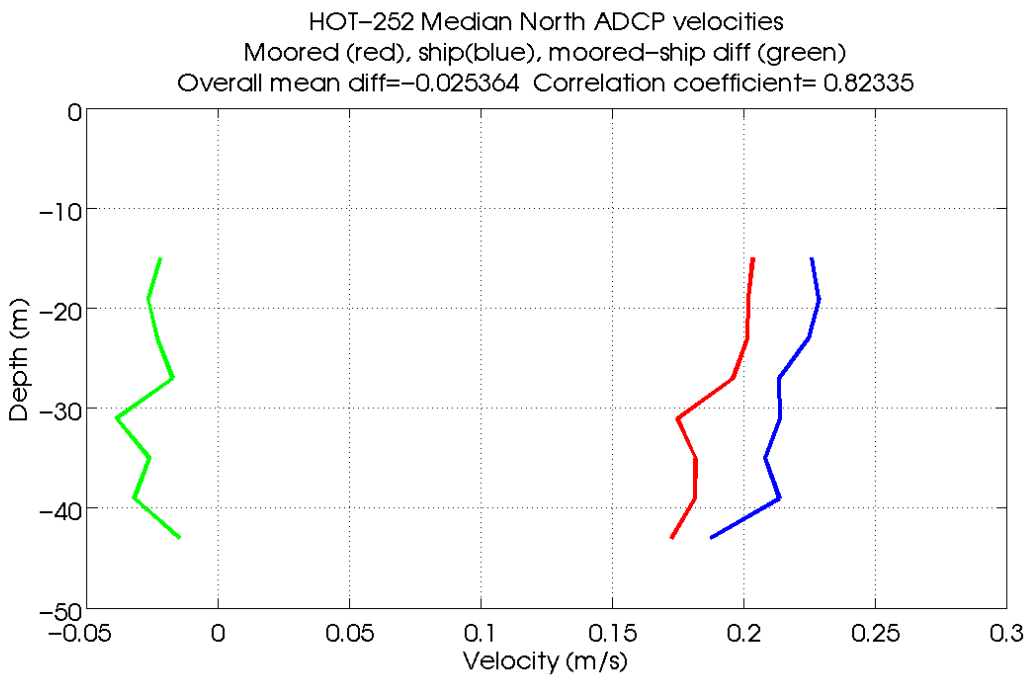

Figure 6-53. Median velocity profiles during shipboard ADCP (blue) versus moored 600 kHz ADCP (red) intercomparisons from HOT-252. Moored minus shipboard ADCP differences shown in green. Top panel shows east velocity components, bottom panel shows north velocity components.

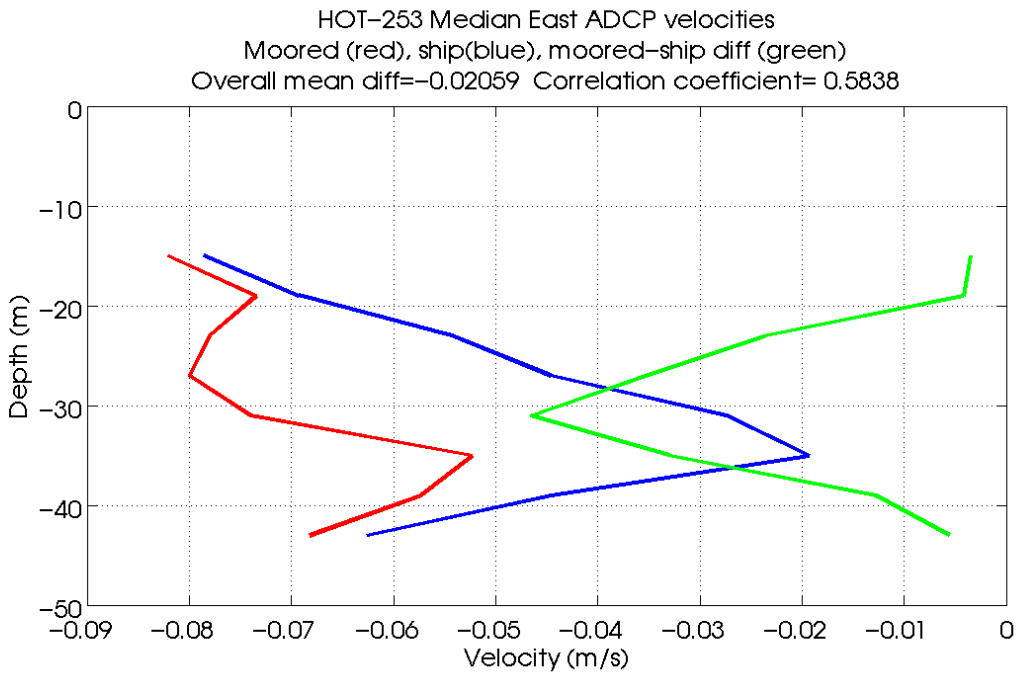

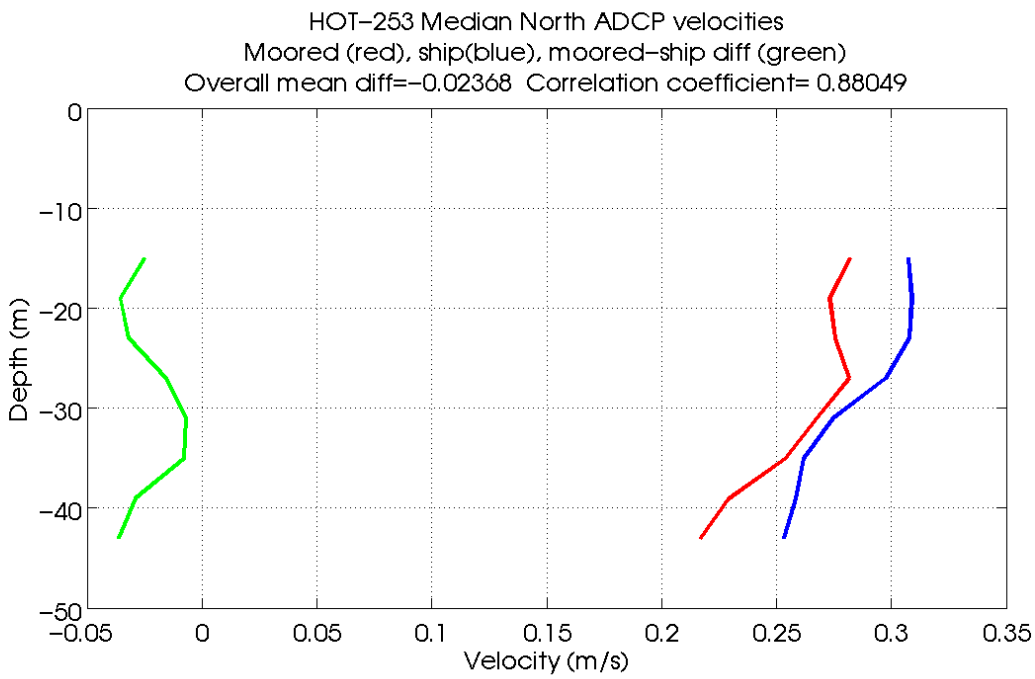

Figure 6-54. Median velocity profiles during shipboard ADCP (blue) versus moored 600 kHz ADCP (red) intercomparisons from HOT-253. Moored minus shipboard ADCP differences shown in green. Top panel shows east velocity components, bottom panel shows north velocity components.

F. Next Generation Vector Measuring Current Meter data (VMCM)

Time-series of daily mean horizontal velocity components for the VMCM current meters deployed during WHOTS-9 at 10 m and 30 m are presented in Figure 6-55.

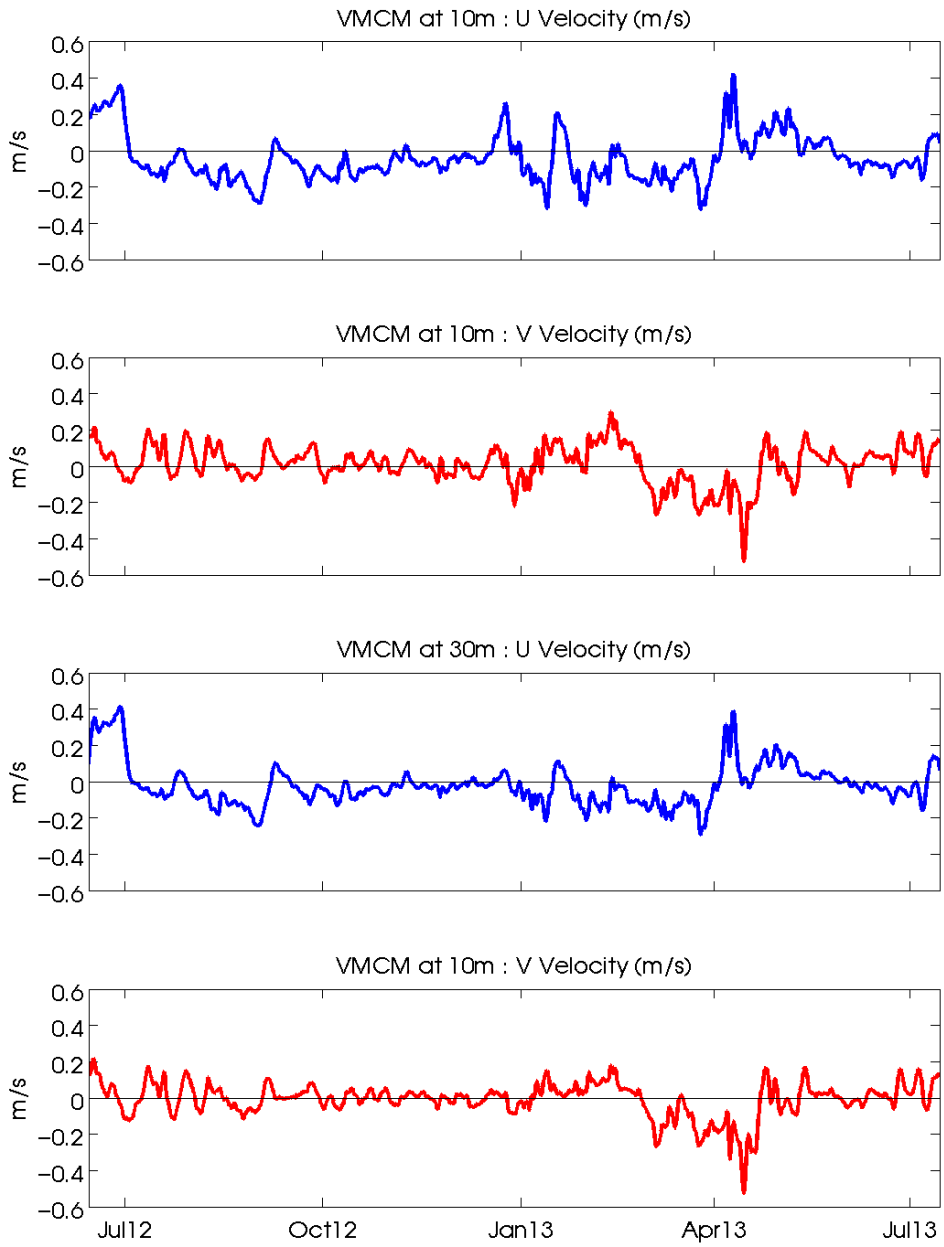

Figure 6-55. Horizontal velocity data (m/s) during WHOTS-9 from the VMCMs at 10 m depth (first and second panel) and at 30 m depth (third and fourth panel).

G. GPS data

Time-series of latitude and longitude of the WHOTS-9 buoy from GPS data are presented in Figure 6-56 and spectra of the time-series is shown in Figure 6-57.

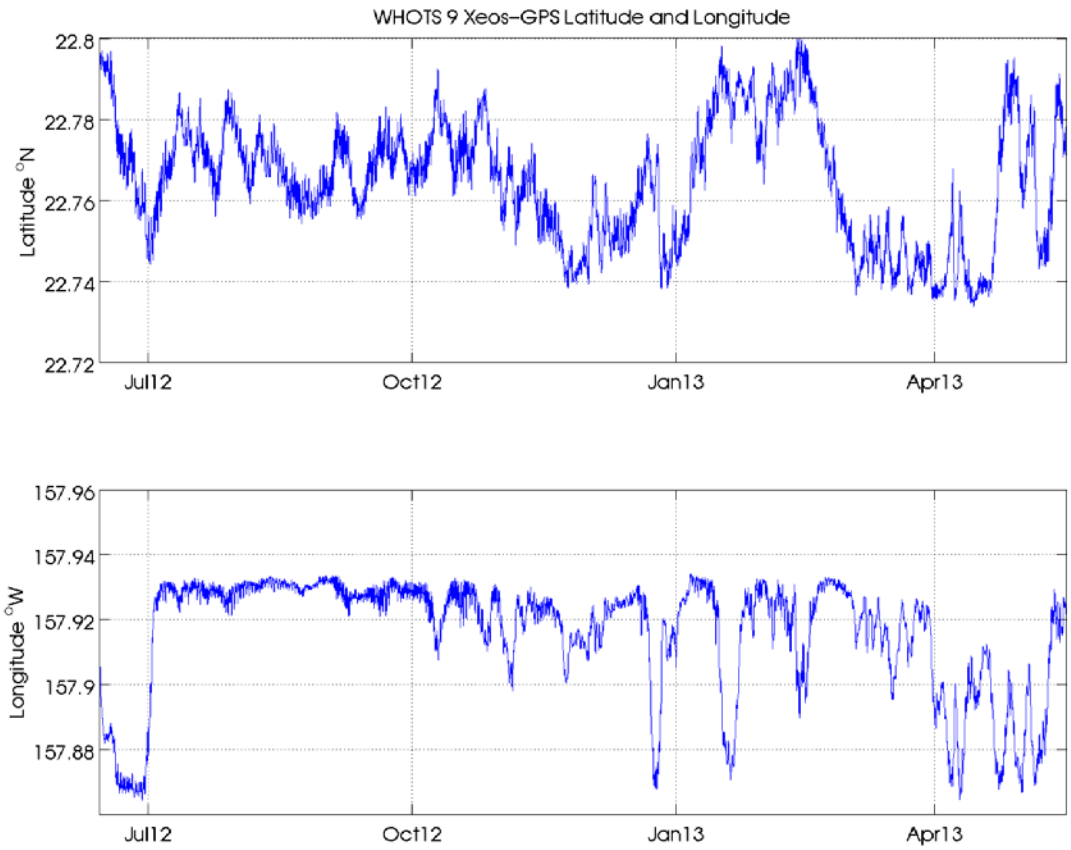

Figure 6-56. GPS Latitude (upper panel) and longitude (lower panel) time series from the WHOTS-9 deployment.

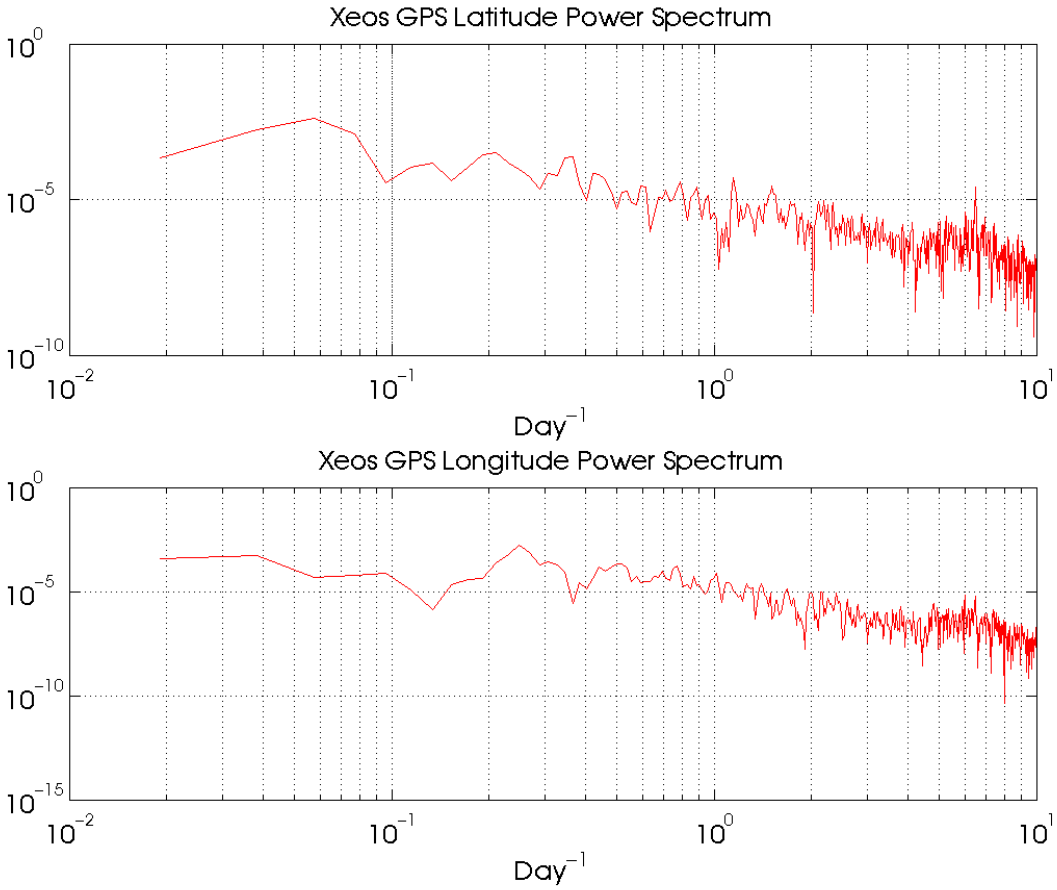

Figure 6-57. Power spectrum of latitude (upper panel) and longitude (lower panel) for the WHOTS-9 deployment.

H. Mooring Motion

The position of the mooring with respect to its anchor was determined from the ARGOS positions as shown in Section 5.D. Additional information of the mooring motion was provided by the ADCP data of pitch, roll and heading, shown in this section.

Figure 6-58 shows the ADCP data of the instrument's tilt (a combination of the pitch and roll), plotted against the buoy's distance from its anchor (derived from ARGOS positions), for both WHOTS ADCP's. The red line in the plot is a quadratic fit to the median tilt calculated every 0.2 km distance bins. The figure shows that during both deployments, the ADCP tilt increased as the distance from the anchor increased. This tilting was caused by the deviation of the mooring line from its vertical position as it was pulled by the anchor. The tilting of the line also caused the rising of the instruments attached to the line.

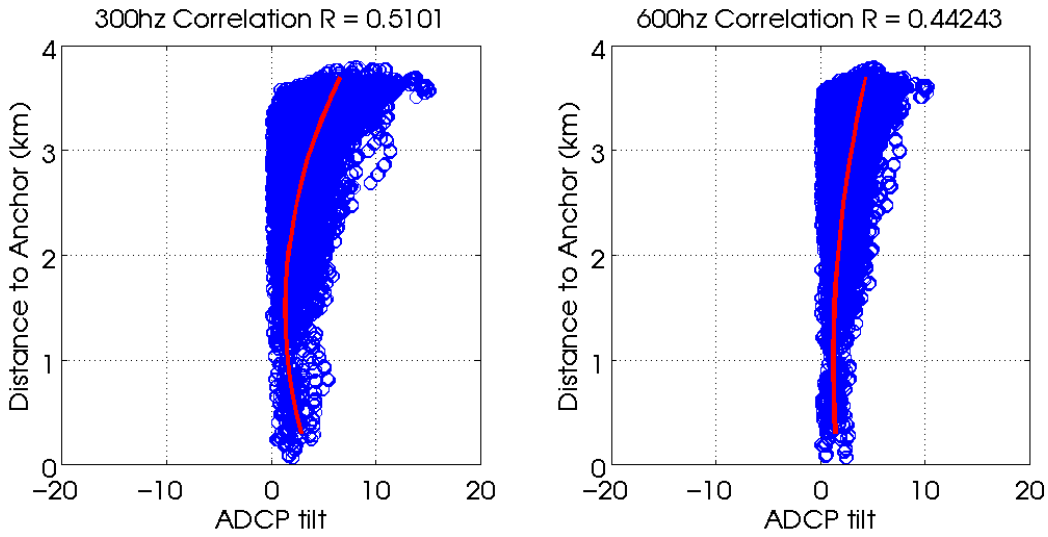

Figure 6-58. Scatter plots of ADCP tilt and distance of the buoy to its anchor for the 300 kHz (left panel), and the 600 kHz ADCP deployments (right panel, blue circles). The red line is a quadratic fit to the median tilt calculated every 0.2 km distance bins.

7. References

Colbo, K., R. Weller, 2009. Accuracy of the IMET Sensor Package in the Subtropics. J. Atmos. Oceanic Technol., 26, 1867-1890.

Firing, E., 1991. Acoustic Doppler Current Profiling measurements and navigation. In *WOCE Hydrographic Operations and Methods.* WOCE Operations Manual, WHP Office Report WHPO 91-1,WOCE Report No. 68/91, 144pp.

Freitag, H. P., M. E. McCarty, C. Nosse, R. Lukas, M. J. McPhaden, and M. F. Cronin, 1999. COARE Seacat data: Calibrations and quality control procedures. NOAA Thechnical Memorandum, ERL PMEL-115. 93 pp.

Hosom, D. R. Weller, R. Payne, and K. Prada, 1995. The IMET (Improved Meteorology) Ship and Buoy Systems. J. Atmos. Oceanic Technol., 12, 527-540.

Howe, B. M., R. Lukas, F. Duennebier, and D. Karl, ALOHA cabled observatory installation, *OCEANS 2011*, 19-22 Sept. 2011.

Kara, A. B., P. A. Rochford, and H. E. Hulburt, 2000. Mixed layer depth variability and barrier layer formation over the North Pacific Ocean, J. Geophys. Res., 105, 16,803–16,821.

Larson, N. and A.M. Pederson, 1996. Temperature measurements in flowing water: Viscous heating of sensor tips. 1st International Group for Hydraulic Efficiency Measurements (IGHEM) Meeting, Montreal, Canada, June 1996.

Lueck, R. G., 1990. Thermal inertia of conductivity cells: Theory. Journal of Atmospheric and Oceanic Technology, 7, 741-755.

Lueck, R. G. and J. J. Picklo, 1990: Thermal inertia of conductivity cells: Observations with a Sea-Bird cell. Journal of Atmospheric and Oceanic Technology, 7, 756-768.

Lukas, R., F. Santiago-Mandujano, F. Bingham and A. Mantyla, 2001. Cold bottom water events observed in the Hawaii Ocean time-series: Implications for vertical mixing. *Deep-Sea Res*. I, 48 (4), 995-1021

Owens, W. B. and R. C. Millard, 1985. A new algorithm for CTD oxygen calibration. Journal of Physical Oceanography, 15, 621-631.

Plueddemann, A.J., R.A. Weller, R. Lukas, J. Lord, P.R. Bouchard, and M.A. Walsh, 2006, WHOI Hawaii Ocean Timeseries Station (WHOTS): WHOTS-2 Mooring Turnaround Cruise Repor**t,** Woods Hole Oceanographic Institution, Technical Report WHOI-2006-08, 68 pp.

Plueddemann, A.J., Ryder, B. Pietro, J. Smith, C. Duncombe Rae, R. Lukas, C. Nosse, J. Snyder, L. Bariteau, S. J. Park, D. Hashisaka, E. Roth, C. Fumar, A. Andrews, and N. Seymour, 2013.

WHOI Hawaii Ocean Timeseries Station (WHOTS): WHOTS-9 2012 Mooring Turnaround Cruise Report, Woods Hole Oceanographic Institution, Technical Report WHOI-2013-04, 93 pp.

Plueddemann, A.J., B. Pietro, S. Whelan, R. Lukas, J. Snyder, C. Fumar, E. Roth, B. Nakahara, D. McCoy, J. George, and D. Wolfe, 2014, WHOI Hawaii Ocean Timeseries Station (WHOTS): WHOTS-10 Mooring Turnaround Cruise Report, Woods Hole Oceanographic Institution, Technical Report WHOI-2014-02, 114 pp.

Santiago-Mandujano, F., P. Lethaby, R. Lukas, J. Snyder, Weller, A. Plueddeman, J. Lord, S. Whelan, P. Bouchard, and N. Galbraith, 2007. Hydrographic Observations at the Woods Hole Oceanographic Institution (WHOI) Hawaii Ocean Timeseries (HOT) Site (WHOTS): 2004-2006. School of Ocean and Earth Science and Technology, University of Hawaii. (http://www.soest.hawaii.edu/whots/data_report1.html)

Tupas, L., F. Santiago-Mandujano, D. Hebel, R. Lukas, D. Karl, and E. Firing 1993. Hawaii Ocean Time-series Data Report 4, 1992, School of Ocean and Earth Science and Technology, University of Hawaii, 93-14, 248 pp.

Tupas, L., F. Santiago-Mandujano, D. Hebel, C. Nosse, L. Fujieki, E. Firing, R. Lukas, D. Karl, 1997. Hawaii Ocean Time-series Data Report 8, 1996, School of Ocean and Earth Science and Technology, University of Hawaii, 97-7, 296 pp.

UNESCO. 1981. Tenth Report of the Joint Panel on Oceanographic Tables and Standards. UNESCO Technical Papers in Marine Science, No. 36, UNESCO, Paris.

Whelan S., R. Weller, R. Lukas, F. Bradley, J. Lord, J. Smith, F. Bahr, P. Lethaby, J. Snyder, 2007. WHOI Hawaii Ocean Timeseries Station (WHOTS): WHOTS-3 Mooring Turnaround Cruise Report. Technical Report. Woods Hole Oceanographic Institution, WHOI-2007-03, 103 pp.

8. Appendices

A. Appendix 1: WHOTS-9 300 kHz ADCP Configuration

File Size 28,408,757 bytes

Data Structure BB/WH/OS
Ensemble Length 752 bytes

Program Version 50.4

System Frequency 300 kHz
Convex
Sensor Configuration #1
Transducer Head Attached TRUE
Orientation UP
Beam Angle 20 Degrees
Transducer 4 Beam Janus

Real Data

CPU Serial Number: 8675

False Target(WA) 70 counts
Band Width (WB) 0
Cor. Thres. (WC) 64 counts
Err Thres. (WE) 2000 mm/s
Blank (WF) 1.76 m
Min PGood (WG) 0
Ref Layer (WL) 1, 5 first bin, last bin
Mode (WM) 1
Bins (WN) 30
Pings/Ens (WP) 40
Bin Size (WS) 4.00 m

Head Align (EA) 0.00 degrees
Head Bias (EB) 9.52 degrees
Coord Xform (EX) 00011111 Earth Coordinates Using Tilts, 3 Beam Solutions, and Bin Mapping
Sens Source (EZ) 01111101 cdhprst
Sens Avail 00011101 cdhprst

Time/Ping (TP) 00:04.00

Hardware 4 Beams
Code Reps. 9
Lag Length 0.49 m
Xmt Length 4.42 m
1st Bin 6.22 m

BT Pings/Ens (BP) 0
BT Ens Delay (BD) 0
BT Cor.Thres. (BC) 0 counts
BT Eval. Thres. (BA) 0 counts

BT PG Thres. (BG) 0
BT Mode (BM) 0
BT Err Thres. (BE) 0 mm/s
BT Max Range (BX) 0 dm

First Ensemble 00000001 07-Jun-2012 00:00:00
Last Ensemble 00058164 15-Jul-2013 21:50:00

B. Appendix 2: WHOTS-9 600 kHz ADCP Configuration

File Size 23,928,361 bytes

Data Structure BB/WH/OS
Ensemble Length 652 bytes

Program Version 50.4

System Frequency 600 kHz
Convex
Sensor Configuration #1
Transducer Head Attached TRUE
Orientation UP
Beam Angle 20 Degrees
Transducer 4 Beam Janus

Real Data

CPU Serial Number: 15009

False Target(WA) 70 counts
Band Width (WB) 0
Cor. Thres. (WC) 64 counts
Err Thres. (WE) 2000 mm/s
Blank (WF) 0.88 m
Min PGood (WG) 0
Ref Layer (WL) 1, 5 first bin, last bin
Mode (WM) 1
Bins (WN) 25
Pings/Ens (WP) 80
Bin Size (WS) 2.00 m

Head Align (EA) 0.00 degrees
Head Bias (EB) 9.52 degrees
Coord Xform (EX) 00011111 Earth Coordinates Using Tilts, 3 Beam Solutions, and Bin Mapping
Sens Source (EZ) 01111101 cdhprst
Sens Avail 00011101 cdhprst

Time/Ping (TP) 00:2.00

Hardware 4 Beams
Code Reps. 9
Lag Length 0.25 m
Xmt Length 2.21 m

1st Bin 3.11 m

BT Pings/Ens (BP) 0
BT Ens Delay (BD) 0
BT Cor.Thres. (BC) 0 counts
BT Eval. Thres. (BA) 0 counts
BT PG Thres. (BG) 0
BT Mode (BM) 0
BT Err Thres. (BE) 0 mm/s
BT Max Range (BX) 0 dm

First Ensemble 00000001 07-Jun-2012 00:00:00
Last Ensemble 00058154 16-Jul-2013 19:59:59

C. Appendix 3: WHOTS-9 VMCM report

WHOTS 9 VMCM Preliminary Processing

N Galbraith, 2013/08/01

General WHOTS 9 platform information

1. Anchor times: 14-Jun-2012 02:23 14-Jul-2013 16:17

2. Water depth: 4668

3. Magnetic_variation:
value_to_be_applied: 9.8701
annual_drift_east: -2.4773
inputs:
latitude: 22.77
longitude: -157.9
date: 2012/12/28
source: NOAA > NESDIS > NGDC
model: International Association of Geomagnetism and Aeronomy (IAGA) International Geomagnetic Reference Field (IGRF)
URL: http://www.ngdc.noaa.gov/geomag-web/#declination
contact: geomag.models@noaa.gov

WHOTS 9 VMCM information

1. From tech docs

a. From Deployment file:

SN	Depth	Start Date	Start Time	Spike Start	Spike Start	Comment
11	10	10-Jun-12	19:50	10-Jun-12	20:39:00	top rotor spun at 20:39, bottom at 20:40:00
61	30	10-Jun-12	21:58	10-Jun-12	22:07:00	top rotor spun at 22:07:00, bottom at 22:08:00

b. From Recovery file:

SN	Depth	UTC	Inst Time	stop	records
11	10	7/17/13 19:31	7/15/13 19:27:15	7/17/13 19:28	578847
61	30	7/17/13 19:42	7/15/13 19:45:43	7/17/13 19:35	578738

WHOTS 9 VMVM Preliminary Processing

1. raw dat files converted to matlab using get_vmcm.m version 2012/5/30.
2. Clock checks and basic inventory

File	ntot	ndepl	lastgood
whots9vmcm11	578847	569574	14-Jul-2013 16:16:30
whots9vmcm61	578739	569574	14-Jul-2013 16:16:45

Preliminary data return; note the clocks were both 1 minute, there were no missing records.

SN	first	last	#points	#expt	%
11	14-Jun-2012 02:23:30	14-Jul-2013 16:16:30	569634	569634	100
61	14-Jun-2012 02:23:45	14-Jul-2013 16:16:45	569634	569634	100

Plots of HOURLY averages of U & V.

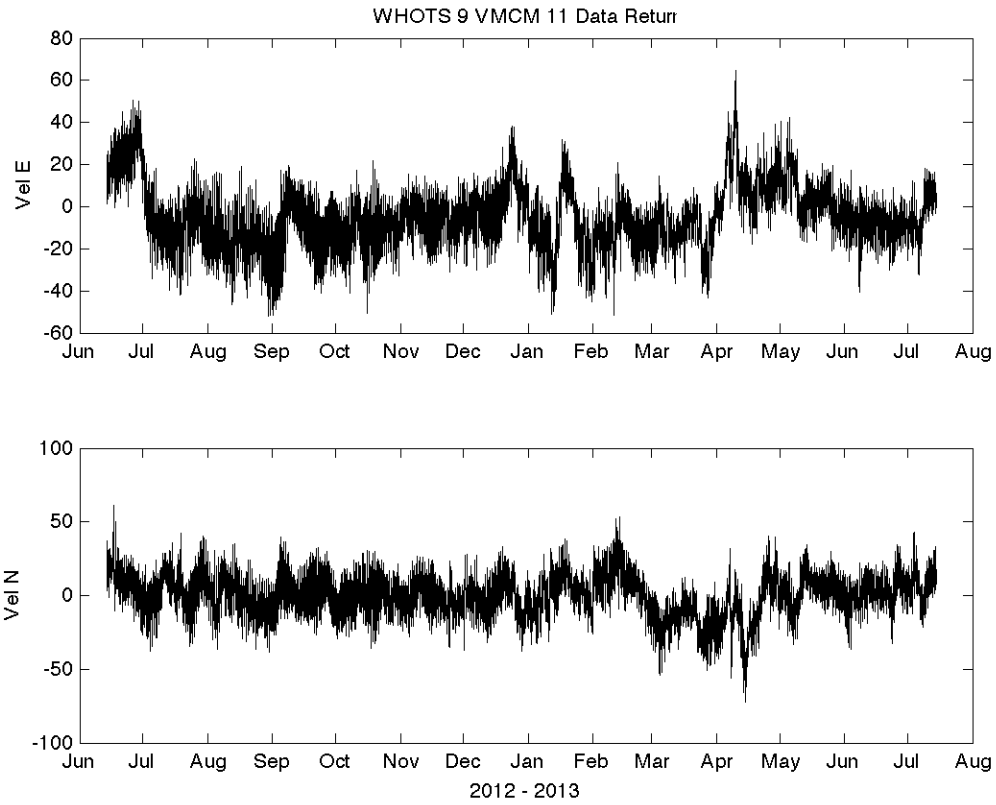
WHOTS 9 VMCM 11 Data Returr
Vel E
80
60
40
20
0
-20
-40
-60
Jun Jul Aug Sep Oct Nov Dec Jan Feb Mar Apr May Jun Jul Aug
Vel N
100
50
0
-50
-100
Jun Jul Aug Sep Oct Nov Dec Jan Feb Mar Apr May Jun Jul Aug
2012 - 2013

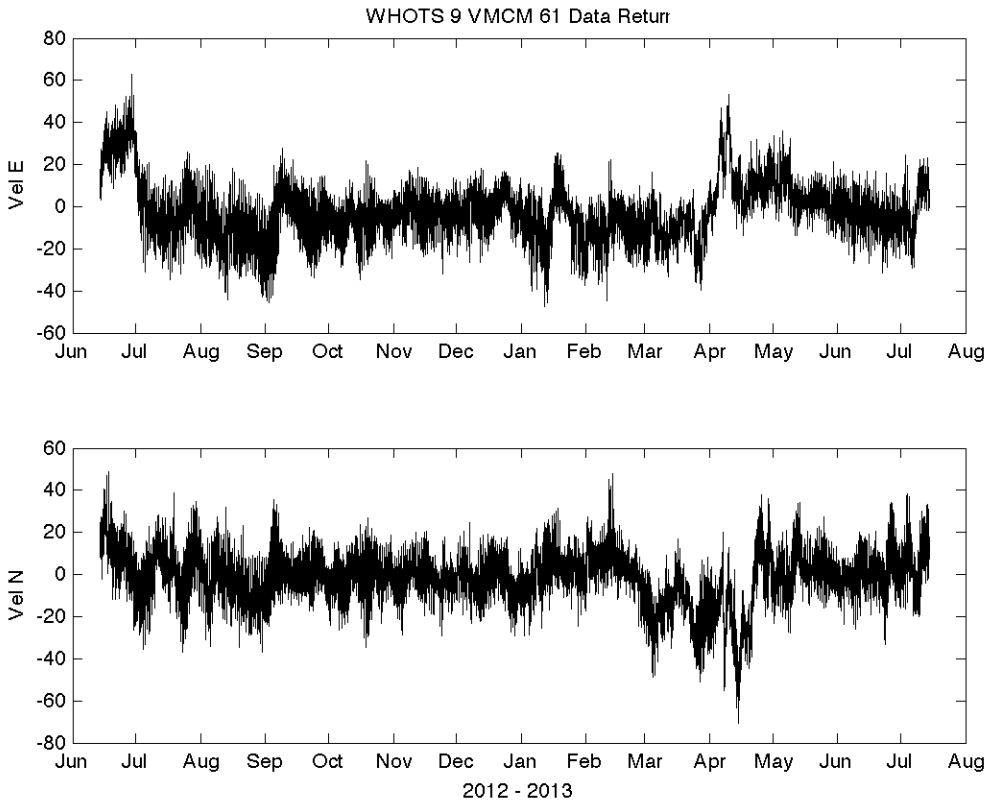
WHOTS 9 VMCM 61 Data Returr
Vel E
80
60
40
20
0
-20
-40
-60
Jun
Jul
Aug
Sep
Oct
Nov
Dec
Jan
Feb
Mar
Apr
May
Jun
Jul
Aug
Vel N
60
40
20
0
-20
-40
-60
-80
2012 - 2013